Regulatory mechanisms of tumor initiation, growth and invasion: the function of isocitrate dehydrogenase 1, acidosis and ephrinB2

Inaugural Dissertation
submitted to the Faculty of Medicine
in partial fulfillment of the requirements
for the PhD-Degree
of the Faculties of Veterinary Medicine and Medicine
of the Justus Liebig University Giessen

by Böğürcü-Seidel, Nuray
from Izmir

Giessen 2018

From the Institute of Neuropathology

Director / Chairman: Prof. Dr. Till Acker

of the Faculty of Medicine of the Justus Liebig University Giessen

First Supervisor and Committee Member: Prof. Dr. Till Acker

Second Supervisor and Committee Member: Prof. Dr. Stefanie Dimmeler

Committee Members:

I declare that I have completed this dissertation single-handedly without the unauthorized help of a second party and only with the assistance acknowledged therein. I have appropriately acknowledged and referenced all text passages that are derived literally from or are based on the content of published or unpublished work of others, and all information that relates to verbal communications. I have abided by the principles of good scientific conduct laid down in the charter of the Justus Liebig University of Giessen in carrying out the investigations described in the dissertation.

Table of contents

Zusammenfassung....1
Summary....5
1 Introduction....8
1.1 The WHO classification and grading of central nervous system tumors....8
1.1.1 Molecular alterations in glioma pathogenesis....10
1.1.2 Transcriptional subtypes of glioblastoma....12
1.2 Tumor microenvironment....14
1.2.1 The brain tumor microenvironment....14
1.2.2 The hypoxic tumor microenvironment....15
1.2.2.1 Hypoxia inducible factors and the hypoxic response....17
1.2.2.2 HIF structure....17
1.2.2.3 The regulation of HIF-α....17
1.2.2.4 The functional role of HIF....20
1.2.2.5 The role of PDHs in tumors....22
1.2.2.5.1 Regulation of PHD activity....24
1.2.2.5.2 PHD regulated HIF-independent signaling pathways....26
1.2.3 Cancer stem cells in glioblastoma....28
1.3 Metabolic reprogramming in cancer....31
1.3.1 2-OG and 2-OG dependent dioxygenases....33
1.3.1.1 Antitumorigenic activity of 2-OG....36
1.3.2 The function of isocitrate dehydrogenases (IDHs)....38
1.3.2.1 IDH mutations and 2-Hydroxglutarate (2-HG)....42
1.3.3 pH regulation and acidic tumor microenvironment....46
1.4 Angiogenesis and anti-angiogenic therapy in brain tumors....48
1.4.1 Eph receptors and ephrin ligands....51
1.4.1.1 Eph-ephrin signaling in tumors....54
1.5 Mesenchymal transition in gliomas....56
1.5.1 EMT regulators....57
1.5.2 Signaling pathways involved in EMT....58
2 Aim of the thesis project....61
3 Materials and methods....62
3.1 Materials....62
3.1.1 Chemicals....62

3.1.2 Antibiotics 62
3.1.3 Antibodies 63
3.1.3.1 Primary antibodies 63
3.1.3.2 Secondary antibodies 64
3.1.4 Protein and DNA ladders 65
3.1.4.1 Protein ladder 65
3.1.4.2 DNA ladders 65
3.1.5 Bacterial strains 65
3.1.6 Cell lines 65
3.1.6.1 Cells generated during the PhD thesis 66
3.1.7 Plasmids 68
3.1.8 Primers 70
3.1.9 siRNA Oligos 71
3.1.10 Media, buffers and other reagents 72
3.1.10.1 Animal experiments 72
3.1.10.2 Bacterial cultures 73
3.1.10.3 Cell Culture 73
3.1.11 Nucleic acid isolation 75
3.1.12 Stainings (FACS, IHC, IF,) 75
3.1.13 Western Blotting 76
3.2 Methods 78
3.2.1 Working with RNA 78
3.2.1.1 RNA extraction 78
3.2.1.2 Reverse transcription 78
3.2.1.3 Microarray analysis 79
3.2.2 Working with DNA 80
3.2.2.1 Bacterial transformation 80
3.2.2.2 Plasmid isolation 80
3.2.2.3 Restriction digestion 80
3.2.2.4 Ligation and recombination 81
3.2.2.5 Agarose gel electrophoresis 81
3.2.2.6 Gel extraction of DNA fragments from agarose gels 82
3.2.2.7 Determination of DNA concentrations 82
3.2.2.8 Quantitative real time polymerase chain reaction (qPCR) 82
3.2.2.9 Sequencing 83
3.2.3 Working with proteins 83

3.2.3.1 Protein extraction 83
3.2.3.2 Nuclear and cytoplasmic protein extraction 84
3.2.3.3 Determination of protein concentration 84
3.2.3.4 SDS-PAGE (Sodium Dodecyl Sulfate Poly Acrylamide Gel Electrophoresis) 85
3.2.3.5 Stripping the western blot membranes 86
3.2.4 Cell culture 86
3.2.4.1 Isolation of primary glioblastoma cells from human tumor samples 86
3.2.4.2 Cell culture conditions and subculturing of primary glioblastoma cells 86
3.2.4.3 Cryopreservation of cells 87
3.2.4.4 Determining the cell number 88
3.2.4.5 Transient transfection 88
3.2.4.6 siRNA transfection 89
3.2.4.7 Production of lentiviruses in 293T cells using calcium phosphate transfection method 89
3.2.4.8 Titration of lentiviral particles 91
3.2.4.9 Lentiviral transduction of cells 92
3.2.4.10 Stable transduction of primary glioblastoma cells 92
3.2.4.11 Stable transduction of cell lines 92
3.2.4.12 Creating knock-out cells 92
3.2.4.13 Hypoxic incubation of cells 93
3.2.4.14 Physiological (pH7.4) and acidic (pH6.7) pH treatment of the cells 93
3.2.4.15 TGFβ, TNFα, 2-OG and FBS treatments of cells 94
3.2.4.16 Sphere formation assay 94
3.2.4.17 Flow cytometry (FACS, Fluorescence activated cell sorting) 95
3.2.4.18 Modified Boyden Chamber assay 95
3.2.4.19 Collagen invasion assay 96
3.2.4.20 Colony formation 96
3.2.4.21 High-performance liquid chromatography-mass spectrometry (HPLC-MS) 97
3.2.4.22 Luciferase assay 97
3.2.5 *In vivo* tumor models 98
3.2.5.1 Intracranial tumor xenograft models 98
3.2.5.2 Subcutaneous xenograft models 99
3.2.5.3 Tumor xenograft model of breast cancer 99
3.2.5.4 Perfusion and tissue preparation 99
3.2.5.5 Quantification of tumor volume and hematoxylin and eosin (HE) staining 100

3.2.5.6 Analysis of invasiveness of xenograft tumors 101
3.2.6 Immunofluorescence and immunohistochemistry stainings 101
3.2.6.1 p65 staining of the cells 101
3.2.6.2 Endomucin staining 102
3.2.6.3 Human nuclei staining 103
3.2.6.4 HIF-1α staining and Hypoxyprobe detection 103
3.2.7 Analysis of patient survival data 103
3.2.8 Statistical analysis 103
4 Results 104
4.1 The impact of 2-OG regulation on glioblastoma and other tumor entities 104
4.1.1 Regulation of 2-OG levels and PHD function by IDH1 104
4.1.1.1 The role of IDH1 in the regulation of the hypoxic response 104
4.1.1.2 Enhanced activation of the NF-κB pathway upon IDH1 silencing 111
4.1.1.3 IDH1 overexpression decreases HIF-α levels and impairs expression of HIF and NF-κB target genes 113
4.1.2 IDH1 knock-down promotes a cancer stem cell (CSC) phenotype 115
4.1.3 Silencing of IDH1 mediates mesenchymal transition in GBM 120
4.1.3.1 Increased expression of Snail and CD44 levels by IDH1 silencing 120
4.1.3.2 IDH1 knock-down elevates the invasive capacity of GBM cells 122
4.1.3.3 HIF-1/2α silencing reverts the Snail upregulation elicited by IDH1 knock-down 123
4.1.4 Microenvironmental signals downregulate IDH1 125
4.1.5 IDH1 level is associated with tumor growth and invasion 126
4.1.6 IDH1 silencing enhances HIF-α and Snail expression levels in breast and lung carcinoma cell lines 129
4.2 An acidosis induced HSP90-HIF-α axis and the cancer stem cell phenotype 131
4.2.1 Acidosis-induced HIF activation and CSC maintenance 131
4.2.1.1 Acidosis controls HIF function through HSP90 *in vitro* and *in vivo* 134
4.2.2 High HSP90 expression in the hypoxic CSC niche 137
4.3 The hypoxia regulated HIF-1α-ZEB2-ephrinB2 axis controls tumor invasion and anti-angiogenic resistance 139
4.3.1 Hypoxia increases invasion through downregulation of ephrinB2 139
4.3.2 Decreased ephrinB2 levels are associated with increased tumor invasiveness and resistance to antiangiogenic treatment 142
5 Discussion 145
5.1 Impaired 2-OG levels controlled by IDH1 elevate the hypoxic response and the invasive/metastatic tumor phenotype 146

5.1.1 IDH1 silencing-mediated 2-OG decrease enhances the hypoxic response in a PHD dependent manner 147
5.1.2 Activation of PHD-controlled HIF-α-independent NF-κB signaling in IDH1 silenced cells 151
5.1.3 The potential role of 2-OG for the maintenance of the cancer stem cell phenotype 153
5.1.4 Metabolic control of mesenchymal transition in glioblastoma 154
5.1.5 Microenvironmental regulation of IDH1 157
5.1.6 The role of IDH1 and 2-OG in tumor growth and progression 160
5.2 Acidosis promotes HIF function and cancer stem cell maintenance through HSP90 162
5.2.1 HIF dependent induction of the CSC phenotype under acidic stress 163
5.2.2 HSP90 controlled HIF function under acidic conditions 165
5.2.3 Targeting the hypoxic CSC niche through HSP90 inhbition 167
5.3 Hypoxia mediates an invasive phenotype and anti-angiogenic therapy resistance through the activation of a HIF-1α-ZEB2-ephrinB2 axis 168
5.3.1 Hypoxia induces invasion and downregulates ephrinB2 168
5.3.2 Loss of ephrinB2 is associated with an invasive tumor phenotype 170
6 Bibliography 172
7 List of figures and tables 208
7.1 List of figures 208
7.2 List of tables 209
8 Abbreviations 210
9 Publications based on the work presented in this dissertation 215
10 Acknowledgments 216

Zusammenfassung

Tumorerkrankungen sind, nach Erkrankungen des Herz-Kreislaufsystems, die häufigste Todesursache weltweit. Unter den Tumoren des zentralen Nervensystems ist das Glioblastoma multiforme die häufigste und aggressivste Tumorentität. Trotz neuentwickelter, multimodaler Therapieansätze und einem besseren Verständnis der molekularen Mechanismen, die der Tumorentstehung zugrunde liegen, bleibt die mittlere Überlebenszeit von Glioblastompatienten mit etwa 15 Monaten seit Jahrzehnten nahezu gleich. Zwei charakteristische Eigenschaften des Mikromillieus im Glioblastom sind die Existenz nekrotischer Bereiche, sowie eine dysfunktionale Gefäßstruktur, die zu Tumorbereichen mit reduzierter Sauerstoffversorgung (Hypoxie) führen. Tumorhypoxie steht in Zusammenhang mit verschiedenen Schlüsselcharakteristiken von Tumorerkrankungen (Hallmarks of Cancer) wie der Adaption des Stoffwechsels, Angiogenese, tumorassoziierte Entzündungsreaktionen, Invasion und Metastasierung. Die Haupteffektoren der zellulären Adaption an Hypoxie sind die hypoxie-induzierten Transkriptionsfaktoren (HIF-1α und HIF-2α), deren Stabilität mittels Hydroxylierung durch Prolylhydroxylasen (PHDs) reguliert wird. Diese PHDs benötigen Sauerstoff und 2-Oxoglutarat (2-OG) als Co-Substrat, um spezifische Prolylreste zu hydroxylieren, was zur Degradation von HIF-α unter Normoxie führt. Unter Hypoxie ist die Aktivität der PHDs inhibiert, was mit einer Stabilisierung von HIF-α einhergeht. Die Aktivierung der Hypoxie Antwort erfolgt indes nicht ausschließlich durch reduzierte Sauerstoffkonzentrationen, sondern kann auch durch die Akkumulation des Onkometaboliten 2-Hydroxyglutarat, dass die Aktivität von PHDs beeinflussen kann, begünstigt werden. Die Identifikation und Charakterisierung pro-onkogener Mutationen, die zur Anreicherung dieses Onkometaboliten, der als 2-Oxoglutarat Analogon dient, unterstreicht die zentrale Rolle, die 2-OG in der Regulation zellulärer Prozesse einnimmt.

Hierauf gründet unsere Hypothese, dass Isocitrat-Dehydrogenase, ein Enzym, das Isocitrat zu 2-OG konvertiert, eine zentrale Rolle in der Aufrechterhaltung der 2-OG Level, und damit der Regulation von 2-OG abhängiger Enzymaktivität, spielt.

Tatsächlich zeigen unsere Ergebnisse, dass ein knock-down von IDH1 zu einer Reduktion adäquater 2-OG Level führt, was mit einer Aktivierung der Hypoxie-Antwort einhergeht. Weiterhin konnten wir anhand verminderter HIF-α-Hydroxylierung zeigen, dass diese Aktivierung des Hypoxie-Response auf einer verminderten Aktivität der 2-OG abhängigen PHDs basiert. Um diese Ergebnisse weiter zu untermauern und eine direkte Abhängigkeit dieser Prozesse von 2-Oxoglutarat zu verifizieren, wurden IDH1 knock-down Zellen mit einer zellpermeablen Variante von 2-OG behandelt. Tatsächlich unterdrückte die Zugabe von 2-OG die, durch den IDH1 knock-down bedingte, Aktivierung der Hypoxie-Antwort. Da diese Ergebnisse eindeutig belegen, dass IDH1-abhängige Veränderungen der 2-OG Level die Aktivität von PHDs regulieren, interessierte uns, ob der knock-down von IDH1 auch weitere PHD-regulierte Signalwege wie den NF-κB Signalweg beeinflusst. In Übereinstimmung mit unseren vorherigen Ergebnissen konnten wir zeigen, dass eine IDH1 knock-down abhängige Inaktivierung der PHDs auch zu einer vermehrten Translokation von NF-κB in den Zellkern, und damit einhergehend einer Aktivierung von NF-κB Zielgenen, führte. Zusätzlich zu diesen Ergebnissen konnten wir zeigen, dass der Tumorstammzellphänotyp, der eng mit der Aktivierung des Hypoxie-Response verknüpft ist, durch IDH1 Silencing erhöht, und anschließend mittels 2-OG Behandlung rückgängig gemacht werden konnte. Interessanterweise konnten wir zudem zeigen, dass anomale 2-OG Level Invasion und die Expression von Snail, einem Schlüsselfaktor der mesenchymalen Transition, der eine wichtige Rolle in der Regulation der Tumorinvasion spielt, modulieren. In Übereinstimmung mit unseren zellkulturbasierten *in vitro* Daten konnten wir die Schlüsselrolle, die IDH1 für die Tumorprogression spielt, auch in *in vivo* Experimenten verifizieren. Im Tumormodell zeigte sich, dass IDH1 knock-down, ebenso wie im Zellkulturexperiment, eine bedeutende Rolle für die Regulation von Tumorinvasion, der Aktivierung der HIF-α und NF-κB Signalwege, sowie des Tumorstammzellphänotyps spielt. Weiterhin konnten wir TGFβ, einen Aktivator der mesenchymalen Transition, als einen IDH1 Regulator identifizieren. Bemerkenswerterweise führte ein IDH1 knock-down in Brust- und Lungenkarzinomen, Tumorentitäten, bei denen sich bildende Metastasen die häufigste Todesursache darstellen, zu ähnlichen molekularen Adaptionen wie der

Aktivierung des HIF-α-Signalweges, oder der erhöhten Expression von Snail, führte. Am interessantesten jedoch war, dass IDH1 knock-down im *in vivo* Tiermodell zu erhöhter Metastasierung der Primärtumore führte.

Zusätzlich zur Akkumulation tumorzellintrinsischer Adaptionen verändern Tumore aktiv das Tumormikromillieu, was mit einer Akquisition weiterer Hallmarks of Cancer und einer erhöhten Tumorprogression einhergeht. Eine typische Folge der Tumorstoffwechseladaption unter Hypoxie ist die Azidifizierung des Tumormikromillieus. Aus diesem Grund haben wir uns im zweiten Teil dieser Arbeit mit molekularen Mechanismen, und deren Einfluss auf die Tumorprogression, beschäftigt, die synergistisch durch Azidose und Hypoxie reguliert werden. Unsere Ergebnisse zeigen, dass ein azidisches Tumormikromillieu die Hypoxieantwort von Tumorzellen potenziert und den Tumorstammzellphänotyp reguliert, was auf eine Rolle der Tumorazidose für Tumorinitiierung und Therapie-Resistenz schließen lässt. Mechanistisch zeigen unsere Ergebnisse, dass Azidose die Hypoxieantwort der Zellen über das Heat Shock Protein 90 (HSP90) aktiviert. Hierbei führte die Inaktivierung oder der knock-down von HSP90 unter azidischen Bedingungen zu verminderter Tumorhypoxie und Tumorwachstum. Übereinstimmend mit diesen Ergebnissen konnten wir in Patientenbiopsien zeigen, dass die Expressionslevel von HSP90 positiv mit denen von Hypoxie- und Tumorstammzellmarkern korrelieren.

Unter den Hallmarks of Cancer, die durch Hypoxie reguliert werde, findet sich neben der Tumorinvasion vor allem die Aktivierung der Tumorangiogenese. Im dritten Teil dieser Arbeit konzentrierten wir uns auf die hypoxieregulierten Mechanismen, die Tumorangiogenese, und damit das Tumorwachstum positiv beeinflussen. Wir konnten zeigen, dass Tumorhypoxie, die auch durch die therapeutische Inhibition von Tumorangiogenese hervorgerufen werden kann, zu einer Herunterregulierung des Zelladhäsionsmoleküls ephrinB2, und daraus resultierend einer lokalen Verstärkung der Tumorinvasion führte. Mechanistisch zeigten unsere Ergebnisse, dass die Reduktion der ephrinB2 Expression direkt durch das HIF-1α Zielgen ZEB2 kontrolliert wird, was erstmals die Existenz einer HIF-1α-ZEB2-ephrinB2 Achse im Glioblastom

beweist, die Tumorinvasion, auch vermittelt durch anti-angiogene Therapeutika, kontrolliert.

Fasst man die Ergebnisse dieser Arbeit zusammen, konnten wir eine zentrale Rolle des Metabolits 2-Oxoglutarat für die Kontrolle der PDH Aktivität und damit der Hypoxieantwort, sowie der durch diese regulierten Mechanismen und Tumorcharakteristika wie Tumorstammzellhomöostase, Invasion und Metastasierung, identifizieren. Weiterhin konnten wir neue Mechanismen entschlüsseln über die eine HIF-1α-ZEB2-ephrinB2 Achse Tumorinvasion, sowie Tumorazidose mittels HSP90 den Tumorstammzellphänotyp reguliert. Unsere Ergebnisse unterstreichen die zentrale Rolle, die Tumorhypoxie für die Regulation von Schlüsselmechanismen des Tumorwachstums spielt und offenbaren hierdurch potenzielle Ziele neuer Therapiestrategien.

Summary

Cancer is one of the leading causes of death worldwide. Among central nervous system tumors, glioblastoma is the most common and most aggressive tumor entity. Despite new therapeutic strategies and a better understanding of the molecular mechanisms leading to tumorigenesis, the median glioblastoma patient survival is only 15 months.

A hypoxic tumor microenvironment is one of the characteristics of glioblastoma and tumor hypoxia has been linked to multiple hallmarks of cancer, including tumor promoting inflammation, metabolic reprogramming, angiogenesis, invasion and metastasis. The main effectors of the cellular response to hypoxia are the hypoxia-inducible transcription factors (HIFs), whose stability is tightly regulated through hydroxylation by the prolyl hydroxylase domain proteins (PHDs). The latter require oxygen and 2-oxoglutarate (2-OG) as co-substrates to hydroxylate specific residues within HIF-α, which eventually leads to HIF-α degradation under normoxia. Under hypoxia, PHDs are inactive and HIF-α is stabilized. Activation of the hypoxic response is not only mediated by hypoxia, but also by the accumulation of the oncometabolite 2-hydroxyglutarate, which can modulate PHD activity. Identification and characterization of oncogenic mutations leading to the accumulation of oncometabolites acting as 2-oxoglutarate (2-OG) analogs, showed the central role of 2-OG in the regulation of cellular responses. We therefore hypothesized that isocitrate dehydrogenases (IDHs), which convert isocitrate to 2-OG, might play a central role in the maintenance of 2-OG levels and hence the regulation of 2-OG dependent enzyme activity. In line with this hypothesis, we show that IDH1 knock-down results in reduction of 2-OG levels, accompanied by the activation of the hypoxic response as a direct result of PHD inhibition, evidenced by reduced HIF-α hydroxylation. In order to directly demonstrate the involvement of 2-OG in this process, we treated IDH1 knock-down cells with cell permeable 2-OG. Importantly, addition of 2-OG suppressed the IDH1 knock-down-mediated increase of HIF-α levels and HIF-α target gene expression. Since these findings demonstrated that IDH1-dependent changes in 2-

OG control PHD activity, we examined if IDH1 silencing also influences other PHD-regulated signaling pathways, such as NF-κB signaling. In line with our previous findings, IDH1 silencing-mediated PHD inactivation led to increased NF-κB nuclear translocation and activation of NF-κB downstream targets. Additionally, we demonstrated that the cancer stem cell (CSC) phenotype, which has been closely linked to HIF-α activation, is also enhanced by IDH1 silencing and reverted by 2-OG treatment. Importantly, we could show that aberrant 2-OG levels also modulate invasion and the expression of Snail, a key regulator of mesenchymal transition, which plays a crucial role in the control of tumor invasion. In line with the cell culture-based data, our *in vivo* experiments verified the effects of IDH1 silencing on the induction of invasive characteristics, as well as activation of HIF-α and NF-κB signaling and the stem cell phenotype in tumors. Additionally, we identified TGFβ, an inducer of mesenchymal transition, as a regulator of IDH1. Strikingly, in breast and lung cancer cells, tumor types in which metastasis is the primary cause of death, IDH1 silencing induced similar molecular changes, including activation of HIF-α signaling and increased expression of Snail. Most importantly, IDH1 silencing in this context resulted in increased metastasis.

In addition to accumulating cancer cell-intrinsic changes, tumors reshape their own microenvironment, contributing to the acquisition of cancer hallmarks and tumor progression. One typical consequence of metabolic reprogramming under hypoxia is acidification of the tumor microenvironment. Therefore, in a second part of this work, we aimed to understand the molecular mechanisms controlled by the combination of acidosis and hypoxia in the tumor microenvironment, and its effect on tumorigenesis. We show that an acidic tumor microenvironment promotes the CSC phenotype and even further potentiates the hypoxic response, suggesting a role for acidosis in tumorigenesis and tumor therapy resistance. We revealed that acidosis controls HIF-α function through heat shock protein 90 (HSP90). Strikingly, absence or inactivation of HSP90 under acidic conditions reduced tumor initiation, tumor hypoxia and tumor growth. Importantly, we found that HSP90 levels correlate with hypoxic and stem cell marker genes in glioblastoma patients.

Among the cancer hallmarks that are regulated by hypoxia, are the activation of invasion and the induction of angiogenesis. In the third part of this work, we focused on hypoxia-dependent mechanisms that regulate these capabilities. We show that hypoxia, which can be promoted by inhibition of angiogenesis, induces local glioma invasion and downregulates the cell adhesion molecule ephrinB2. Importantly, we reveal that ephrinB2 downregulation is directly controlled by ZEB2, a target of HIF-1α, establishing a critical role of a HIF-1α-ZEB2-EphrinB2 axis in glioma invasion, including invasion induced by anti-angiogenic agents. Notably, absence of ephrinB2 increased tumor invasiveness, whereas ephrinB2 overexpression decreased it, revealing a crucial function of ephrinB2 in the control of the invasive capacity of gliomas.

Taken together, our results demonstrate the pivotal role of 2-OG for the control of PHD activity, the hypoxic response and downstream biological processes, such as CSC maintenance, invasion and metastasis. Additionally, we also revealed distinct molecular mechanisms through which hypoxia regulates cancer hallmarks, namely enhancing tumor invasion via a HIF-1α-ZEB2-EphrinB2 axis, or synergizing with acidosis to control the CSC phenotype and tumor growth through HSP90. These findings identify several mechanisms, centered around the control of hypoxic signaling in tumors, which regulate cancer hallmarks and may provide targets for future therapeutic strategies.

1 Introduction

Brain tumors consist of cells that originate from different cell lineages and grow abnormally in the brain and/or spinal cord. The World Health Organization (WHO) established a classification and grading system for benign and malignant brain tumors, which is accepted and used worldwide (Louis et al., 2016). The estimated brain tumor incidence in Europe in 2012 was 6.6 cases per 100000 with a higher incidence rate in men (7.8 cases per 100000) compared to women (5.6 cases per 100000) (Ferlay et al., 2013).

The most common and most aggressive malignant brain and central nervous system tumor is glioblastoma followed by diffuse astrocytomas. Glioblastomas represent 15.1% of all brain and central nervous system tumors and account for 46.1% of primary malignant brain tumors, exhibiting an increased frequency rate with patient age (Ostrom et al., 2015). The median survival of patients diagnosed with glioblastoma is between 12 to 15 months, and only 5% of the patients survive longer than 5 years (Gallego, 2015, Global Burden of Disease Cancer, 2015, Ostrom, et al., 2015, Young et al., 2015).

1.1 The WHO classification and grading of central nervous system tumors

According to the recent WHO classification of brain tumors, glioblastoma is included in the group of diffuse gliomas along with astrocytic tumors, oligodendrogliomas and diffuse gliomas of the childhood (Louis, et al., 2016). Previously, in the 2007 WHO classification, the astrocytic and oligodendroglial gliomas were grouped separately. Unlike the 2007 version, the 2016 WHO classification provides a combination of phenotypic and genotypic classification of the tumors. Tumors with similar growth pattern, behaviors and shared genetic driver mutations, such as mutations in the isocitrate dehydrogenase (IDH) gene, are grouped together. The 2016 WHO

classification is based on a combination of histological and molecular features of the tumors and leads to a better definition of the tumor entities (Table 1.1) (Louis et al., 2007, Louis, et al., 2016).

Depending on tumor malignancy, the WHO grading system categorizes astrocytomas from grade I to IV, as an indicator of therapy response and patient outcome (Louis, et al., 2007). Grade I tumors, such as pilocytic astrocytomas and subependymal giant cell astrocytomas, consist of slow-proliferating cells, are nonmalignant and can in general be successfully cured by surgical resection. Grade II tumors are infiltrative and slow-growing, but often recur as higher grade tumors. IDH-mutant diffuse astrocytoma, IDH-mutant and 1p/19q-codeleted oligodendrogliomas and pleomorphic xanthoastrocytoma are classified as grade II. Anaplastic oligodendrogliomas and anaplastic astrocytomas are classified as grade III. These tumors are characterized by a high mitotic activity and anaplasia and are highly malignant tumors. Moreover, the WHO defines the highly infiltrative astrocytic tumors with high mitotic activity and tumors displaying high malignancy, endothelial cell proliferation, necrosis or perinecrotic areas as grade IV (Louis, et al., 2007, Louis, et al., 2016). Grade IV tumors such as glioblastoma and diffuse midline glioma grow rapidly and a combination of surgical resection, chemo and/or radio therapy still remains insufficient to eradicate all tumor cells, leading to frequent recurrence of these tumors. Patients diagnosed with a grade II tumor frequently survive longer than 5 years, whereas patients with a grade IV tumor typically have a median survival of 15 months (Stupp et al., 2005, Gallego, 2015, Rahman et al., 2015). However, glioblastoma patients with a mutation in the IDH1 gene and/or silenced O^6-alkylguanine DNA alkyltransferase (MGMT) due to promoter methylation, show prolonged survival rates (Louis, et al., 2007, Louis, et al., 2016).

Table 1.1. Examples of gliomas according to the 2016 WHO classification of central nervous system tumors (Louis, et al., 2016).

WHO Grade	Tumor Type
I	Pilocytic astrocytoma Subependymal giant cell astrocytoma
II	Diffuse astrocytoma Oligodendrogliomas Pleomorphic xanthoastrocytoma
III	Anaplastic oligodendrogliomas Anaplastic astrocytoma Anaplastic pleomorphic xanthoastrocytoma
IV	Glioblastoma Diffuse midline glioma

1.1.1 Molecular alterations in glioma pathogenesis

Glioblastomas can be classified as primary and secondary glioblastomas depending on their pathological development. The majority of glioblastomas arise *de novo* without any identified precursor lesion and are defined as primary glioblastoma. Secondary glioblastomas arise from initially lower grade gliomas such as diffuse astrocytomas or anaplastic astrocytomas (Fig. 1.1) (Ohgaki and Kleihues, 2013, Wilson et al., 2014). Around 90% of glioblastomas are primary glioblastomas. The incidence of primary glioblastoma is higher in elderly patients (>50 years old), whereas secondary glioblastoma develop in younger patients with a mean age of 45. The incidence rate of primary glioblastoma is 1.3 to 1.5 times higher in men compared to women (Phillips et al., 2006, Ohgaki and Kleihues, 2013).

Comprehensive genomic analysis of glioblastoma samples revealed that at least one component within three main pathways, RTK signaling, p53 and RB tumor-suppressor pathway, is altered during tumorigenesis (Cancer Genome Atlas Research, 2008). However, primary and secondary glioblastomas carry distinct genetic alterations (Fig. 1.1), indicating that they are derived from different genetic precursors. The common alterations in primary glioblastoma are EGFR amplification, PTEN mutation and loss of chromosome 10, whereas IDH1/2 mutations, TP53 mutations and 19q loss are more common in secondary glioblastoma. Although primary and secondary

glioblastomas exhibit a different molecular profile, identification and characterization of IDH1/2 mutation and its exclusive presence in secondary glioblastoma has allowed reliable differentiation of primary and secondary glioblastoma (Ohgaki and Kleihues, 2013, Wilson, et al., 2014). Eventually, in the recent 2016 WHO classification of central nervous system tumors, the IDH mutation status is described as the primary criteria to differentiate secondary glioblastoma from primary glioblastoma (Louis, et al., 2016).

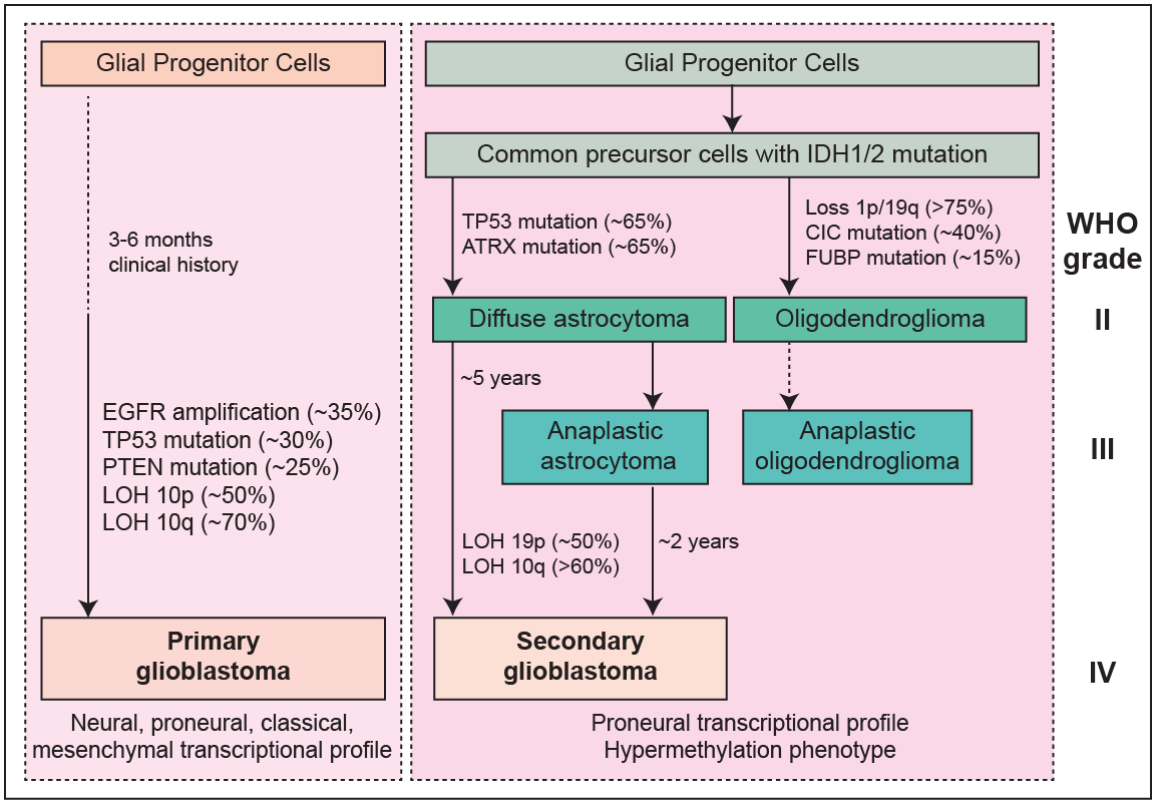

Figure 1.1. Summary of most frequent molecular abnormalities found in primary and secondary glioblastomas.
Redrawn from Ohgaki and Kleihues 2013.(Ohgaki and Kleihues, 2013).

Identification of exclusive alterations in glioblastoma or in lower grade glioma types has allowed some of them to be used as clinically relevant molecular markers. Some of these alterations such as IDH mutation, loss of 1p/19q, ATRX mutation and MGMT promotor methylation have become important molecular markers as they provide diagnostic, prognostic and predictive information (Ohgaki and Kleihues, 2013, Nicolaidis, 2015, Louis, et al., 2016). IDH mutations are associated with a better

prognosis and patients with an IDH mutation are significantly younger with a mean age of 32-41 than patients with wild-type IDH. A mutation in the 2-oxoglutarate (2-OG) producing enzyme IDH leads to a reduced activity of IDH and, importantly, the production of 2-hydroxyglutarate, an oncometabolite. (Crespo et al., 2015, Louis, et al., 2016). It is therefore considered to be a gain-of-function.

The combination of loss of 1p/19q and IDH1 mutation has been clinically used to identify oligodendrogliomas. Patients with 1p/19q loss showed longer survival after genotoxic or adjuvant therapy (Huse and Aldape, 2014). ATRX mutation together with TP53 and IDH1 mutation is a specific marker for diffuse astrocytoma and anaplastic astrocytoma that are grade II and III tumors with better prognosis (Louis, et al., 2016). Silencing of the MGMT gene by hypermethylation of its promotor is associated with prolonged survival of the patients. Patients with MGMT promotor hypermethylation exhibit better response to chemotherapy, as the cells cannot repair the therapy-induced DNA damage, leading to cell death (Crespo, et al., 2015).

1.1.2 Transcriptional subtypes of glioblastoma

Recently, efforts have been made to provide more insight into the gene expression pattern of different glioma subtypes. Comparison of high grade versus low grade gliomas or primary versus secondary glioblastomas, identified differentially expressed genes, indicating distinct transcriptional signatures of these subtypes (Karcher et al., 2006, Tso et al., 2006a, Tso et al., 2006b, Vital et al., 2010). In addition to these studies, genetic alterations and gene expression profiling studies led to a division of glioblastomas (as defined in the 2007 WHO classification) into four subclasses: proneural, neural, classical and mesenchymal (Phillips, et al., 2006, Verhaak et al., 2010).

Glioblastomas with a proneural signature express genes related to an oligodendrocytic signature. The proneural subclass is characterized by PDGFRA alteration, IDH1 mutation, TP53 mutation and loss of heterozygosity. Furthermore, the proneural phenotype is associated with secondary glioblastomas and lower grade

gliomas and shares a gene profile with neural stem cell lines. As the majority of proneural glioblastomas are secondary glioblastomas, the proneural phenotype is associated with longer survival and diagnosed in younger patients (Phillips, et al., 2006, Verhaak, et al., 2010).

Tumors with a neural phenotype do not exhibit a distinctive gene expression profile. The gene expression pattern is similar to normal brain tissue with high expression of neuronal markers such as NEFL, GABRA1, SYT1 and SLC12A5 (Verhaak, et al., 2010).

Glioblastomas with a classical phenotype exhibit a profile associated with high proliferation and are frequently characterized by chromosome 7 amplification paired with chromosome 10 loss and EGFR amplification. Additionally, the tumors with classical phenotype lack TP53, NF1 and IDH1 mutations (Phillips, et al., 2006, Verhaak, et al., 2010).

The mesenchymal subtype expresses higher levels of mesenchymal and astrocytic markers, such as CD44, MERTK, YKL40 and MET. Loss, or lower expression of NF1 frequently occurs in this subtype. In addition, altered tumor necrosis factor family and NF-κB signaling pathways are commonly seen in the mesenchymal subtype (Phillips, et al., 2006, Verhaak, et al., 2010). Interestingly, Phillips et al. showed that recurrent tumors shift their phenotype to a mesenchymal phenotype (Phillips, et al., 2006) and Verhaak et al. showed that the majority of immortalized cell lines resemble the mesenchymal phenotype (Verhaak, et al., 2010).

The gene expression based molecular classification of tumors highlights the importance of genomic sequence and transcriptional analysis. The diversity of genetic alterations, leading to different subtypes of glioblastoma, proposes no effective single therapy approach. Further studies characterized diffuse gliomas even in more detail with the help of datasets available from The Cancer Genome Atlas (TCGA) (Brennan et al., 2013, Frattini et al., 2013, Cancer Genome Atlas Research et al., 2015, Ceccarelli et al., 2016) and identified the association between prognosis and genetic alteration, gene expression and DNA methylation pattern, defining new subtypes of gliomas (Noushmehr et al., 2010, Sturm et al., 2012).

1.2 Tumor microenvironment

Tumors consist not only of tumor cells, but also of a variety of different stromal cells such as endothelial and inflammatory cells. The tumor microenvironment contains cells, signaling molecules, soluble factors, chemokines, extracellular matrix proteins and mechanical cues, which facilitate tumor growth, progression, invasion and therapy resistance (Fig. 1.2). The tumor microenvironment supports tumor cells by providing proliferative and proinvasive signals, inducing angiogenesis, reprogramming energy metabolism and protecting the tumor cells from immune cells. Therefore, careful analysis and targeting of the supportive tumor microenvironment may be necessary to provide effective treatments (Hanahan and Weinberg, 2011, Balkwill et al., 2012, Hanahan and Coussens, 2012) .

1.2.1 The brain tumor microenvironment

Tumor cells not only display heterogeneity at the gene expression and genetic alteration level, but also reside in different microenvironments and interact with different cell types (Balkwill, et al., 2012, Charles et al., 2012, Lorger, 2012). Genetic instability of tumor cells and local distribution of environmental factors such as hypoxia, starvation, acidosis, oxidative stress, biomechanical stress and therapeutic interventions create this heterogeneity. Microenvironmental signals and environmental factors in turn influence the tumor progression and patient prognosis (Charles, et al., 2012, Kucharzewska and Belting, 2013). The tumor microenvironment is organ-specific and has a complex role. The brain is a highly vascularized organ and brain tumors possess a particular microenvironment with a broad variety of cell types such as endothelial cells, pericytes, astrocytes, neurons, microglia and tumor-associated macrophages. These cells and tumor cells themselves produce signaling molecules and growth factors, which, together with environmental cues, create the supportive tumor microenvironment (Fig. 1.2) (Hoelzinger et al., 2007, Charles, et al., 2012). For instance, TGFβ, which is produced by tumor cells, suppresses the

activation and proliferation of microglia, leading the repression of immune response to the tumor cells (Grauer et al., 2007, Hoelzinger, et al., 2007).

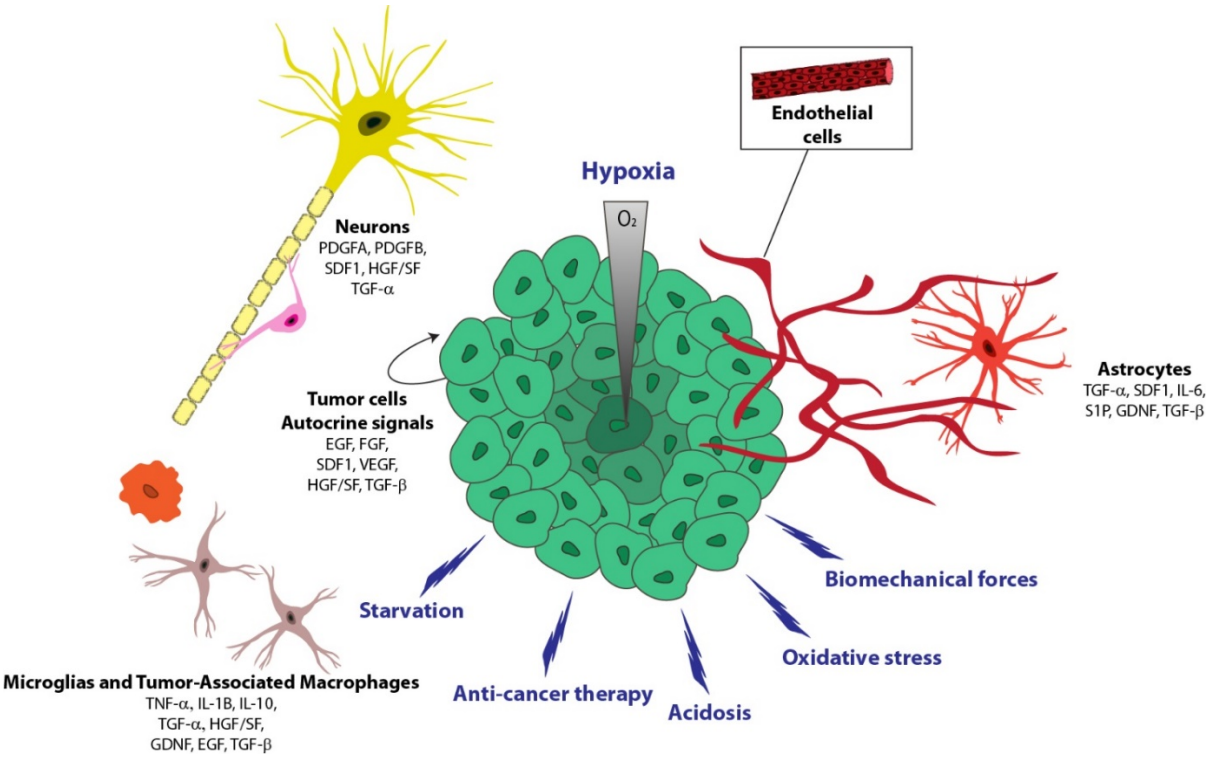

Figure 1.2. The tumor microenvironment in the brain.
Brain tumor cells interact with a variety of different stromal cells such as neurons, endothelial cells, pericytes, astrocytes, microglia and tumor-associated macrophages (TAM), releasing signaling molecules and cytokines. Tumor cells and stromal cells communicate and respond to the signaling molecules and cytokines that are produced. The rapid progression of the tumor itself generates environmental factors such as hypoxia, starvation, acidosis, oxidative stress, biomechanical stress through the limitation of nutrient/oxygen supply or accumulation of metabolic products.

1.2.2 The hypoxic tumor microenvironment

Tumor hypoxia is one of the characteristics of solid tumors and is associated with an aggressive tumor phenotype (Muz et al., 2015). Hypoxia occurs due to the imbalance between oxygen delivery and oxygen consumption. Rapid growth of the tumor mass creates areas with limited oxygen availability within the tumor. Oxygen levels in the tumor depend on the organ, as well as the size and the stage of the tumor. Oxygen levels in different organs vary widely (Emily G. Armitage et al., 2014, Muz, et al., 2015, Span and Bussink, 2015). The average oxygen concentration under physiological

conditions for the brain is 4.6%, for the breast 8.5%, for the lung 5.6%, whereas tumors of these organs show oxygen concentrations of as low as 1.7% O_2, 1.5% O_2, 2.2% O_2, respectively (Muz, et al., 2015).

Hypoxia can occur in two different forms: chronic (diffusion-limited) hypoxia and acute (perfusion-limited) hypoxia. Chronic hypoxia occurs when the tumor cells are beyond the diffusion capacity of oxygen leading to long-term cellular changes and genomic instability. The different periods of better and worse oxygenation of tumor areas cause the acute hypoxia which induces survival mechanisms in tumor cells by activating autophagy, apoptotic and metabolic adaptation. A mixture of chronic and acute hypoxia results in formation of hypoxic tumor areas (Muz, et al., 2015, Span and Bussink, 2015, Patel and Sant, 2016).

Hypoxia induces changes in the physicochemical characteristics of the tumor, in signaling pathways and in the behavior of TAMs (tumor associated macrophages) and other stromal cells. Hypoxia induced physicochemical changes include (1) acidic pH as a result of a metabolic shift towards glycolysis, (2) ROS generation which leads to genomic instability within the tumor and (3) intracellular and extracellular redox potential difference (Patel and Sant, 2016). Different signaling pathways are activated by hypoxia, which mostly result in tumor cell adaptation and survival under hypoxic stress. Hypoxic activation of the HIF (hypoxia inducible factor) signaling pathway is the most and best-studied pathway. Besides HIF, the UPR (unfolded protein response) pathway, the AKT-mTOR pathway, the ERK pathway and the NF-κB pathway are the other pathways that are activated by hypoxia (Span and Bussink, 2015, Patel and Sant, 2016). In addition to hypoxia, cytokines, chemokines and growth factors can also activate these pathways in a hypoxia independent manner. Hypoxia not only leads to changes in these pathways, but also leads to changes in the mRNA/miRNA expression profile, epigenetics and metabolism of the cells (Muz, et al., 2015, Span and Bussink, 2015). The contribution of hypoxia towards the metastatic phenotype, cancer stem cell phenotype and immunologic microenvironment has also become a great interest of many researchers (Muz, et al., 2015, Span and Bussink, 2015, Patel and Sant, 2016).

1.2.2.1 Hypoxia inducible factors and the hypoxic response

1.2.2.2 HIF structure

Hypoxic activation of the HIF pathway is the major mechanism mediating the adaptive responses to hypoxia through the regulation of transcription by HIF. HIF is a heterodimer, which consists of an α and a β subunit (Wang and Semenza, 1995). The β subunit is constitutively expressed. In contrast, the α subunit is oxygen-regulated and stabilized under hypoxic conditions (Li et al., 1996). Both subunits belong to the PAS subfamily of the basic Helix-Loop-Helix (bHLH) transcription factor family (Iyer et al., 1998). The bHLH-PAS motif is responsible for heterodimer formation between the α and β subunits and the binding to the hypoxia response element (HRE) within the promotor of the respective target genes (Semenza et al., 1991, Jiang et al., 1996, Jiang et al., 1997). HIF-α has three different isoforms, namely HIF-1α, HIF-2α and HIF-3α. Unlike HIF-3α, HIF-1α and HIF-2α show sequence similarity and both isoforms have two transactivation domains (TAD). The N-terminal (N-TAD) and C-terminal (C-TAD) TADs control HIF-α transcriptional activity by interacting with co-activators stabilizing HIF (Semenza, et al., 1991, Jiang, et al., 1996, Jiang, et al., 1997). Importantly, distinct from the β subunit, all α subunits have an oxygen-dependent degradation domain (ODD), which is important for the regulation of HIF-α stability in an oxygen-dependent manner (Wang and Semenza, 1995, Bruick and McKnight, 2001, Kaelin and Ratcliffe, 2008).

1.2.2.3 The regulation of HIF-α

HIF-α expression is regulated at the levels of transcription, translation and protein stability (Kallio et al., 1997, Gorlach et al., 2000, Dengler et al., 2014). Signaling pathways such as mTOR or the ERK pathway, which are activated by growth factors or cytokines, modulate the transcription or translation of HIF-α. MicroRNAs (miRNA) and mRNA destabilizing proteins can also decrease HIF-α levels (Dengler, et al., 2014). In addition, especially under hypoxic conditions, HIF-α protein stability and activity is regulated via post-translational modifications including hydroxylation, acetylation, sumoylation, ubiquitination and phosphorylation (Bruick and McKnight,

2001, Jeong et al., 2002, Bae et al., 2004, Keith et al., 2011). Besides the post-translational modifications, interaction of HIF-α with other proteins such as p53, SHARP1 and HSP90 (heat shock protein 90) also modulates HIF-α stability (Fig. 1.3) (Ravi et al., 2000, Isaacs et al., 2002, Montagner et al., 2012).

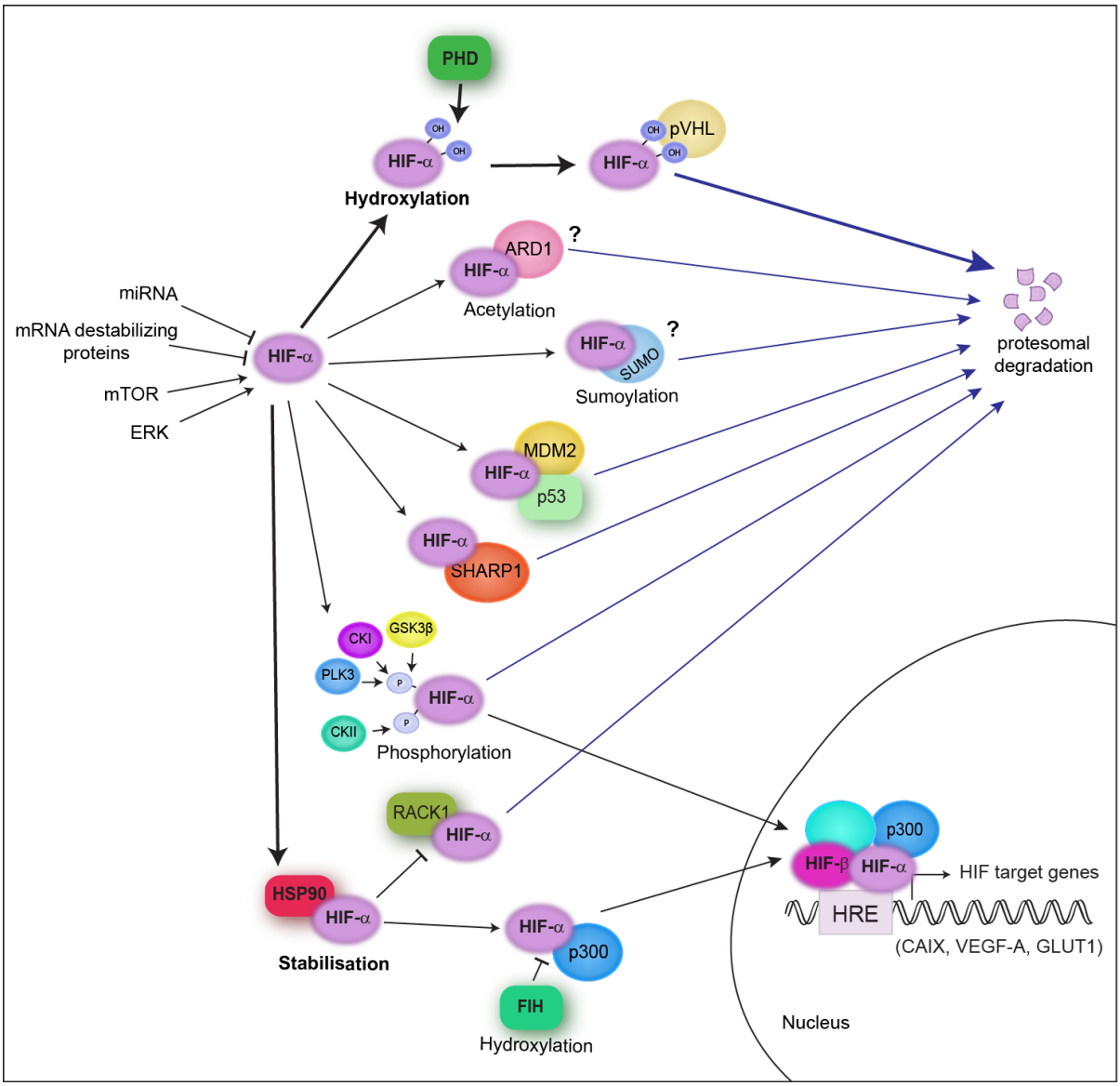

Figure 1.3. The regulation of HIF-α levels and transactivity.
Overview of pathways that involve in the HIF-α regulation at the different levels such as transcription, translation and post-translational modifications.

Under normoxia, HIF-α is hydroxylated on at least one of the two proline residues (at the positions 402 and 564 in HIF-1α and at the positions 405 and 531 in HIF-2α) within the ODD by oxygen-dependent prolyl hydroxylases (PHD1, PHD2 and PHD3),

allowing the recognition by the von Hippel-Lindau tumor-suppressor protein (pVHL). Interaction of HIF-α with pVHL recruits a E3 ubiquitin protein ligase for catalyzing HIF-α ubiquitination, thereby targeting HIF-α for proteasomal degradation (Fig. 1.3). PHDs require oxygen for their catalytic activity. Therefore, under hypoxia, absence of oxygen leads to diminished HIF-α hydroxylation, which prevents the interaction of HIF-α with pVHL, resulting in the accumulation of HIF-α in the nucleus (Iwai et al., 1999, Maxwell et al., 1999, Bruick and McKnight, 2001, Kaelin and Ratcliffe, 2008). Another oxygen-dependent hydroxylase named factor inhibiting HIF (FIH) is responsible for the negative regulation of the transcriptional activity of HIF-α by hydroxylation of the asparagine-803 residue. Under normoxia, hydroxylation at the asparagine-803 residue by FIH blocks the interaction between HIF-α and its co-activators CBP/p300 (Fig. 1.3) (Lando et al., 2002, McNeill et al., 2002).

The acetylation status is also critical for HIF-α stabilization. Depending on the location of the acetyl residues, acetylation has been shown to regulate HIF-α negatively or positively. Acetylation of Lys532 by the acetyl-transferase arrest defective 1 (ARD1) has been reported to lead to HIF-α destabilization (Fig. 1.3). By contrast, several other groups have failed to observe either ARD1 mediated HIF-α acetylation or interaction between ARD1 and HIF-α (Jeong, et al., 2002, Bilton et al., 2005, Murray-Rust et al., 2006). The role of ARD1 in HIF-α acetylation remains controversial. Additionally, deacetylases such as histone deacetylases (HDAC) and the family of sirtuins (SIRT1-7) also regulate HIF-α stability negatively or positively, depending on the HIF-α isoform and the acetylated residues (Dioum et al., 2009, Zhong et al., 2010, Geng et al., 2011). Another post-translational modification of HIF-α, whose role remains unclear, is sumoylation. Sumoylation has been reported to enhance or inhibit the HIF-α transactivation (Fig. 1.3) (Bae, et al., 2004, Berta et al., 2007).

Phosphorylation is another modification, which is crucial for HIF-α stability and activity. It has been reported that the different residues of HIF-α are directly phosphorylated by several different kinases. HIF-α phosphorylation mediated by casein kinase II (CKII), ERK and protein kinase A (PKA), leads to enhanced activation of HIF-α (Richard et al., 1999, Minet et al., 2000, Gradin et al., 2002). However,

phosphorylation of HIF-α by casein kinase I (CKI), glycogen synthase kinase 3β (GSK3β) and polo-like kinase 3 (PLK3) decreases the HIF-α stability or activity (Fig. 1.3) (Mottet et al., 2003, Kalousi et al., 2010, Xu et al., 2010a).

Elevated HIF-α levels are associated with loss of the p53 tumor-suppressor gene. Moreover, interaction between HIF-α and p53 leads to MDM2 mediated ubiquitination directing HIF-α to proteasomal degradation. Tumors with loss of p53 show increased tumor angiogenesis indicating activation of HIF-α target genes such as VEGFA. This mechanism shows that loss of p53 in the tumors contributes to enhanced transcriptional regulation by HIF-α (Ravi, et al., 2000, Roe and Youn, 2006). In addition, interaction between HIF-α and SHARP1 regulates HIF-α stability. SHARP1 binding to HIF-α promotes HIF-α proteasomal degradation in a pVHL independent manner resulting in suppression of invasive, metastatic and angiogenic capacity of the cells (Montagner, et al., 2012, Piccolo et al., 2013, Liao et al., 2014).

HSP90 and RACK1 are also involved in the mechanism controlling HIF-α stability in an oxygen independent manner. It has been reported that HSP90 and RACK1 compete to bind to the same site in the PAS domain of HIF-α. RACK1 binding recruits Elongin-C to HIF-α, resulting in HIF-α ubiquitination and proteasomal degradation, whereas HSP90 binding increases HIF-α stability and transactivity (Fig. 1.3) (Gradin et al., 1996, Katschinski et al., 2004, Liu et al., 2007). In addition, the HSP90 inhibitors geldanamycin and 17-allylaminogeldanamycin disrupt the HIF-α-HSP90 interaction leading to increased HIF-α proteasomal degradation (Isaacs, et al., 2002, Mabjeesh et al., 2002, Zagzag et al., 2003).

Altogether, these pathways demonstrate that a variety of physiological conditions are involved in HIF regulation and highlight the importance of the balance between HIF-α synthesis, stabilization and degradation.

1.2.2.4 The functional role of HIF

Oxygen-dependent or independent activation of HIF-1α and HIF-2α regulate a variety of target genes, which are involved in diverse biological processes including glycolysis, pH regulation, angiogenesis, metastasis/invasion, stemness/self-renewal,

proliferation and apoptosis (Fig. 1.4). HIF-α directly upregulates several glycolytic enzymes and transporters such as glucose transporters (GLUT1 and GLUT3), hexokinases (HK 1 and 2), pyruvate dehydrogenase kinase 1 (PDK1) and lactate dehydrogenase A (LDHA), as well as monocarboxylate transporter 4 (MCT4) and carbonic anhydrase IX (CAIX), which play a role in pH regulation. HIF-α mediated regulation of these enzymes and transporters rewire the tumor metabolism to support tumor survival and proliferation (Iyer, et al., 1998, Semenza, 2001, Kim et al., 2006, Denko, 2008, Benita et al., 2009, Semenza, 2012, Dengler, et al., 2014).

Another hypoxia regulated biological process is metastasis. The key mediators of metastasis such as chemokine receptor 4 (CXCR4), metalloproteinases (MMP-2 and MMP-9) and lysyl oxidase (LOX) are HIF targets and associated with poor patient outcome. In addition, the EMT (epithelial to mesenchymal transition) regulators Snail, Slug, ZEB1, ZEB2 and Twist have been shown to be regulated by HIF (Petrella et al., 2005, Erler et al., 2006, Yang et al., 2008, Semenza, 2012).

Activated HIF-α also induces several pro-angiogenic factors such as vascular endothelial growth factor (VEGF), erythropoietin (EPO) and angiopoietin 2 (ANG2) that stimulate new blood vessel formation to ensure oxygen availability for the tumor cells (Takeda et al., 2004, Covello et al., 2006). HIFs also induce several genes that are required in stem cell homeostasis including the key regulator of stem cell behavior, OCT4, as well as many genes that are involved in proliferation and apoptosis (Pugh and Ratcliffe, 2003, Seidel et al., 2010).

The contribution of HIF-1α and/or HIF-2α to regulate the expression of their target genes has been shown to be cell-type specific. Moreover, HIF-1α and HIF-2α are shown to bind preferentially to specific genes, whereas some genes are induced by both isoforms (Hu et al., 2007, Lau et al., 2007, Lofstedt et al., 2007, Keith, et al., 2011). For example, glycolytic pathway genes are mostly regulated by HIF-1α, whereas stem cell homeostasis related genes are preferentially regulated by HIF-2α. Under acute hypoxia, transactivation of target genes is primarily mediated by HIF-1α. However, HIF-2α is stabilized upon prolonged and mild levels of hypoxia, where it induces the transactivation of specific target genes (Holmquist-Mengelbier et al.,

2006, Hu, et al., 2007, Lau, et al., 2007, Lofstedt, et al., 2007, Keith, et al., 2011, Koh et al., 2011).

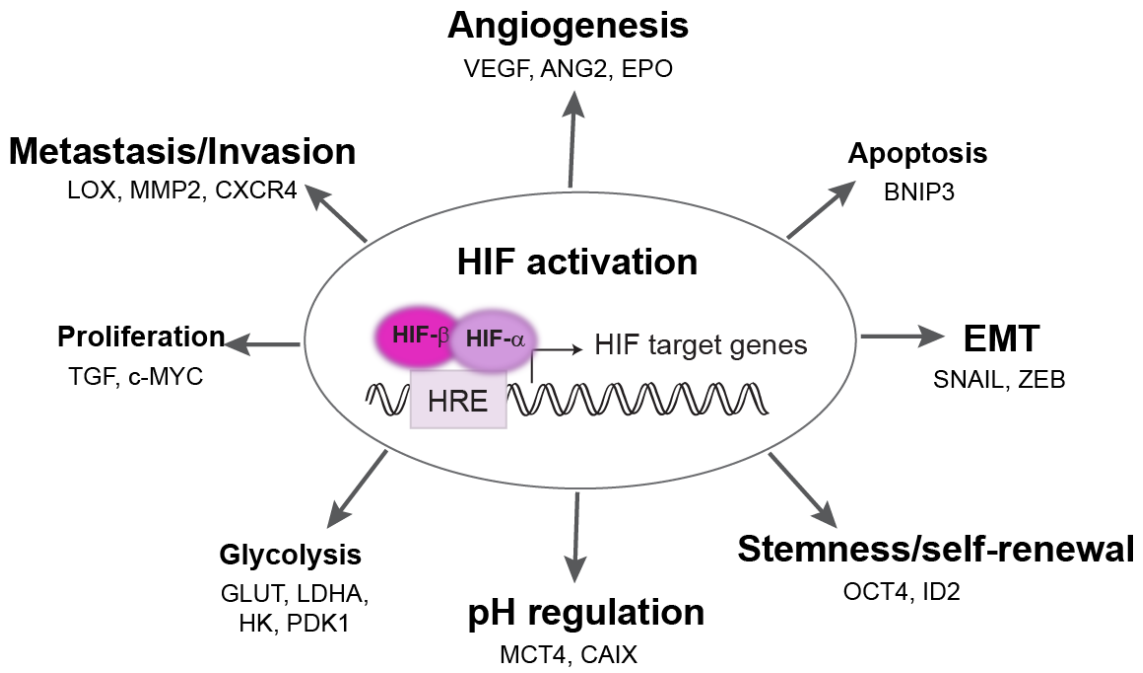

Figure 1.4. The biological pathways activated by HIF-1α and HIF-2α.
HIF-1α and HIF-2α regulate a variety of genes involved in different biological processes. These processes and some examples of genes that are regulated by HIF-1α and/or HIF-2α are shown in the schematic.

1.2.2.5 The role of PDHs in tumors

Oxygen-dependent regulation of HIF-α levels is mainly mediated by hydroxylation, followed by ubiquitination and proteasomal degradation (PHD mediated HIF-α regulation is described in detail under the “Hypoxia inducible factors and hypoxic response” section). HIF-α hydroxylation on the proline residues is a post-translational modification, which is catalyzed by prolyl hydroxylase domain proteins (PHDs) (Bruick and McKnight, 2001, Epstein et al., 2001). HIF prolyl hydroxylases have three different isoforms, PHD1, PHD2 and PHD3 (also known as EglN2, EglN1 and EglN3, respectively). PHDs belong to a family of 2-OG dependent, non-haem iron binding dioxygenases which require oxygen and 2-OG as co-substrates and iron (Fe^{2+}) as co-factor (Huang et al., 2002). PHDs have low affinity to oxygen with high K_m (~200-250

μM) values. Therefore, PHDs are highly sensitive to changes in oxygen levels within the physiological ranges, making them bona fide cellular oxygen sensors (Bruick and McKnight, 2001, Epstein, et al., 2001, Huang, et al., 2002, Hirsila et al., 2003, Schofield and Ratcliffe, 2004).

PHD1 and PHD2 are longer isoforms with 407 and 426 amino acids respectively, whereas PHD3 is the shortest isoform with only 239 amino acids. The hydroxylase domains at the C-terminus of PHDs are well conserved (Bruick and McKnight, 2001). PHD isoforms are expressed at different levels in the tissues. PHD2 is the most abundant isoform, which is found in most tissues, while PHD1 and PHD3 expression is more restricted. PHD1 is abundant in the testis and placenta whereas PHD3 is highly expressed in the heart. All PHDs have been reported to be expressed in the brain (Lieb et al., 2002, Cioffi et al., 2003, Willam et al., 2006a). Not only are the expression levels of PHDs across the tissues distinct, but also their subcellular localizations. PHD1, which contains a nuclear localization signal, is predominantly localized in the nucleus. PHD2 is localized in the cytoplasm while PHD3 is distributed evenly in the cytoplasm and the nucleus (Metzen et al., 2003, Yasumoto et al., 2009, Henze et al., 2010).

Although all the PHD isoforms have been reported to hydroxylate HIF-α *in vitro*, their affinities on the HIF-α isoforms and specificities towards the hydroxylation sites differ. PHD1 and PHD3 hydroxylate HIF-2α whereas PHD2 hydroxylates HIF-1α more efficiently. Under normoxia and mild hypoxia, PHD2 is the main regulator of HIF-1α. Under prolonged and severe hypoxia, PHD3 has more influence on HIF-2α. Moreover, PHD3 has been reported to hydroxylate Pro564 but not Pro402 in HIF-1α. In addition, isoform and cell type specific effects were also obtained in mouse models. Germline *Phd2* knock-out leads to embryonic lethality due to placental defects and heart failure, whereas Phd1 and Phd3 knock-out mice are viable (Epstein, et al., 2001, Berra et al., 2003, Hirsila, et al., 2003, Appelhoff et al., 2004, Takeda et al., 2006, Takeda et al., 2007). Altogether, these studies indicate the complexity of hydroxylation of HIF-α by different PHDs. It seems that different PHDs have preferences under certain conditions, which are also cell type specific.

1.2.2.5.1 Regulation of PHD activity

PHD activity is not only dependent on oxygen availability. Besides oxygen, PHDs require 2-OG and iron (ferrous iron, Fe^{2+}). As the first step of the reaction, ferrous iron (Fe^{2+}) is bound to the PHD catalytic domain, allowing the binding of oxygen, 2-OG and HIF-α. Then, molecular oxygen is used to convert 2-OG into succinate and CO_2, while HIF-α as a substrate is hydroxylated (Fig. 1.5) (Schofield and Ratcliffe, 2004, Smirnova et al., 2012). When the availability of other co-substrates and co-factors are not limited, the presence of oxygen is crucial for PHD activity and cannot be substituted by another molecule. The high K_m values of PHDs for oxygen make PHDs highly sensitive to concentration changes of oxygen levels (K_m values of PHDs for oxygen define the concentration of oxygen when the reaction reaches 50% of the maximal catalytic rate). A hypoxic tumor microenvironment leads to inactivation of PHDs, HIF-α stabilization and HIF-α mediated transcriptional reprogramming (Smirnova, et al., 2012, Nguyen and Duran, 2016).

ROS and nitric oxide (NO) have also been reported to regulate PHD activity. The potential mechanism of ROS induced PHD inactivation includes reduced iron availability by oxidation of ferrous iron (Fe^{2+}) to ferric iron (Fe^{3+}). Another proposed mechanism implies that ROS increase the mitochondrial respiration, leading to decreased oxygen availability for PHD activity. However, it has not been proven whether ROS directly affect PHD activity. The findings to date suggest indirect effects of ROS on PHD function (Bell and Chandel, 2007, Yang et al., 2012, Nguyen and Duran, 2016). NO also acts as a PHD inhibitor that is a potential competitor of oxygen for binding to iron at the catalytic sites of PHDs. However, there are accumulating data on the controversial effect of NO under normoxia and hypoxia (Berchner-Pfannschmidt et al., 2010, Chowdhury et al., 2011a, Nguyen and Duran, 2016).

To maintain the full activity, PHDs also require ascorbate as a reducing agent. When the reaction is completed by PHDs, 2-OG is converted to succinate and CO_2 and a ferrous iron (Fe^{2+}) is converted to a ferryl iron (Fe^{4+}) which then, due to its cytotoxicity, is directly reduced to the ferric iron (Fe^{3+}). Therefore, new ferrous iron (Fe^{2+}) is needed for the reactivation of PHD; ascorbate reduces the ferric iron (Fe^{3+}: storage form of

iron in the cells) to the ferrous state (Fe^{2+}) (Myllyla et al., 1984, Kuiper and Vissers, 2014, Nguyen and Duran, 2016). Additionally, Co^{2+} and Ni^{2+} have been shown to directly compete with Fe^{2+} binding to PHDs resulting inactivation of PHDs (Yuan et al., 2003, Davidson et al., 2005, Nguyen and Duran, 2016). A recent study revealed an additional mechanism controlling PHD function, by showing that L-cysteine protects PHD2 from self-inactivation through preventing the oxidation of specific cysteine residues within PHD2 that are critical for its activity (Briggs et al., 2016).

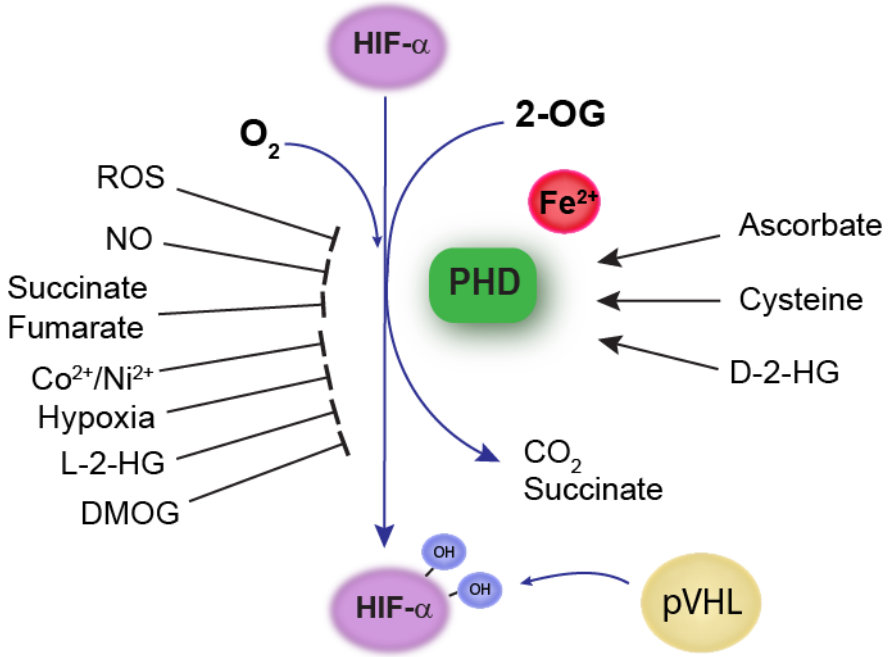

Figure 1.5. Regulation of PHD activity.
PHDs require oxygen, 2-OG, Fe2+, ascorbate and cysteine to maintain its hydroxylation function. A variety of factors, such as ROS, NO, TCA cycle intermediates, other ions and 2-OG analogs also negatively regulate PHD activity.

2-OG, an intermediate of the TCA cycle, is needed as a co-substrate and serves as an electron donor for the hydroxylation reaction. Amino acid starvation has been shown to lead to reduced 2-OG levels and thereby inactivation of PHDs (Duran et al., 2013). Moreover, the 2-OG analog DMOG has been used as a PHD inhibitor (Cummins et al., 2008). In addition to competitive inhibition of PHDs by DMOG, TCA cycle intermediates, such as succinate, fumarate, isocitrate, malate, oxaloacetate, and

pyruvate can also modulate PHD activity (Koivunen et al., 2007). Succinate and fumarate are known as oncometabolites and accumulation of these metabolites has been identified in cancer. Succinate and fumarate are structural analogs of 2-OG and inhibit PHDs competitively. Normally, TCA intermediates cannot compete with 2-OG due to their cellular localization, as TCA intermediates are mostly produced and consumed in the mitochondria. However, accumulation of succinate and fumarate in high amounts still results in PHD inactivation in the cytoplasm (Isaacs et al., 2005, Selak et al., 2005, Koivunen, et al., 2007).

Besides the factors which are described above, several other microenvironmental factors including hypoxia, growth factors and cytokines regulate PHDs (Appelhoff, et al., 2004, Jokilehto and Jaakkola, 2010). PHD2 and PHD3 expression levels have been shown to be upregulated under hypoxic conditions which in turn downregulate HIF-α, resulting in a negative feedback loop (Henze and Acker, 2010). PHD2 within its promotor and PHD3 within its enhancer region contain hypoxic response elements (HREs), where HIF-α binds to regulate their transcription. PHD1 has been shown to be estrogen inducible in breast cancer cells, whereas TGFβ has been reported to downregulate PHD2 and stabilize HIF-α (Appelhoff, et al., 2004, McMahon et al., 2006, Jokilehto and Jaakkola, 2010). Taken together, PHDs do not only sense oxygen levels, but also other molecules such as 2-OG, iron, ascorbate, L-cysteine, ROS, NO, succinate and fumarate, acting as the central metabolic sensors of the cell.

1.2.2.5.2 PHD regulated HIF-independent signaling pathways

Even if the best-characterized function of PHDs is the regulation of HIF-α stability, PHDs have also been shown to have HIF-independent binding and hydroxylation targets. These targets include a variety of genes that are involved in cell signaling, apoptosis and transcriptional regulation. (Yasumoto, et al., 2009, Yang et al., 2014, Nguyen and Duran, 2016, Zurlo et al., 2016).

The nuclear factor kappa-light-chain-enhancer of activated B cells (NF-κB) is an important regulator of the immune response, which is stimulated by cytokines and growth factors. The NF-κB pathway has been shown to be controlled by PHDs. The

basal and TNFα induced NF-κB activity is negatively regulated by PHDs (Cummins et al., 2006, Fu and Taubman, 2010). Reduced PHD levels or hypoxia result in an increase of NF-κB activity (Winning et al., 2010, Xue et al., 2010). PHD1 and PHD3 regulate NF-κB activity to a greater extent than PHD2. Furthermore, it was reported that PHD2 deficient macrophages displayed activated NF-κB signaling. The proposed molecular mechanism is the elevation of NF-κB activity via a hydroxylation dependent regulation of IKKβ, which carries a putative hydroxylation motif (LXXLAP) (Cummins, et al., 2006, Hamm et al., 2013). Normally, NF-κB subunits form a complex with IκBα that prevents NF-κB subunits (p50 and p65) from entering into the nucleus to activate the target genes. Inflammatory stimuli or growth factors dissociate this complex via proteasomal degradation of IκBα, which is mediated by the IKK (IκB kinase) complex, which includes IKKβ, IKKα, IKKγ and HSP90 (Oliver et al., 2009). IKKβ has been proposed to be targeted by PHDs, lower levels or inactivation of PHDs would result in more active IKKβ to inhibit IκBα, therefore activating NF-κB (Cummins, et al., 2006). Another proposed mechanism is PHD3 mediated blockade of the IKKβ and HSP90 interaction, which is required for activation of NF-κB (Xue, et al., 2010). .

PHDs also negatively regulate the transcription factors ATF4 (Activating transcription factor 4), Pax2 (paired box gene 2) and FOXO3a (Koditz et al., 2007, Hiwatashi et al., 2011, Yan et al., 2011, Zheng et al., 2014). It still remains unclear whether ATF4 and Pax2 regulation is hydroxylation dependent, whereas FOXO3 is hydroxylated at Pro426 and Pro437 sites. In addition to transcription factors, PHDs also contribute to the control of transcription and translation via targeting RNA polymerase II and eEF2 kinase (Eukaryotic elongation factor 2 kinase) in a hydroxylation dependent manner (Koditz, et al., 2007, Mikhaylova et al., 2008, Hiwatashi, et al., 2011, Yan, et al., 2011, Zheng, et al., 2014, Moore et al., 2015). Different groups identified proteins including EPOR, Akt, MAPK6, p53, erythropoietin receptor, EGFR and many more that are involved in the regulation of signaling pathways, as direct or indirect PHD targets. (Wong et al., 2013, Garvalov et al., 2014, Henze et al., 2014, Yang, et al., 2014, Zurlo, et al., 2016). All these findings emphasize the central role of PHDs as not only the regulator of the HIF pathway, but also other cellular processes where PHD functions rely on their hydroxylation and/or binding activity.

1.2.3 Cancer stem cells in glioblastoma

Tumors are composed of heterogeneous cells. Two different models have been described to explain tumor development and heterogeneity. The stochastic model (also known as clonal evolution model) postulates that tumor heterogeneity is the result of genetic changes and mutations occurring over time in individual cells. These events, with the contribution of the tumor microenvironment, are followed by the selection of the best-adapted clones, which are driving the tumor progression. In this model, all the tumor cells possess the similar potential to divide and drive the tumor growth (Nowell, 1976). The hierarchical model (also known as the cancer stem cell model) proposes that, similar to normal tissues, tumors are organized in a hierarchical manner, suggesting that only a distinct subset of tumor cells, the so-called cancer stem cells (CSCs), are responsible for tumor initiation and maintenance. In the hierarchical model, the tumor consists of CSCs displaying stem cell properties and differentiated cells, which are generated by CSCs (Reya et al., 2001, Dalerba et al., 2007).

CSCs were first isolated from acute myeloid leukemia (AML) samples. Only the tumor cells expressing the surface markers that are associated to normal hematopoietic stem cells were able to initiate AML in immunodeficient mice (Bonnet and Dick, 1997). Later, CSCs have also been identified in many solid tumors including breast, lung, colon, prostate, brain and other solid tumor types (Al-Hajj et al., 2003, Singh et al., 2004, Collins et al., 2005, Kim et al., 2005, Ricci-Vitiani et al., 2007). CSCs share several features with normal stem cells, such as self-renewal capacity, multi-lineage differentiation and cell surface marker expression. In addition, CSCs show a strong tumorigenic capacity, are resistant to therapeutics and are able to recapitulate the heterogeneity of the parental tumor, making them clinically relevant targets (Fig. 1.6) (Reya, et al., 2001, Borovski et al., 2011).

As observed in other solid tumors, glioblastoma stem cells (GSCs) were also shown to be involved in tumor initiation, maintenance, propagation and therapeutic resistance. GSCs possess self-renewal and differentiation capacity, and, when

transplanted in animal models, they drive the formation of tumors consisting of heterogeneous cells, as found in the parental tumor (Singh et al., 2003, Singh, et al., 2004, Folkins et al., 2007). Whether CSCs originate from neural stem cells or from differentiated cells, still remains unclear. GSCs display similar gene expression patterns to neural stem cells, supporting a neural stem cell origin, whereas the switch between the differentiated and stem cells state, the so-called cellular plasticity, supports the possibility of dedifferentiation and regaining of self-renewal capacity. Possibly, GSCs may have different cells of origin in different tumors (Jackson and Alvarez-Buylla, 2008, Modrek et al., 2014, Sundar et al., 2014).

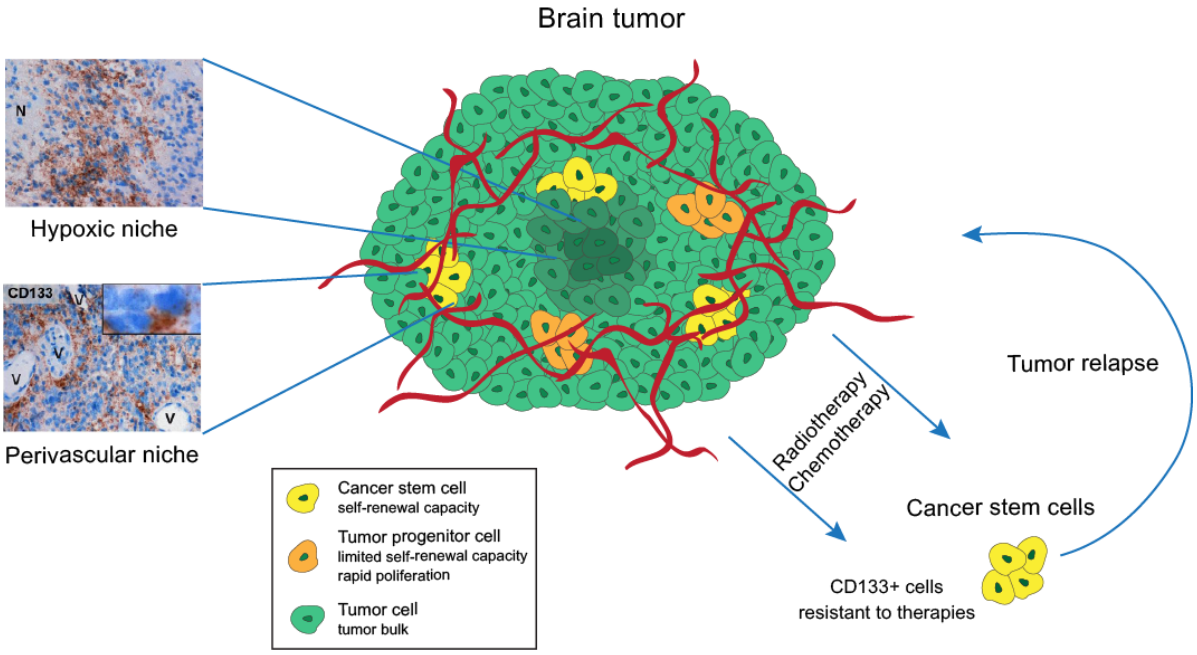

Figure 1.6. Cancer stem cell model.
Tumors consist of CSCs, less differentiated tumor progenitor cells and more differentiated tumor cells. CSCs reside in two different niches – a hypoxic and a perivascular one – which contribute to the maintenance of the CSC state. Cells expressing a well characterized CSC marker, CD133, are resistant to therapies, and are likely responsible for tumor relapse.

The best-studied GSC marker is CD133 (Prominin 1), which is also used to identify cancer stem cells in lung, colon, prostate, pancreatic and ovarian cancers. CD133 is commonly used for the enrichment of cancer stem cells. CD133 positive glioblastoma cells show increased self-renewal capacity, which is typically assessed by neurosphere forming assays. Moreover, compared to CD133 negative cells, CD133 positive cells demonstrate more tumorigenic capacity in xenotransplantation studies.

Gene profiling studies have also shown that CD133 positive glioblastoma cells exhibit a similar gene profile with embryonic stem cells, suggesting that CD133 plays a role in the stem cell state. Furthermore, it has been shown that CD133 positive cells are resistant to therapy due to the activation of DNA repair mechanisms and cell cycle check points (Singh, et al., 2004, Bao et al., 2006, Liu et al., 2006, Ricci-Vitiani, et al., 2007, Garvalov and Acker, 2011). Even if CD133 is a commonly used tool to enrich for CSCs, several other cell surface makers such as CD15, integrin α6, A2B5, L1CAM, CXCR4 and CD44 have been identified and used. Cell surface markers provide advantages by facilitating isolation and sorting of live CSCs. Another method to enrich for CSCs is the sorting of the side population, which is based on exclusion of Hoechst 33342, a lipophilic DNA staining dye (Ogden et al., 2008, Bleau et al., 2009, Son et al., 2009, Anido et al., 2010, Lathia et al., 2010, Sundar, et al., 2014). In addition to cell surface markers, the CSC population expresses stem cell marker genes such as Olig2, Sox2, Bmi1 and Musashi, which are known from physiological stem cells (Heddleston et al., 2011).

Analogous to physiological stem cells, CSCs reside in specialized microenvironments, known as niches. Dynamic interactions between CSCs and their microenvironment, which includes other cell types, the extracellular matrix, signaling molecules, soluble factors and chemokines, play a crucial role in the maintenance of CSCs. Normal stem cells are known to be located in the subventricular zone and the hippocampus in close proximity to endothelial cells (Shen et al., 2008, Tavazoie et al., 2008). Similarly, CSCs are enriched in the perivascular niche. The perivascular niche supplies signals to regulate CSC maintenance and CSCs in turn secrete factors like VEGF, TGFβ and TNFα, which remodel the microenvironment (Sundar, et al., 2014, Plaks et al., 2015). For instance, NO secreted by endothelial cells, leads to enhanced Notch activity (Charles et al., 2010). It has also been shown that CD133 positive CSCs express higher levels of VEGF, leading to increased tumor vascularization (Yao et al., 2008).

Another characteristic of solid tumors is the existence of perinecrotic hypoxic areas, which have been reported to be the second niche for CSCs (Li et al., 2009). The cellular response to low oxygen levels is mainly mediated by the HIF pathway. Hypoxia

has been reported to enhance self-renewal and the expression of CSC marker genes (Covello, et al., 2006, Seidel, et al., 2010, Heddleston, et al., 2011, Yun and Lin, 2014). HIF-1α and HIF-2α directly regulate CSC marker genes. In glioblastoma, HIF-2α but not HIF-1α, seems to be the main regulator of the CSC phenotype and HIF-2α is highly expressed in GSCs (Heddleston et al., 2009, Seidel, et al., 2010). The side population approach under hypoxic conditions has also identified GSCs maker genes, ASPHD2, MAML3, NFE2L2, ABL2 and NFATC2, which are also regulated by HIF-2α (Seidel, et al., 2010).

1.3 Metabolic reprogramming in cancer

Altered metabolism is one of the key biological features of tumor cells and has been linked to tumorigenesis and therapy resistance. Tumor cells reprogram their metabolism to meet their needs during tumor progression. Even if tumors exhibit a heterogeneous distribution of crucial nutrients such as oxygen, glucose and glutamine, tumor cells are able to sustain their energy production, biosynthesis of macromolecules and maintenance of cellular redox states at appropriate levels by reprogramming their metabolism (DeBerardinis et al., 2007, Yeung et al., 2008, Hanahan and Weinberg, 2011, Ward and Thompson, 2012). Metabolic reprogramming in tumor cells is characterized by elevated glycolysis, glutaminolysis, pentose phosphate pathway, lipid metabolism, mitochondrial biogenesis and macromolecule biosynthesis. Metabolic rewiring not only provides energy, but also macromolecules to support the tumor cells for survival, rapid proliferation and other processes indispensable for tumor progression (DeBerardinis et al., 2008, Cairns et al., 2011, Hanahan and Weinberg, 2011).

The Warburg effect, the first described metabolic alteration in tumor cells, describes the metabolic shift from oxidative phosphorylation to glycolysis, even in the presence of oxygen (aerobic glycolysis) (Warburg, 1956a). Besides the aerobic glycolysis, hypoxia, due to the absence of oxygen, also leads to a shift from oxidative phosphorylation to glycolysis, a phenomenon termed anaerobic glycolysis (Gatenby and Gillies, 2004, Cairns, et al., 2011). In contrast to normal cells, tumor cells

preferentially use glycolysis to generate ATP for energy even if it is less efficient compared to oxidative phosphorylation. In addition to ATP, glycolysis provides the precursors for nucleotide, lipid and amino acid biosynthesis. Moreover, glycolysis also entails an acidic tumor microenvironment. By favoring glycolysis, tumor cells generate carbonic and lactic acids that are exported to the extracellular space. The expression of glycolytic enzymes (such as HK1, HK2, PDK1 and LDHA) and glucose transporters (such as GLUT1-4) are remarkably elevated in tumors (Gatenby and Gillies, 2004, DeBerardinis, et al., 2008, Cairns, et al., 2011, Phan et al., 2014). HIF-1α, p53 and c-Myc are the master inducers of glycolysis through the regulation of glycolytic genes (HIF function is described in detail under “Hypoxia inducible factors and hypoxic response” section) (Yeung, et al., 2008). .

The interaction between tumor cells to the tumor microenvironment plays a key role in reprogramming the metabolism. Profound effects of oncogenes on metabolism and identification of mutations in metabolic enzymes such as isocitrate dehydrogenase (IDH), fumarate hydratase (FH), succinate dehydrogenase (SDH) and alterations in pyruvate kinase (PKM) have demonstrated their contribution to tumorigenesis and tumor progression by reprogramming the metabolism.

Mutations in metabolic enzymes such as IDH1, SDH and FH have been shown to lead to the accumulation of oncometabolites. The IDH gene encodes an enzyme that catalyzes the conversion of isocitrate to 2-OG (2-oxoglutarate, also known as α-ketoglutarate) within the tricarboxylic acid cycle (TCA) (Plaut et al., 1983). Similarly, SDH and FH are mitochondrial enzymes that catalyze the conversion of succinate to fumarate and fumarate to malate, respectively (Baysal et al., 2000, Tomlinson et al., 2002, Isaacs, et al., 2005). IDH, SDH and FH mutations cause the accumulation of 2-hydroxyglutarate (2-HG), succinate and fumarate, respectively. Importantly, these metabolites have been shown to compete with 2-OG and act as oncometabolites. Accumulation of these oncometabolites affects 2-oxogluatarate dependent dioxygenases that catalyze protein hydroxylation, DNA and histone methylation. IDH, SDH and FH mutations have been identified in cancers, especially in glioma, paraganglioma and papillary renal cancers, respectively (Baysal, et al., 2000, Isaacs,

et al., 2005, Parsons et al., 2008, Dang et al., 2009). Particularly, SDH and FH mutations have been shown to activate the hypoxic response even in the presence of oxygen (so-called pseudo-hypoxia), whereas the role of IDH1 mutation on the hypoxic response seems to be more complex and controversial (Tomlinson, et al., 2002, Isaacs, et al., 2005, Selak, et al., 2005, Zhao et al., 2009). In summary, understanding the molecular basis and mechanism of altered metabolism, which depends on the tumor type, seems to be crucial to efficiently target the tumor growth.

1.3.1 2-OG and 2-OG dependent dioxygenases

2-OG (2-oxoglutarate, also known as α-ketoglutarate (α-KG)) is a small molecule involved in a variety of metabolic and cellular pathways. 2-OG is an intermediate of the TCA cycle and is produced by oxidative decarboxylation of isocitrate, or by oxidative deamination of glutamate. As an important biological molecule, 2-OG contributes to the cellular anabolism and catabolism by regulating ATP production, NAD^+/NADH generation, reductive carboxylation and amino acid production. More importantly, 2-OG is also needed as a co-substrate for 2-OG dependent dioxygenases that catalyze hydroxylation reactions of a large number of substrates (Fig. 1.7) (Krebs and Johnson, 1980, Schofield and Zhang, 1999, McDonough et al., 2010, Loenarz and Schofield, 2011).

There are approximately 70 different 2-OG dependent oxygenases in humans. Their activity relies on the availability of key nutrients including 2-OG, oxygen, Fe^{2+} and ascorbate. 2-OG dependent oxygenases can target DNA, RNA and proteins for modification (Loenarz and Schofield, 2011, Rose et al., 2011). DNA/RNA modifying 2-OG dependent oxygenases include ten-eleven translocation hydroxylases (TET1-3) and alkylated DNA repair protein alkB homologs (ALKBH2-3). During the oxidative decarboxylation of 2-OG, 5-methylcytosine (5-mC, a key epigenetic modification) is hydroxylated by TETs as a substrate, generating 5-hydroxy-methylcytosine (5-hmC) that may represent an intermediate for 5-methylcytosine demethylation (Huang and Rao, 2014, Kroeze et al., 2015). Another modification mediated by 2-OG dependent oxygenases resulting in epigenetic effects is histone demethylation. Jumonji-domain-

containing demethylases (KDMs and JMJDs) need 2-OG as a co-substrate to remove the methyl groups from histones to influence the chromatin structure (Tsukada et al., 2006). 2-OG dependent oxygenases targeting proteins include PHDs, P3H, P4H, ASPHD and FIH. These 2-OG dependent oxygenases hydroxylate the prolyl, aspartyl, lysyl and asparaginyl residues of proteins that regulate the hypoxic response and collagen production (Markolovic et al., 2015). The role of PHDs in the regulation of the hypoxic response is discussed in detail under “The role of PDHs in tumors”.

The amounts of the key metabolite 2-OG, produced in the cell, depends on the cellular redox status. Under increased concentrations of NAD^+, 2-OG is produced in the TCA cycle by oxidative decarboxylation of isocitrate by IDH1/2 and further converted to succinate, whereas NADH accumulation results in transamination of 2-OG, producing glutamate from 2-OG (Owen et al., 2002, Xiao et al., 2016). 2-OG can be transported to the cytoplasm by oxoglutarate carriers and anion channels to be used in reactions in the cytoplasm (Fig. 1.7) (Monne et al., 2013). 2-OG contributes to energy metabolism as a precursor of glutamine and glutamate, which are energy fuels of the cells. In some physiological and pathological cases, nutrition therapy is applied to overcome the glutamine and glutamate deficiencies to supply the energy needed in the body. Due to the instability of glutamine and the toxicity of glutamate, direct glutamine and/or glutamate supplementations have limited success. Therefore, the use of the glutamine and glutamate precursor 2-OG, became an alternative nutrition therapy. It has been reported that 60% of dietary 2-OG can be absorbed in the intestine, whereas 20% of 2-OG can be detected in the bloodstream, which is then metabolized to glutamine and glutamate (Stehle et al., 1989, Hermanussen and Tresguerres, 2005, Junghans et al., 2006, Stein et al., 2009, Al Balushi et al., 2013, Zdzisinska et al., 2017).

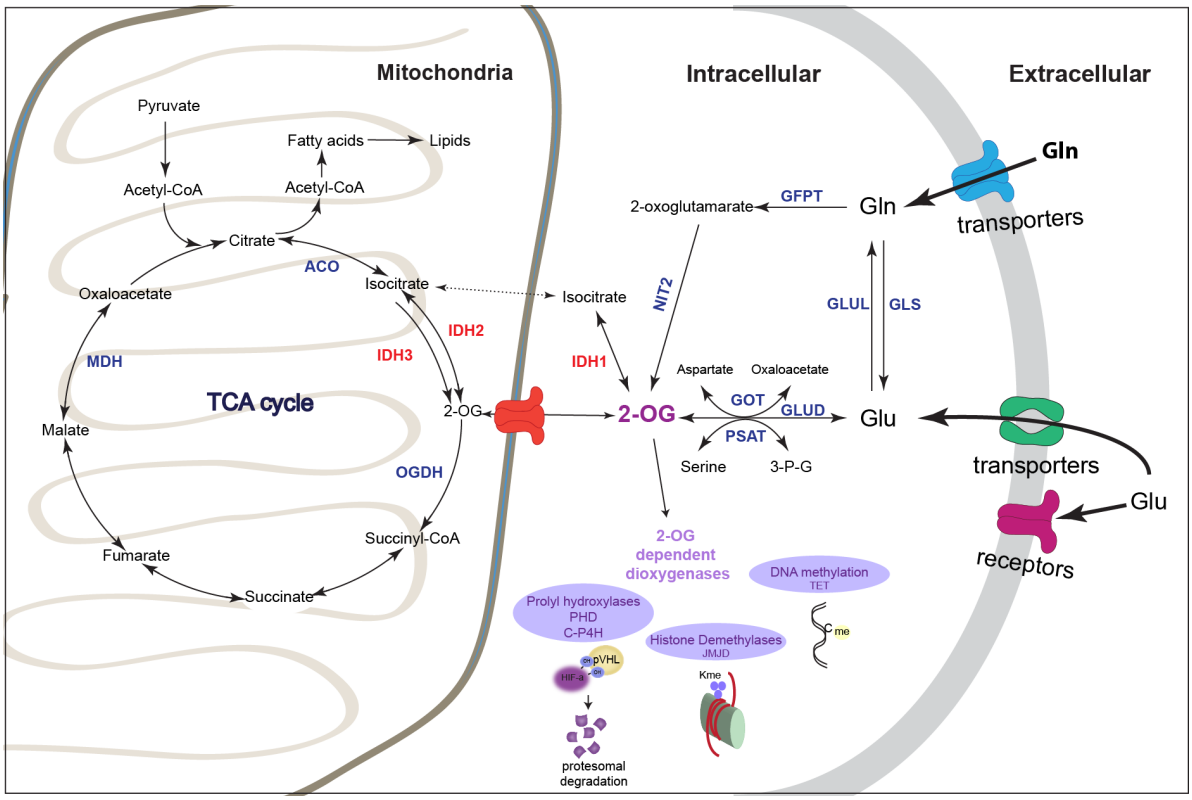

Figure 1.7. The metabolic processes producing 2-OG.
2-OG is produced either by oxidative decarboxylation of isocitrate by IDHs or by oxidative deamination of glutamate and glutamine. During the oxidative deamination of glutamate (Glu) and glutamine (Gln), which produces 2-OG, several enzymes, such as GLS (Glutaminase), GLUD (glutamate dehydrogenase), GOT (Aspartate transaminase), PSAT (Phosphoserine aminotransferase), GFPT (glutamine--fructose-6-phosphate transaminase) and NIT2 (ω-amidase) (shown in blue) take part in the conversion. On the other hand, oxidative decarboxylation of isocitrate is catalyzed by IDH isoforms (IDH1-3) either in cytoplasm, or in the mitochondria. 2-OG produced in the cell is used by the 2-OG dependent dioxygenases as a co-substrate to regulate a variety of biological processes (protein hydroxylation, histone demethylation and DNA methylation).

The use of 2-OG in medical treatment is not limited to nutrition therapy, 2-OG is also used as an antioxidant antagonizing oxidative stress, as an enhancer of wound healing in patients with severe burns and as a modulator of immune cells. Moreover, it has been reported that 2-OG supplementation has a positive effect on bone density and strength, an effect that has been linked to two possible mechanisms. The first mechanism proposes that collagen prolyl 4-hydroxlase (C-P4H), a 2-OG dependent dioxygenase, enhances the collagen type I production in bone cells, resulting in increased bone density and strength. The second mechanism suggests that 2-OG induced proline production plays a central role in collagen metabolism to regulate

bone density and strength (Wu et al., 2016, Zdzisinska, et al., 2017). Another interesting role of 2-OG is described as a regulator of the aging process. It has been reported that 2-OG extends the lifespan of adult *Caenorhabditis elegans* by reducing ATP synthase and mTOR activity, thereby leading to a reduction in ATP content and oxygen consumption (Chin et al., 2014, Salminen et al., 2014).

1.3.1.1 Antitumorigenic activity of 2-OG

Recently, some studies have shown that the accumulation of 2-OG analogs (succinate, fumarate and 2-HG) are involved in carcinogenesis. These findings drew the attention to 2-OG and its potential anticancer activity. Accumulation of succinate and fumarate, caused by mutations in SDH and FH, leads to pseudo-hypoxia via competitive inhibition of 2-OG dependent dioxygenases, such as PHDs. This is especially typical in paraganglioma and papillary renal cancers, which frequently have SDH and FH mutations, respectively (Baysal, et al., 2000, Isaacs, et al., 2005, Selak, et al., 2005). Reduced PHD activity mediated by 2-OG analogs is reversed by 2-OG addition, demonstrating that 2-OG can be used to regain PHD activity in SDH and FH mutated tumors (Briere et al., 2005, MacKenzie et al., 2007, Tennant et al., 2009). Not only PHD activity, which modulates the hypoxic response, but also TET and KDM activities are elevated by succinate and fumarate, leading to enhanced DNA and histone methylation, which, in turn, regulates gene expression at the epigenetic level. Interestingly, the effect of succinate and fumarate accumulation on DNA and histone methylation can also be reversed by 2-OG (Cervera et al., 2009, Chowdhury et al., 2011b, Xiao et al., 2012). These findings show that 2-OG to succinate and 2-OG to fumarate ratios are critical for the maintenance of 2-OG dependent dioxygenase activity, and that 2-OG itself has an antitumorigenic effect.

The utilization of 2-OG as an antitumorigenic agent was investigated by a number of researchers. Increased VEGF and erythropoietin levels that are regulated by the hypoxic tumor microenvironment lead to enhanced angiogenesis in tumors. Matsumoto et al. showed that exogenous 2-OG application inhibits angiogenesis via the reduction of HIF-α, VEGF and erythropoietin levels. 2-OG decreases the VEGF and erythropoietin production, as well as HIF-α levels in a dose dependent manner

(Matsumoto et al., 2006). Moreover, similar results were observed in Lewis lung carcinoma (LLC) cells. In a LLC tumor xenograft model, 2-OG treated mice developed significantly smaller tumors, which was accompanied by reduced tumor angiogenesis. Importantly, administration of 2-OG combined with 5-fluorouracil to the tumor bearing mice reduced the tumor growth and angiogenesis, suggesting the potential clinical use of 2-OG as an antitumor agent (Matsumoto et al., 2009). Tennant et al. also showed that derivatized 2-OG could be used to overcome tumor hypoxia by reactivating PHDs *in vivo*. More importantly, 2-OG permeates into the tumor resulting in reduced HIF-α levels and induction of PHD dependent hypoxic cell death (Tennant, et al., 2009). An anti-proliferative effect of 2-OG is also observed under normoxia. The cell cycle is affected by elevated expression of the cyclin-dependent kinase inhibitors p21 Waf1/Cip1, p27 Kip1 and Rb phosphorylation in 2-OG treated colon cell carcinoma cells. However, the mechanism through which 2-OG elicits these effects remains unclear (Rzeski et al., 2012).

Due to limited perfusion, tumors exhibit an inadequate nutrient and oxygen supply. A recent study showed that tumor cells in the core region of the tumor starve due to glutamine deficiency. Low glutamine levels in the tumor core result in decreased 2-OG levels, thereby inactivating Jumonji-domain-containing histone demethylases, leading to histone hypermethylation. Low levels of 2-OG, which is required as a co-substrate by histone demethylases, promotes cancer cell dedifferentiation (cancer stem cell state) and therapeutic resistance. Strikingly, glutamine injection into the tumor core recovers 2-OG levels and 2-OG supplementation to the glutamine-deprived cells reverts the hypermethylation phenotype, suggesting that the tumor microenvironment and 2-OG play a central role in tumor cell fate (Hojfeldt and Helin, 2016, Pan et al., 2016). A number of studies also investigated the impact of intracellular 2-OG on normal stem cells. Intriguingly, 2-OG supports the self-renewal capacity of embryonic stem cells (ESCs) while it induces the differentiation of primed pluripotent stem cells (pPSCs). Even more interestingly, these opposite effects are mediated by similar mechanisms, the regulation of histone methylation (Carey et al., 2015, Hwang et al., 2016, TeSlaa et al., 2016).

Taken together, all these studies support the potential utilization of 2-OG as an antitumorigenic agent. However, the effect of 2-OG should be considered carefully, as exemplified by the finding that opposite effects are observed in ESCs and pPSCs, suggesting that the effect of 2-OG might be context and cell type dependent. Even if the pharmacokinetic behavior of 2-OG as a cancer treatment is under investigation, additional studies and clinical trials are needed (Donnarumma et al., 2013).

1.3.2 The function of isocitrate dehydrogenases (IDHs)

IDHs are enzymes catalyzing the oxidative decarboxylation of isocitrate to 2-OG (Fig. 1.7). In human cells, three different isoforms of IDH are expressed: IDH1, IDH2 and IDH3. IDH1 and IDH2 are $NADP^+$-dependent enzymes and function as homodimers, whereas IDH3 is NAD^+-dependent and consists of three different subunits (α, β and γ), functioning as a heterotetramer (Dalziel, 1980, Xu et al., 2004). IDH1 is localized in the cytoplasm and peroxisomes while IDH2 and IDH3 are active in the mitochondria. IDH3, NAD^+-dependent and structurally unrelated to the other isoforms, only catalyzes an irreversible reaction, while the reactions catalyzed by IDH1 and IDH2 are reversible, depending on substrate and co-factor availability. The directionality of the enzymatic reaction is regulated by the availability of isocitrate, 2-OG, metal ions and the redox status ($NADP^+$ and NADPH) in the cell (Dalziel, 1980, Xu, et al., 2004, Mellai et al., 2013).

Each IDH1 monomer contains a large domain, a clasp domain and a small domain (Fig. 1.8). The large and small domains are held together by the clasp domain to form the active site (active site cleft). Each homodimer contains two asymmetric and identical IDH1 monomers, which shift between an inactive and active conformation. In the inactive open form, the regulatory segment unfolds and the active site is blocked by the interaction between Asp279 (D279) and Ser94 (S94) (Fig. 1.8, left). When isocitrate reaches a certain level, IDH1 forms the active closed conformation. In the active closed form, hydrogen bonding between Asp279 and Ser94 breaks and the metal-isocitrate complex binds to the active site producing 2-OG, CO_2 and NADPH (Fig. 1.8, right and Fig. 1.9). $NADP^+$-dependent IDHs require a divalent metal ion,

ideally, Mn^{2+} or Mg^{2+}, but Ca^{2+} could also be used as a substitute. Since the regulatory segment of IDH is located in the protein core and therefore not accessible by other proteins it is thought that protein-protein interactions could not directly influence IDH activity. Therefore, IDH activity might primarily rely on the availability of substrate and co-factors. (Dalziel, 1980, Ceccarelli et al., 2002, Xu, et al., 2004, Mellai, et al., 2013).

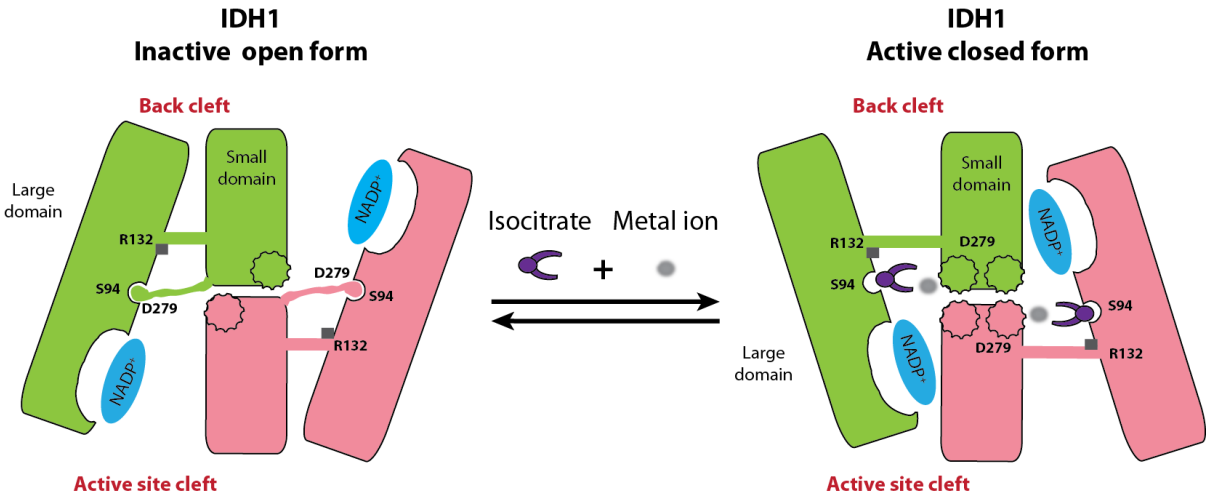

Figure 1.8. Structure of IDH1 homodimer and IDH1 conformational changes.
$NADP^+$-dependent IDH1 shifts between an inactive open and active closed conformation. The IDH1 homodimer is composed of two asymmetric and identical IDH1 monomers. Each IDH1 monomer contains a large domain, a clasp domain and a small domain, which requires $NADP^+$, isocitrate and metal ions for its activity. (Redrawn and modified from (Xu, et al., 2004)).

The main function of IDHs is catalyzing the conversion of isocitrate to 2-OG. However, the different IDH isoforms have overlapping, but distinct roles in metabolic processes. Since IDH1 is localized in the cytoplasm and peroxisomes, 2-OG, which is needed as a co-substrate for cytoplasmic and nuclear 2-OG dependent dioxygenases, is mainly produced by IDH1. In addition, IDH1 also contributes to lipid synthesis and cellular protection from oxidative stress by generating NADPH. NADPH is required as a reducing agent and consumed during lipid synthesis. Moreover, NADPH plays a crucial role in the regeneration of glutathione, which neutralizes ROS. Even if the main source of NADPH is the pentose phosphate pathway, the contribution of IDH1 and IDH2 is equally important. It has been shown that IDH1 protects the cells from oxidative and radiation damage (Jo et al., 2002, Lee et al., 2002, Losman and Kaelin, 2013, Mellai, et al., 2013). In an IDH1 knock-out mouse model, it has been shown that

the IDH1 level is important to protect the cells against oxidative stress. IDH1 knock-out hepatocytes display an impaired $NADP^+$/NADPH ratio leading to increased ROS levels. In the same mouse model, IDH1 deficiency impairs the alanine utilization through elevated 2-OG levels in the liver (Itsumi et al., 2015, Ye et al., 2017). In another study, miR-181 has been reported to inhibit lipid accumulation via directly targeting IDH1, displaying a miR-181-IDH1 axis in the regulation of lipid metabolism (Chu et al., 2015). Moreover, sterol regulatory element-binding proteins (SREBPs), which are required for cholesterol and fatty acid biosynthesis, transcriptionally regulate IDH1. SREBPs activated IDH1 contributes to the production and maintenance of fatty acids by supplying NADPH and lowering the phytanic acid levels (Shechter et al., 2003). Under hypoxic conditions, glutamine is described as the major carbon source via glutaminolysis and reductive carboxylation. IDH1 has been shown to catalyze the reductive carboxylation of 2-OG to isocitrate under hypoxia or mitochondrial dysfunction, contributing to the conversion of glutamine to other cellular intermediates used for lipid synthesis (Metallo et al., 2011, Mullen et al., 2011, Scott et al., 2011, Le et al., 2012, Fan et al., 2013, Mullen et al., 2014). The function of IDH1 seems not to be limited to lipid synthesis or protection from oxidative stress; IDH1 levels functionally determine the cell fate under stress conditions. IDH1 is transcriptionally upregulated by CHOP and C/EBPβ in response to ER (endoplasmic reticulum) stress, promoting apoptosis in human melanoma cells (Yang et al., 2015). Notably, IDH1 upregulation also inhibits proliferation, invasion and migration, as well as tumor growth in osteosarcoma cells (Hu et al., 2014).

In contrast to IDH1, IDH2 and IDH3 are localized in the mitochondria. IDH3 contributes to mitochondrial respiration by the production of 2-OG in an irreversible reaction, whereas IDH2 could regulate both isocitrate and 2-OG levels, to balance metabolite levels in the mitochondria. Similar to IDH1, IDH2 has been reported to play a crucial role in reductive carboxylation. The mitochondrial NADPH, which can counteract mitochondrial oxidative stress, is produced by IDH2 (Lee et al., 2004, Wise et al., 2011, Filipp et al., 2012, Losman and Kaelin, 2013). An interesting tumor study showed that IDH2 deficient tumor bearing mice display high ROS levels in the tumors and elevated tumorigenesis (Kim et al., 2014). In glioblastoma, IDH2 has been

reported to be targeted by miR-183 which, in this tumor entity, is expressed at higher levels compared to normal brain. miR-183 downregulates IDH2, thereby leading to reduced 2-OG levels. Moreover, decreased 2-OG levels abrogate the 2-OG dependent dioxygenase activity resulting in an increased HIF-α level (Tanaka et al., 2013). Interestingly, in diffuse large B-cell lymphoma patients, IDH2 activity and levels are positively regulated by D-2-HGDH (D-2-hydroxyglutarate dehydrogenase) expression. D-2-HGDH is an enzyme which converts D-2-HG (D-2-Hydroxglutarate) to 2-OG. In line with the previous study, the patients carrying D-2-HGDH mutations leading to inactivation of the enzyme, display reduced IDH2 levels along with decreased 2-OG levels. D-2-HGDH mutations result in reduced HIF-α hydroxylation, increased histone methylation and elevated DNA methylation due to the lacking 2-OG for the 2-OG dependent dioxygenases, PHDs, JMJDs and TETs, respectively. Moreover, ectopic expression of IDH2 rescues the effect of D-2-HGDH deficiency, showing the importance of IDH2 especially for the regulation of epigenetic remodeling in diffuse large B-cell lymphoma (Lin et al., 2015).

The function of IDH3 in tumors seem to be more complicated. Zhang et al. showed that IDH3α is downregulated by TGFβ in cancer-associated fibroblasts (CAF), leading to reduced 2-OG levels and subsequently increased HIF-α levels and tumorigenesis (Zhang et al., 2015a). Even if IDH3 is stated to perform an irreversible reaction, Zeng et al showed that aberrant IDH3α expression is related to increased HIF-α levels and tumorigenesis in adenocarcinoma cells via regulating the reductive carboxylation. Interestingly, IDH3α silencing increased the 2-OG levels and reduced the HIF-α level (Zeng et al., 2015). In summary, IDH3 function seems to be cell type specific or context dependent.

Taken together, these studies suggest that activity and levels of IDHs are crucial for the maintenance of levels of the antitumorigenic metabolite 2-OG, to regulate the activity of 2-OG dependent enzymes, reductive carboxylation, lipid metabolism and tumor cell characteristics such as invasiveness.

1.3.2.1 IDH mutations and 2-Hydroxglutarate (2-HG)

Metabolic dysregulation is one of the hallmarks of tumor cells. Not only signals by the tumor microenvironment, but also mutations in metabolic enzymes reprogram tumor metabolism. Recently, mutations in IDH1 and IDH2 were identified first in glioma and colon tumor. It was a striking discovery that had a major impact on the diagnosis of tumor patients, marking a shift towards the inclusion of molecular alterations for the classification of central nervous system tumors. (Louis, et al., 2016).

Comprehensive analysis in glioblastoma and colon cancer patients identified a somatic and heterozygous mutation in the IDH gene, which occurs at the active site of the enzyme on arginine residues of IDH1 (R100 or R132) or IDH2 (R140 or R172) (Fig. 1.8) (Sjoblom et al., 2006, Parsons, et al., 2008, Yan et al., 2009). Subsequently, IDH mutations have been observed in AML, cholangiocarcinoma, cartilaginous tumors and some few cases in other solid tumors such as bladder cancer, melanoma, prostate cancer, breast cancer and lung cancer (Mardis et al., 2009, Amary et al., 2011a, Sequist et al., 2011, Borger et al., 2012). In glioblastoma the mutation of IDH1 is more commonly found than an IDH2 mutation and it occurs in more than 80% of the secondary glioblastoma. Importantly, IDH mutation is associated with a better prognosis in glioblastoma (Balss et al., 2008). However, IDH mutation status correlates with a worse prognosis in AML that has progressed from myelodysplastic syndrome (MDS) and myeloproliferative neoplasms (MPN), and in breast cancers (Thol et al., 2010, Tefferi et al., 2012, Terunuma et al., 2014). Notably, in the recent 2016 WHO classification, IDH1 mutation status is defined as the first criteria to differentiate lower grade glioma from higher grade glioma (Louis, et al., 2016). It still remains unclear whether the differences between the IDH1 mutated and wild-type patients are driven by the IDH1 mutation or the reflection of biological differences between the lower grade and higher gliomas. Nevertheless, IDH mutations seem to possess a prognostic value, are implicated as an early/driver event during the progression of glioma and represent a subtype of tumors with a distinct origin. It is speculated that IDH mutant cells, which later on accumulate p53 and ATRX mutations, give rise to diffuse astrocytoma, whereas IDH mutant cells with the deletion of 1p/9q

and TERT promoter mutations give rise to oligodendrogliomas (Fig. 1.1) (Ohgaki and Kleihues, 2013, Wahl and Venneti, 2015, Dang and Su, 2017).

Interestingly, IDH mutations are heterozygous missense mutations occurring always at the active site of the enzyme, resulting in the loss of one wild-type IDH copy. Initially, IDH mutations were thought to promote tumorigenesis through the loss of IDH function (Yan, et al., 2009, Zhao, et al., 2009). However, subsequent studies found that IDH mutations cause a neomorphic activity of the enzyme by enabling the conversation of 2-OG to D-2-HG, revealing a gain of function of the mutant IDH (Dang, et al., 2009, Ward et al., 2010). The oncometabolites D-2-HG and L-2-HG are the two chiral isoforms of 2-HG, which are produced in negligible quantities in normal cells. Normally, 2-HG is converted back to 2-OG by enantiomer specific (D-2-HG and L-2-HG) dehydrogenases (D-2-HGDH and L-2-HGDH) to prevent their accumulation in the cells (Steenweg et al., 2010, Struys, 2013). Intriguingly, IDH mutant enzymes exclusively produce the D enantiomer of 2-HG, which accumulates to extremely high levels (Fig. 1.9). Due to the slower catalytic rate of D-2-HGDH compared to mutant IDH, D-2-HGDH is not able to convert these high amounts of D-2-HG back to 2-OG, resulting in accumulation of D-2-HG (Dang, et al., 2009, Engqvist et al., 2009). Moreover, due to their structural similarity, accumulation of the oncometabolite D-2-HG has been shown to competitively inhibit 2-OG dependent dioxygenases, impairing a variety of cellular processes by altered epigenetic remodeling, hypoxic response and collagen maturation.

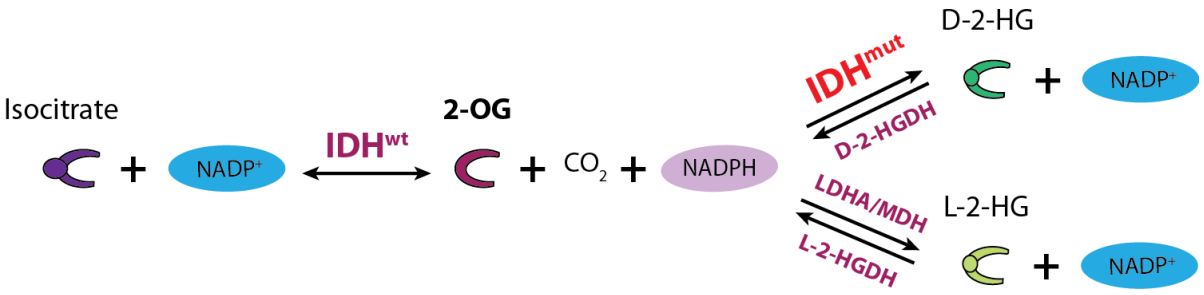

Figure 1.9. The reactions catalyzed by IDH wild-type (IDH^{wt}) and IDH mutant (IDH^{mut}) enyzmes.
IDH wild-type enzymes converts isocitrate to 2-OG while producing byproducts CO_2 and NADPH, in TCA cycle. Mutation in IDH active site leads to gain of function with a neomorphic activity of the enzyme. IDH mutant enzymes use 2-OG and NADPH as substrates and exclusively produce D-2-HG. D-2-HG and L-2-HG have been shown to act as oncometabolites, which are normally produced at very low levels in the cells, whereas accumulation of 2-HG is known to be linked to the pathogenesis of cancer and some rare disorders. LDHA, lactate dehydrogenase A; MDH, malate dehydrogenase.

Whether IDH mutation and D-2-HG induced metabolic changes contribute to the initiation or progression of cancer is still a topic of some debate. However, since the identification of IDH mutation, several studies have been performed to reveal the underlying molecular mechanisms. One proposed mechanism how mutant IDH contributes to tumorigenesis is through changes in DNA and histone methylation, which regulate gene expression epigenetically. The strongest support for this hypothesis comes from studies in glioma and AML. Expression of mutant IDH induces histone hypermethylation and alters genome-wide DNA methylation (Chowdhury, et al., 2011b, Xu et al., 2011, Duncan et al., 2012, Turcan et al., 2012, Venneti et al., 2013). Moreover, IDH mutation status is correlated with the CpG island methylation phenotype in glioma (Noushmehr, et al., 2010). It was shown that elevated D-2-HG levels by IDH mutation inhibit differentiation, which was demonstrated by overexpressing mutant IDH and treatment with cell permeable D-2-HG, whereas an inhibitor of mutant IDH induced differentiation. Moreover, expression of mutant IDH or D-2-HG treatment enhanced the proliferation and colony formation of astrocytes and TF-1 cells. D-2-HG produced by mutant IDH inhibits TET2 function, blocks the differentiation and increases stem cell maintenance in hematopoietic cells. In line with these findings, D-2-HG inhibits histone demethylase activity, thereby leading to impaired histone methylation, resulting in cell differentiation blockage. Altogether,

different studies demonstrated that IDH mutation and elevated D-2-HG levels abrogate cellular differentiation in tumors through epigenetic rewiring (Figueroa et al., 2010, Koivunen et al., 2012, Lu et al., 2012, Losman and Kaelin, 2013, Rohle et al., 2013, Wang et al., 2013a). Even if overexpression of mutant IDH confers a growth advantage to astrocytes and TF-1 cells, IDH mutation decreases the cell proliferation in the primary glioblastoma cell line U87. Conversely, in a biologically more relevant model, inhibition of IDH mutant enzyme in patient derived glioma cells, carrying IDH mutation in one allele, reduces proliferation and enhances glioma differentiation (Bralten et al., 2011, Rohle, et al., 2013).

Other 2-OG dependent dioxygenases, involved in the response to oxygen availability, are PHDs. Initially it has been reported that IDH mutation inhibits PHD activity, thereby leading to HIF-α stabilization (Zhao, et al., 2009, Xu, et al., 2011, Sasaki et al., 2012a, Izquierdo-Garcia et al., 2015). Subsequent studies had challenged this observation by reporting either unchanged (Metellus et al., 2011, Sasaki et al., 2012b, Bardella et al., 2016) or diminished HIF-α levels (Koivunen, et al., 2012, Chesnelong et al., 2014, Kickingereder et al., 2015, Miroshnikova et al., 2016). These studies reflect the complexity of the link between mutant IDH-induced D-2-HG and HIF activity. Koivunen et al. claimed that D-2-HG does not inhibit, but rather stimulate PDH activity (Koivunen, et al., 2012). However, it was shown that 2-HG is oxidized to 2-OG non-enzymatically, which might explain the 2-HG induced PHD activity (Tarhonskaya et al., 2014). Collagen hydroxylases such as P4H (Prolyl 4-hydroxylase) and PLOD (procollagen lysyl hydroxylase) are 2-OG dependent hydroxylases, involved in the biosynthesis and stability of collagen. D-2-HG has also been shown to inhibit P4HA1 (Prolyl 4-hydroxylase subunit alpha-1) and cause defects in collagen maturation (Koivunen, et al., 2012, Sasaki, et al., 2012a).

In addition to cancer, IDH mutation has been linked to the pathogenesis of rare disorders, including Ollier disease, Maffucci syndrome and D-2-hydroxyglutaric aciduria (D-2-HGA). Patients with Ollier disease and Maffucci syndrome develop cartilaginous tumors, glioma or AML during childhood. Interestingly, around 65% of the patients develop IDH mutated tumors while their physiological tissue expresses

wild-type IDH, suggesting that IDH mutations occur during the embryonic development in a somatic mosaic pattern (Balss, et al., 2008, Amary, et al., 2011a, Amary et al., 2011b, Pansuriya et al., 2011). D-2-HGA is a rare inherited neurometabolic disease, characterized by elevated D-2-HG levels and caused by mutations in D-2-HGDH or IDH genes. D-2-HGA patients are characterized by cardiomyopathy, mental retardation, hypotonia, and cortical blindness. Another neurometabolic disease with severe symptoms is L-2-hydroxyglutaric aciduria (L-2-HGA) which is a result of a mutation in L-2-HGDH. Interestingly, L-2-HGA affects the central nervous system and the patients have an increased incidence of glioma (Kranendijk et al., 2010a, Kranendijk et al., 2010b, Kranendijk et al., 2012, Akbay et al., 2014).

1.3.3 pH regulation and acidic tumor microenvironment

One characteristic of solid tumors is the acidification of the tumor microenvironment, which is caused by hypoxia and altered metabolism in tumor cells (Warburg, 1956b, Gatenby and Gillies, 2004). Upregulation of glycolysis, a highly active pentose phosphate pathway, increased glutaminolysis and hypoxia in tumor cells produce lactate and CO_2, which are the main source of the extracellular acidosis (Fig. 1.10) (Kato et al., 2013, Bohme and Bosserhoff, 2016). Tumor cells not only produce acidic metabolites but also enhance the export of acidic metabolites to the extracellular space to maintain intracellular pH levels. In most tumors, the intracellular pH is between 7.0 and 7.4, whereas extracellular pH values are much lower. In brain tumors, extracellular pH has been shown to reach as low as 5.9, while the mean in all tumors is around 6.9 (Vaupel et al., 1989, Kato, et al., 2013, Bohme and Bosserhoff, 2016).

Glycolysis is elevated under normoxia or hypoxia in tumor cells (Warburg effect). Tumor cells exhibit up to 200 times higher glycolysis rates than normal cells (Warburg, 1956b). Tumor cells adapt their metabolism to favor glycolysis by increased glucose uptake, thereby promoting higher lactate production (Bohme and Bosserhoff, 2016). Hypoxia regulates the expression or activity of glycolytic enzymes, HK1, HK2, PDK, LDH and transporters, GLUT1 as well as CAIX and MCT4. Increased GLUT

expression and HK activity elevate the intracellular glucose availability. Furthermore, upregulation of LDH increases the conversion of pyruvate to lactate and hypoxic inhibition of PDK prevents pyruvate to enter the TCA cycle. Monocarboxylate transporters (MCT), which are co-transporters of hydrogen protons with lactate, and carbonic anhydrases (CA), which hydrate the CO_2 to hydrogen protons and bicarbonate, contribute to the maintenance of intracellular alkaline pH (Swietach et al., 2007, Chiche et al., 2010, Kato, et al., 2013). Therefore, hypoxic regulation of several genes, which play a role in pH regulation, shows that the HIF pathway is closely linked to the acidification of the tumor microenvironment. However, the presence of oxygenated but acidic tumor regions demonstrate that hypoxia is not the only driver of an acidic tumor microenvironment (Fukumura et al., 2001, Swietach, et al., 2007, Chiche, et al., 2010, Kato, et al., 2013, Bohme and Bosserhoff, 2016).

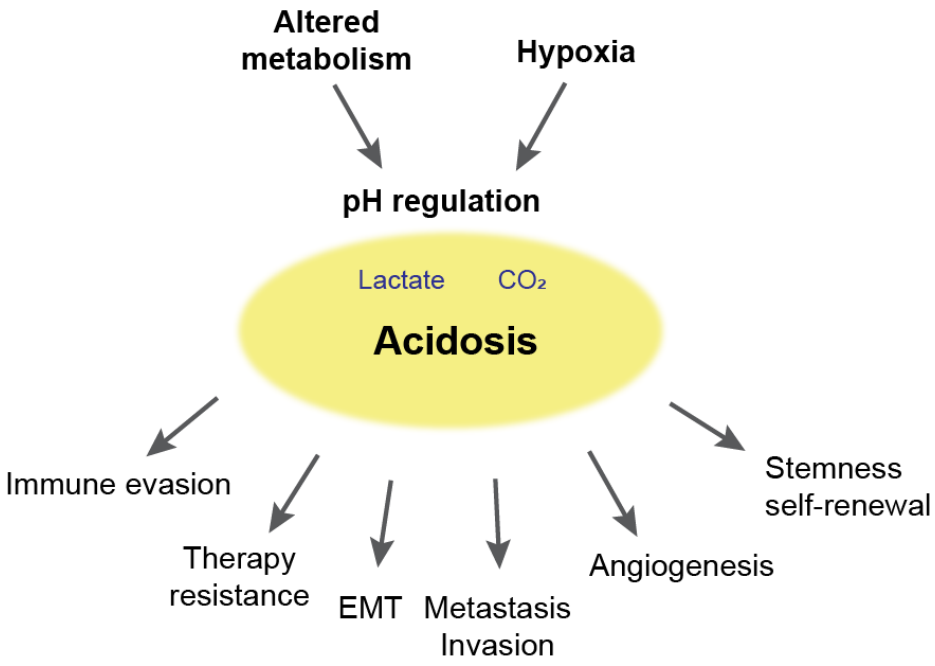

Figure 1.10. The acidic tumor microenvironment.
Altered metabolism and hypoxia cause the production of acidic metabolites (e.g. lactate and CO_2) that are exported to the extracellular space. In turn, the acidic tumor microenvironment stimulates multiple biological processes in the tumor.

The acidic tumor microenvironment regulates multiple biological processes, including immune evasion, therapy resistance, angiogenesis, EMT, metastasis and stem cell maintenance (Fig. 1.10). The acidic tumor microenvironment also affects stromal cells,

immune cells and the blood vessel system. Acidosis has been reported to reduce the activity of natural killer cells and the release of cytokines, affecting the immune response. Acidosis also induces apoptosis and inhibits cell proliferation. However, acidosis can select tumor cells that are resistant to the acidic tumor microenvironment, which may give an advantage for tumor growth. In addition, acidic pH also affects the uptake of drugs, thereby modulating therapy response (Gatenby and Gillies, 2004, Kato, et al., 2013).

In gliomas, acidosis has been shown to induce VEGFA expression, which potentially increases angiogenesis (Fukumura, et al., 2001). Additionally, in other solid tumors, acidosis has been shown to induce MMP-2, MMP-9, cathepsin B, VEGFA and IL-8, contributing to enhanced metastasis, invasion and angiogenesis. Inhibition of MMPs, which play an important role in proteolysis of the extracellular matrix, reduces tumor cell invasion, growth and angiogenesis in glioblastoma (Xu et al., 2002, Kato et al., 2005, Kato, et al., 2013). Acidosis also plays a role in stem cell maintenance in glioblastoma. Hjelmeland *et al.* showed that an extracellular pH of 6.5 increases the expression of stem cell markers, such as Oct4, Olig2 and Nanog, and angiogenic factors like IL-8 and VEGFA, which is associated with increased HIF-2α (Hjelmeland et al., 2011).

An acidic microenvironment is toxic for many cells, including normal and tumor cells. However, tumor cells adapt to the acidic stress, which results in aggressive and therapy resistant tumors. Therefore, understanding the mechanisms that play a role in pH sensing and acidic adaptation are important in order to elucidate the role of acidosis in tumor growth.

1.4 Angiogenesis and anti-angiogenic therapy in brain tumors

Angiogenesis is a process that plays a pivotal role in cancer progression by providing oxygen and nutrients to support the growth and survival of tumor cells. Physiological angiogenesis is regulated by the balance between pro-angiogenic and anti-angiogenic

factors generating normal vessels capable of sustaining the perfusion of the tissue. In contrast, tumors lack this balance and the tumor vasculature is structurally and functionally abnormal, leading to reduced perfusion. Different types of angiogenic processes have been reported to be involved in tumor development: sprouting angiogenesis, intussusceptive angiogenesis (also known as nonsprouting or splitting angiogenesis), postnatal vasculogenesis, vasculogenic mimicry and vascular co-option (Ronca et al., 2017). Sprouting angiogenesis, the growth of new blood vessels from preexisting ones, is the general form of angiogenesis. Sprouting angiogenesis is endothelial cell growth towards a pro-angiogenic stimulus, such as VEGF, from preexisting vessels, generating new sprouts. In this multistep process, tip cells, stalk cells and pericytes are involved (Welti et al., 2013). In intussusceptive angiogenesis, new blood vessels are created by splitting a preexisting blood vessel into two (Ribatti and Djonov, 2012). Postnatal vasculogenesis is the recruitment of endothelial progenitor cells from the bone marrow to the tumor site to increase vascularization (Dimova et al., 2014, Moschetta et al., 2014). Vascular mimicry is the formation of microvascular channels by tumor cells providing an opportunity to tumor cells for invasion and metastatic spread (Seftor et al., 2012). Recent studies showed that CSCs may also transdifferentiate to endothelial cells or pericytes to support and generate blood vessels (Ricci-Vitiani et al., 2010, Wang et al., 2010a, Cheng et al., 2013). Another angiogenic process, vascular co-option, is a mechanism, which does not include the generation of blood vessels. Instead, tumor cells hijack the existing vessels and migrate along them, therefore requiring little or no neo-angiogenesis (Leenders et al., 2002, Donnem et al., 2013).

Angiogenic factors are important stimuli for the initiation of angiogenesis. VEGF-A is the most potent pro-angiogenic factor, due to its high expression and regulation as a response to the tumor microenvironment in glioblastoma and other tumor entities. Importantly, VEGFA is involved in several steps of angiogenesis: endothelial cell proliferation, sprouting and capillary formation (Schmidt et al., 1999, Chaudhry et al., 2001). Therefore, anti-angiogenic therapy, the blockage of angiogenic signals, has become an attractive option to restrain angiogenesis-dependent tumor growth. The anti-angiogenic therapeutics commonly used in the clinic include bevacizumab,

sunitinib, sorafenib and pazopanib. Bevacizumab (also known as Avastin) is a humanized monoclonal antibody against VEGFA, which blocks its binding with its receptors (VEGFR). Clinical studies using bevacizumab showed improved overall survival (OS) and progression-free survival (PFS) in colorectal cancer and non-small lung cancer, whereas only improvement of PFS but not OS was observed in recurrent glioma patients (Cohen et al., 2009, Castro and Aghi, 2014, Gilbert et al., 2014, Keating, 2014, Taal et al., 2014).

Anti-angiogenic therapy confers antitumor effects through the modulation of several processes. In general, anti-angiogenic therapy is believed to starve the tumor by curtailing its oxygen and nutrient supply. However, it has been shown that anti-angiogenic treatment can – at least transiently - lead to vascular normalization, thereby improving oxygen and drug delivery. Strikingly, anti-angiogenic therapy induced oxygenation has been reported to increase the tumor radiosensitivity and potentially induce the efficiency of chemotherapeutics (Winkler et al., 2004, Myers et al., 2010, Tamura et al., 2016, Tamura et al., 2017). Moreover, anti-angiogenic therapy has been reported to reduce the CSCs population, an effect potentially mediated by the depletion of the CSC niche (Calabrese et al., 2007, Folkins, et al., 2007). Importantly, VEGF blockade improves the efficiency of immunotherapy and induces apoptosis of glioma cells and CSCs (Knizetova et al., 2008, Hamerlik et al., 2012, Voron et al., 2015, Wallin et al., 2016). Although positive aspects of anti-angiogenic therapy and improved PFS were demonstrated, these effects were transient and did not improve the OS due to intrinsic or acquired resistance (Gilbert, et al., 2014, Tamura, et al., 2017).

Bevacizumab inhibits angiogenic processes relying on VEGFA, however, it does not inhibit the other angiogenic processes, such as intussusceptive angiogenesis, vasculogenic mimicry and vascular co-option. Indeed, bevacizumab treatment results in increased vascular co-option. Intrinsic or acquired resistance to anti-angiogenic therapy causes therapy failure and remains a challenge (Jimenez-Valerio and Casanovas, 2017, Mahase et al., 2017, Ronca, et al., 2017). Therefore, several groups have been focusing on the mechanisms involved in resistance to anti-

angiogenic therapy. Those include vascular independence of tumor cells, activation of alternative pro-angiogenic mechanisms and factors, hijacking the preexisting vessels, recruitment of pro-angiogenic stromal cells and adaptation to anti-angiogenic therapy-induced hypoxia (Jimenez-Valerio and Casanovas, 2017, Ronca, et al., 2017, Tamura, et al., 2017). Bevacizumab itself and bevacizumab-induced hypoxia enhance invasion and migration in glioma. MMPs have been shown to be upregulated after bevacizumab treatment and they are associated with anti-angiogenic therapy resistance. In addition, c-MET, Dll4 and β1 integrin expression, as well as STAT3 pathway activation are correlated to anti-angiogenic therapy resistance in glioma (Zhang et al., 2015b, Tamura, et al., 2017).

Taken together, anti-angiogenic therapy and the mechanism of anti-angiogenic therapy resistance remain an important challenge. However, understanding the molecular mechanisms of resistance might help to identify new therapeutic strategies or a better pre-selection of patient groups.

1.4.1 Eph receptors and ephrin ligands

Dissection of angiogenic processes at the molecular level revealed that among the multiple factors involved in the regulation of angiogenesis, axon guidance molecules like netrins, Slit proteins, semaphorins and ephrins play an important role (Ronca, et al., 2017). The largest receptor protein-tyrosine kinase (RTK) family, the Eph (erythropoietin-producing human hepatocellular carcinoma) receptors, and their ligands, the ephrins, were initially regarded as axon guidance molecules. Now, ephrins and Ephs are known to be involved in various biological processes; development, tissue homeostasis, angiogenesis, cell migration and cancer (Pitulescu and Adams, 2010, Kania and Klein, 2016). Eight ephrin ligands and fourteen Eph receptors have been identified in humans. Based on their structure and linkage to the cell membrane, ephrin ligands are divided into two subgroups. There are five ephrinA ligands which are glycosylphosphatidylinositol-linked to the membrane and three transmembrane ephrinB ligands (Fig. 1.11). Therefore, based on Eph receptor structure similarity and binding affinity to their ligands ephrinA or ephrinB, Eph receptors are also divided into

two subclasses, the EphA and EphB receptors (Eph Nomenclature, Hirai et al., 1987, Gale et al., 1996).

In contrast to most of the RTK ligands, ephrinA and ephrinB ligands are membrane bound proteins, mediating signal transduction by cell-cell contact. Both classes of ephrin ligands share Eph receptor-binding domains at the extracellular part. Receptors of the ephrinA class are anchored to the membrane with a glycosylphosphatidylinositol (GPI) domain, whereas the ephrinB class contains a transmembrane domain, a short cytoplasmic region with several phosphorylation sites and an intracellular PDZ binding motif. EphA and EphB receptors have similar structures, consisting of the same domains: a ligand-binding domain followed by a cysteine-rich region and Fibronectin III repeats at the extracellular part; at the intracellular part, Eph receptors are composed of a juxtamembrane region, a kinase domain, a SAM (sterile α motif) domain and a PDZ binding motif at the C-terminus (Fig. 1.11) (Gale, et al., 1996, Himanen et al., 2001, Toth et al., 2001, Himanen and Nikolov, 2003).

One of the unique characteristics of Eph-ephrin signaling is the initiation of bidirectional signaling upon Eph-ephrin binding; Eph activated signaling in Eph expressing cells (forward signaling) and signaling activated by ephrin in ephrin expressing cells (reverse signaling) occurs. Moreover, depending on the cellular context, activation of the same Eph-ephrin signaling might result in an opposite outcome. One of the attributes making the Eph-ephrin system so complex is the activation of various signaling modes; forward, reverse, bidirectional, parallel and anti-parallel modes. Modes, or the direction of signal transduction might vary depending on the distribution of Ephs and ephrins in the cells and different Eph-ephrin pairs. In addition to this complexity, ligand-dependent and ligand-independent crosstalk with other RTKs and extracellular matrix proteins are known to occur (Pasquale, 2010, Gucciardo et al., 2014, Kania and Klein, 2016).

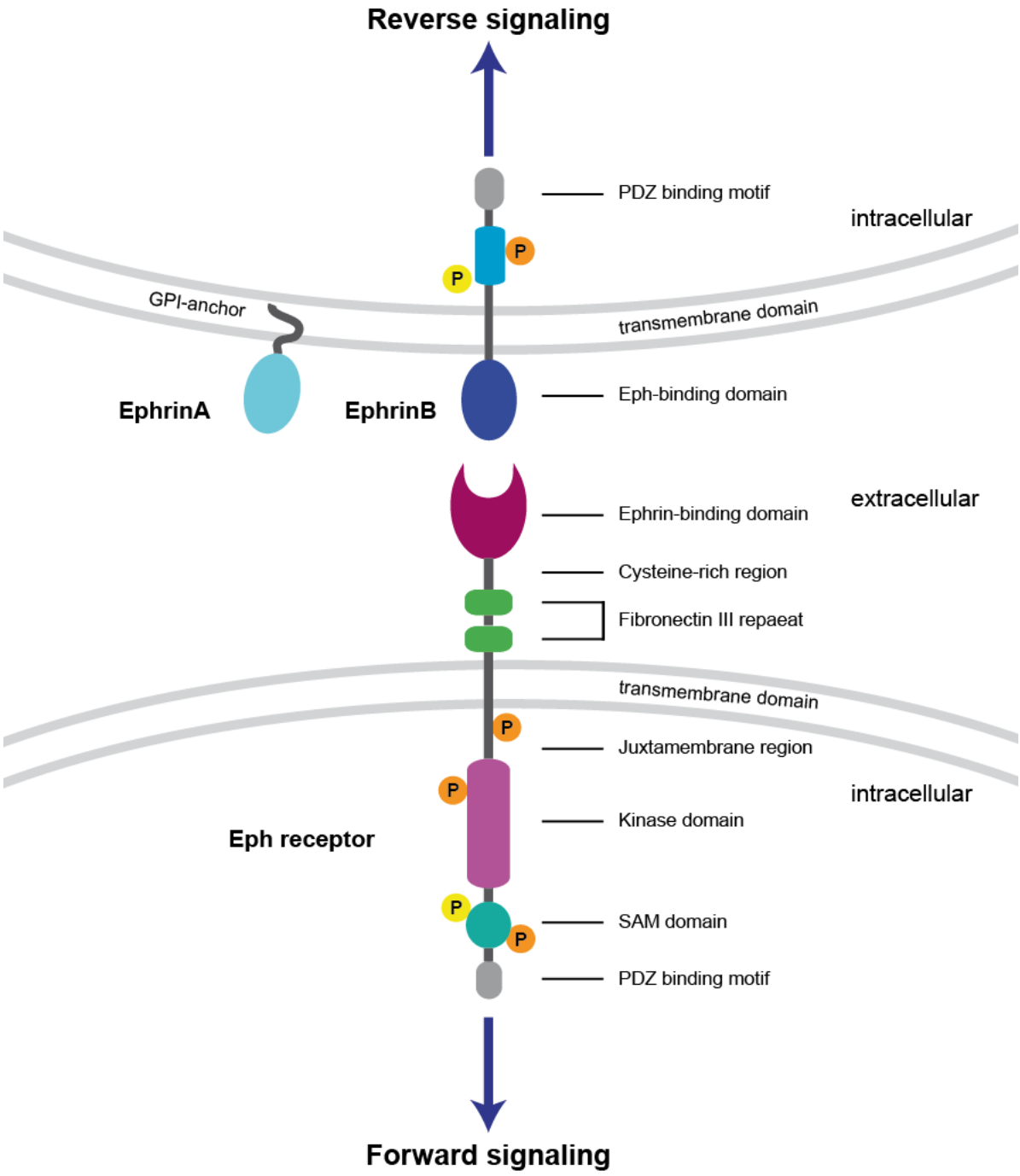

Figure 1.11. Structure of Eph receptors and ephrin ligands.
Eph receptors and ephrin ligands are membrane bound molecules mediating signal transduction by cell-cell contact. Eph receptors and ephrin ligands are divided into two classes, A and B. EphA and EphB receptors consist of the same domains whereas ephrinA and ephrinB ligands differ in domain structure. Eph-ephrin binding triggers bidirectional signaling; forward signaling in the Eph expressing cell and reverse signaling in the ephrin expressing cell. Depending on the direction of signal, the mode of signal transduction varies. Redrawn and modified from (Kania and Klein, 2016).

Forward signaling upon ligand binding is activated by Eph clustering, forming signaling centers, as well as the phosphorylation of tyrosine residues in the juxtamembrane region and kinase domain. Phosphorylated tyrosine residues in the receptor serve as docking sites for the adaptor proteins such as Src Homology 2 (SH2) and phosphotyrosine binding domain-containing proteins (PTP) (Binns et al., 2000, Himanen et al., 2010, Janes et al., 2012). Adaptor proteins link the receptors and multiple downstream signaling molecules resulting in activation of the PI3K-AKT, JNK/STAT, and RAS/MAPK pathways. In addition to these pathways, Eph receptor activation regulates focal adhesion kinase (FAK) and Scr kinase mediated signals and Rho GTPase-mediated actin dynamics (Pasquale, 2008, Gucciardo, et al., 2014, Kania and Klein, 2016). Eph-ephrin (receptor-ligand) interaction triggers also reverse signaling in ephrin expressing cells. ephrinA mediated reverse signaling relies on lipid raft-mediated clustering with Src kinases, whereas Eph-ephrinB interaction transduces the signaling via phosphorylation in the cytoplasmic tail and the recruitment of SH2 and PDZ containing proteins. Reverse signal activation modulates biological processes such as cell-cell contact and cell migration (Palmer et al., 2002, Gucciardo, et al., 2014, Kania and Klein, 2016).

1.4.1.1 Eph-ephrin signaling in tumors

Eph-ephrin signaling has been well studied in neural development, where it contributes to neuronal progenitor proliferation, differentiation, axon guidance and synaptic plasticity. Moreover, Eph-ephrin signaling is involved in other biological processes including the establishment of stable tissue boundaries and tissue separation, remodeling of vessels, cell motility and migration, maintenance of stem cells and modulation of angiogenesis (Pasquale, 2008, Kania and Klein, 2016). Interestingly, all these processes are known to be deregulated in cancer. Eph receptors and ephrin ligands have been shown to be upregulated or downregulated in cancer, co-operating with multiple pathways (Pasquale, 2010, Gucciardo, et al., 2014).

The studies on the involvement of the Eph-ephrin system in tumor initiation or progression produced incongruous results. Depending on the cellular context and the specific Eph-ephrin pair, the same Ephs and ephrins are able to mediate tumor-

suppressive or oncogenic signals, showing that Eph-ephrin signaling is fraught with complexity and nuance (Pasquale, 2010, Gucciardo, et al., 2014, Lodola et al., 2017). It has been shown that EphB2 signaling suppresses the proliferation of tumor cells and abrogates cell migration and invasive tumor growth, therefore functioning as a tumor-suppressive system. Interestingly, EphB2 expression is shown to be downregulated or lost by mutation in prostate and colorectal cancers. Furthermore, EphB2 downregulation is associated with higher tumor grade in colorectal cancer (Huusko et al., 2004, Batlle et al., 2005, Cortina et al., 2007). Similar to EphB2, EphB4 signaling has been shown to inhibit tumor cell invasion and motility in a ligand-dependent manner in breast cancer (Noren et al., 2006). In contrast to these studies, EphB2 expression has been shown to be higher in lung cancer cells, and high EphB2 expression is correlated with poor patient survival, indicating an oncogenic role of EphB2 in this tumor entity (Zhao et al., 2017). EphA2 overexpression or EphB1 phosphorylation suppress glioblastoma cell migration and invasion (Wykosky and Debinski, 2008, Ferluga et al., 2013, Teng et al., 2013), whereas EphB2 overexpression promote an invasive phenotype in glioblastoma cells and GSCs (Nakada et al., 2004, Wang et al., 2012), displaying opposite outcome depending on the Eph receptor type.

Not only tumor cells, but also stromal cells such as endothelial and inflammatory cells, express Ephs and ephrins, might interact with tumor cells and initiate the crosstalk between tumor and stromal cells by mediating repulsive or attractive signals. Ephs and ephrins are involved in tumor angiogenesis and upregulated in the tumor vasculature. EphB4 expressing tumor cells can activate ephrinB2 reverse signaling in endothelial cells stimulating tumor angiogenesis. Regulation of tumor angiogenesis by ephrinB2 has been shown to be mediated through VEGFR signaling (Noren et al., 2004, Sawamiphak et al., 2010, Wang et al., 2010b).

Taken together, all these studies implicate the importance of the Eph-ephrin system in cancer. Therapies targeting Eph-ephrin signaling might be a promising strategy for the inactivation of oncogenic Eph-ephrin signals. However, different cellular outcomes in Eph or ephrin expressing cells and activation of different signaling pathways even

with the same Eph-ephrin pair might limit the success of the treatments. Therefore, elucidating downstream mediators of Ehp-ephrin signaling remains an important task to understand and differentiate Eph-ephrin mediated tumor-suppressive or oncogenic signals.

1.5 Mesenchymal transition in gliomas

Glioblastomas are aggressive and infiltrative tumors, limiting the efficiency of current therapies. Aggressive glioblastomas are characterized by enhanced invasive behavior of tumor cells into the brain parenchyma. The majority of the aggressive glioblastomas with highly invasive nature and poor prognosis exhibits a mesenchymal phenotype (Verhaak, et al., 2010, Louis, et al., 2016). These observations indicate the existence of mesenchymal transition in gliomas, analogous to the epithelial-to-mesenchymal transition (EMT)-like processes observed in carcinomas, driving the key molecular changes necessary for invasion.

EMT has been studied extensively in epithelial tumors, which commonly metastasize to distant organs. EMT is a biological process changing cellular features of the tumor cells, including the loss of cell-cell contacts and increased cell motility, leading to the acquisition of an invasive/mesenchymal phenotype. EMT is associated with tumor therapy resistance and is regulated by factors in the tumor microenvironment, such as hypoxia and TGFβ (Lee et al., 2006, Kalluri and Weinberg, 2009, Lamouille et al., 2014).

EMT is also involved in the acquisition of a stem cell phenotype in tumors (Mani et al., 2008). Mesenchymal transition and the cancer stem cell phenotype display overlapping features such as therapy resistance and aggressive tumor formation. A recent study showed the overlap of the mesenchymal phenotype with both EMT markers and CD133 expression levels in glioblastoma patients. In another study, association between the mesenchymal subtype and CD44, a stem cell and EMT marker, was shown. In addition, CD44 expression levels are correlated with increased tumor invasion and poor prognosis. These findings suggest a link between the

molecular phenotype of tumors and the EMT process, controlling tumor aggressiveness (Kim et al., 2013, Zarkoob et al., 2013, Karsy et al., 2016).

1.5.1 EMT regulators

During the process of EMT, epithelial tumor cells detach from the basement membrane. Glioma cells lack the tissue components and important cell-cell contact factors, existing in epithelial cells, but still both cell types are able to migrate, spread and disseminate to the surrounding tissue. Recent studies have shown that several EMT regulators, such as Snail, Slug, Twist, ZEB1 and ZEB2, known from epithelial tumors, play a critical role in the activation of mesenchymal features in glioma. Interestingly, recurrent glioblastomas, which originate from low grade gliomas, displayed high expression levels of EMT regulators and markers (Mikheeva et al., 2010, Cheng et al., 2012b, Kahlert et al., 2013, Myung et al., 2014, Iser et al., 2016, Iwadate, 2016).

Snail (also known as Snail1) and Slug (also known as Snail2) are members of the SNAIL family of transcriptional factors mostly acting as repressors. Both members regulate the EMT phenotype through repression of various epithelial markers and the upregulation of mesenchymal markers (Lamouille, et al., 2014). Snail and Slug expression levels are regulated at transcriptional and protein level. Snail and Slug expression levels are controlled by direct binding of several transcription factors, such as Notch intracellular domain, LOXL2, NF-κB, HIF-1α, IKKα, SMAD, HMGA2, Egr-1, PARP-1, STAT3, MTA3 and Gli1. Tumor microenvironment induced signaling pathways including hypoxia, TGFβ, TNF, Wnt and Notch lead to activation of these transcription factors. Posttranscriptional modifications such as phosphorylation also control the translocation or degradation of the Snail and Slug (Kaufhold and Bonavida, 2014, Iser, et al., 2016, Iwadate, 2016).

Studies investigating the role of Snail and Slug in glioblastoma showed that depletion of Snail in glioblastoma cells decreased proliferation, invasion and migration of the cells, whereas overexpression of Snail increased the invasion (Han et al., 2011,

Savary et al., 2013, Myung, et al., 2014). Slug is also involved in the invasive phenotype. Slug expression levels correlate with the malignancy of glioblastoma in patients. Overexpression of Slug in glioblastoma cells increases the proliferation and invasion *in vitro* and enhances the tumor growth *in vivo* (Yang et al., 2010).

Another EMT regulator, Twist has also been reported to be associated with EMT in gliomas. A higher Twist expression level correlates with higher malignancy of glioma cells and Twist promotes invasion in glioma cells. EMT related genes such as Slug, MMP-2, HGF, FAP and FN1 are upregulated by Twist and inhibition of Twist results in decreased invasive capacity of glioma cells (Elias et al., 2005, Mikheeva, et al., 2010, Nagaishi et al., 2012). Another study showed that Twist and Sox2 synergistically induce the invasive phenotype in glioblastoma. In addition, knock-down of Twist or Sox2 reduced cancer stem cell maintenance and downregulated mesenchymal markers (Velpula et al., 2011). Interestingly, a hypoxic tumor microenvironment which is known to control cancer stem cell maintenance, also induces the expression level of Twist directly by HIF-1α (Yang, et al., 2008).

ZEBs are known to regulate tumor invasiveness, resistance to therapy and tumor progression in other cancer types (Sanchez-Tillo et al., 2011). ZEB1 and ZEB2 are also related to mesenchymal transition in glioblastoma. Siebzehnrubl *et al.* observed that ZEB1 expression is associated with shorter patient survival. ZEB1 controls tumor invasiveness, chemoresistance and stem cell capacity of the cells through miR-200 inhibition (Siebzehnrubl et al., 2013). Similarly, ZEB2 levels correlate with tumor malignancy and ZEB2 knock-down abrogates the invasive phenotype and reduces the proliferation of glioma cells (Qi et al., 2012). Multiple signaling pathways such TGFβ/SMAD signaling and hypoxia have been shown to regulate ZEB expression levels (Postigo et al., 2003, Depner et al., 2016).

1.5.2 Signaling pathways involved in EMT

EMT is a complex and reversible biological process and several signals from the tumor microenvironment orchestrate this process by activating multiple signaling pathways,

resulting in induced EMT. The cells at the invasive front of the tumor commonly undergo EMT. These cells with more mesenchymal characteristics enter the blood stream, migrate into distant organs and there microenvironmental signals subsequently revert this process (mesenchymal to epithelial transition, MET) to establishes metastasis.

The TGFβ signaling pathway is well known for its tumor suppressing and tumor promoting effects. Tumor cells develop mechanisms that enable the cells to evade TGFβ mediated tumor suppressive signals, so that TGFβ starts acting as an oncogenic factor (Seoane, 2006). TGFβ activates two signaling pathways, one of them SMAD-dependent, the other a SMAD-independent. In the SMAD-dependent pathway, after TGFβ binding to its receptors, SMAD2/3 proteins are activated by the receptors. The active SMAD complex translocates into the nucleus, interacts with DNA binding proteins and recruits corepressors or coactivators to regulate the target genes. In the SMAD-independent pathway, TGFβ activates the PI3K/AKT and ERK/MAPK signaling pathway (Iser, et al., 2016, Moustakas and Heldin, 2016, Zhang et al., 2016).

Recent studies investigated the contribution of the TGFβ signaling pathway to glioma tumorigenesis. Seoane *et al.* showed that glioblastoma cells escape from the antiproliferative effect of TGFβ by FoxG1 and PI3K mediated inhibition of the SMAD/FoxO complex (Seoane et al., 2004). Moreover, PDGF-B methylation status has been shown to be critical for the oncogenic role of TGFβ. In highly aggressive and proliferative gliomas, hyperactivated TGFβ/SMAD signaling induces PDGF-B expression, leading to glioblastoma proliferation, whereas a methylated PDGF-B status blocks the proliferative effect of TGFβ/SMAD signaling. High TGFβ/SMAD activity is associated with poor prognosis in PDGF-B unmethylated patients, indicating that the methylation status of the PDGF-B gene defines the oncogenic role of TGFβ in glioma patients (Bruna et al., 2007). TGFβ also acts as an inducer of EMT like processes in glioblastoma, resulting in enhanced invasion and migration. TGFβ mediated increase in SMAD2 activation and ZEB1 levels promote the mesenchymal phenotype, which is associated with enhanced invasion and mesenchymal marker expression (Joseph et al., 2014). High expression of TGFβ and Twist adjacent to

pseudopalisading necrotic areas, correlating with decreased patient overall survival, has also been reported (Iwadate et al., 2016).

The Wnt/β-catenin pathway is another pathway regulating the EMT phenotype. Activation of Wnt causes β-catenin translocation into the nucleus where it acts as a transcription factor activating its target genes. The Wnt/β-catenin pathway is associated with reduced overall patient survival and the mesenchymal subgroup in glioblastoma. The Wnt/β-catenin pathway has been shown to regulate EMT associated genes such as Twist, ZEB1, Snail and Slug (Liu et al., 2011, Kahlert et al., 2012, Paul et al., 2013).

One of the hallmarks of glioblastoma is the existence of necrotic areas resulting from limited oxygen supply. Necrotic areas are surrounded by highly hypoxic pseudopalisading areas. Hypoxia regulates the mesenchymal phenotype and enhances invasion and migration in glioblastoma. Anti-VEGF antibody treatment by bevacizumab, induces more hypoxic areas leading to overexpression of EMT regulators such as Twist, ZEB1, ZEB2, Snail and Slug in patients (Joseph et al., 2015, Kahlert et al., 2015, Xu et al., 2015, Karsy, et al., 2016).

2 Aim of the thesis project

Glioblastomas are the most common and the most aggressive malignant brain tumors. Conventional therapies such as chemo and/or radiotherapy after surgical resection still remain insufficient to cure the patients, as incomplete eradication frequently results in tumor recurrence. Molecular alterations in the tumor cells, the reprogramming of tumor cell metabolism, as well as the crosstalk between tumor cells and the tumor microenvironment assist adaptive and evasive behaviors of tumor cells. Importantly, the tumor microenvironment, metabolism and phenotype interact with each other. Recent studies have demonstrated that tumor metabolism and metabolic enzymes contribute to tumor initiation and progression. Moreover, a hypoxic and acidic tumor microenvironment and signaling pathways regulated by this tumor microenvironment are known to control cellular dedifferentiation, invasion and evasive response to anti-angiogenic therapy. However, the molecular mechanisms involved in these processes and the contribution of metabolism are so far only partly understood.

The project presented in this thesis aimed to examine three questions at the intersection of tumor metabolism and the tumor microenvironment. **First**, we aimed to analyze the function of IDH1 in the regulation of 2-OG and 2-OG dependent enzyme activity, specifically PHD activity, and identify microenvironmental factors regulating IDH1 levels. Furthermore, we wanted to examine the 2-OG dependent phenotypical changes mediated by IDH1 (such as cancer stem cell maintenance and epithelial-to-mesenchymal transition) using cell culture based assays and *in vivo* tumor models. **Second**, we aimed to investigate the molecular mechanisms mediating the role of acidosis in regulating the hypoxic response and cancer stem cell maintenance. In particular, we wanted to assess the role of HSP90 in the acidosis induced hypoxic response and its effect on tumor cell self-renewal and tumor growth. **Third**, we aimed to characterize the function of ephrinB2 in the hypoxic tumor microenvironment, especially its role in mediating an anti-angiogenic therapy-induced invasive phenotype.

3 Materials and methods

3.1 Materials

3.1.1 Chemicals

Solvents and standard chemicals were, if not indicated differently, purchased from Sigma-Aldrich, Carl Roth, Merck, or AppliChem.

3.1.2 Antibiotics

All the stock solutions were sterile filtered before use (0.22 µm, # SLGV033RS, Millipore).

Table 3.1. Antibiotics for selection of bacterial cells.

Antibiotic	Stock solution	Final concentration
Kanamycin (# K-1377, Sigma-Aldrich)	100 mg/ml in distilled water	100 µg/ml
Ampicillin (# A9598, Sigma-Aldrich)	100 mg/ml in distilled water	50-100 µg/ml

Table 3.2. Antibiotics for selection of mammalian cells.

Antibiotic	Stock solution	Final concentration	
		Cells	Concentration
Blasticidin S HCL (# R210-01, Invitrogen)	6 mg/ml in distilled water	G55 cells	6 µg/ml
Puromycin (# P9620, Sigma-Aldrich)	10 mg/ml commercial stock solution	G55 cells	5 µg/ml
		U87 cells	2.5 µg/ml
		GBM46	2.5 µg/ml
		MDA-MB-231	5 µg/ml
G418 (Geneticin) (Gibco)	50mg/ml	Astrocytoma	500 µg/ml

3.1.3 Antibodies

3.1.3.1 Primary antibodies

Table 3.3. Primary antibodies. WB; western blotting, IHC; Immunohistochemistry, IF; Immunofluorescence

Antibody	Species	Order No.	Company	Dilution	Used for
Anti-HIF-1α	Rabbit (polyclonal)	# 10006421	Cayman Chemical	1:3000	WB, IHC
Anti-HIF-2α	Rabbit (polyclonal)	# NB100-122	Novus Biologicals	1:1000	WB
Anti-OH-HIF-1α$^{(Pro564)}$	Rabbit (monoclonal)	# 3434	Cell Signaling	1:1000	WB
Anti-IDH1	Goat	# sc-49996	Santa Cruz	1:1000	WB
Anti-IDH2	Mouse	# ab55271	Abcam	1:1000	WB
Anti-p65 (RelA) (D14E12)	Rabbit (monoclonal)	# 8242	Cell signaling	1:8000	WB, IF
Anti-CD133	Rabbit (polyclonal)	# ab19898	Abcam	1:500	WB
Anti-CD133/2 clone 293C3 APC conjugated	Mouse (monoclonal)	# 130-090-854	Miltenyi Biotech		FACS
Anti-CD133 clone W6B3C1	Mouse (monoclonal)	# 130-092-395	Miltenyi Biotech	1:100	IHC
Anti-CD15	Mouse (monoclonal)	# 642917	BD Horizon		FACS
Anti-Snail	Rat (monoclonal)	# 4719	Cell Signaling	1:500	WB
Anti-Slug	Rabbit (monoclonal)	# 9585	Cell Signaling	1:500	WB
Anti-T-cadherin	Mouse (monoclonal)	# sc-166875	Santa Cruz	1:1000	WB

Anti-CD44	Mouse (monoclonal)	# 3570	Cell Signaling	1:5000	WB
Anti-ZEB1	Rabbit (polyclonal)	# sc-25388	Santa Cruz	1:1000	WB
Anti-ZEB2	Mouse (monoclonal)	# sc-271984	Santa Cruz	1:1000	WB
Anti-HSP90	Mouse (monoclonal)	# SPA-830	Stressgen	1:5000	WB, IHC
Anti-HA tag	Mouse (monoclonal)	# 901513	BioLegend	1:1000	WB
Anti-ephrinB2	Goat (polyclonal)	# AF496	R&D Systems	1:2000	WB
Anti-EphB4	Goat (polyclonal)	# AF446	R&D Systems	1:1000	WB
Anti-Tubulin	Mouse (monoclonal)	# DLN-09992	Dianova	1:8000	WB
Anti-Endomucin	Mouse (monoclonal)	# 14-5851-82	eBioscience	1:500	IF
Anti-human nuclei	Mouse (monoclonal)	# MAB4383	Millipore/ chemicon	1:200	IF

3.1.3.2 Secondary antibodies

Table 3.4. Secondary antibodies. WB; western blotting, IHC; Immunohistochemistry, IF; Immunofluorescence

Antibody	**Order No.**	**Company**	**Dilution**	**Used for**
Goat anti rabbit IgG (H+L) HRPO conjugated	# 111-035-144	Dianova	1:5000	WB, IHC
Donkey IgG anti-Goat IgG (H+L)-HRPO conjugated	# 705-035-147	Dianova	1:5000	WB, IHC
F(ab')2 Rat IgG (H&L) Antibody Peroxidase Conjugated Pre-Adsorbed	# 712-1333	Rockland	1:3000	WB, IHC

Goat IgG anti-Mouse IgG+IgM (H+L)-HRPO conjugated	# 115-035-146	Dianova	1:5000	WB, IHC
Alexa Fluor 568 goat anti rabbit IgG	# A11036	Life Technologies	1:1000	IF
Alexa Fluor 568 goat anti rat IgG	# A11077	Life Technologies	1:500	IF
Alexa Fluor 568 goat anti mouse IgG	# A11031	Life Technologies	1:500	IF

3.1.4 Protein and DNA ladders

3.1.4.1 Protein ladder

Spectra Multicolor High Range Protein Ladder, # 26616, Thermo Scientific
PageRuler Prestained Protein Ladder, # 26625, Thermo Scientific

3.1.4.2 DNA ladders

100 bp DNA Ladder, Invitrogen # 15628-018
1 kb DNA Ladder, Invitrogen # 15615-024

3.1.5 Bacterial strains

Escherichia coli DH5α: This strain was used for transformations except for the lentiviral vectors (Invitrogen).
One Shot® Stbl3™ chemically competent *E. coli*: This strain was used for cloning into lentiviral vectors.

3.1.6 Cell lines

G55: Human glioblastoma cell line (M. Westphal and K. Lamzus, Hamburg, Germany) (Westphal et al., 1994).
U87: Human glioblastoma cell line (ATCC # HTB-14)
GBM46: Primary human glioblastoma cell line obtained from a 41 year old female patient**.**

MDA-MB-231: Human breast carcinoma cell line (ATCC # HTB-26) transduced with a luciferase construct consist of firefly luciferase under control of HIF-2α-ODD and constitutively active *Renilla* luciferase. Single cell clone was created by Omelyan Trompak.

A549: Human lung carcinoma cells (ATCC # CCL-185)

Wild-type and ephrinB2 knockout astrocytoma cells: Murine high-grade gliomas (Depner, et al., 2016)

HEK293T: Human embryonic kidney cells (ATCC # CRL-3216)

3.1.6.1 Cells generated during the PhD thesis

Table 3.5. Cell pools generated in this work

Name	Construct/Lentivirus	MOI	Selection
GBM46 Co	non silencing control (Thermo Scientific)	10	Puromycin
GBM46 shIDH1 #1	pGIPZ-shIDH1 #1 (Thermo Scientific)	10	Puromycin
GBM46 shIDH1 #2	pGIPZ-shIDH1 #2 (Thermo Scientific)	10	Puromycin
GBM46 shIDH1 #3	pGIPZ-shIDH1 #3 (Thermo Scientific)	10	Puromycin
G55 Co	non silencing control (Thermo Scientific)	20	Puromycin
G55 shIDH1	pGIPZ-shIDH1 #3 (Thermo Scientific)	20	Puromycin
U87 Co	non silencing control (Thermo Scientific)	40	Puromycin
U87 shIDH1	pGIPZ-shIDH1 #3 (Thermo Scientific)	40	Puromycin
U87 shIDH2	pGIPZ-shIDH2 (Thermo Scientific)	40	Puromycin
U87 shIDH1+2	pGIPZ-shIDH1 #3 / pGIPZ-shIDH2 (Thermo Scientific)	20+20	Puromycin
MDA-MB 231 Co	non silencing control (Thermo Scientific)	50	Puromycin
MDA-MB 231 shIDH1	pGIPZ-shIDH1 #3 (Thermo Scientific)	50	Puromycin

MDA-MB 231 Co KO #1	pSpCas9(BB)-2A- Puro (PX459) V2.0 cell clone 1	-	Puromycin
MDA-MB 231 Co KO #2	pSpCas9(BB)-2A- Puro (PX459) V2.0 cell clone 2	-	Puromycin
MDA-MB 231 IDH1 KO #1	pSpCas9(BB)-2A- Puro (PX459) V2.0 IDH1 KO cell clone 1	-	Puromycin
MDA-MB 231 IDH1 KO #2	pSpCas9(BB)-2A- Puro (PX459) V2.0 IDH1 KO cell clone 2	-	Puromycin
A549 Co KO #1	pSpCas9(BB)-2A- Puro (PX459) V2.0cell clone 1	-	Puromycin
A549 231 Co KO #2	pSpCas9(BB)-2A- Puro (PX459) V2.0 cell clone 2	-	Puromycin
A549 IDH1 KO #1	pSpCas9(BB)-2A- Puro (PX459) V2.0 IDH1 KO cell clone 1	-	Puromycin
A549 IDH1 KO #2	pSpCas9(BB)-2A- Puro (PX459) V2.0 IDH1 KO cell clone 2	-	Puromycin
G55 Co	non silencing control (Thermo Scientific)	20	Puromycin
G55 shHSP90	pGIPZ-shHSP90α / pGIPZ-shHSP90β (Thermo Scientific)	10+10	Puromycin
G55 Co	pLenti6 GFP	20	Blasticidin
G55 HSP90DN	pLenti6 HA-HSP90DN	20	Blasticidin
Astrocytoma Control	pECFP-N1 (Clontech)	-	Geneticin
Astrocytoma eB2KO Control	pECFP-N1 (Clontech)	-	Geneticin
Astrocytoma eB2KO+eB2	pECFP ephrinB2-HA	-	Geneticin
G55 Control	pECFP-N1 (Clontech)	-	Geneticin
G55 ephrinB2OE	pECFP ephrinB2-HA	-	Geneticin

3.1.7 Plasmids

pCI-VSVG: Lentiviral packaging plasmid, expresses the envelope protein glycoprotein-G (#1733 Addgene, Garry Nolan)

psPAX2: Lentiviral packaging plasmid (# 12260 Addgene, Didier Trono)

pGIPZ non silencing control: Lentiviral expression vector (non targeting), The non-silencing shRNA is a negative control for any transduction experiment performed using GIPZ shRNA constructs (Open Biosystems # RHS4346)

pGIPZ-shIDH1 #1: Short hairpin RNA against human IDH1 (sequence 1) in pGIPZ lentiviral vector, (Open Biosystems # V2LHS_217815)

Mature antisense TTTCGTATGGTGCCATTTG

pGIPZ-shIDH1 #2: Short hairpin RNA against human IDH1 (sequence 2) in pGIPZ lentiviral vector, (Open Biosystems # V3LHS_320102)

Mature antisense ATGCTTCTTTATAGCTTCT

pGIPZ-shIDH1 #3: Short hairpin RNA against human IDH1 (sequence 3) in pGIPZ lentiviral vector, (Open Biosystems # V3LHS_320103)

Mature antisense TGTTATCAAGCTTTGCTCT

pGIPZ-shIDH2: Short hairpin RNA against human IDH2 in pGIPZ lentiviral vector, (Open Biosystems # V3LHS_387076)

Mature antisense TCAGTATGGTGTTCTTGGT

pGIPZ-shHSP90α: Short hairpin RNA against human HSP90α in pGIPZ lentiviral vector, (Open Biosystems # V3LHS_364791)

Mature antisense TTGTTGCAACATCTCACGG

pGIPZ-shHSP90β: Short hairpin RNA against human HSP90α in pGIPZ lentiviral vector, (Open Biosystems # V2LHS_86053)

Mature antisense TGCTTTAGTACCAGACTTG

pLenti6 GFP/V5: Lentiviral expression vector for lentiviral-based expression of GFP. GFP protein was cloned into pLenti6/V5 CMV (#V49610, Open Biosystems).

pLenti6 HA-HSP90DN: Lentiviral expression vector for lentiviral-based expression of human dominant negative mutant HSP90β. Dominant negative mutant HSP90β (#22480, Addgene) was cloned into pLenti6/V5 CMV (#V49610, Open Biosystems).

pcDNA3.1 D/V5-His-TOPO: Mammalian expression vector, CMV promoter, mammalian selection: neomycin, bacterial resistance: ampicillin, contains V5 epitope and polyhistidine (6X His) tag, (Invitrogen).

pcDNA3.1 IDH1wt: Mammalian expression vector with human IDH1.

pcDNA3.1 IDH1-3DN: Mammalian expression vector with human IDH1 with the point mutations at aspartic acid residues (273, 275 and 270) leading to an enzymatically inactive IDH1 (Koivunen, et al., 2012).

pcDNA3.1D/V5-His-TOPO.HIF-1α: Mammalian expression vector with human HIF-1α (Julia Wenner).

pcDNA3.1D/V5-His-TOPO.HIF-2α: Mammalian expression vector with human HIF-2α (Julia Wenner).

pcDNA3.1D/V5-His-TOPO.HIF-1α mPPN: Mammalian expression vector with a non-degradable sequence of human HIF-1α with mutated prolyl hydroxylation sites (Julia Wenner).

pcDNA 9X HRE luciferase: The pcDNA 9X HRE luciferase contains nine copies of an hypoxia responsive element (HRE) that drives transcription luciferase (This plasmid was a gift from Dr. Massimiliano Mazzone).

pNL3.2.NF-κB-RE[NlucP/NF-κB-RE/Hygro] Vector: The pNL3.2.NF-κB-RE[NlucP/NF-κB-RE/Hygro] Vector(a,b) contains five copies of an NF-κB response element (NF-κB-RE) that drives transcription of a destabilized form of NanoLuc® luciferase, an engineered 23.3kDa luciferase fusion protein. (# N1111, Promega)

SBE4-Luc: Firefly luciferase expression vector containing four copies of the SMAD binding element (# 16495, Addgene)

pRL-SV40: *Renilla* luciferase internal control reporter, promoter: SV40, early enhancer promoter (Promega)

pSpCas9(BB)-2A-Puro (PX459) V2.0: CRISPR mammalian expression vector carrying Cas9 (# 62988, Addgene) (Ran et al., 2013)

pSpCas9(BB)-2A-Puro (PX459) V2.0 IDH1 KO: CRISPR mammalian expression vector carrying Cas9 with guide sequence for IDH1 gene

Guide sequence 1 in exon 3: GTGTAGATCCAATTCCACGTAGGG

Guide sequence 2 in exon 7: GCATAGGCTCATCGACGACATGG

pECFP-N1: Mammalian expression vector under control of CMV promotor expressing enhanced cyan fluorescent variant of the Aequorea victoria green fluorescent protein gene (ECFP) (Clontech).

pECFP ephrinB2-HA: Mammalian expression vector under control of CMV promotor expressing enhanced cyan fluorescent variant of the Aequorea victoria green fluorescent protein gene (ECFP) (Clontech) and mouse ephrinB2 (Essmann et al., 2008).

3.1.8 Primers

All oligonucleotides were ordered from Sigma-Aldrich.

The primers were designed to be intron spanning to prevent the amplification of genomic DNA sequences.

Table 3.6. Primers for quantitative real time PCR

Primer	Sequence (5´- 3´)
ANG fw	CTGGGCGTTTTGTTGTTGGTC
ANG rev	TGGTTTGGCATCATAGTGCTG
ASPHD2 fw	CTTCGGACCTGTATTGGGAAC
ASPHD2 rev	CAGCTCACAGCCATTTGGAG
CAIX fw	AAGAAGAGGGCTCCCTGAAG
CAIX rev	TAGCGCCAATGACTCTGGTC
CCL-2 fw	TTCTGTGCCTGCTGCTCATAG
CCL-2 rev	CAGGTGACTGGGGCATTGA
CD133 fw	TTGACCGACTGAGACCCAAC
CD133 rev	AGGTGCTGTTCATGTTCTCCAAC
CD15 fw	GGTCTATCGCCGCTACTTCC
CD15 rev	AGTTCCGTATGCTCTTGGGC
Glut1 fw	GATTGGCTCCTTCTCTGTGG
Glut1 rev	CAGGATCAGCATCTCAAAGG
hephrinB2 fw	AGTTCGACAACAAGTCCCTTTG
hephrinB2 rev	AGCAATCCCTGCAAATAAGG
HIF-1α fw	CCATTAGAAAGCAGTTCCGC
HIF-1α rev	TGGGTAGGAGATGGAGATGC
HIF-2α fw	CGAACACACAAGCTCCTCTC
HIF-2α rev	GTCACCACGGCAATGAAAC

HPRT fw	TATGGCGACCCGCAGCCC
HPRT rev	GCAAGACGTTCAGTCCTGTCCAT
IDH1 fw	AGAAGCATAATGTTGGCGTCA
IDH1 rev	CGTATGGTGCCATTTGGTGATT
IDH2 fw	ACACGTGGCCTGGAGCACCG
IDH2 rev	CACATTGCTGAGGCCGTGAATGC
IDH3A fw	ACTGGTGGTGTTCAGACAGT
IDH3A rev	TGAATGGCAGTGACGTTCCG
IL-8 fw	TTTTGCCAAGGAGTGCTAAAGA
Il-8 rev	AACCCTCTGCACCCAGTTTTC
MAML3 fw	CAGCAGGTCAATCAGTTTCAAG
MAML3 rev	GGTTCTGGGAGGGTCCTATTC
Musashi fw	CCGGCTTCGGCCACAGTCTTGGG
Musashi rev	GCAGGCAGTAGCGGGTCCGAGTCG
Nanog fw	GCAGAAGGCCTCAGCACCTA
Nanog rev	AGGTTCCCAGTCGGGTTCA
Nestin fw	AGACTTCCCTCAGCTTTCAGG
Nestin rev	TGGGAGCAAAGATCCAAGAC
NFATc2 fw	CAGTGGCAGAATCGTCTCTTTAC
NFATc2 rev	GCTGTCTGTGTCTTGTCTTTCAAC
NFE2L2 fw	GACATTCCCGTTTGTAGATGAC
NFE2L2 rev	GGTGACTGAGCCTGATTAGTAGC
Oct4 fw	GCTCGAGAAGGATGTGGTCC
Oct4 rev	CGTTGTGCATAGTCGCTGCT
RelA (p65 subunit) fw	CGCATCCAGACCAACAACAA
RelA (p65 subunit) rev	CAGATCTTGAGCTCGGCAGT
Snail fw	CTTCCAGCAGCCCTACGAC
Snail rev	CGGTGGGGTTGAGGATCT
Sox2 fw	GCCGGCGGCAACCAGAAAAACAG
Sox2 rev	CCGCCGGGGCCGGTATTTAT
TNFA fw	CTTCTGCCTGCTGCACTTTG
TNFA rev	GGCCAGAGGGCTGATTAGAG
VEGFA fw	AGCCTTGCCTTGCTGCTCTA
VEGFA rev	GTGCTGGCCTTGGTGAGG

3.1.9 siRNA Oligos

siRNA oligos for transient knockdown experiments were obtained from Dharmacon. Knockdowns were performed using a pool of 4 targeting sequences.

siControl: (D-001810-10-05, SMARTpool: ON-TARGETplus Non-targeting Control siRNAs, Dharmacon)

siHIF-1α: NM_181054 (L-004018-00-0005,SMARTpool: ON-TARGETplus Human HIF-1α siRNA, Dharmacon)

siHIF-2α: NM_001430 (L-004814-00-0005,SMARTpool: ON-TARGETplus Human HIF-2α siRNA, Dharmacon)

siRELA: NM_021975.3 (L-003533-00-0005,SMARTpool: ON-TARGETplus Human RELA siRNA, Dharmacon)

siTWIST1: NM_000474.3 (LQ-006434-00-0002 ON-TARGETplus Human TWIST1 siRNA, Dharmacon)

siTWIST2: NM_057179.2 (LQ-012862-02-0002, ON-TARGETplus Human TWIST2 siRNA, Dharmacon)

siZEB1: NM_001128128.2 (LQ-006564-01-0002, ON-TARGETplus Human ZEB1 siRNA, Dharmacon)

siZEB2: NM_014795.3 (LQ-006914-02-0002, ON-TARGETplus Human ZEB2 siRNA, Dharmacon)

siSnail: NM_005985.3 (LQ-010847-01-0002, ON-TARGETplus Human Snail siRNA, Dharmacon)

siSlug: NM_003068.4 (LQ-017386-00-0002, ON-TARGETplus Human Slug siRNA, Dharmacon)

siLOXL2: NM_002318.2 (LQ-008020-01-0002, ON-TARGETplus Human LOXL2 siRNA, Dharmacon)

siLOXL3: NM_032603.3 (LQ-008021-00-0002, ON-TARGETplus Human LOXL3 siRNA, Dharmacon)

3.1.10 Media, buffers and other reagents

3.1.10.1 Animal experiments

Anesthesia: 9 ml 0.9% sterile NaCl solution, 2 ml Ketamine 10% (# FS1670041, bela-pharm GmbH), 0.5 ml Xylazin 2% (CEVA Tiergesundheit GmbH)

Analgesia: 14 ml 0.9% sterile NaCl solution, 1 ml (0.05 mg/ml) Buprenorphine (Essex Pharma), 50 µg/kg

Phosphate-buffered saline (PBS): 140 mM NaCl, 2.7 mM KCl, 10 mM $Na_2HPO_4.2H_2O$, 1.8 mM KH_2PO_4, pH 7.4.

4% Paraformaldehyde (PFA): 80 g PFA (# 0335.3, Roth) were dissolved in 1.5 liter of 1X PBS, adjusted the pH to 11 with 5 M NaOH and stired until the solution gets clear. Afterwards the pH was adjusted to 7.4 and the solution filled up to 2 liter with 1X PBS. The solution was stored at -20°C.

0.5 M phosphate buffer (PB): 115 mM $NaH_2PO_4.H_2O$, 385 mM $Na_2HPO_4.7H_2O$, adjust the pH to 7.4

Cryoprotection solution (CPS): 500 ml 0.1 M PB pH 7.4, 250 ml ethylene glycol (# 9516.1, Roth) and 250 ml Glycerin (# 3783.1, Roth) were stirred until a clear solution was obtained. The CPS was stored at RT (room temperature).

30% sucrose in 0.1M PB pH7,4: 333.3 g D(+)- Sucrose (# 4621.2, Roth) was filled up to 1 liter with 0.1M PB, sterile filtered and stored at 4 °C.

3.1.10.2 Bacterial cultures

LB-Agar (Luria-Bertani-Medium): 32g LB-Agar powder (# 22700025, Invitrogen) was used per 1 liter of ultrapure water. The solution was autoclaved at 121 °C for 15 minutes, cooled down to 40°C, the appropriate amount of antibiotics added, swirled to mix and poured in 10 cm dishes in a horizontal flow hood. The plates were stored at 4°C.

LB-Medium (Luria-Bertani-Medium): 20g LB powder (# X964.1, Roth) was suspended in 1 liter of ultrapure water and autoclaved at 121°C for 15 minutes. The medium was stored at 4°C.

3.1.10.3 Cell Culture

CO_2-independent Medium without L-Glutamine: # 18045-054, Gibco

D-MEM/F12 (1:1) (with Glutamine): # 11320-033, Gibco

D-MEM (Dulbecco´s Modified Eagle Medium High Glucose (with Glutamine, 4.5 g/l D-Glucose, Sodium Pyruvate): # 11995-065, Gibco

Opti-MEM® I Reduced Serum Medium: # 31985-047, Gibco

FBS (Fetal Bovine Serum): # 10270-106, Gibco

General cell culture medium for adherent cells: 500 ml DMEM, 10% FBS

Tumor sphere medium: 500 ml DMEM/F12, 10ml B-27 Supplement (50X), minus vitamin A (# 12587-010, Gibco), 5 ml amphotericin B (# A2942, Sigma-Aldrich), 2.5 ml 1M HEPES (# 1563-056, Gibco), 0.5 ml gentamicin (50 mg/ml) (# 15750-045, Gibco). Add freshly to the dishes human recombinant EGF (final concentration 20 ng/ml) (# AF-100-15, PeproTech) and human recombinant bFGF (final concentration 20 ng/ml) (# 100-18B, PeproTech).

Astrocytoma culture medium: 422 ml Basal Medium Eagle (BME) (# 41010, Gibco), 15 ml 20% glucose solution in ultrapure water, sterile filtered (# G-8270, Sigma-Aldrich), 5 ml sodium pyruvate (# 11360, Gibco), 5 ml 1M HEPES (# 1563-056, Gibco), 2.5 ml Penicillin/Streptomycin (# P11-010, PAA Laboratories GmbH), 50 ml horse serum (# H1270, Sigma-Aldrich), 500 µl MITO+ serum extender (# 355006, BD Biosciences)

Trypsin/EDTA: # 25300-62, Gibco

Accutase: # A11105-01, Gibco

Growth factor stock solutions: Recombinant human EGF (# AF-100-15, PeproTech) and recombinant human bFGF (# 100-18B, PeproTech) were reconstituted in 5 mM Tris, 0.1% BSA (bovine serum albumin), pH 7.6 to a final concentration of 20 µg/ml. Aliquots were stored at -20°C.

Dimethyl sulfoxide (DMSO): # A994.1, Roth

Cryo-Medium SFM: # C-29910, Promocell

2xHBS: 281 mM NaCl, 100 mM HEPES, 1.5 mM Na_2HPO_4 in distilled water, pH 7.12, sterile filtered and stored at -20°C

1xPBS: # 10010-056, Gibco

2.5M $CaCl_2$: dissolved in ultrapure water, sterile filtered and stored at 4°C

10mM Chloroquine: dissolved in distilled water, sterile filtered an stored at 4°C

Polybrene: (# H9268-5G, Sigma-Aldrich) 6 mg/ml in ultrapure water, sterile filtered and stored at -20 °C

Poly (2-hydroxyethyl methacrylate) (pHEMA): 10 mg/ml pHEMA (# P3932-25g, Sigma-Aldrich) was dissolved in 95% ethanol, sterile filtered and stored at RT

Collagen solution (10 ml): 5.1 ml bovine collagen (Biomatrix), 3.5 ml TSM, 1.36 ml HEPES

Ultrapure water: 0.22 µm sterile filtered water (18.2 MΩ)

3.1.11 Nucleic acid isolation

RNeasy Mini Kit: (# 74106, Qiagen)

β-Mercaptoethanol: (# M6250, Sigma-Aldrich)

RNase-Free DNase Set: (# 79254, Qiagen)

DEPC-H_2O: 1 ml Diethylpyrocarbonate (# K028, Roth) was dissolved overnight in 1 liter distilled water and autoclaved subsequently.

Precellys 24 Homogenizer (Bertin Instruments).

Ceramic beads (VWR, CK14 Soft Tissue Homogenizing Kit, Beads in Bulk Format, 325 g of inert 1.4 mm ceramic beads).

Screw cap Micro tubes (# 72.694.005, Sarstedt).

3.1.12 Stainings (FACS, IHC, IF,)

FACS Staining buffer: 1x PBS, 0.5% BSA, 2 mM EDTA, pH 7.2

DNase I: (# DN25-100MG, Sigma-Aldrich)

Cytoseal XYL: (# 8312-4, Richard Allan Scientific)

DAB (3,3'-diaminobenzidine) solution: Mix 1 drop of DAB chromogen with 1 ml of DAB substrate (# K3467, Dako)

DAPI/Antifade-Solution (ultra) (4',6-diamidino-2-phenylindole) (DAPI): 1000 ng/ml, (working concentration 1:5000), (# D1306, Invitrogen)

Eosin: 1% Eosin Y disodium salt (# E4382-256, Sigma-Aldrich) was dissolved in 70% ethanol. 1 drop of glacial acetic acid was added per 100 ml of solution. The solution was stored at RT.

Fluorescent mounting medium: (# S3023, Dako)

Goat serum: (# B11-035, PAA Laboratories GmbH)

H_2O_2 (30%): (# 8070.2, Roth), stored at 4°C. (Diluted in PBS according to requirements)

Mayer's Haematoxylin: (# A4840-500, Applichem)

20X PBS (Phosphate Buffered Saline): 140 mM NaCl, 2.7 mM KCl, 10 mM $Na_2HPO_4.2H_2O$, 1.8 mM KH_2PO_4, pH 7.4, stored at RT.

0,01M Sodium citrate buffer pH 6.0: 1.47 g tri-sodium citrate (dehydrate) in 500 ml ultrapure water (pH 6.0).

TBS: 0.05 M Tris, 0.3 M NaCl in ultrapure water, pH 7.6.

TBST: TBS with 0.1% Triton™ X-100 (# T8787, Sigma-Aldrich)

Tris/EDTA (TE) buffer pH 8.0: 10 mM Tris base, 1 mM EDTA, 0.05% Tween 20 (# A49740100, Applichem)

Xylol: (# 95692, Fluka)

3.1.13 Western Blotting

Ammonium persulfate (APS): 1 g of powdered APS solved in 100 ml distilled water and stored in 1 ml aliquots at -20 °C (# 9592.1, Roth).

TEMED: Tetramethylenediamine (# A1148, Applichem)

Lower-buffer: 0.5 M Tris base (pH to 8.8), 0.4% SDS in distilled water.

Upper buffer: 0.5M Tris base, 0.4% SDS, filled up with distilled water.

Lysis buffer (Laemmli): 10 mM Tris HCl, 2% SDS, 2 mM EGTA, 20 mM NaF in distilled water.

Blocking buffer: 5% milk powder in 1x PBS-Tween-20 (0.1%).

20x PBS: 140 mM NaCl, 2.7 mM KCl, 10 mM $Na_2HPO_4.2H_2O$, 1.8 mM KH_2PO_4 in distilled water (pH 7.4).

10x Running buffer: 250mM Tris base, 2M glycine, 1% SDS in with distilled water.

Sample buffer: 40 ml 10% SDS, 16 ml 1 M Tris pH 6.8, 20 ml glycerol, 19 ml distilled water, stored in 800 µl aliquots, for usage mixed with 200 µl 1% bromphenol blue and 50 µl β-mercaptoethanol.

8% separating gel: 2.7 ml 30% poly-Acrylamide (# 3029, Roth), 2.6 ml lower buffer, 4.5 ml distilled water, 100 µl APS (10%), 10 µl TEMED.

12% separating gel: 4 ml 30% poly-Acrylamide, 2.6 ml lower buffer, 3.5 ml distilled water, 100 µl APS (10%), 10 µl TEMED.

Stacking gel: 0.65 ml 30% poly-Acrylamide, 1.3 ml upper buffer, 4.5 ml distilled water, 100 µl APS (10%), 10 µl TEMED.

10x Wet Transfer buffer: 200 mM Tris base, 1.5 M glycine in distilled water.

Stripping buffer: 200 mM glycine, 0.05% Tween-20 in distilled water.

Washing buffer (PBS-T): 1x PBS, 0.1% Tween-20 in distilled water.

3.2 Methods

3.2.1 Working with RNA

3.2.1.1 RNA extraction

Depending on the experimental duration and the cell lines, between $1x10^4$ and $1x10^6$ cells were seeded in 6-well plates or 10 cm dishes. The following day treatment (e.g. hypoxia, TNFα, TGFβ, 2-OG, FBS, transfection) was started. At the end of the treatment, adherent cells were washed with PBS, scraped off and lysed in 350µl RLT buffer (RNeasy Mini Kit, (# 74106, Qiagen); 1 ml RLT + 10 µl β-Mercaptoethanol). The cells grown as tumor sphere culture were spun down and lysed in 350 µl RLT buffer. In case of the tumor samples, first, cryopreserved tumor samples were weighted. Between 5 mg to 30 mg of tumor samples were mechanically homogenized for 1 minute in RLT buffer by using a Precellys sample homogenizer (Bertin Instruments) with ceramic beads in micro tubes. The beads were spun down and the supernatant was collected for RNA extraction. RNA extraction from cells or tumor samples was performed following the manufacturer's instructions (RNeasy Mini Kit, (# 74106, Qiagen). In order to remove residual amounts of genomic DNA, the optional on-column DNase digestion was carried out using the RNase-Free DNase Set (# 79254, Qiagen). The concentration of the RNA was determined by NanoDrop (Peqlab) photometric measurement at a wavelength of 260 nm. The isolated total RNA was stored at -80°C.

3.2.1.2 Reverse transcription

After 1 µg of RNA was filled up with DEPC-water to 11 µl, 1 µl random hexamer was added. The mix was incubated for 5 minutes at 70°C to unfold RNA secondary structures and then cooled down on ice immediately. Afterwards, 7 µl of a previously prepared mix containing 4 µl 5x reverse transcriptase reaction buffer (# EP0451,Thermo), 2 µl dNTP-Mix (10 mM) (# NO447L, NEB) and 1 µl RNase-Inhibitor (# 03335402001, Roche) were added and the whole mixture was briefly centrifuged

and incubated for 5 minutes at room temperature (RT). 1 µl of Revert Aid H Minus M-MuLV Reverse transcriptase (# EP0451, Thermo) was added and the reaction mix briefly centrifuged and incubated for another 10 minutes at RT followed by 60 minutes incubation at 42 °C. The reaction was inactivated for 10 minutes at 70°C. After the reaction was cooled down on ice, 1 µl RNase H (# 10786357001, Roche) was added, briefly centrifuged and incubated for 20 minutes at 37°C. For further analysis with a qPCR system, the cDNA was diluted at a 1:10 ratio with 180 µl DEPC-water.

3.2.1.3 Microarray analysis

U87 cells were treated with hypoxia (1% O_2) or TGFβ (5ng/ml) for 72 hours. RNA was extracted using the RNeasy kit (# 74106, Qiagen). Purified total RNA was amplified and Cy3-labeled using the LIRAK kit (Agilent) following the kit instructions. Per reaction, 200 ng of total RNA was used. The Cy3-labeled aRNA (amplified RNA) was hybridized overnight to 8x60K 60mer oligonucleotide spotted microarray slides (Agilent Technologies, design ID 072363). Hybridization and subsequent washing and drying of the slides was performed following the Agilent hybridization protocol.
The dried slides were scanned at a 2 µm/pixel resolution using the InnoScan is900 microarray scanner (Innopsys, Carbonne, France). Image analysis was performed with Mapix 6.5.0 software, and calculated values for all spots were saved as GenePix results files. Stored data were evaluated using the R software (Team, 2007) and the limma package (Ritchie et al., 2015) from BioConductor(Gentleman et al., 2004). Mean spot signals were background corrected with an offset of 1 using the NormExp procedure on the negative control spots. The logarithms of the background-corrected values were quantile-normalized (Silver et al., 2009, Ritchie, et al., 2015). The normalized values were then averaged for replicate spots per array. From different probes addressing the same NCBI gene ID, the probe showing the maximum average signal intensity over the samples was used in subsequent analyses. Genes were ranked for differential expression using a moderated t-statistic (Ritchie, et al., 2015). Pathway analyses were done using gene set tests on the ranks of the t-values.

3.2.2 Working with DNA

3.2.2.1 Bacterial transformation

Amplification of plasmid DNA was carried out by incubating 100 µl chemically competent *E. coli* with either 10 ng of plasmid DNA or 5 µl output of ligation reaction for 20 minutes on ice. After a 30 seconds heat shock at 42°C, the vial was placed back on ice for 2 minutes. About 500 µl LB-medium was added and the vial was incubated at 37°C for 1 hour (shaking horizontally at 220 rpm). 50-150 µl of the bacterial culture was spread on LB plates containing the appropriate amount of antibiotics. If ligated plasmid DNA was transformed, up to 250 µl of the bacterial culture was used. After 12-16 hours of incubation at 37°C, colonies where picked and 4 ml of a starter culture was inoculated in S.O.C. medium (# 15544034, Thermo).

3.2.2.2 Plasmid isolation

Small amounts of plasmid DNA were isolated from starter cultures between 4 to 6 ml by using the GeneJET Plasmid Miniprep Kit (# K0503, Fermentas Life Science) according to the manufacturer's instruction. The isolation of larger amounts of plasmid DNA from overnight cultures up to 300 ml was done by using the PureLink® HiPure Plasmid Maxiprep Kit (# K2100-06, Invitrogen) as described in the manufacturer's instruction manual.

3.2.2.3 Restriction digestion

In order to clone the desired insert into the vector, a restriction digestion with one or double restriction enzymes was performed to prepare the vector/insert for ligation. The 50 µl reaction mixture consisted of 10 µg plasmid DNA, 5 µl buffer, 1.75 µl enzyme and residual volume of water was incubated at the optimal enzyme temperature. All the enzymes were purchased from Thermo Fisher Scientific, single or double digestions were usually conducted as recommended on the following website.

https://www.thermofisher.com/de/de/home/brands/thermo-scientific/molecular-biology/thermo-scientific-restriction-modifying-enzymes/restriction-enzymes-thermo-scientific.html
pcDNA3.1 IDH1-3DN vector was created by PCR amplification of insert from pBabe-HA-hygro IDH1-3DN (Koivunen, et al., 2012) into pcDNA3.1 by using EcoRI and BamHI restriction.

3.2.2.4 Ligation and recombination

For ligation reaction, 50 ng linearized vector, 2-10 µl insert, 2 µl T4 DNA ligase (# EL0011, Fermentas) were mixed together and filled up to 20 µl with DEPC-water in a sterile 1.5 ml tube. Usually a 1:3 vector:insert ratio was used as a starting point. The reaction was performed at RT for 1 hour or overnight at 16°C. A recombination reaction was performed according to the manufacturer's instructions by using Gateway pDONR Vectors (Thermo Scientific). For the generation of a lentiviral HA-tagged dominant-negative mutant of HSP90β (HSP90 DN) or a GFP expressing control construct, primers containing attB1 and attB2 recombination sites were designed. Following amplification by PCR, the inserts were recombined into the pDONR221 vector (Thermo Scientific) following the manufacturer's instructions. Subsequently, a second recombination reaction was performed to transfer the expression constructs into the pLenti6/V5-DEST expression vector (Thermo Scientific) according the manufacturer's instructions.

3.2.2.5 Agarose gel electrophoresis

For separation and analysis of DNA after digestion or PCR amplification, agarose gel electrophoresis was used. Depending on the size of the DNA fragments 1-4% gels were casted. The appropriate amount of agarose was dissolved in 1xTBE by boiling and 0.5 µg/ml ethidium bromide (# 2218.2, Roth) was added to allow detection of DNA bands under UV light. After addition of sample buffer, the gel was loaded with the appropriate marker (10bp-, 100bp-, or 1kb-DNA ladder, Invitrogen), run at 80 V until separation had occurred.

3.2.2.6 Gel extraction of DNA fragments from agarose gels

The purification of DNA fragments from agarose gels was performed using the QIAquick Gel Extraction Kit (# 28704, Qiagen) according to the manufacturer's instruction.

3.2.2.7 Determination of DNA concentrations

The DNA sample was analyzed by NanoDrop (Peqlab) photometric measurement at a wavelength of 260 nm and 280 nm. DNA concentration and the ratio of A260/A280 were displayed automatically. A clean DNA preparation should have an A260/A280 of 1.7 to 2.0.

3.2.2.8 Quantitative real time polymerase chain reaction (qPCR)

Quantitative real time PCR allows amplification and simultaneously quantification of the amount of DNA/cDNA molecules of interest in the sample, either as an absolute number of copies or as relative amount to a normalizing gene. Quantification is based on the detection of fluorescent signals, which are produced from the fluorescent dye SYBR green during PCR cycles. SYBR green intercalates with double-stranded DNA and emits light when excited. The PCR reactions were performed with the Absolute QPCR SYBR Green ROX Mix (# AB-1162/a, ABgene) on a StepOne Plus system (ABgene, Thermo-Scientific).
Reactions were performed in triplicates with 2-4 µl of diluted cDNA (~20-40 ng), 100 nM forward (fw) primer, 100 nM reverse (rev) primer, 12,5 µl 2X ABsolute™ QPCR SYBR Green Mix and DEPC-water in a total volume of 25 µl. The amount of target mRNA was determined using the comparative threshold cycle method and normalized relatively to the amount of the housekeeping genes HPRT or β-actin mRNA.

Table 3.7. qPCR program used for SYBR green method

Step	Temperature	Time	Number of cycle
Enzyme activation	95°C	15 min	1
Denaturation	95°C	30 sec	45
Annealing	60°C	30 sec	
Extension	72°C	30 sec	
Denaturation	95°C	1 min	1
Annealing/Extension	60°C	1 min	1
Melt curve	55°C	15 sec	0.5°C stepwise increase in temperature
End	4°C	hold	

3.2.2.9 Sequencing

All the plasmids created, bought or taken from other groups were sequenced. All sequencing reactions were performed by SeqLab.

3.2.3 Working with proteins

3.2.3.1 Protein extraction

Depending on the experimental duration, $1.5x10^5$ to $1x10^6$ million cells were seeded under sphere conditions into sterile petri dishes. The tumor spheres were collected into 15 ml conical tubes in the hood or in the hypoxic chamber, transferred on ice immediately and centrifuged at 2500 rpm for 1 minute at 4°C. After aspiration of supernatant, cells were lysed in 75-200 µl Laemmli buffer. In case of adherent cells, $1.5x10^5$ to $5x10^5$ cells were seeded into the cell culture dishes. At the end of the experiment, cells were placed on ice, washed with cold PBS and scraped off in 100-200 µl Laemmli buffer (without bromphenol blue) with a cell scraper. Lysates were transferred to 1.5 ml tubes and sonicated at 90% amplitude with 0.5 s pulse period durations for 30 seconds (Sonopuls mini20, Bandelin) to shear genomic DNA. To denature the proteins, lysates were incubated at 95°C for 5 minutes. The protein lysate was stored at -80°C until further use.

To isolate protein from tumors samples, cryopreserved tumors were weighted and 20 times the amount of Laemmli buffer to the tumor samples was added in 1.5 ml or 2 ml tubes (e.g. for 50 mg of tumor tissue, 1000 µL Laemmli buffer was used). The tumor samples in Laemmli buffer were mechanically disrupted by using an ULTRA-TURRAX disperser for 1 minute until the samples were homogenized. Subsequently, the samples were sonicated at 90% amplitude with 0.5 s pulse period durations for 30 seconds to shear genomic DNA. After centrifugation at 17000 g for 5 minutes at RT, the supernatants were collected in new 1.5 tubes. Lysates were incubated at 95°C for 5 minutes to denature the proteins. The protein lysates were stored at -80°C until further use.

3.2.3.2 Nuclear and cytoplasmic protein extraction

To analyze nuclear translocation of p65, $4x10^5$ cells were seeded under sphere conditions in sterile petri dishes. Two days after seeding, the cells were treated with TNFα (# 300-01A, Peprotech, final concentration 10ng/ml) for 30 minutes. Nuclear and cytoplasmic protein extraction was done using the nuclear and cytoplasmic extraction reagents (# 78833, Thermo Scientific) according to manufacturer's instruction.

3.2.3.3 Determination of protein concentration

Protein concentration was determined using the colorimetric DC Protein Assay Reagents Package (BIO-RAD # 500-0116), which is based on the Lowry method (Lowry et al., 1951). The alkaline copper tartrate solution (Reagent A), the diluted Folin Reagent (Reagent B) and Reagent S were prepared according to the manufacturer's instructions. 25 µl of the mixture of reagent B and S were added to the sample (5 µl of protein lysate) and combined with 200 µl reagent B in a 96 well plate. After 15 minutes incubation at RT, the absorbance was measured at 750 nm in a microplate reader. Pure Laemmli buffer without bromphenol blue was measured as a blank. The protein concentration was determined using a calibration curve measured with increasing concentrations of BSA (bovine serum albumin).

3.2.3.4 SDS-PAGE (Sodium Dodecyl Sulfate Poly Acrylamide Gel Electrophoresis)

The principle behind this method lies in separation of proteins according to their size. Due to binding of SDS, proteins have identical charge per unit mass, which leads to a size dependent fractionation. Depending on the size of the protein being analyzed 8%, 10% or 12% separating gels were prepared. 30 µg of protein from each sample was taken and filled up to a final volume of 18 µl with Laemmli buffer in a new tube to load the same amount of protein from each sample in equal volume. Sample buffer was added to the protein lysate in a 1:3 ratio and heated at 95°C for 5 minutes to denature proteins. The protein samples were loaded on the gel and the proteins were separated using a standard discontinuous SDS-polyacrylamide denaturing gel electrophoresis in Mini-Protean Tetra cells (BIO-RAD). The separated proteins were transferred electrophoretically from the SDS gel to PVDF membranes (Hybond ECL, Amersham) at 100 mA per gel for 2 hours using a Wet Blot System (BIO-RAD). Membranes were incubated for 1 hour in 5% milk blocking buffer (PBS, 0.1% Tween-20, 5% milk powder) to prevent unspecific antibody binding followed by primary antibody incubation in the blocking buffer at 4°C overnight. Blots were rinsed 3 times (15 minutes each) in washing buffer (PBS, 0.1% Tween 20) and incubated for 1 hour at RT with the appropriate secondary HRP-conjugated antibody diluted in blocking buffer. After 3 times washing with washing buffer and once with PBS (each 15 minutes), chemiluminescent signal was produced using ECL Western Blotting Detection System (Thermo Scientific), ECL plus System (Perkin Elmer) or ECL Pico/Femto System (Thermo Scientific) depending on the abundance of the protein and peroxidase activity of the secondary antibody. The membrane was placed into a developing cassette and the luminescent signals detected with an X-ray film (# 34089, Thermo Scientific) with exposure times of 1 second to 1 hour, depending on the signal strength.

3.2.3.5 Stripping the western blot membranes

To detect another protein in the same western blot membrane, the membrane was incubated in stripping buffer for 1 hour at RT, washed with PBS for 5-10 minutes and subsequently blocked with 5% blocking buffer again for 1 hour. Afterwards, the new primary antibody was added and incubated overnight at 4°C. The procedure was continued as described above.

3.2.4 Cell culture

3.2.4.1 Isolation of primary glioblastoma cells from human tumor samples

Isolation and primary glioblastoma cell culture from human tumor specimen were carried out as previously described (Seidel et al., 2015). All steps of the tissue dissociation were carried out under sterile conditions in a laminar flow cell culture hood to reduce the risk of contamination of the primary culture.

3.2.4.2 Cell culture conditions and subculturing of primary glioblastoma cells

Primary glioblastoma cells were cultured in tumor sphere medium (TSM), in which the cells grow as three-dimensional spheroids with stem cell characteristics. Depending on the tumor sphere size, primary glioblastoma cells were split every 7 to 10 days. The spheres were centrifuged for 3 minutes at 900 rpm, the supernatant discarded and the pellet was incubated with 1 ml accutase solution at 37°C for 15 minutes. The cell suspension was triturated gently with a 1000 µl pipette tip, 9 ml TSM was added and filtered over a cell strainer (40-100 µm). The cell were filtered over a 100 µm cell strainer to subculture the cells. If an experiment was set, 70 µm cell strainer was used. To guarantee the single cell platting for the sphere formation assay, 40 µm cell strainer was used. After another round of centrifugation the cells were resuspended in fresh TSM medium including growth factors (EGF and FGF).
U87, G55, MDA-MB-231, A549, LN229 and HEK293T cells were cultured in DMEM supplemented with 10% FBS on tissue culture dishes or flasks under adherent conditions. Astrocytomas were cultured in astrocytoma medium, consisting of BME,

0.6% glucose, 1mM sodium pyruvate, 10 mM HEPES, 10% horse serum and 0.1% MITO serum extender under adherent conditions.
Adherent cells were washed with PBS and covered with 2 ml Trypsin-EDTA solution and incubated at 37°C for 3 to 5 minutes until the cells detached. Hereafter 8 ml of complete growth medium were added and the cells aspirated by gently pipetting up and down. The cell suspension was centrifuged at 1000 rpm for 3 minutes, the supernatant discarded and the cells resuspended in fresh complete growth medium and subcultured in ratios between 1:5 and 1:20 depending on the cell line.

3.2.4.3 Cryopreservation of cells

The primary glioblastoma cells were used at low passage number, as there is a risk of genetic alterations and phenotypic shifts over the course of prolonged culture with multiple passaging. Therefore, a substantial number of aliquots were cryopreserved at the earliest passage when they can be sufficiently expanded. Subsequently, fresh frozen aliquots were periodically thawed and cultured for a limited number of passages and new fresh aliquots at low passages were frozen.
To cryopreserve the primary glioblastoma cells, the cells were collected 2 days after splitting by centrifugation at 900 rpm for 3 minutes. The pellet of 1 petri dish was resuspended in 2 ml of Cryo-SFM cryopreservation medium and distributed to 2 cryo vials, which were placed into a cell freezing container (# BCS-405, Biocision) used to control the freezing rate of cells (1 °C/minute when placed at -80°C). The following day the vials were transferred to liquid nitrogen for long-term storage.
70-90% confluent adherent cells were trypsinized, centrifuged at 1000 rpm for 3 minutes and resuspended in 2 ml DMEM, 20% FBS, 10% DMSO, transferred to 2 cryo vials and frozen as described above.
Cryopreserved cells were rapidly thawed in a water bath at 37°C and mixed with 10 ml of the corresponding culture medium and seeded on the respective culture dishes. The following day the medium was changed and, if necessary, replaced with medium containing antibiotics for transgene expression or selection.

3.2.4.4 Determining the cell number

Cell number was determined by using the CASY Cell Counter and Analyzer System Model TT (# 05651697001, Roche Diagnostics GmbH), which works via electronic pulse area analysis and measures cell number, size distribution and viability of a sample. Cell counting was performed by diluting 100 µl cell suspension in 10ml CASY ton solution (# 05651808001, Roche Diagnostics GmbH) and analyzed according to the manufacturer's instructions.

3.2.4.5 Transient transfection

In order to perform transfection, glioblastoma cell lines were seeded on tissue culture 6 well plates at a density of 3-4x10^5 cells per well. The following day, transfection was performed by using Lipofectamine 2000 (# 116680, Thermo Scientific) for G55 cells or Fugene HD (# E2311, Promega) for U87cells. 1:3 ratio of µg DNA to µl of Lipofectamine 2000 and 1:4 ratio of µg DNA to µl of Fugene HD were used to transfect 2 to 4 µg of DNA. Transfection mixes were prepared in Opti-MEM medium and transfections were done in 10% FBS medium without antibiotics according to manufacturer's instruction. On the next day, the cells were reseeded to sphere conditions.

In order to transfect primary cells, 4 hours after seeding 5x10^5 primary glioblastoma cells into the 6 well plates, transfection was performed by using Fugene HD in TSM without antibiotics according to manufacturer's instruction.

To create stable control or ephrinB2-HA overexpressing cells, G55 cells were transfected with pECFP-N1 or pECFP ephrinB2-HA plasmids by using Lipofectamine 2000 and selected with 500 µg/ml geneticin for 2 weeks. EphrinB2 KO and WT astrocytomas were transfected with pECFP-N1 (Clontech) or pECFP ephrinB2-HA plasmids by using Fugene HD. Transfected cells were selected in medium containing 500 µg/ml geneticin for 2 weeks.

3.2.4.6 siRNA transfection

siRNAs against HIF-1α, HIF-2α, RelA or nontargeting control siRNA were obtained as a pool of 4 siRNA oligos (ONTARGETplus SMART pool, Dharmacon). Reverse siRNA transfection of U87 cells was performed with 20 pmol per HIF-1α, HIF-2α, RelA siRNA by using Lipofectamine RNAiMAX (Thermo Scientific) in antibiotic free 10% FBS medium according to the manufacturer's instructions. 24 hours after transfection, cells were reseeded to sphere culture conditions. Subsequently, the cells were cultured under normoxia or hypoxia (1% O_2). Reverse siRNA transfection of GBM015 cells was performed with 10 pmol siHIF-1α and 50 pmol siHIF-2α, or 60 pmol nontargeting siRNA, respectively, with Lipofectamine RNAiMAX (Thermo Scientific) in antibiotic free TSM according to the manufacturer's instructions. 24 hours after transfection, the cells were seeded in CO_2-independent TSM at pH 7.4 and preincubated under normoxic conditions for 48 h. Subsequently, the cells were cultured under hypoxia in TSM at pH 7.4 or 6.7. To repress gene expression of the EMT repressors, LN229 cells were transiently transfected twice at 24 hours intervals with Oligofectamine (Invitrogen) and a 20 nM pool of three ON-TARGETplus siRNA oligonucleotides (Thermo Scientific).

3.2.4.7 Production of lentiviruses in 293T cells using calcium phosphate transfection method

All steps were carried out in a S2 (biosafety level 2) laboratory.

Expression Arrest pGIPZ lentiviral shRNA vectors, pGIPZ non silencing control and pLenti6/V5 CMV were purchased from Thermo Scientific. GFP and dominant negative mutant HSP90β (# 22480, Addgene) was cloned into pLenti6/V5 CMV vector (# V49610, Open Biosystems). Viral particles were produced through calcium phosphate co-transfection with lentiviral vector and packaging vectors.

The day before the calcium phosphate transfection, HEK293T cells were seeded at a density of $4x10^6$ cells per T75 tissue culture flask in full medium (DMEM with 10% FBS). Next day, 2 hours before the transfection, the medium was changed to 9 ml of serum containing medium. For each transfection 25 µg specific lentiviral vector, 12.5

µg of ENV plasmid (pCI-VSVG) and 12.5 µg of core packaging plasmid (psPAX2) were added to 450 µl sterile filtered water in a 15 ml tube. Subsequently 50 µl 2.5 M $CaCl_2$ was added. DNA was precipitated by dropwise addition of 500 µl 2xHBS to the DNA/$CaCl_2$ mixture while vortexing the mixture vigorously. The mixture was vortexed for an additional 1 minute and incubated at RT for 30 minutes. During the incubation time, 10 µl of 10 mM chloroquine stock (final concentration 10 µM, # C6628-25g, Sigma) was added to the flasks. 1 ml of precipitated DNA solution was slowly pipetted into the flask and cells were placed at 37 °C for 16 hours. The transfection mixture was aspirated and replaced by 10 ml of standard culture medium. The virus containing supernatant was collected 48 and 72 hours post-transfection into a sterile tube, which was stored at 4 °C. Addition of 10 ml fresh standard culture medium was carried out by pipetting slowly at the rim of the flask as HEK293T cells easily detach.

Before virus concentration, the supernatant was filtered through a sterile, 0.45 µm low protein binding filter (Millex-HV 0.45 µm PVDF filters, # SLHVR25LS, Millipore) to remove any remaining cellular debris. Viral supernatant was pipetted into a sterile 38.5 ml ultracentrifuge tube (PA thick-walled-UC-tube, Herolab), which was already placed in the centrifuge bucket on a balance under the tissue culture hood. Tubes were balanced to 0.1 g exactly and ultracentrifugation was performed at 20000 g for 4 hours at 4°C in a Sorvall Pro 80 Ultracentrifuge and an AH-629 swinging bucket rotor. The supernatant was discarded by decanting and residual liquid was removed by placing the tube upside down on a beforehand UV-lighted paper for few minutes. The desired resuspension volume (100-250 µl) of DMEM (without serum) was pipetted at the bottom of the tube. In order to dislodge the viral particles from the protein pellet the suspension was incubated for 5-10 minutes at 4°C and then gently pipetted about 30 times up and down trying to avoid formation of air bubbles. The resuspended pellet was transferred to a sterile 1.5 ml tube and centrifuged in a microfuge at full speed for 5 minutes at 4°C. The supernatant was placed in a new, sterile 1,5 ml tube, aliquoted into multiple vials at 10-20 µl and stored at -80°C. Usually, the virus production per lentiviral vector was performed by using at least two T75 flasks per lentivirus and the concentrated virus was combined at the end to obtain higher viral titers.

3.2.4.8 Titration of lentiviral particles

For determining the titer of viruses expressing fluorescent proteins, $2.5x10^4$ G55 cells were seeded in a 24 well plates and titration was performed for according to the manufacturer's instruction (Open Biosystems) by using 25 µl of virus including the addition of 8 µg/ml polybrene (# H9268-5g, Sigma). Transduced cells were counted as described in the manual Trans-Lentiviral shRNA Bulk Packaging System (Open Biosystems) and transducing units per ml determined using the following formula:

Number of GFP positive colonies counted x dilution factor x 40 = # TU/ml

The final titer (in TU/ml) was obtained by assessing the average titers from the successive dilutions.

For determining the virus titer of vector that do not express fluorescent proteins, such as the pLenti6/V5 CMV vectors, $5x10^4$ G55 cells were seeded in 6 well plates. The following day, 10 fold serial dilutions of the lentiviral supernatant (10^{-2} to 10^{-9}) were prepared in 24 well plate by using dilution medium (DMEM containing 10% FBS and 8 µg/ml polybrene). To prepare the first dilution (10^{-2}), 11µl of the lentiviral supernatant was carefully resuspended in 1089 µl of dilution medium. For preparing the following dilution (10^{-3}) 110 µl of the first dilution was transferred to the next well containing 990 µl of dilution medium and the same procedure was repeated for the following dilutions. The medium over the cells was replaced with the prepared serial dilutions of lentivirus. The last well of the plate was used as a control without lentiviral transduction. The medium was replaced 24 hours after transduction. The following day, the medium was changed with fresh medium containing the selective antibiotic. The antibiotic-containing medium was refreshed every 2 to 3 days until the cells in the control well were dead. After washing the cells twice with PBS, the crystal violet staining (0.5% Crystal violet (# 61135, Fluka) in 20% Methanol/H_2O, sterile-filtered through a 0.45 µm PDVF filter; stored at +4°C) was performed for 5 to 10 minutes. Subsequently, the cells were washed again twice with PBS. Colonies formed by transduced cells were counted and transducing units per ml determined using the following formula:

(n1 x d1+ n2 x d2) / 2 = # TU/ml

where n is number colonies of a dilution, d is a dilution (e.g. 10^{-7}).

The average from two serial dilutions were taken to obtain TU/ml.

3.2.4.9 Lentiviral transduction of cells

All steps were carried out in a S2 (biosafety level 2) laboratory.

3.2.4.10 Stable transduction of primary glioblastoma cells

GBM46 primary glioblastoma cells were seeded at a density of $3x10^5$ (6 well plate, 1000 µl total volume including medium, polybrene and virus) cells in cell 6 well plates coated with laminin (Sigma-Aldrich # L2020 solution in PBS (10 µg/ml). The cells were incubated at 37°C for 3-5 hours in TSM without antibiotics, containing 8 µg/ml polybrene. Lentiviral particles were added according to the desired multiplicity of infection (MOI) and the cells were incubated overnight. The following day the cells were washed with PBS and new TSM was added. To select the transduced cells, antibiotic selection was started with the corresponding antibiotic two days after transduction. Three to five days after viral transduction, cells were detached from the monolayer on laminin using accutase and seeded as sphere cultures in 6 well suspension culture plates in TSM containing antibiotics.

3.2.4.11 Stable transduction of cell lines

Depending on the cell line and desired MOI, cells were seeded at a density of $5x10^3$ cell per well in a 24 well cell culture plate (500 µl total volume including medium, polybrene and virus stock) or $5x10^5$ cell per well in a 6 well cell culture plate (1000 µl total volume including medium, polybrene and virus stock) in medium containing 10% FBS and 8 µg/ml polybrene. Lentiviral particles were added according to the desired MOI and the cells were incubated overnight. The following day cells were washed with PBS and new medium was added. Antibiotic selection was started with the corresponding antibiotic. When the cells reached a confluence of around 80%, transduced cells were split to larger cell culture dishes.

3.2.4.12 Creating knock-out cells

CRISPR mammalian expression vectors carrying Cas9 (pSpCas9(BB)-2A-Puro (PX459) V2.0, #62988, Addgene) (Ran, et al., 2013) were used to create IDH1 knock-

out cells. IDH1 guide sequences were designed by CRISPR Design Tool (http://crispr.mit.edu/), purchased from Sigma and cloned into the pSpCas9n vector as described before (Ran, et al., 2013). The cells were seeded to 6 well plates and the choice of transfection protocol was performed depending on the cell line (see the section Transient transfection above). To create the polyclonal knock-out pool, 24 hours after transfection puromycin selection was started. After 3 to 4 days of antibiotic selection, cells were propagated and checked for knock-out efficiency. To select a knock-out cell clone originated from a single cell, 0.2 cell per well was seeded in 96 well plate. Within 2 to 3 weeks single cell clones were transferred to lager dishes and checked for absence of IDH1.
Control and ephrinB2 knock-out gliomas were created by C. Depner and H. zum Buttel as described (Depner, et al., 2016).

3.2.4.13 Hypoxic incubation of cells

For hypoxic treatment cells were grown at 1% O_2 and 5% CO_2 at 37 °C for the indicated time points in an O_2 controlled Hypoxic Workstation (Coy Lab, Grass Lake, USA). Usually 24 hours after seeding the experiment under normoxia, dishes or plates were put into the hypoxic chamber for the indicated time points. For different pH treatments, before cells were cultured under hypoxic conditions, medium was changed in all corresponding samples of the experiment to be compared. For hypoxic time courses, all cells were seeded at the same time under normoxia, placed under hypoxia at different time points and harvested at the same time at the end of the experiment, to control for the effect of cell density on oxygen concentration in the medium.

3.2.4.14 Physiological (pH7.4) and acidic (pH6.7) pH treatment of the cells

The cells were seeded in 6 well plates or 10 cm dishes the day before the pH treatments. The pH of the medium was preadjusted to pH7.4 or pH6.7 with 1 M HCl or 1 M NaOH at 37°C. The next day, the medium of the cells was changed with fresh pH7.4 or pH6.7 medium. The glioma cell lines were incubated in CO_2-independent medium (# 18045-054, Invitrogen), supplemented with 2 mmol/l L-glutamine and 10%

FBS, whereas the primary glioma cells lines were incubated in CO_2-independent medium supplemented with 2% B-27 serum-free supplement without vitamin A, 2 mM L-glutamine, 20 ng/ml bFGF, and 20 ng/ml EGF. The cells were grown for the indicated time points under pH7.4 or pH6.7, combined with normoxia or hypoxia.

3.2.4.15 TGFβ, TNFα, 2-OG and FBS treatments of cells

For TGFβ treatment of glioblastoma cells, when the cells were seeded as spheres, TGFβ1 (transforming growth factor β1, # 100-21C, Peprotech, final concentration 5 ng/ml) was added to the dishes for the indicated times. In the case of MDA-MB-231 and A549 cells, cells were seeded in growth medium (with 10% FBS) under adherent conditions. The next day, the medium was replaced with 1% FBS-containing medium. 24 hours after medium change, TGFβ (final concentration 5 ng/ml) was added to the dishes for indicated times.

For TNFα treatments, one day after seeding the cells under sphere conditions, TNFα (# 300-01A, Peprotech, final concentration 10 ng/ml) treatment was started.

24 hours after seeding the cells as spheres, treatment with cell permeable 2-OG (dimethyl 2-oxoglutarate [Dm-2-OG], # 349631, Sigma, final concentration 6 mM or 8 mM) was started and cells were cultured for the indicated times.

For FBS treatments, the cells were seeded in pHEMA coated dishes in TSM. The following day FBS was added to a final concentration of 10% and the cells were cultured for the indicated times.

All the samples of an experiment were harvested at the same time.

3.2.4.16 Sphere formation assay

To determine secondary sphere formation (sphere forming units (SFU)), cells were seeded at a density of $5x10^5$ cells on either petri dishes (primary glioblastoma cells) or pHEMA coated tissue culture dishes (glioblastoma cell lines) in TSM for 5 to 7 days. The cells were then split and 6 wells per condition were seeded in 6 well suspension plates (# 657185, Greiner) (primary glioblastoma cells, 1000 cells per well) or pHEMA coated 6 well tissue culture plates (glioblastoma cell lines, 500 cells per well). Spheres

consisting of 4 or more cells were counted and presented as the percentage of sphere forming cells after 7 days.

3.2.4.17 Flow cytometry (FACS, Fluorescence activated cell sorting)

Flow cytometry was performed using BD FACSCanto II (BD Biosciences). At the end of the treatments, as indicated in figures legends, tumor spheres were dissociated into single-cell suspension by accutase (PAA) treatment for 15 minutes at 37°C. After washing the cells twice with FACS Staining buffer (PBS, pH 7.2, 0.5% BSA, 2 mmol/l EDTA), single cells were blocked with 20 µl (60 µg) normal mouse IgG (# 10400C, Invitrogen) for 20 minutes at 4°C and stained with 10 µl of CD133/2 (293C3)-PE-conjugated antibody (130-090-853, Miltenyi Biotec) or 5 µL of CD15-V450–conjugated antibody (642917, BD Biosciences) for 30 minutes at 4°C. The background staining was determined using matching isotype control antibodies from the same manufacturers at the same concentration as the specific antibodies. 5 minutes before analysis, 1 mM SYTOX Blue (Invitrogen; CD133/2-PE) or SYTOX Red (CD15) nucleic acid stain was added to exclude dead cells. Data were analyzed using FlowJo v7/9 (Tree Star) by gating for live cells based on SYTOX staining, then for singlets using forward scatter area versus width and side scatter area versus width, followed by gating for the CD133 or CD15 positive populations, respectively.

3.2.4.18 Modified Boyden Chamber assay

The migration ability of the cells was assessed by a modified Boyden chamber assay. Following incubation under normoxia or hypoxia for 24 hours, $5x10^4$ cells were seeded in the upper compartment of transwell filter inserts (with 12 polycarbonate membrane inserts with a pore size of 8.0 µm; # 3422 Corning/Costar) in 100 µl matrigel medium mix (final concentration 1 mg/ml matrigel, Becton Dickinson). Matrigel was polymerized at 37°C for 1 hour. The upper compartment of the transwell was filled with 1% FBS-supplemented medium and the lower compartment with 10% FBS-supplemented medium and incubated at normoxia or hypoxia. After 24 hours incubation at 37°C, the cells were fixed for 10 minutes by replacing the medium of the lower compartment with 70% ethanol and rehydrated by a washing step with PBS. Invaded cells were

stained with DAPI (1:5000 in 1x PBS; 10 minutes incubation) and non-invaded cells in the Matrigel on the upper surface were removed with a Q-tip. Images were acquired with a 4x objective on a LEICA BM IL LED inverted fluorescence microscope with a LEICA DFC420C camera and were quantified with ImageJ (Schneider et al., 2012) by thresholding stained cells (n=6).

3.2.4.19 Collagen invasion assay

Cell culture dishes and plates were coated with 10 mg/ml pHEMA, dried and rinsed with PBS. Glioblastoma cells were seeded in pHEMA dishes in TSM and cultured under normoxia or hypoxia for 48 hours. The collagen gel consisting of 50% PureCol bovine collagen type I (Advanced Biomatrix, USA), 2% B-27 Serum-Free Supplement, 48% DMEM-F12 (serum free) and HEPES with 20 ng/ml bFGF and 20 ng/ml EGF was prepared on ice. 12 well plates were covered with 300 µl of collagen gel and the gel was polymerized for 1 h at 37°C. Tumor spheroids of equal size were then picked and plated in a second layer of 360 µl collagen gel. For hypoxic experiments, the plates were incubated in a hypoxic chamber. Images were taken with a 4x objective. The first image was taken 2 hours after experiment was set, afterwards images were taken every 24 hours. The invasion of the spheres was analyzed with the programs Adobe Photoshop and ImageJ (Schneider, et al., 2012). ImageJ was used for quantification of the invasion index of the spheroids (n=8-12) using the formula:
Invasion Index = $(\text{Perimeter})^2/\text{Area}$.

3.2.4.20 Colony formation

To assess the tumor colony forming capacity of the cells, 500 cells per 6 well plate were seeded in triplicate in the growth medium. To allow the single cells to form colonies, the cells were cultured for 2 weeks and every 2 to 3 days the medium was changed. After washing the cells twice with PBS, the crystal violet staining (0.5% Crystal violet (# 61135, Fluke) in 20% Methanol/H_2O, sterile-filtered through a 0.45 µm PDVF filter; stored at +4°C) was performed for 5 to 10 minutes. Subsequently, the cells were washed again twice with PBS and colony numbers were counted.

3.2.4.21 High-performance liquid chromatography-mass spectrometry (HPLC-MS)

$5x10^6$ U87 cells, which were incubated under normoxia or hypoxia for 18 hours in 15 cm dishes, were collected in 50 ml tubes. After 2 times washing with cold PBS, 500 µl of dry-ice-cold methanol/PBS (85/15 v/v) were added to the cells. The samples were stored at -80°C until further analysis. 200 µl of sample was transferred to the new tubes and centrifuged at 15000 g for 5 minutes at 4°C. The supernatant was collected and evaporated to complete dryness in Eppendorf concentrator plus (30°C) for 1 hour. The pellet was dissolved in DATAN (50 mg/ml DATAN in 4:1 Acetonitrile/Acetic acid) and incubated at 75°C for 30 minutes by shaking at 12000 rpm and centrifuged for 1 minute at 4°C (15000 g). The samples were diluted 1:3 with dH_2O and analyzed with HPLC-MS. 2-oxoglutarate (2-OG) and succinate levels were measured and concentrations were determined from a standard curve. Concentrations were normalized to cell amount.

3.2.4.22 Luciferase assay

This method measures the level of expression of firefly luciferase, which is driven by specific promoters (or transcription factor binding sites) located upstream of it. Changes in the promoter activity, e.g. as a result of different levels of transcription factors bound to it, are reflected as changes in firefly luciferase signal. The pRL-SV40 vector, which constitutively expresses Renilla luciferase was used as internal transfection control for normalization.

$3.5x10^5$ cells were transfected with 750 ng 9xHRE (HIF response element), 1400 ng NF-κB-RE (NF-κB binding sites) or 950 ng SBE4-luc (SMAD binding element) together with 100 ng pRL-SV40 by using Fugene (U87 cells) or Lipofectamine (G55 cells) transfection in 6 well plates. In the case of HRE activity measurement, 1200 ng HIF-1α, 200 ng HIF-2α or 1200 ng HIF-1α mPPN were additionally transfected as indicated under the respective figures. To transfect the same amount of DNA in each well, DNA amounts were adjusted with empty pcDNA3.1 vector to a total of 2 µg per 6 well. The following day, the cells were split in triplicate into 24 well plates under sphere

conditions. TGFβ treatment was started the same day whereas hypoxia or TNFα treatments were started the next day. At the end of the treatments, the cells were collected and lysed in passive lysis buffer (Dual-Luciferase Reporter Assay System, Promega) according to the manufacturer's instruction. *Renilla* luciferase and firefly luciferase activity were measured using the Dual-Luciferase Reporter Assay System (Promega) in a microplate reader (TriStar LB 941, Berthold Technologies). Firefly luciferase signal was normalized to *Renilla* luciferase activity and plotted as relative luciferase units (RLU).

3.2.5 *In vivo* tumor models

Animal experiments were approved by the veterinary department of the regional council in Darmstadt, Germany. Xenograft transplantations were performed in athymic 6-8 week-old female NMRI nu/nu mice (Janvier Labs) that were kept in a specific pathogen-free animal facility according to the institutional guidelines.

3.2.5.1 Intracranial tumor xenograft models

For intracranial tumor xenograft transplantations mice were anesthetized (through intraperitoneal injection of 150 µl/20 g bodyweight of 2 ml 10% ketamine, 0.5 ml 2% xylazine in 9 ml 0.9% saline) and placed into a stereotactic apparatus (Kopf Instruments). The scalp was disinfected with a swab dipped in 70% ethanol and opened with a type 15 scalpel. A burr hole was made 2 mm left of the sagittal suture and 0.5 mm anterior to the bregma using a micro drill 0.7 mm in diameter. The cells, resuspended in cold CO_2-independent medium, were slowly implanted at a depth of 3 mm from the dura using a 2.5 µl Hamilton syringe equipped with an unbeveled 33 G needle. The mice were kept until the development of neurological symptoms and, in case of comparative experiments, sacrificed at the same time point.
For intracranial tumor implantations, 5000 cells in 1µl for G55 control and shIDH1 cells, 200000 cells in 2 µl for GBM46 control and shIDH1 cells, 7500 cells in 1µl for G55 control and shHSP90 cells, as well as for G55 control and HSP90 DN cells, were transplanted.

3.2.5.2 Subcutaneous xenograft models

For subcutaneous tumor injections, mice were anesthetized as described above. 75000 G55 cells suspended in 100 µl PBS/Matrigel per flanks were injected subcutaneously into both flanks of 6-8 week-old female nude (NMRI nu/nu) mice. The tumor size was measured at regular intervals using a caliper according to the formula $V = L \times W^2 / 2$.

V: volume, L: length, W: width

Mice were maintained until tumors exceeded a volume of 2000 mm^3 or upon the onset of morbidity symptoms (>20% weight loss, tumor ulceration).

3.2.5.3 Tumor xenograft model of breast cancer

To analyze the primary tumor growth and metastasis of MDA-MB-231 cells, orthotopic injection into the mammary fat pad of mice was performed. $4x10^6$ cells suspended in 100 µl PBS were injected orthotopically into one mammary fat pad of 6-8 week-old female nude (NMRI nu/nu) mice. The tumor size was measured at regular intervals using a caliper according to the formula

$V = L \times W^2 / 2$.

V: volume, L: length, W: width

Mice were maintained until one of the tumor exceeded a volume of 2000 mm^3. The mice were sacrificed at the same time point. Primary tumors were isolated and snap frozen. Metastatic nodules in the lungs were counted by two independent people.

3.2.5.4 Perfusion and tissue preparation

Tumor-bearing mice were anesthetized through intraperitoneal injection of 250 µl/20 g bodyweight of 2 ml 10% ketamine, 1 ml 2% xylazine in 9 ml 0.9% saline. At the endpoint of the shHSP90 and HSP90 DN experiments, the tumor-bearing mice were injected with 60 µg/g Hypoxyprobe (Hypoxyprobe Plus Kit (FITC-Mab), Hypoxyprobe-1, HP2-kit, NPI Inc.) intraperitoneally 90 minutes prior to cardiac perfusion with cold 0.9% NaCl solution. Afterwards, the chest was opened and vascular perfusion was performed using 0.9% saline for 3 minutes and 4% PFA as a fixative for 6 minutes via

a 13 gauge needle inserted through the left ventricle. The brains or the subcutaneous tumors were dissected and additionally fixed in 4% PFA at 4°C overnight. The brains were dehydrated in 30% sucrose for about 4 days at 4°C and subsequently rapidly frozen on dry ice for sectioning with a sliding microtome (Leica # SM2010R). The whole brain was sectioned by collecting 10 x 40 µm sections followed by 4 x 20 µm sections in 14 sequential microcentrifuge tubes containing cryoprotection solution (CPS). When the last section was stored in the tube, collection of sections was performed in the first tube again, resulting in brain sections at 480 µm intervals in every microcentrifuge tube. The sections were stored at -20°C. Alternatively, after overnight PFA fixation, the brains were transferred to PBS until paraffin embedding with a Sakura Tissue-Tek VIP 5 Jr vacuum infiltration processor. 4-6 µm thin sections of the paraffin embedded tissue were cut using a microtome and transferred on glass slides.

3.2.5.5 Quantification of tumor volume and hematoxylin and eosin (HE) staining

The hematoxylin solution (# A4840-500, Applichem) consists of sodium iodide, an oxidizing agent that converts hematoxylin to hematein and a mordant, usually aluminium or iron compounds. The hematoxylin-metal complex acts as a basic dye, staining nucleic acids in the nucleus and cytoplasm blue. Eosin (1% eosin in 70% EtOH, add 1 drop of concentrated acetic acid per 100 ml), acting as an alcohol-based acidic dye, stains more basic proteins within the cytoplasm pink.

For quantifying the tumor volume in G55 control, G55 shIDH1, GBM46 control, GBM46 shIDH1, control glioma and ephrinB2 knock-out glioma tumors, a series of brain sections covering the whole brain at 480 µm intervals was mounted on microscope slides and dried at room temperature overnight. The slides were fit into a removable glass slide rack and rehydrated in PBS for 2 minutes, followed by a rinse in ultrapure dH_2O. Hematoxylin staining was performed for 8-10 minutes in a staining jar. The slides were rinsed in ultrapure dH_2O and blued in tap water for 2 minutes, followed by an additional rinse in ultrapure dH_2O. Cytoplasmic eosin staining was performed for 6 minutes followed by dehydration in an ascending alcohol series (2 times 70% and 96% ethanol for 30 s and 2 times for 5 minutes in 100% ethanol).

Finally the slides were transferred to xylol 2 times for 5 minutes each and subsequently mounted with Cytoseal™ XYL (Richard-Allen Scientific) and dried under the chemical hood. The tumor volume was calculated by tracing the tumor area using the semi-automated stereological system Stereo Investigator 4.34 (MicroBrightField Inc.) or ImageJ and calculating the volume with the following formula:
V [mm^3] = total tumor area [mm^2] x12 x 0.04 mm (thickness of sections)
For quantifying the tumor volume in G55 control, G55 shHSP90 andG55 HSP90 DN tumors: The brains were cut at the injection site where the largest tumor diameter is located and the tumors were imaged. Tumor volume was analyzed using the section with the biggest tumor area by measuring the largest diameter (L) and largest perpendicular diameter (W), using the formula $V = L \times W^2/2$.

3.2.5.6 Analysis of invasiveness of xenograft tumors

The invasiveness of the xenograft tumors was analyzed based on the fluorescent signal from GFP expressing tumor cells or human nuclei staining. 6-10 pictures of the tumor rim per tumor were taken with a fluorescence microscope (LEICA TCS SPE, camera: LEICA DFC420C; 20x objective). The length of the tumor rim and the area of the invading tumor cells was measured with ImageJ. The tumor invasive index was calculated as the area of tumor invading the parenchyma per tumor rim length.

3.2.6 Immunofluorescence and immunohistochemistry stainings

3.2.6.1 p65 staining of the cells

To assess the PHD controlled NF-κB activity (nuclear translocation of p65), p65 staining was performed. The cells were cultured and treated in 8 well chamber slides (177402, Thermo). At the end of the experiment, the cells were washed twice with PBS and fixed with 4% PFA for 15 minutes at RT, followed by 3 times washing in PBS. After 60 minutes blocking in blocking buffer (1X PBS / 20% normal goat serum (#5425, Cell Signalling) / 0.3% Triton X-100) at RT, the cells were incubated with primary antibody (1:500 dilution of NF-κB p65 (D14E12) XP antibody (# 8242, Cell Signaling)

in antibody dilution buffer (1X PBS / 1% BSA / 0.3% Triton X-100)) at 4°C overnight. The cells were washed 3 times with PBS and subsequently incubated with fluorochrome-conjugated secondary antibody (Alexa Flour 568 (1:1000 diluted in Antibody Dilution Buffer)) for 2 hours at RT in dark, followed by 3 times washing in PBS. Afterwards, DAPI staining was performed (1:5000 in 1X PBS; 10 minutes incubation). The slides were mounted and three different staining areas per condition were imaged at 40X magnification. Nuclear p65 signal of 10-12 cells per area was analyzed with ImageJ and mean fluorescence intensity (MFI) was calculated.

3.2.6.2 Endomucin staining

To analyze angiogenesis (new vessel formation) in intracranial tumor xenograft models, endomucin staining which stains the mouse endothelial cells, was performed. The 40 µm brain sections were rehydrated in PBS, transferred in a 24-well plate (per well maximum 3 sections) and permeabilized for 1 hour in PBS with 1% Triton X-100 at RT by shaking on an orbital shaker. Afterwards the sections were blocked (1x PBS / 5% normal goat serum / 0.5% Triton X-100) for 1 hour at RT. The sections were incubated with primary endomucin antibody (1:500 in blocking buffer (20% normal goat serum/1X PBS/0.01% Triton X-100)) for two nights at 4°C while shaking on an orbital shaker. After the primary antibody incubation, the sections were washed 3 times for 15 minutes in PBS (with 0.01% Triton X-100) and once with PBS for 15 minutes. The secondary antibody (goat anti rat Alexa Fluor 568, 1:200 in blocking buffer) was added and incubated at 4°C overnight. The following day, the sections were washed 3 times for 15 minutes in PBS (with 0.01% Triton X-100) and once with PBS for 15 minutes. After washing steps, the sections were stained with DAPI (1:5000 in 1X PBS) to visualize the nuclei and mounted with fluorescence mounting medium (# S3023 Dako). The vessel area was analyzed as percentage of the tumor area with ImageJ. 8-10 pictures were analyzed per tumor and mean values were calculated for each tumor.

3.2.6.3 Human nuclei staining

To detect the human tumor cells, human nuclei staining was performed. 40 µm thick tumor sections were rehydrated in PBS. Antigen retrieval was performed in a steamer for 5 minutes in citrate buffer, pH 6.0 followed by 2 times washing in PBS (with 0.01% Triton X-100) and 1 time washing in PBS for each 5 minutes. Subsequently, the sections were blocked with 20% NGS/0.01% Triton X-100 in PBS for 3 hours and treated for 2 nights at 4°C with human nuclei antibody (1:200 dilution, MAB4383, Millipore / Chemicon). After washing 2 times in PBS (with 0.01% Triton X-100) and 1 time in PBS, the sections were incubated with secondary antibody (Alexa Fluor 568 , 1:1000). The sections were washed with PBS and stained with DAPI (1:5000 in 1x PBS; 10 minutes incubation). Invading cells were quantified with ImageJ.

3.2.6.4 HIF-1α staining and Hypoxyprobe detection

Stainings were performed as described in detail in (Bogurcu et al., 2018).

3.2.7 Analysis of patient survival data

Glioblastoma patient survival data, retrieved in 2013, and lung adenocarcinoma patient survival data, retrieved in 2014, were downloaded from The Cancer Genome Atlas (TCGA) database, cBioPortal (http://www.cbioportal.org/) (Cerami et al., 2012, Gao et al., 2013). IDH1 expression levels (z-scores) of the same glioblastoma and lung adenocarcinoma patients were also downloaded from cBioPortal. Patient survival versus IDH1 expression was analyzed by using GraphPad Prism.

3.2.8 Statistical analysis

Results are presented as mean + standard error of mean (SEM). Statistical comparisons between groups were done using the Student's t-test or Mann-Whitney U test. Statistical significance is indicated as * $P<0.05$; ** $P<0.01$; *** $P<0.001$ ***.

4 Results

4.1 The impact of 2-OG regulation on glioblastoma and other tumor entities

The first part of the thesis aims to examine the role of IDH1 in the regulation of 2-OG and 2-OG dependent enzyme activity. We were particularly interested in the metabolic changes and responses, which are mediated by reduced IDH1 levels in glioblastoma. Tumor cell lines of different tumor entities, such as breast and lung cancer, were also used for validation. Parts of the following work have been performed with the help of the members of the Institute of Neuropathology within the group of Prof. Till Acker (Giessen, Germany), the Institute of Vascular Signaling within the group of Prof. Ingrid Fleming (Frankfurt, Germany), the University of Giessen Lung Center (Giessen, Germany) and the Institute of Cell Biology and Neuroscience within the group of Prof. Amparo Acker-Palmer (Frankfurt, Germany) who are mentioned in the respective figure legends.

4.1.1 Regulation of 2-OG levels and PHD function by IDH1

4.1.1.1 The role of IDH1 in the regulation of the hypoxic response

IDH proteins are enzymes producing 2-OG, an intermediary metabolite of the TCA cycle and an essential co-substrate of 2-OG dependent dioxygenases, by converting isocitrate to 2-OG. Among 2-OG dependent dioxygenases, PHDs play an important role in coordinating the cellular responses to hypoxia or low oxygen tension by direct regulation of HIF-α levels (Nguyen and Duran, 2016). To examine the role of IDH isoforms in the regulation of the hypoxic response, we first created IDH1 and/or IDH2 knock-down cell lines. Knock-down of IDH1 by three different shRNA constructs (Fig. 4.1A) or knock-down of IDH1 and/or IDH2 (Fig. 4.1A-C) showed increased levels of HIF-1α and HIF-2α in different glioblastoma cell lines. Furthermore, well established

HIF target genes, such as carbonic anhydrase 9 (CAIX), vascular endothelial growth factor A (VEGFA) and glucose transporter 1 (GLUT1), were upregulated, confirming the elevated hypoxic response upon IDH1 silencing (Fig. 4.1D, E).

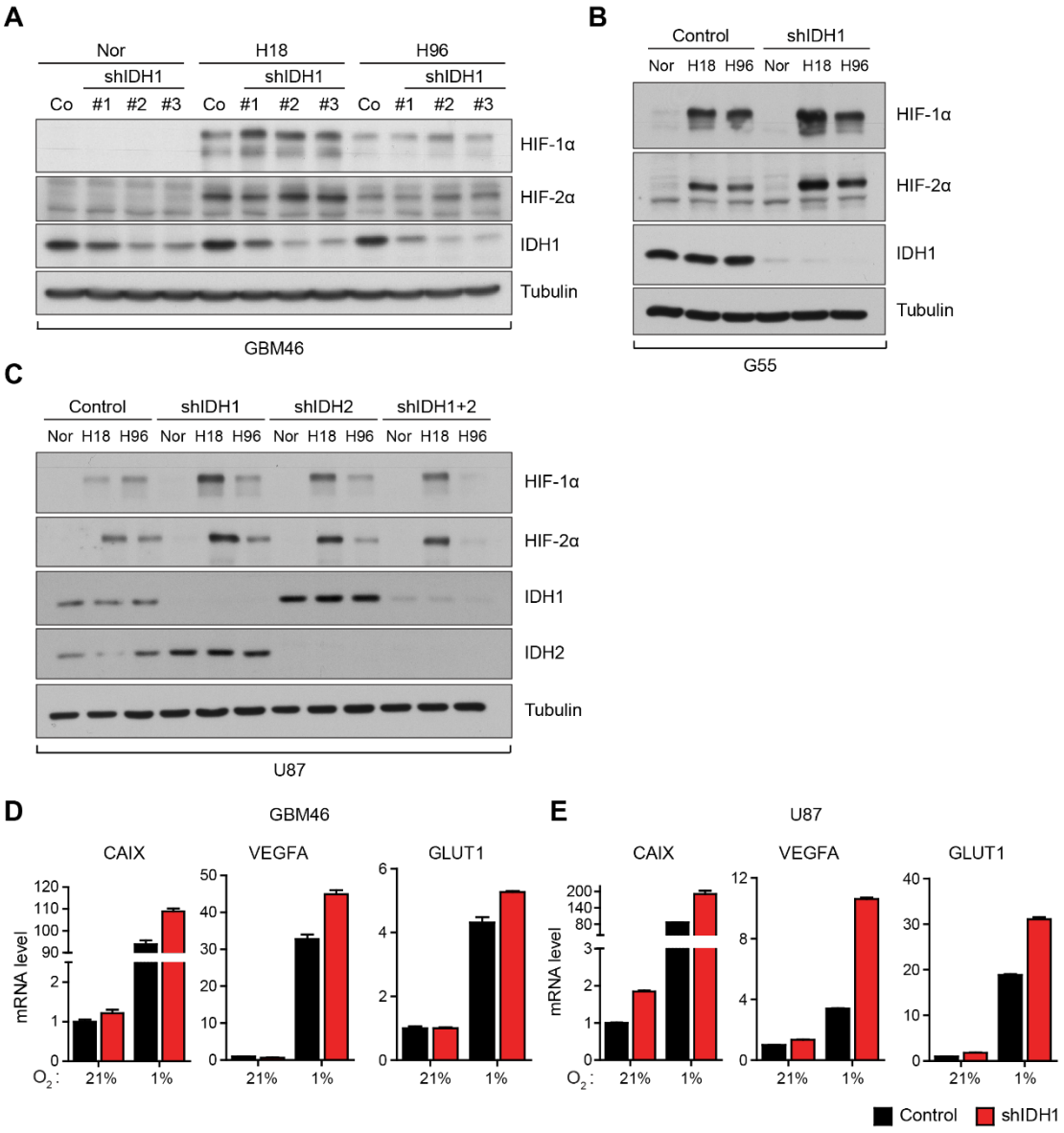

Figure 4.1. IDH1 knock-down increases HIF-α levels and HIF target genes expression. **A,** GBM46 glioblastoma cells were transduced with lentiviruses carrying non-silencing control (Co) and three different IDH1 shRNA knock-down constructs. Construct 3 was used for subsequent experiments. Whole cell extracts were analyzed by immunoblotting with the indicated antibodies. **B, C,** G55 and U87 glioblastoma cells were transduced with lentiviruses carrying non-silencing control (Control), IDH1 shRNA and/or IDH2 shRNA. Cells were grown under sphere conditions and incubated under normoxia (Nor, 21% O_2) or hypoxia (1% O_2) for 18 or 96 hours (H18/H96). Knock-down of IDH1 and/or IDH2 resulted in increased HIF-α levels

under hypoxia. **D, E,** GBM46 and U87 control or IDH1 knock-down cells were analyzed for the expression levels of HIF target genes by qPCR. Target gene expression levels increased in IDH1 knock-down cells.

Furthermore, microarray analysis of U87 control and IDH1 knock-down cells under normoxia and hypoxia for 72 hours revealed that IDH1 knock-down increases the expression of a set of HIF-regulated genes (Koivunen, et al., 2012) under both normoxia and hypoxia, confirming the HIF mediated transcriptional reprograming (Fig. 4.2A, B). The expression of a set of HIF target genes was significantly upregulated upon IDH1 knock-down under normoxia or hypoxia (Fig. 4.2B). Consistently, microarray analysis confirmed that HIF target genes analyzed previously (Fig. 4.1E), CAIX, VEGFA and GLUT1, were expressed at higher levels in IDH1 silenced cells.

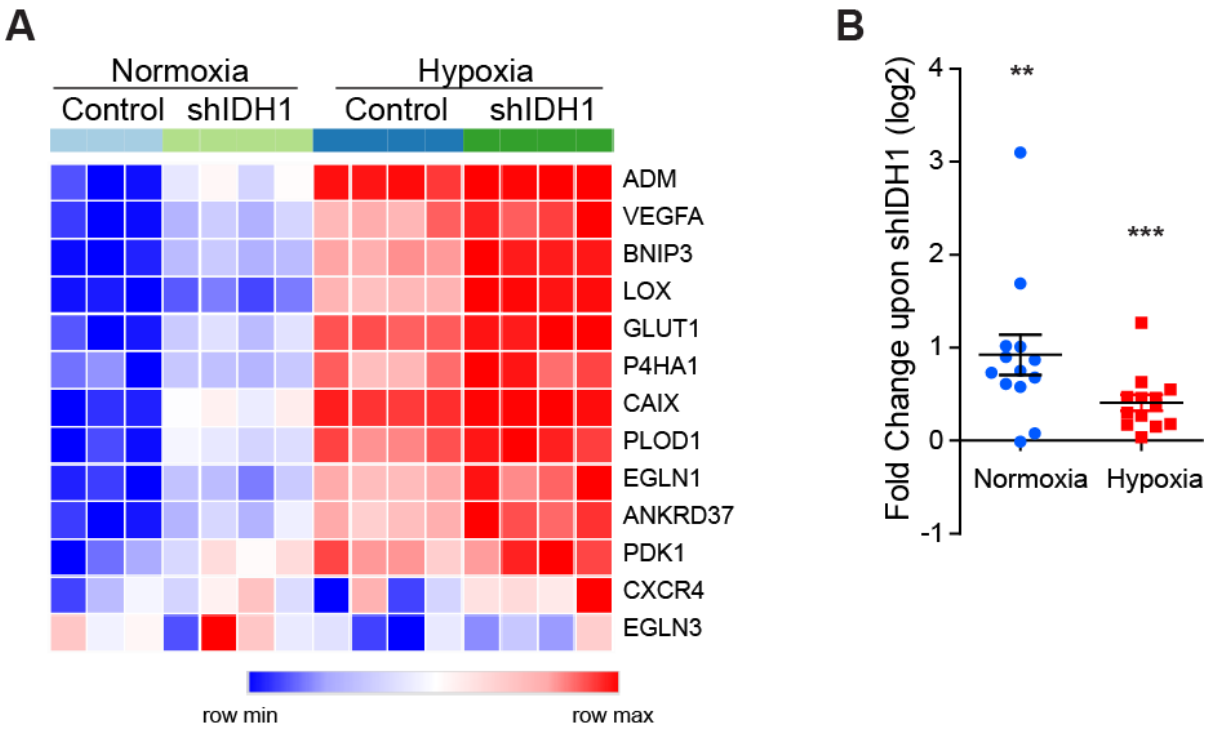

Figure 4.2. Increased expression levels of HIF-regulated genes.
A, U87 control and IDH1 knock-down cells were analyzed in a mRNA microarray. mRNA expression level of a set of HIF-regulated genes were sorted and represented in the heatmap. **B,** Fold change in HIF-regulated gene expression upon IDH1 knock-down are shown, each dot represents one gene listed in the heatmap (left). Microarray analysis was performed in collaboration with Jochen Wilhelm and Susanna Ziegler from the University of Giessen Lung Center (Giessen, Germany). ***P*<0.01, ****P*<0.001

To further verify the HIF-α activating effect of IDH1 knock-down, we performed dual luciferase transactivation reporter assays to detect HIF activity (firefly luciferase under

the control of HIF response elements, HRE) in U87 and G55 cell lines. IDH1 silencing was sufficient to increase the endogenous and exogenous HIF activity in cells overexpressing a control vector, wild-type HIF-1α and/or HIF-2α under normoxia or hypoxia (Fig. 4.3A, B), whereas cells overexpressing HIF-1α that cannot be hydroxylated by PHDs (undegradable form of HIF-1α) did not show an increased HIF activity (Fig. 4.3C). This result indicated that IDH1 silencing regulates HIF activity in a PHD dependent manner. To further confirm this result, we analyzed the levels of hydroxylated HIF-1α at the proline 564 site (OH-HIF-1α Pro^{564}) with a specific antibody by western blotting; cells were treated with the proteasome inhibitor MG132 to prevent the proteasomal degradation of hydroxylated HIF-α. Under hypoxia, PHDs are inactivated due to reduced oxygen levels, leading to decreased HIF-α hydroxylation and therefore increased HIF-α stability, whereas HIF-α is hydroxylated at high levels under normoxia. Western blot analysis showed that HIF hydroxylation (OH-HIF-1α Pro^{564}) is decreased in IDH1 knock-down cells under normoxia and hypoxia (Fig. 4.3D), indicating that reduced hydroxylation can explain HIF-α stabilization upon IDH1 silencing. In addition, IDH1 cells were cultured under hypoxia and subsequently transferred to normoxia for different time points to allow reoxygenation of the cells. HIF-1α degradation upon reoxygenation was also hampered following IDH1 depletion (Fig. 4.3E), providing an additional evidence of reduced PHD activity in IDH1 knock-down cells.

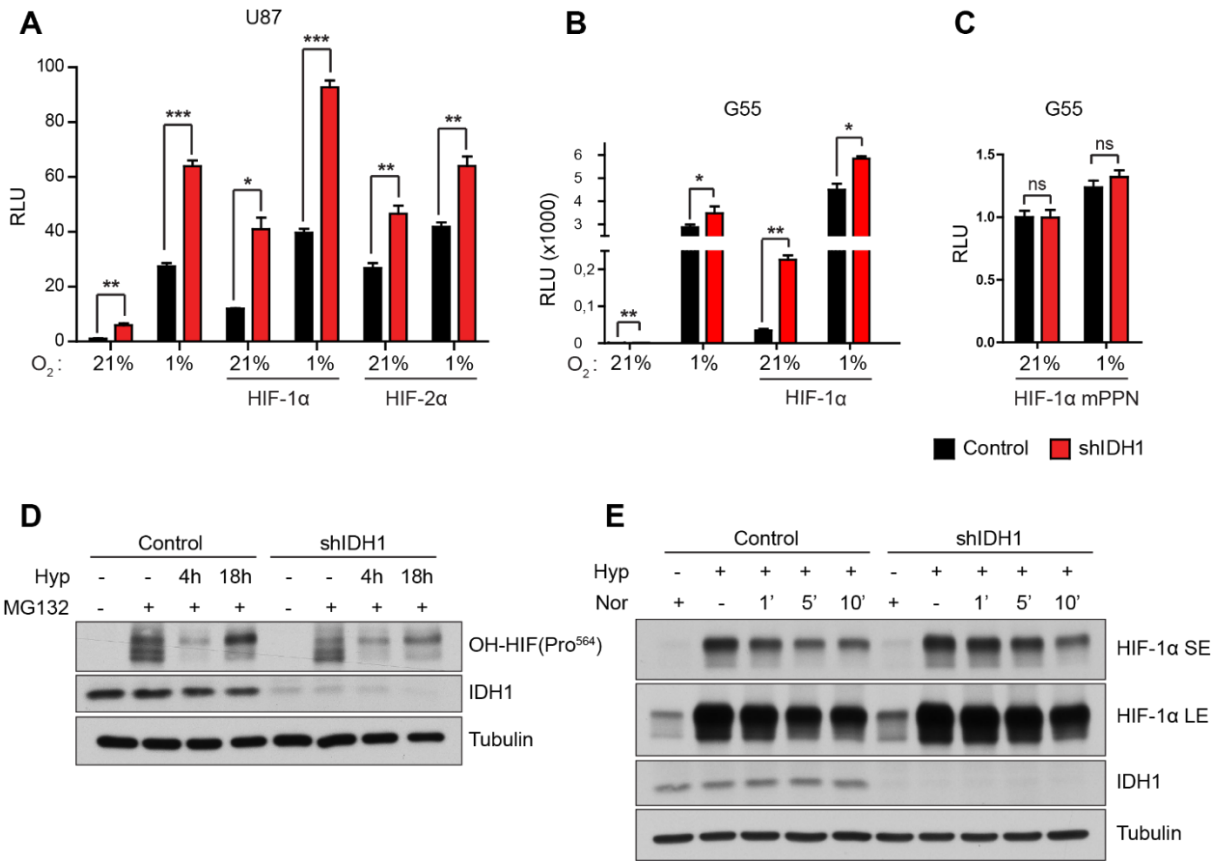

Figure 4.3. PHD dependent reduction of HIF-α hydroxylation leads to increased HIF activity and delayed reoxygenation in IDH1 silenced cells.
A-C, U87 and G55 glioblastoma cells were transfected with a firefly luciferase reporter construct under the control of HIF response elements (HRE). IDH1 knock-down cells showed increased HIF activity under normoxic (21% O_2) and hypoxic (1% O_2) conditions, as well as in cells overexpressing wild-type HIF-1α and HIF-2α **(A, B),** confirming the HIF-α stabilizing effect of IDH1 knock-down. G55 cells which overexpress HIF-1α that cannot be hydroxylated by PHDs (HIF-1α mPPN) did not show an increased HIF activity, showing that the HIF-α stabilizing effect of IDH1 knock-down is PHD dependent **(C)**. **D,** Control and IDH1 knock-down G55 cells were grown under hypoxia (4 and 18 hours) in the presence of the proteasome inhibitor MG132 to prevent the degradation of hydroxylated HIF-1α (OH-HIF-1α Pro564). Knock-down of IDH1 resulted in decreased OH-HIF-1α Pro564 levels. **E,** G55 cells were treated with hypoxia for 18 hours, then transferred to normoxic conditions for 1-10 min, revealing delayed HIF-α degradation following reoxygenation of cells with IDH1 silencing. Data are means +SEM. *P<0.05, **P<0.01, ***P<0.001.

2-OG dependent dioxygenases rely on the presence of their co-factors and co-substrates. For instance, PHD activity depends on the availability of oxygen, Fe^{2+} and 2-OG, which makes PHDs important nutrient sensors to regulate the cellular response to microenvironmental changes. Here we showed that IDH1 knock-down increases HIF-α levels through abrogating PHD activity (Fig. 4.1, Fig. 4.3). Therefore, to address

the question whether regulation of IDH1, as one of the 2-OG producing enzymes, might regulate 2-OG levels, or change the 2-OG-to-succinate ratio, we performed mass spectrometry analysis. IDH1 silenced cells produced remarkably lower levels of 2-OG (Fig. 4.4A) and had a lower 2-OG-to-succinate ratio (Fig. 4.4B). Furthermore, the HIF-α stabilizing effect of IDH1 was abolished by addition of Dm-2-OG, a cell permeable derivative of 2-OG, in U87 (Fig. 4.4C) and G55 (Fig. 4.4D) cells. Importantly, not only HIF-α levels, but also the expression of the HIF target genes CAIX and VEGFA was reduced by addition of Dm-2-OG (Fig. 4.4E, F). Taken together, these data identify IDH1 as an important regulator of 2-OG levels to control PHD activity and the hypoxic response.

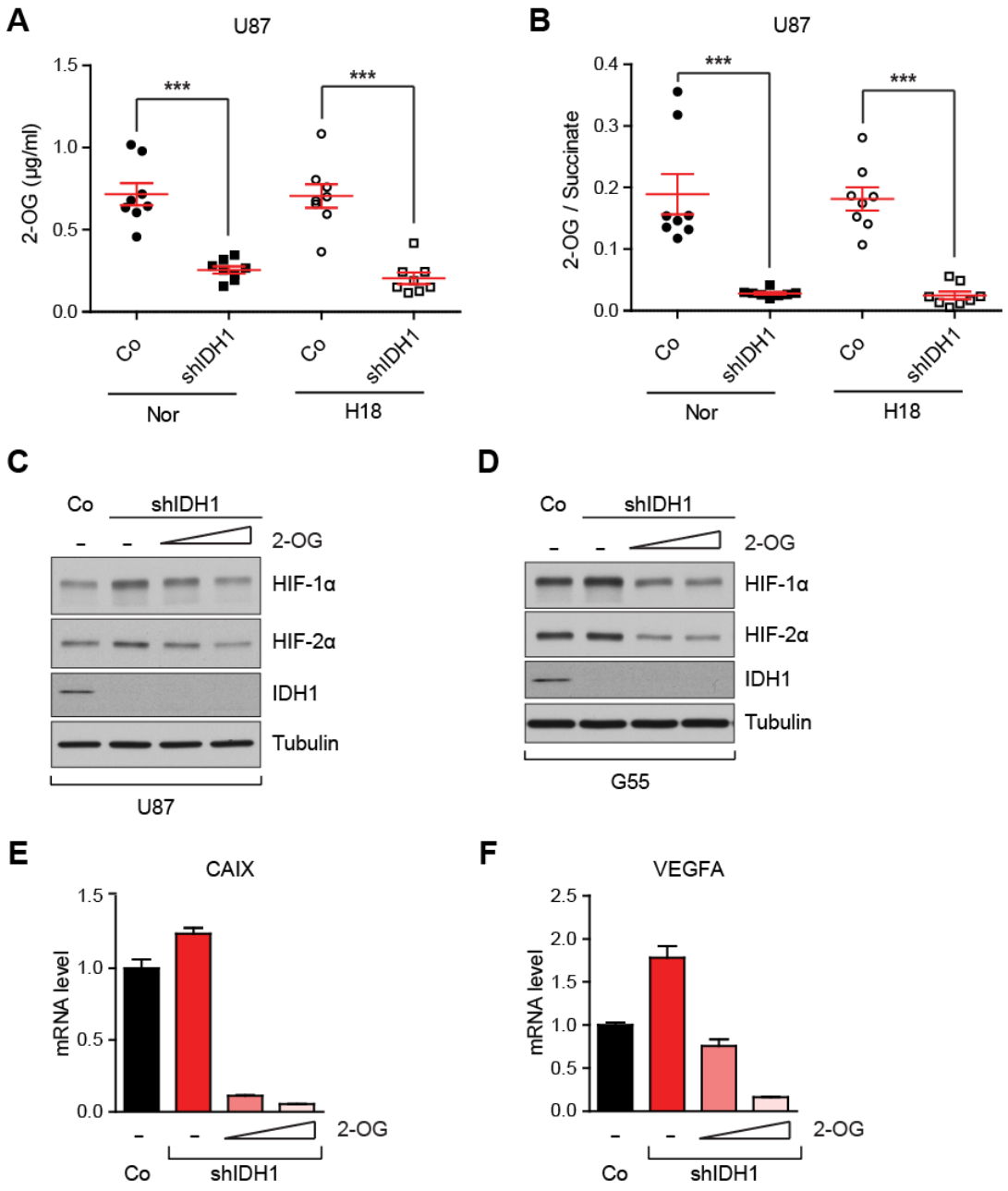

Figure 4.4. IDH1 knock-down results in reduced 2-OG levels and addition of Dm-2-OG reverts the IDH1 knock-down effects.
A, B, U87 control and IDH1 knock-down cells were incubated under normoxia or hypoxia for 18 hours (H18). 2-oxoglutarate (2-OG) and succinate levels were quantified by UPLC-MS/MS and concentrations were normalized to the cell amount (n=8). IDH1 silencing leads to the reduction of 2-OG concentration and 2-OG-to-succinate ratio. Mass spectrometry analysis was performed by Sven Zukunft in the group of Prof. Ingrid Fleming at the Institute of Vascular Signaling (Frankfurt, Germany). **C-F,** Addition of Dm-2-OG reverts the effect of IDH1 silencing on HIF-α levels and HIF target genes expression. U87 and G55 cells were treated with 6 mM and 8 mM of a cell permeable form of Dm-2-OG (dimethyl 2-oxoglutarate) for 3 hours under hypoxia (**C, D**). To detect the HIF target gene expression, U87 cells were treated with 6 mM and 8 mM Dm-2-OG for 18 hours under hypoxia (**E, F**). Data are means ± SEM. ****P*<0.001.

4.1.1.2 Enhanced activation of the NF-κB pathway upon IDH1 silencing

Besides the control of the hypoxic response, PHDs have been also reported to regulate other signaling pathways. NF-κB, which is the master regulator of the inflammatory response, is regulated by PHD hydroxylase activity. PHDs act as negative regulators of NF-κB and inhibition of PHDs leads to the activation of NF-κB signaling by allowing the nuclear translocation of NF-κB subunits to activate the target genes (Cummins, et al., 2006, Wong, et al., 2013). Therefore, we examined the NF-κB signaling in IDH1 knock-down cells. NF-κB activation was induced by TNFα and the subsequent nuclear translocation of p65 (RelA), a subunit of NF-κB, was analyzed. Western blotting and immunofluorescence analysis showed increased translocation of p65 into the nucleus in IDH1 knock-down cells (Fig. 4.5A, B). In addition to p65 nuclear translocation, the expression of the known NF-κB target genes interleukin-8 (IL-8), tumor necrosis factor alpha (TNFα), C-C motif chemokine 2 (CCL-2) and angiogenin (ANG) was increased upon IDH1 silencing, indicating higher NF-κB activity (Fig. 4.5C, D). We also measured the NF-κB activity with a luciferase assay which confirmed the enhanced activation of NF-κB. Interestingly, not only TNFα and hypoxia induced NF-κB activity, but also basal NF-κB activity was increased upon IDH1 silencing (Fig. 4.5E). We therefore wanted to assess if inactivation of PHDs through decreased 2-OG levels causes the enhanced NF-κB activation. To that end, we restored 2-OG levels in shIDH1 cells by adding cell-permeable Dm-2-OG into the medium. Increased expression of CCL-2 upon IDH1 knock-down was reduced to control levels following addition of Dm-2-OG (Fig. 4.5F), indicating that IDH1 regulates PHD activity by maintaining 2-OG levels and Dm-2-OG supplementation reverses the effects of IDH1 knock-down.

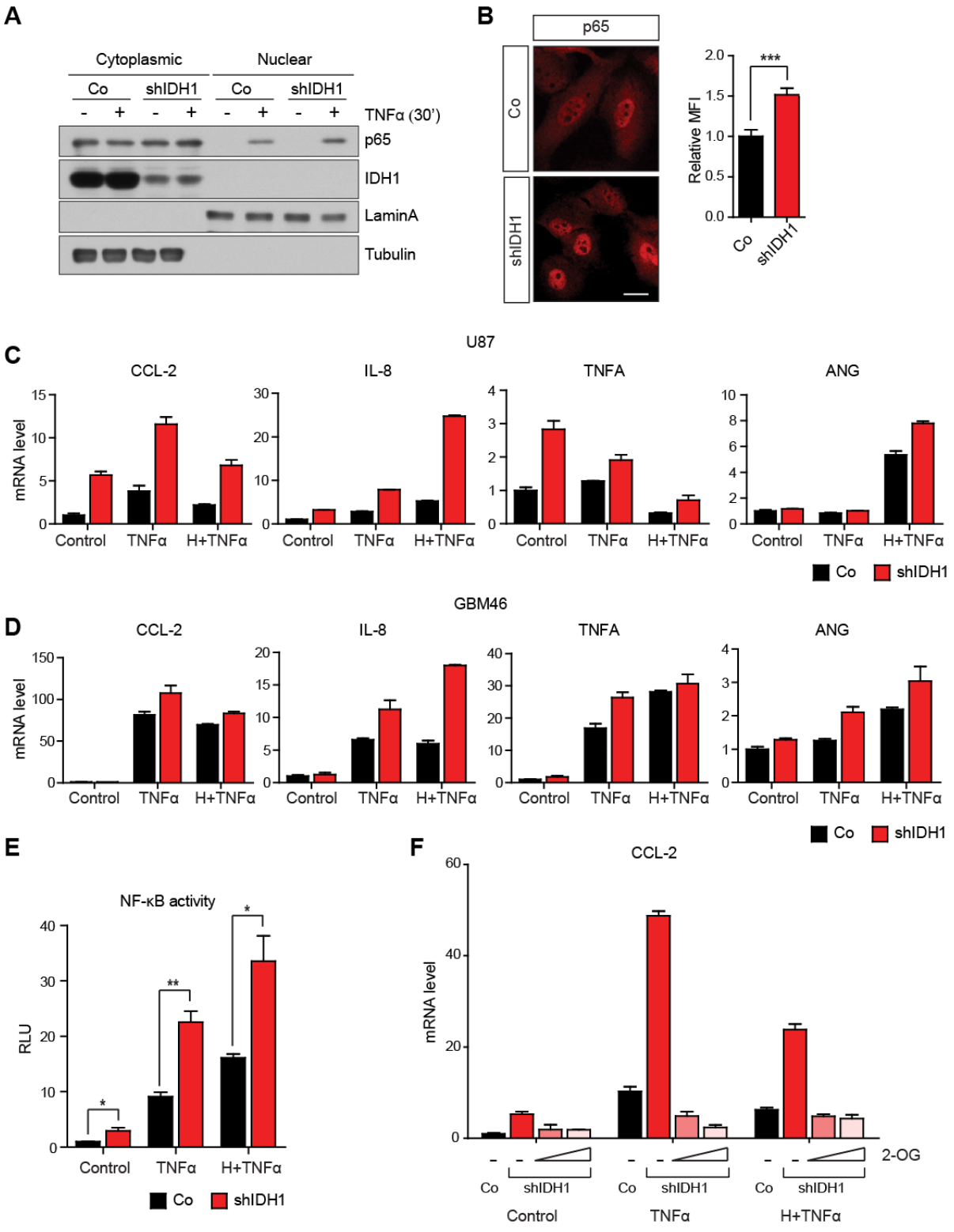

Figure 4.5. Regulation of the NF-κB pathway by IDH1 silencing.
A, B, U87 control and IDH1 knock-down cells were treated with TNFα and/or hypoxia. After 30 min of TNFα stimulation, nuclear and cytoplasmic proteins were analyzed to assess the nuclear translocation of the NF-κB subunit p65 by western blot and immunofluorescence.

Mean fluorescence intensity (MFI) was measured with ImageJ. **C, D,** U87 and GBM46 cells were analyzed for the expression levels of NF-κB target genes by qPCR. Expression levels of the NF-κB target genes interleukin-8 (IL-8), tumor necrosis factor alpha (TNFα), C-C motif chemokine 2 (CCL-2) and angiogenin (ANG) were increased in IDH1 knock-down cells. **E,** U87 glioblastoma cells were transfected with a firefly luciferase reporter construct under the control of NF-κB biding sites. IDH1 knock-down cells showed an increased NF-κB activity. **F,** U87 cells were treated with 6 mM and 8 mM of a cell permeable form of Dm-2-OG under TNFα treatment and/or hypoxia. Addition of Dm-2-OG to IDH1 knock-down cells reduced the expression levels of CCL-2 to the control levels. Scale bar, 20 μm (**B**). Data are means ± SEM. **P*<0.05, ***P*<0.01, ****P*<0.001.

4.1.1.3 IDH1 overexpression decreases HIF-α levels and impairs expression of HIF and NF-κB target genes

The regulation of HIF-α and NF-κB signaling in IDH1-depleted cells by diminished 2-OG levels suggested that IDH1 levels play a crucial role in the regulation of PHD-dependent signaling. To further test this, we examined the effect of increased IDH1 expression. Overexpression of IDH1 in different glioblastoma cells diminished HIF-1α and HIF-2α levels (Fig. 4.6A-C), displaying the reversed effect of IDH1 silencing. Moreover, overexpression of wildtype IDH1 in IDH1 knock-down cells also abolished HIF-α stabilization relative to control cells, whereas overexpression of an enzymatically inactive form of IDH1 (IDH1-3DN) (Losman et al., 2013) did not reduce HIF-α levels (Fig. 4.6D), demonstrating that IDH1 enzymatic activity is required for IDH1 mediated control of PHD activity.

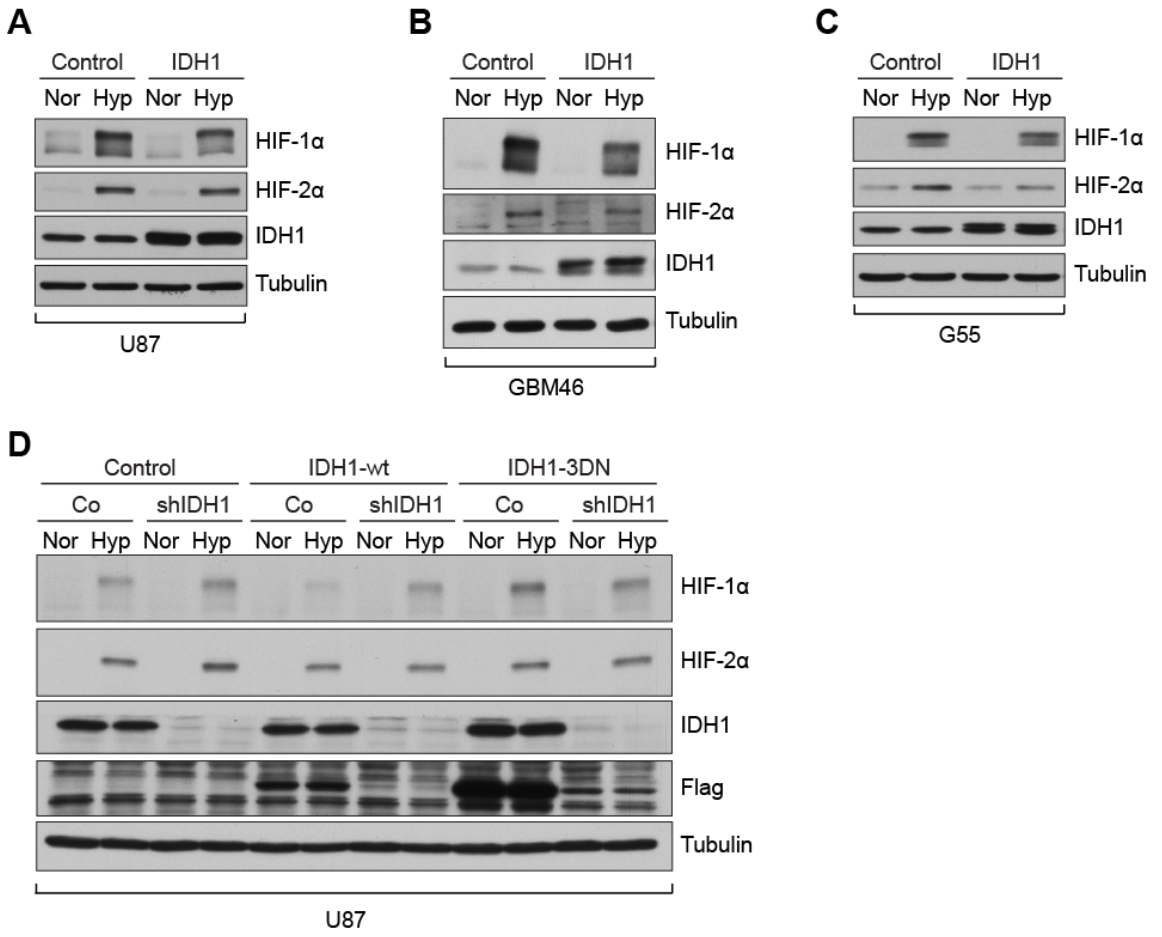

Figure 4.6. IDH1 overexpression reduces the hypoxic response.
A-C, U87, GBM46 and G55 cells were transfected with control and IDH1 wildtype overexpressing constructs and cultured under normoxia (Nor, 21% O_2) and hypoxia (Hyp, 1% O_2). IDH1 overexpression reduced HIF-α expression. **D,** U87 control and IDH1 knock-down cells were transfected with control (Co), wildtype IDH1 (IDH1-wt) and enzymatically inactive IDH1 (IDH1-3DN) constructs. Overexpression of wildtype IDH1 resulted in decreased HIF-α levels while overexpression of enzymatically inactive IDH1 did not reduce HIF-α levels.

In line with these results, IDH1 overexpression downregulated the expression of HIF target genes such as CAIX, VEGFA and GLUT1 (Fig. 4.7A). Moreover, we examined the expression of NF-κB target genes upon IDH1 overexpression. Our previous results showed that IDH1 silencing leads to increased NF-κB activity and upregulation of NF-κB target gene expression (Fig. 4.5). Thus, IDH1 overexpression displayed the contrary effect (Fig. 4.7B). Together, these results confirm that maintenance of IDH1 levels as well as its enzymatic activity is essential for controlling the hypoxic and inflammatory response.

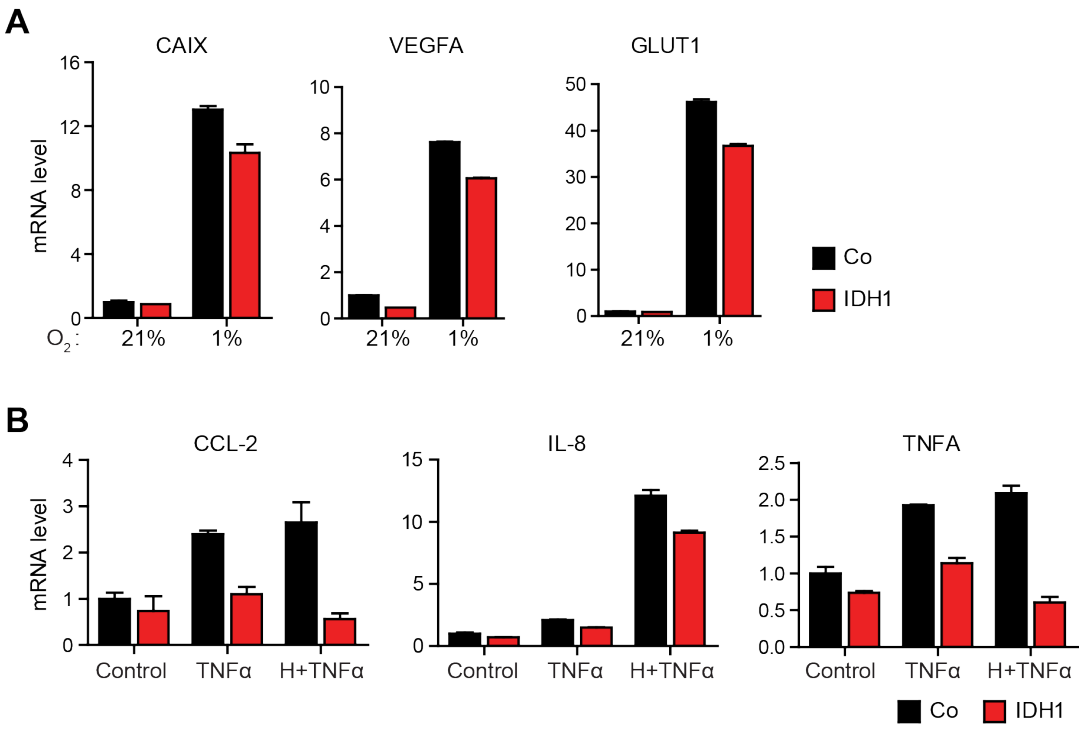

Figure 4.7. IDH1 overexpression reduces expression of HIF-α and NF-κB target genes. **A, B,** IDH1 wildtype overexpressing U87 cells under normoxia, hypoxia and/or TNFα treatment express lower levels of HIF and NF-κB target genes.

4.1.2 IDH1 knock-down promotes a cancer stem cell (CSC) phenotype

Cancer stem cells (CSCs), which are a specific subpopulation of tumor cells with self-renewal and differentiation capacity, have been reported to be regulated by the tumor microenvironment, including the hypoxic response/HIFs, and are involved in GBM pathogenesis. We therefore wanted to investigate if metabolic changes mediated by IDH1 are involved in the maintenance of the CSC phenotype in glioblastomas. To this end, we assessed the expression level of the well-established glioblastoma stem cell marker CD133 in IDH1 knock-down cells by western blotting. GBM46 primary glioblastoma cells transduced with three different IDH1 knock-down constructs displayed higher expression levels of CD133, especially after extended exposure to hypoxia (Fig. 4.8A), as well as under normoxia (Fig. 4.8D). This result was confirmed by fluorescence activated cell sorting (FACS) and qPCR (Fig. 4.8B, C), showing an

increased CD133 positive cell population and mRNA level after IDH1 knock-down, respectively. Moreover, IDH1 silenced cells also exhibited increased expression levels of the glioblastoma stem cell signature genes aspartate beta-hydroxylase domain containing 2 (ASPHD2) and mastermind like transcriptional coactivator 3 (MAML3) (Seidel, et al., 2010) (Fig. 4.8C). Interestingly, the separation of CD133 positive and negative cells revealed that CD133 positive cells express lower levels of IDH1 (Fig. 4.8F), suggesting that the regulation of IDH1 in glioblastoma cells contributes to key metabolic changes for the maintenance of the CSC phenotype. To functionally confirm the involvement of IDH1 in the regulation of the CSC phenotype, we performed a sphere formation assay, which assesses the self-renewal capacity of the cells. IDH1 knock-down cells exhibited an increased self-renewal capacity (Fig. 4.8G), validating the enhanced CSC phenotype. Furthermore, overexpression of IDH1 reduced the expression levels of CD133 (Fig. 4.8E).

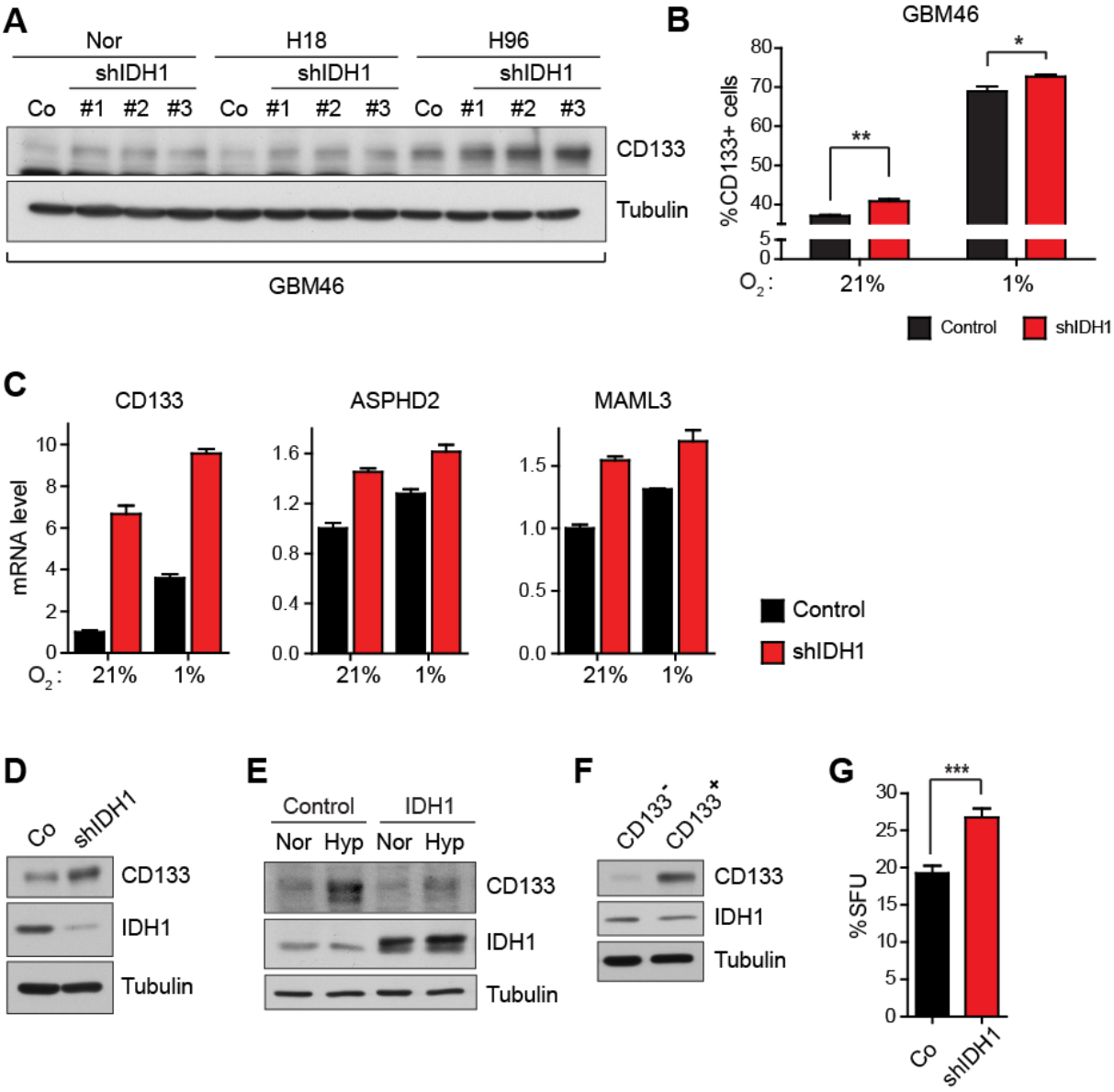

Figure 4.8. Enrichment of cancer stem cells by IDH1 silencing.
A, GBM46 glioblastoma cells were transduced with lentiviruses carrying non-silencing control (Co) and three different IDH1 shRNA knock-down constructs (the same as those in Fig. 4.1A) and cultured under normoxia (Nor, 21% O_2) and hypoxia (1% O_2) for 18 or 96 hours (H18 or H96). The expression levels of the cancer stem cell (CSC) marker CD133 were increased in all three different IDH1 knock-down cell lines. **B-D,** Increased CD133 expression levels following IDH1 silencing were confirmed by FACS analysis (**B**), qPCR (**C,** left) and western blotting (**D**). GBM46 IDH1 knock-down cells also resulted in increased expression levels of the glioblastoma stem cell signature genes Aspartate Beta-Hydroxylase Domain Containing 2 (ASPHD2) and Mastermind Like Transcriptional Coactivator 3 (MAML3), as assessed by qPCR (**C,** middle and right). **E,** IDH1 overexpression reduced CD133 expression. **F,** GBM46 cells were sorted for CD133 negative and positive cells with magnetic bead (MACS) separation. CD133 positive cells exhibited lower IDH1 levels. The magnetic bead separation of CD133 positive and negative cells, which were used for the immunoblot analysis, was performed by Sarah Goos from the group of Prof. Till Acker at the Institute of Neuropathology

(Giessen, Germany).**G,** Knock-down of IDH1 increases the self-renewal capacity of glioblastoma cells as assessed in a sphere forming assay. Data are means ± SEM. **P*<0.05, ***P*<0.01, ****P*<0.001.

The enhanced CSC phenotype following IDH1 knock-down was further confirmed in U87 cells by FACS and qPCR analysis. IDH1 knock-down U87 cells also showed an increased CD133 positive cell population and expression of CSC marker genes (Fig. 4.9A, B). Addition of Dm-2-OG to the culture medium was able to revert the effect of IDH1 silencing on CD133 levels (Fig. 4.9C, D). These experiments demonstrated that IDH1 silencing elevates the CSC phenotype through dysregulated 2-OG levels and Dm-2-OG addition abolishes this phenotype.

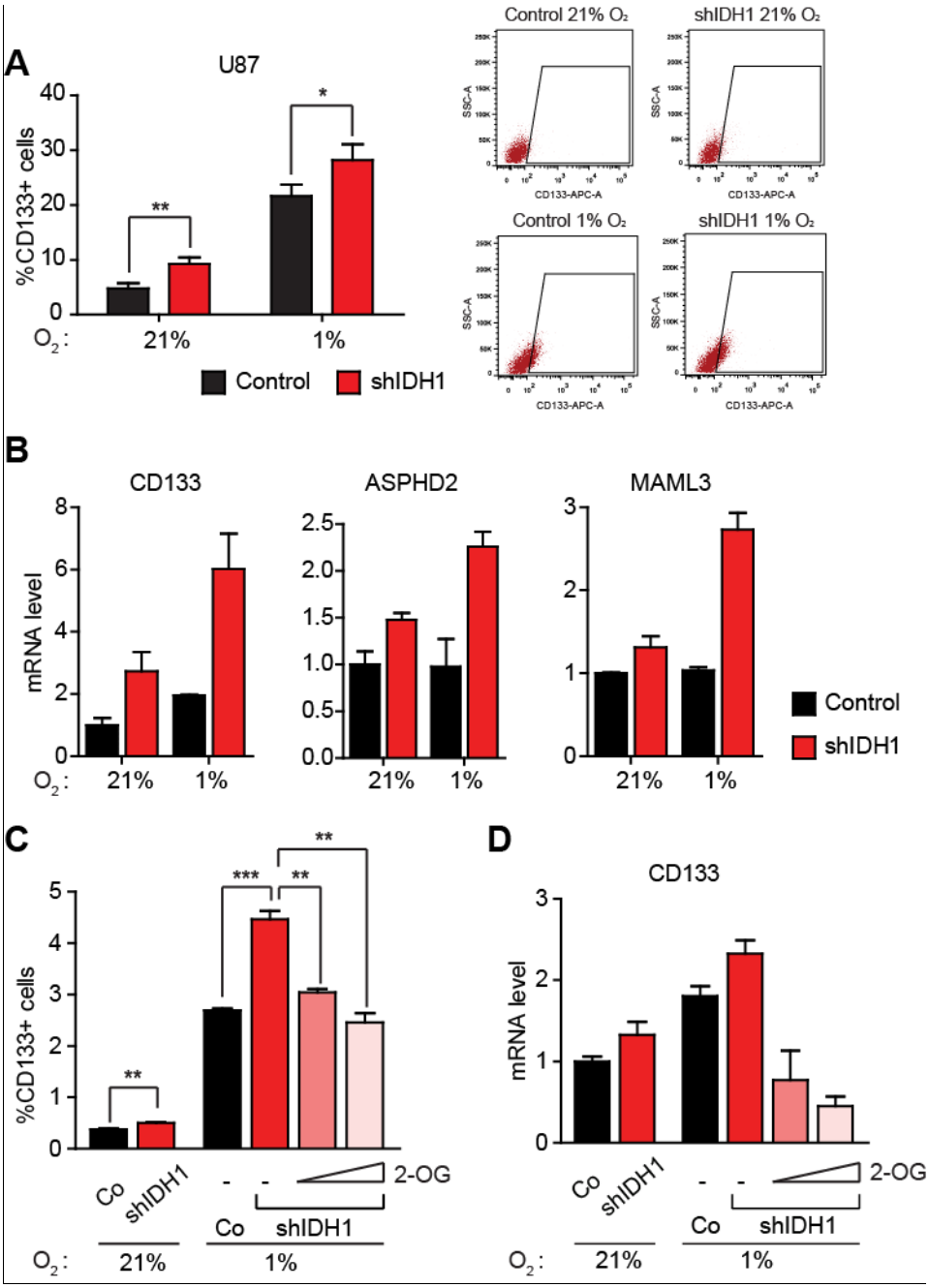

Figure 4.9. Addition of Dm-2-OG abrogates the increased self-renewal capacity upon knock-down of IDH1.

A, B, The increased CD133 expression levels following IDH1 knock-down were analyzed by FACS and qPCR (**B**, left) under normoxia (21%) and hypoxia (1%) for 96 hours in U87 cells. The expression levels of the glioblastoma CSC signature genes ASPHD2 and MAML3 were also increased upon IDH1 silencing (**B**, middle and right). **C, D,** The effect of IDH1 silencing on CD133 levels was reversed by addition of Dm-2-OG. U87 IDH1 knock-down cells were treated with 6 mM and 8 mM Dm-2-OG for 24 hours under hypoxia. The cells were analyzed by FACS (**C**) and qPCR (**D**). Data are means ± SEM. **P*<0.05, ***P*<0.01, ****P*<0.001.

4.1.3 Silencing of IDH1 mediates mesenchymal transition in GBM

4.1.3.1 Increased expression of Snail and CD44 levels by IDH1 silencing

Mesenchymal transformation of GBM resembles epithelial-to-mesenchymal transition (EMT) in epithelial cancers in many aspects. EMT transcription factors such as Snail, Slug, Twist, ZEB1 and ZEB2 have been reported to be important for mesenchymal transformation of GBM and to regulate the stem cell phenotype and tumor aggressiveness via promoting tumor growth, invasion and migration (Mikheeva, et al., 2010, Cheng, et al., 2012b, Kahlert, et al., 2013, Myung, et al., 2014, Iser, et al., 2016, Iwadate, 2016). EMT regulators are directly or indirectly regulated by TGFβ and hypoxia in glioblastoma cells (Karsy, et al., 2016). Activation of the SMAD signaling pathway is known to be one of the first steps in TGFβ induced EMT, which has also been reported to be activated by hypoxia. Importantly, a mesenchymal transition has been linked to the establishment of a CSC phenotype by various lines of evidence (Joseph, et al., 2015, Iser, et al., 2016, Moustakas and Heldin, 2016, Zhang, et al., 2016). Therefore, we wanted to assess if the activation of the hypoxic response and the induction of a CSC phenotype by IDH1 knock-down is also linked to a mesenchymal transition in GBM cells .

First, we examined the activation of TGFβ signaling using a luciferase assay which measures SMAD activity. We observed that IDH1 and/or IDH2 knock-down cells displayed increased SMAD activity (Fig. 4.10A). Furthermore, these cells also showed high expression levels of the EMT regulator Snail, which was analyzed by western blotting and qPCR (Fig. 4.10B, C). The strongest effect on Snail levels was observed after IDH1 silencing, showing the dominant role of IDH1, as compared to IDH2. Thus, in further experiments, we focused on the function of IDH1 in the control of the mesenchymal phenotype in GBM cells. Analysis of the expression levels of other EMT regulators and markers demonstrated that the mesenchymal marker CD44 is highly upregulated upon IDH1 silencing, whereas the proneural marker T-cadherin is downregulated analogous to epithelial marker such as E-cadherin in epithelial cancer (Fig. 4.10D).

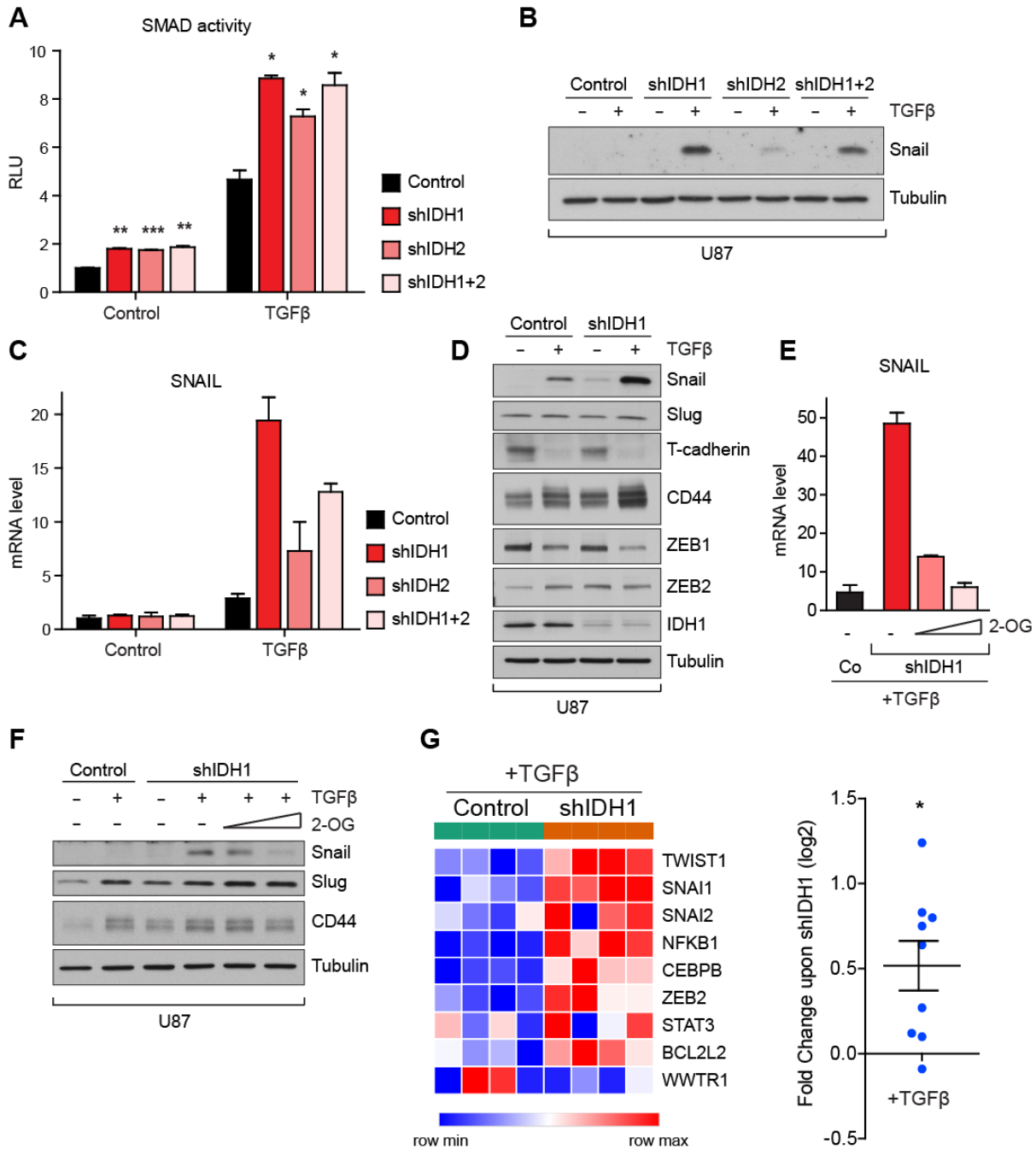

Figure 4.10. IDH1 silencing enhances TGFβ signaling and increases Snail expression levels.

A, U87 Control, IDH1 and/or IDH2 knock-down cells were transfected with a firefly luciferase reporter construct under the control of SMAD binding sites. U87 IDH1 and/or IDH2 knock-down cells showed increased SMAD activity. **B, C,** U87 control, IDH1 and/or IDH2 knock-down cells were treated with 5 ng/ml TGFβ for 72 hours. Western blotting (**B**) and qPCR (**C**) analysis showed that the epithelial to mesenchymal transition (EMT) regulator Snail is highly upregulated by IDH1 silencing. **D,** The expression levels of the EMT regulators Snail, Slug, ZEB1, ZEB2, the mesenchymal marker CD44 and the proneural marker T-cadherin were analyzed by western blotting under treatment with or without 5 ng/ml TGFβ. **E, F,** The

upregulation of Snail and CD44 following IDH1 silencing was reversed by addition of Dm-2-OG. U87 control and IDH1 knock-down cells were treated with or without 5 ng/ml TGFβ for 72 hours, Dm-2-OG was added for the last 6 hours of TGFβ treatment for western blotting (**F**) and the last 18 hours of TGFβ treatment for qPCR (**E**). **G,** TGFβ treated U87 control and IDH1 knock-down cells were analyzed in a mRNA microarray. mRNA expression levels of a set of EMT regulators (Karsy, et al., 2016) were sorted and represented in the heatmap (left). Fold change in expression of EMT regulators upon IDH1 knock-down, relative to control, are shown (right), each dot represents one gene listed in the heatmap (left). Microarray analysis was performed by Jochen Wilhelm and Susanna Ziegler from the University of Giessen Lung Center (Giessen, Germany). Data are means ± SEM. **P*<0.05, ***P*<0.01, ****P*<0.001.

To further verify that upregulation of Snail and CD44 is mediated directly by IDH1 silencing, the cells were treated with Dm-2-OG for 6 hours to restore 2-OG levels in the cells. Addition of Dm-2-OG reduced Snail and CD44 expression levels (Fig. 4.10E, F). Moreover, microarray analysis confirmed that the expression of EMT regulators, which were reported to be involved in GBM pathology (Karsy, et al., 2016), are increased upon IDH1 knock-down following TGFβ treatment (Fig. 4.10G, right). The expression of this set of EMT regulators was significantly elevated upon IDH1 silencing (Fig. 4.10G, left).

4.1.3.2 IDH1 knock-down elevates the invasive capacity of GBM cells

A characteristic feature of EMT in epithelial cancers, as well as mesenchymal transition in GBM, is enhanced local invasion. To confirm that IDH1 knock-down functionally elevates the mesenchymal phenotype, the invasive capacity of the cells was assessed by a modified Boyden chamber assay, which allows the cells to invade through a porous membrane covered with a layer of Matrigel. We observed that IDH silencing significantly increased the invasion of U87 and G55 cells (Fig. 4.11A, B), confirming that that IDH1 knock-down induces a mesenchymal, pro-invasive phenotype.

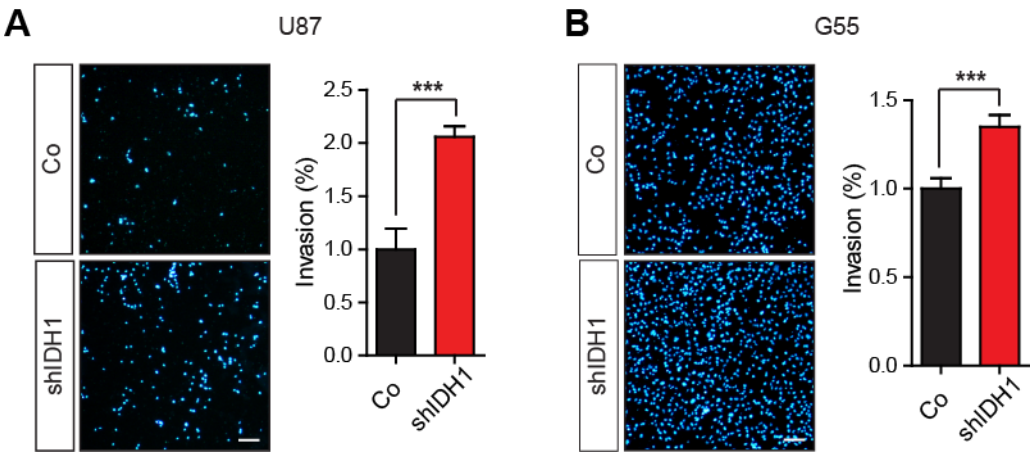

Figure 4.11. IDH1 silencing enhances the invasion capacity of tumor cells.
A, B, Invasion of U87 (**A**) and G55 (**B**) cells cultured for 24 hours was assessed using a modified Boyden chamber assay. Representative images show invading tumor cells at the lower side of the membranes. Quantification of the area covered by invaded cells in the lower compartment, normalized to the area covered by non-invaded cells in the upper compartment (n=6). Data are means ± SEM. Scale bars, 200 µm. *** *P*<0.001.

4.1.3.3 HIF-1/2α silencing reverts the Snail upregulation elicited by IDH1 knock-down

To investigate the mechanisms of the enhanced mesenchymal phenotype in IDH1 knock-down cells, we examined the impact of signaling pathways such as HIF-α and NF-κB, which we showed to be activated in IDH1 silenced cells (Fig. 4.1-5) as a result of reduced 2-OG levels. Interestingly, Snail expression was induced upon IDH1 knock-down (Fig. 4.10C), similarly to the expression of HIF-α (Fig. 4.1D, E) and NF-κB (Fig. 4.5C, D) target genes. Moreover, restoration of 2-OG levels resulted in decreased Snail expression (Fig. 4.10E, F) again similar to the expression levels of HIF and NF-κB target genes (Fig. 4.4E, F and 4.5 F). These data suggested that the signaling pathways regulated by IDH1 knock-down may be involved in the maintenance of the mesenchymal phenotype through controlling Snail expression. Therefore, we silenced HIF-1α and/or HIF-2α in TGFβ treated U87 cells. HIF-1/2α double knock-down reduced the expression levels of Snail, whereas silencing either HIF-1α or HIF-2α alone did not result in a significant effect, indicating that both isoform of HIF-α take part in the control of mesenchymal transition in IDH1-depleted cells. In addition, knock-down of RelA (p65 subunit of NF-κB) and HIF-1/2α under hypoxic (Fig. 4.12B)

or TGFβ (Fig. 4.12C) treatment revealed that HIF-1/2α play a dominant role in the control of the mesenchymal phenotype as seen by a significant reduction of Snail levels. HIF-1α, HIF-2α and RelA knock-down efficiency was determined by qPCR (Fig. 4.12D), which also showed that Snail mRNA upregulation upon IDH1 silencing was partially reverted by HIF-1/2α silencing (Fig. 4.12D).

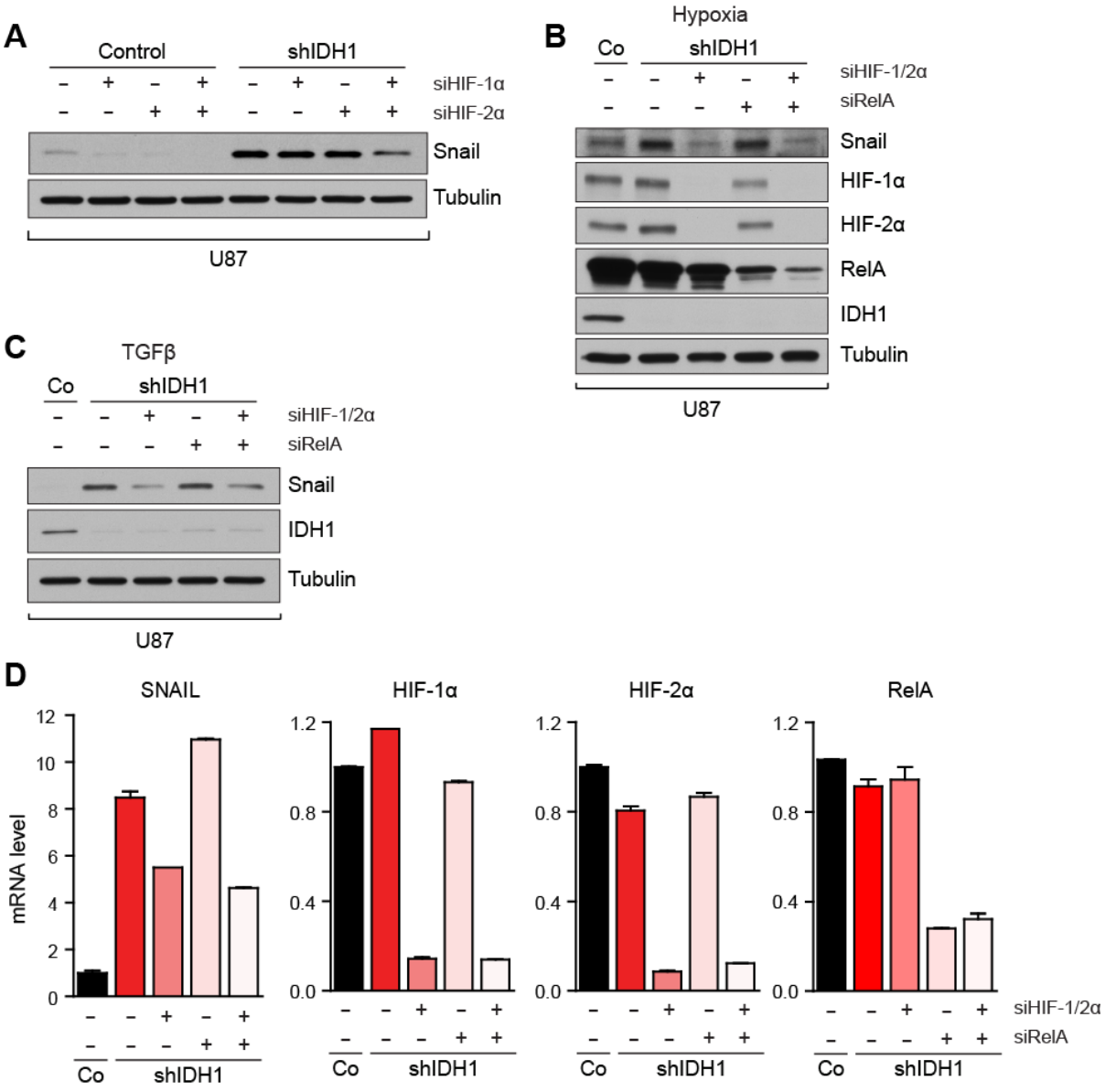

Figure 4.12. HIF-1/2α silencing but not RelA silencing reduces Snail expression levels upon IDH1 silencing.
A, Control, HIF-1α and/or HIF-2α siRNA transfected U87 control and IDH1 knock-down cells were treated with 5 ng/ml TGFβ. Only HIF-1/2α double knock-down leads to reduced Snail expression levels. **B-D,** U87 IDH1 knock-down cells were transfected with control, HIF-1/2α (HIF-1α and HIF-2α) and/or RelA (p65) siRNA. One day after the transfection, the cells were

treated with hypoxia (1% O_2, 48 hours) (**B**) or TGFβ (5 ng/ml, 48 hours) (**C, D**). HIF-1/2α silencing but not RelA silencing reduced Snail expression levels, as determined by immunoblotting (**B, C**) and qPCR (**D**). siRNA knock-down efficiencies were confirmed by qPCR (**D**).

4.1.4 Microenvironmental signals downregulate IDH1

IDH1 is an enzyme which converts isocitrate to 2-OG in the TCA cycle. Since our previous results proposed a key function of IDH1 in the production and maintenance of 2-OG to supply an essential co-substrate for 2-OG dependent enzymes such as PHDs, we investigated whether IDH1 is regulated in response to microenvironmental stimuli. Therefore, we treated the cells with FBS, which contains a variety of growth factors, or TGFβ, an EMT inducer. GMB cells cultured under stem cell conditions in a serum free medium showed a marked reduction in IDH1 expression upon FBS and TGFβ treatment (Fig. 4.13A, B). Interestingly, TGFβ treated CD133 positive GBM46 primary glioblastoma cells expressed much lower levels of IDH1 (Fig. 4.13C), confirming our previous results (Fig. 4.8E) that CSCs express lower levels of IDH1, showing that TGFβ treatment potentiates this effect. Changes in microenvironmental conditions regulate mainly IDH1 expression levels among the IDH isoforms, as shown by qPCR analysis (Fig. 4.13D). IDH1 is 40% to 50% downregulated following TGFβ and FBS treatment, whereas the mitochondrial forms IDH2 and IDH3 showed slight changes at expression levels, indicating a specific regulatory mechanism on IDH1 by the microenvironment.

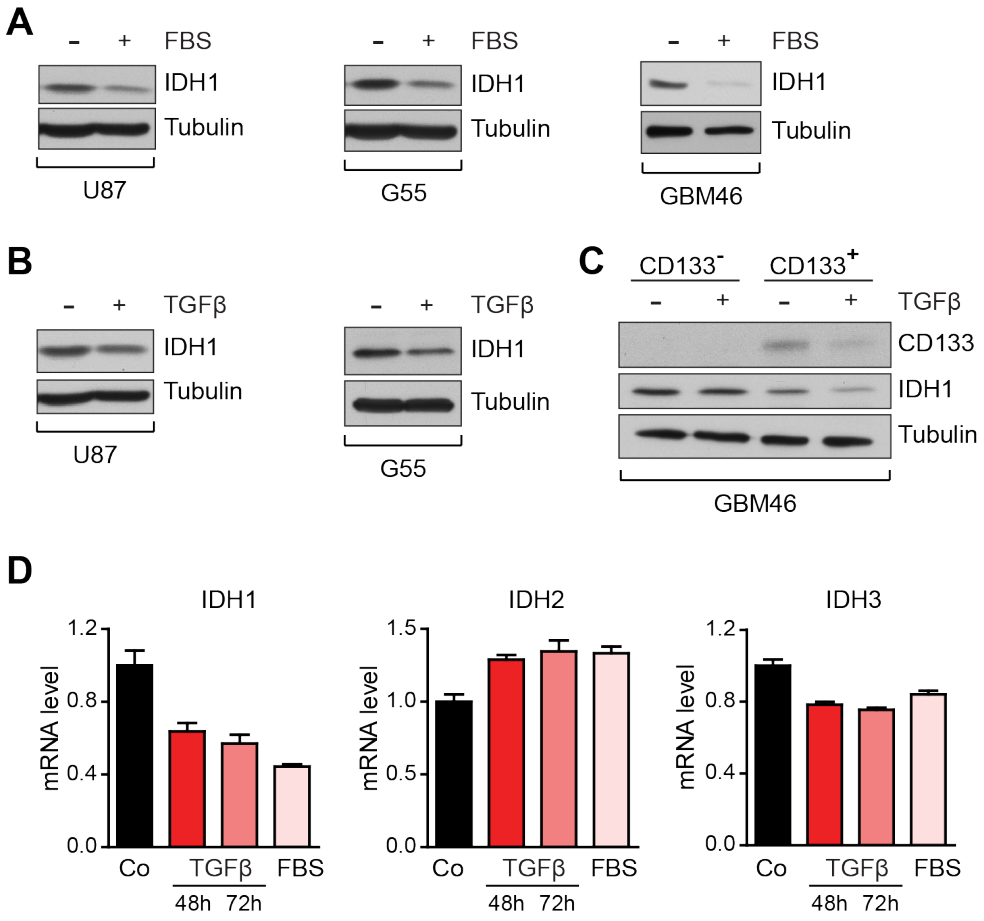

Figure 4.13. Regulation of IDH1 by microenvironmental stimuli.
A, Glioblastoma cells were cultured in tumor stem cell medium, upon addition of 10% FBS IDH1 levels were downregulated. **B,** Glioblastoma cells, treated with TGFβ for 72 hours, showed reduced IDH1 expression levels. **C,** GBM46 primary glioblastoma cells were treated with TGFβ and subsequently sorted for CD133 negative and positive cells with magnetic bead separation. TGFβ treatment downregulates IDH1 levels in CD133 positive cells. The magnetic bead separation of CD133 positive and negative cells, which were used for the immunoblot analysis, was performed by Sarah Goos from the group of Prof. Till Acker at the Institute of Neuropathology (Giessen, Germany). **D,** IDH1 mRNA levels were markedly regulated by TGFβ and FBS treatment in U87 cells, as determined by qPCR.

4.1.5 IDH1 level is associated with tumor growth and invasion

To investigate the impact of IDH1 levels in GBM patient prognosis, we analyzed the data in the publicly available “The Cancer Genome Atlas” (TCGA) cohort. Analysis of IDH1 expression level and survival of individual patients revealed a correlation between low IDH1 expression and decreased overall patient survival (Fig. 4.14A), supporting the utility of IDH1 as a prognostic marker and in line with the pro-

tumorigenic phenotype induced by IDH1 deficiency. Furthermore, intracranial injection of control and IDH1 knock-down cells into immunocompromised mice showed that IDH1 silenced cells formed significantly larger tumors (Fig. 4.14B), confirming the important function of IDH1 in tumor growth. Consistent with our previous data on invasion in cell culture (Fig. 4.11), G55 and GBM46 IDH1 knock-down tumors exhibited increased local tumor invasion *in vivo* (Fig. 4.14C, D), one of the characteristics of glioblastomas. Moreover, IDH1 knock-down tumors showed increased tumor vascularization (Fig. 4.14E).To support our *in vitro* data on the enhanced HIF and NF-κB pathway and CSC phenotype, we isolated RNA from tumors and analyzed gene expression. Elevated levels of VEGFA, a HIF target gene and inducer of angiogenesis, CD133, a CSC marker, and CCL-2, an NF-κB target gene, were observed in tumors with silenced IDH1 *in vivo* (Fig. 4.14F).

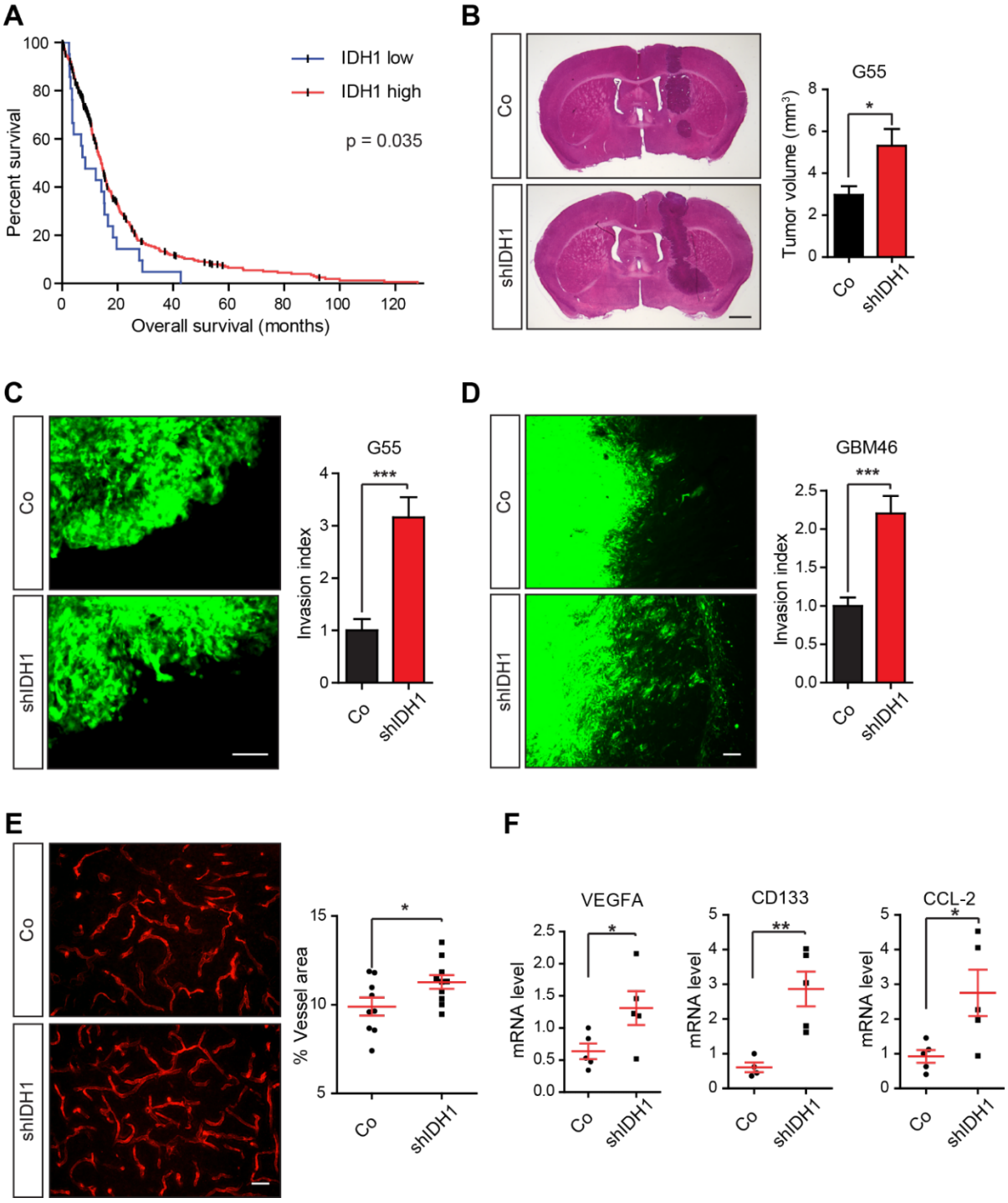

Figure 4.14. Reduced IDH1 levels correlate with poor GBM patient prognosis, increased tumor growth and invasion.
A, Analysis of glioblastoma (GBM) patient survival data and IDH1 expression levels from the TCGA cohort. Low expression levels of IDH1 correlated with a decreased median overall patient survival (n=427). **B,** G55 control and shIDH1 cells were orthotopically transplanted into the brain of immunocompromised mice. IDH1 knockdown cells formed significantly larger tumors (n=10-9 (Co-shIDH1)). **C, D,** G55 (n=9-9 (Co-shIDH1)) and GBM46 (n=9-10 (Co-

shIDH1)) IDH1 knockdown tumors showed increased invasiveness. The orthotopic transplantation of tumor cells into the brain of immunocompromised mice was performed by Sascha Seidel from the group of Prof. Till Acker at the Institute of Neuropathology (Giessen, Germany). GFP signal of tumor cells was used to assess the area of invading tumor cells evading the tumor core. **E,** Endothelial cell staining in GBM46 control and IDH1 knock-down tumors showed increased tumor vascularization in IDH1 silenced tumors (n=9-10 (Co-shIDH1)). **F,** qPCR analysis showed that GBM46 IDH1 knockdown tumors have enhanced expression of VEGFA, CD133 and CCL-2. Data are means ± SEM. Scale bars, 1mm (**B**), 100 µm (**C, D, E**). **P*<0.05, ***P*<0.01, ****P*<0.001.

4.1.6 IDH1 silencing enhances HIF-α and Snail expression levels in breast and lung carcinoma cell lines

To examine if the effect of IDH1 on the hypoxic response and the mesenchymal phenotype, which we observed in GBM, can be validated in other cancer types, we silenced IDH1 in MDA-MB-231 breast cancer cells. Similarly to glioblastoma cell lines, IDH1 silencing resulted in increased HIF-1α and HIF-2α levels under hypoxia (Fig. 4.15A) and a marked increase in the expression level of Snail (Fig. 4.15B). In addition, upon TGFβ treatment, IDH1 was downregulated (Fig. 4.15C), indicating that IDH1 is modulated by external signals in breast carcinoma cell lines analogous to glioblastomas. Consistently, IDH1 knock-out MDA-MB-231 and A549 cells, generated by CRISPR/Cas9-mediated gene targeting, also showed increased levels of Snail (Fig. 4.15D, E). Moreover, hypoxia treated A549 cells showed an enhanced hypoxic response (Fig. 4.15E). Next, we performed a colony forming assay, revealing that IDH1 knock-down cells formed a significantly higher number of colonies (Fig. 4.15F). Moreover, orthotopic transplantation of MDA-MB-231 control and IDH1 knock-down cells into the mammary fat pad of immunocompromised mice showed that IDH1 knock-down cells possess a significantly elevated metastatic capacity, whereas primary tumor growth was not altered (Fig. 4.15H). To further test whether IDH1 is associated with patient prognosis, we analyzed the correlation between IDH1 expression levels and overall survival of lung adenocarcinoma patients. The data obtained from TCGA cohort (n=223) revealed that low IDH1 expression is associated with a worse prognosis (Fig. 4.15G), supporting the importance of IDH1 in cancer pathology.

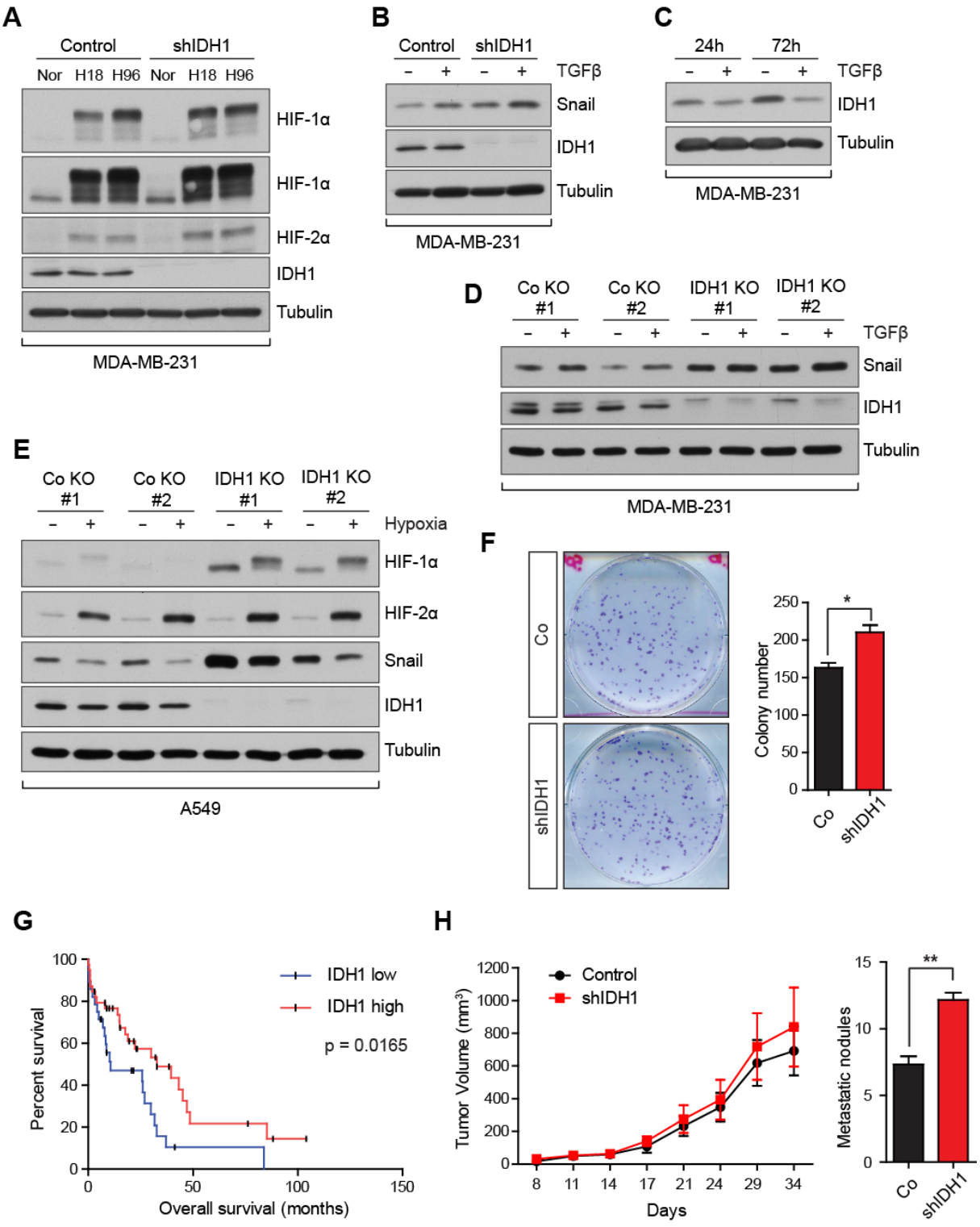

Figure 4.15. IDH1 silencing in breast and lung cancer cell lines
A, MDA-MB-231 breast cancer cells were transduced with lentiviruses carrying non-silencing control (Control) and IDH1 shRNA. Cells were grown under adherent conditions and incubated under normoxia (Nor, 21% O_2) or hypoxia (1% O_2) for 18 or 96 hours (H18/H96). Knock-down of IDH1 leads to increased HIF-α levels. **B,** MDA-MB-231 control and IDH1 knock-down cells

were treated with 5 ng/ml TGFβ for 72 hours. Western blotting analysis showed that the EMT regulator Snail is upregulated upon IDH1 silencing. **C,** IDH1 expression levels are markedly downregulated upon TGFβ treatment. Cells were treated with 5 ng/ml TGFβ for 24 or 72 hours. **D, E,** Increased Snail expression levels and/or enhanced HIF response were verified in IDH1 knock-out (IDH1-KO) MDA-MB-231 and A549 cell clones. MDA-MB-231 and A549 control and IDH1-KO cells were created with the CRISPR-Cas9 system and single cell clones were analyzed. **F,** MDA-MB-231 control and IDH1 knock-down cells were seeded for a colony formation assay (500 cells per well, n=3). IDH1 knock-down cells formed significantly more colonies compared to control cells. **G,** Analysis of lung adenocarcinoma survival data for patients from TCGA cohort stratified according to IDH1 expression revealed a correlation between low levels of IDH1 and decreased overall patient survival (n=223). **H,** MDA-MB-231 control and shIDH1 cells were orthotopically transplanted into the mammary fat pad of immunocompromised mice. IDH1 knockdown cells displayed a significantly higher metastatic capacity, whereas primary tumor growth was not elevated. Orthotopic transplantation of the breast cancer cells into immunocompromised mice and counting of lung metastases were performed with the help of Omelyan Trompak from the group of Prof. Till Acker at the Institute of Neuropathology (Giessen, Germany) and Angel M. Cuesta from the group of Prof. Amparo Acker-Palmer at the Institute of Cell Biology and Neuroscience (Frankfurt, Germany). Data are means ± SEM. **P*<0.05, ***P*<0.01.

4.2 An acidosis induced HSP90-HIF-α axis and the cancer stem cell phenotype

The second part of the thesis focuses on the pH mediated regulation of the hypoxic response and CSC maintenance. Within the project Alina Filatova focused on the mechanism of the cellular response to acidosis and the regulation of the HSP90-HIF axis) *in vitro* (Filatova et al., 2016), whereas Sascha Seidel and I focused on the acidosis-induced HIF dependent regulation of the CSC phenotype and the effect of HSP90 regulation on tumor hypoxia and growth. The presented data was conjointly generated with Sascha Seidel. Analysis of VEGF, CD133 and Nestin expression in glioblastoma patients with low and high HSP90 levels presented in figure 19A was performed by Boyan Garvalov and immunohistochemical analysis of serial sections of patient samples presented in figure 19B was performed by Till Acker.

4.2.1 Acidosis-induced HIF activation and CSC maintenance

Altered metabolism following hypoxia, including a shift from oxidative phosphorylation to glycolysis for energy production is one of the hallmarks of cancer. Due to the

limitation of oxygen supply and accumulation of lactate originating from glycolysis, rapidly growing solid tumors such as glioblastomas become hypoxic and acidic. Decreased extracellular pH accompanied by hypoxia is one of the characteristics of glioblastomas and has been reported to be associated with increased resistance to chemotherapy, elevated VEGF expression levels and a pronounced CSC phenotype (DeBerardinis, et al., 2008, Phan, et al., 2014). Therefore, we examined the contribution of acidosis to tumor hypoxia and CSC maintenance. Cells cultured at physiological pH (pH7.4) or acidic pH (pH6.7) under normoxia or hypoxia showed higher HIF-1α and HIF-2α expression levels in G55 cells (Fig. 4.16A) which was also validated in primary glioblastoma cell lines (data not shown). It has been reported that hypoxia promotes the CSC phenotype through HIFs. To elucidate whether acidosis would also influence the CSC phenotype, GBM15 primary glioblastoma cells were cultured at pH7.4 and pH6.7. Analysis of CSC marker CD133 or CD15 expressing cells by FACS revealed that acidosis increased the fraction of CSCs (Fig. 4.16E, F). Similarly, low pH also increased the expression of side population signature genes, which are associated with a CSC phenotype (Fig. 4.16H). Double knock-down of HIF-1α and HIF-2α (HIF-1/2α; Fig. 4.16B, C) in GBM15 cells demonstrated that the acidosis induced expression of the HIF target gene CAIX, was abrogated and depended on HIF-1/2α (Fig. 4.16D). Moreover, not only HIF target gene expression levels, but also the increased CD133 positive cell fraction and self-renewal capacity were abrogated by HIF-1/2α knock-down (Fig. 4.16E, G), confirming that promotion of the CSC phenotype by acidosis is HIF dependent.

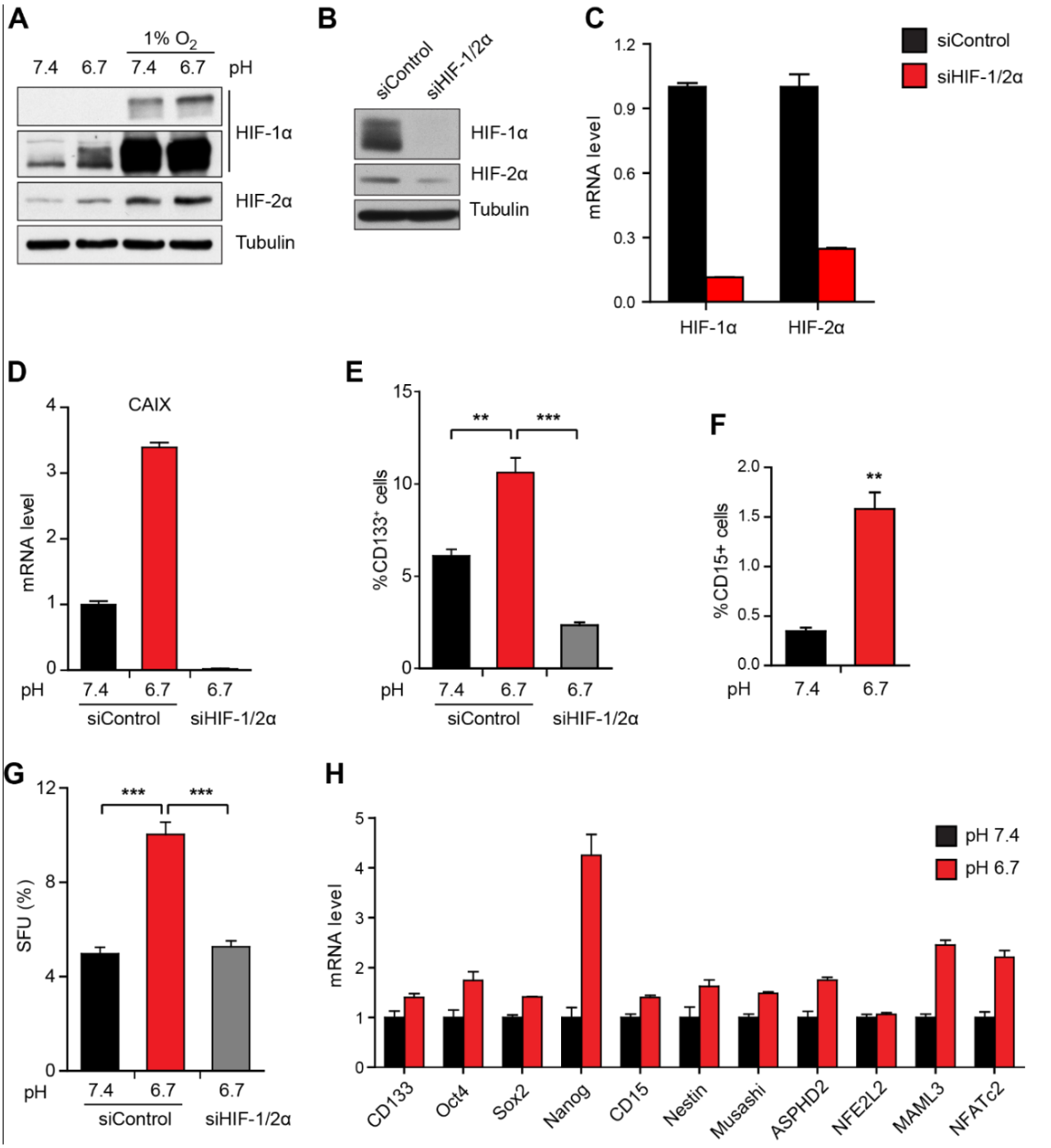

Figure 4.16. Acidosis induces HIF-α function and CSC self-renewal.
A, Acidic pH increases HIF-1/2α levels. Immunoblot of G55 cells grown under normoxia or hypoxia (1% O_2) in CO_2-independent medium with acidic pH (6.7) or physiological pH (7.4). **B-H,** Acidosis induces the CSC phenotype and expression levels of CSC marker genes through HIF-1/2α. GBM015 cells were co-transfected with control or HIF-1/2α siRNA, and after 18 hours of incubation at 1% O_2 the level of HIF-1/2α protein (**B**) and mRNA (**C**) was determined by immunoblot and qPCR, respectively. Quantification of the expression of the HIF target gene CAIX (**D**), the fraction of $CD133^+$ and $CD15^+$ cells (n=3) (**E, F**), the sphere forming capacity (n=6) (**G**) and expression of a panel of CSC marker genes (**H**). GBM015 primary glioblastoma cells were transfected with non-silencing control or HIF-1/2α siRNA and incubated at pH7.4 or 6.7 at 1% O_2 for 96 hours. Data are means ± SEM, $^{**}P<0.01$, $^{***}P<0.001$.

4.2.1.1 Acidosis controls HIF function through HSP90 *in vitro* and *in vivo*

PHD/VHL dependent posttranslational regulation of HIF-α is one of the best-studied molecular mechanisms. Besides the PHD/VHL dependent mechanism, HSP90 competes with RACK1 for HIF-α-binding and the HSP90-HIF-α interaction prevents HIF-α degradation (Katschinski, et al., 2004, Liu, et al., 2007). HSP90 functions as homodimer, each HSP90 monomer consist of three domains: N-terminal domain, which is connected to middle domain by a linker and the c-terminal domain (Csermely et al., 1998, Ali et al., 2006). There are two different cytoplasmic isoforms of HSP90: the inducible HSP90α and the constitutive HSP90β (Krone and Sass, 1994). Previous work in the lab showed that the acidosis mediated increase in HIF function is PHD/VHL independent but instead controlled by HSP90 *in vitro*. In addition, low pH upregulates HSP90, suggesting that acidosis induced HSP90 regulates HIF-α levels and CSC maintenance (Filatova, et al., 2016). To further confirm the role of HSP90 in acidosis induced HIF-α levels, we created HSP90α and HSP90β double knock-down cells. Knock-down of HSP90α/β suppressed the acidosis mediated increase in HIF-α levels (Fig. 4.17A). Importantly, knock-down of HSP90α/β reduced tumor growth in an intracranial tumor model (Fig. 4.17B). Even if both,the control and HSP90α/β knock-down tumors exhibited perinecrotic hypoxic areas as shown by Hypoxyprobe staining, HIF-1α levels were reduced in HSP90α/β knock-down tumors (Fig. 4.17C). Moreover, analysis of RNA and protein samples from tumors revealed that HIF-1/2α levels, as well as the expression of the HIF target gene VEGF were remarkably reduced upon HSP90 knock-down (Fig. 4.17D-F). Furthermore, HSP90 silencing increased the survival of mice and reduced the tumor initiating capacity of the cells (Fig. 4.17G, H), indicating that HSP90 plays a key role under acidic conditions in regulating HIF function and the CSC phenotype.

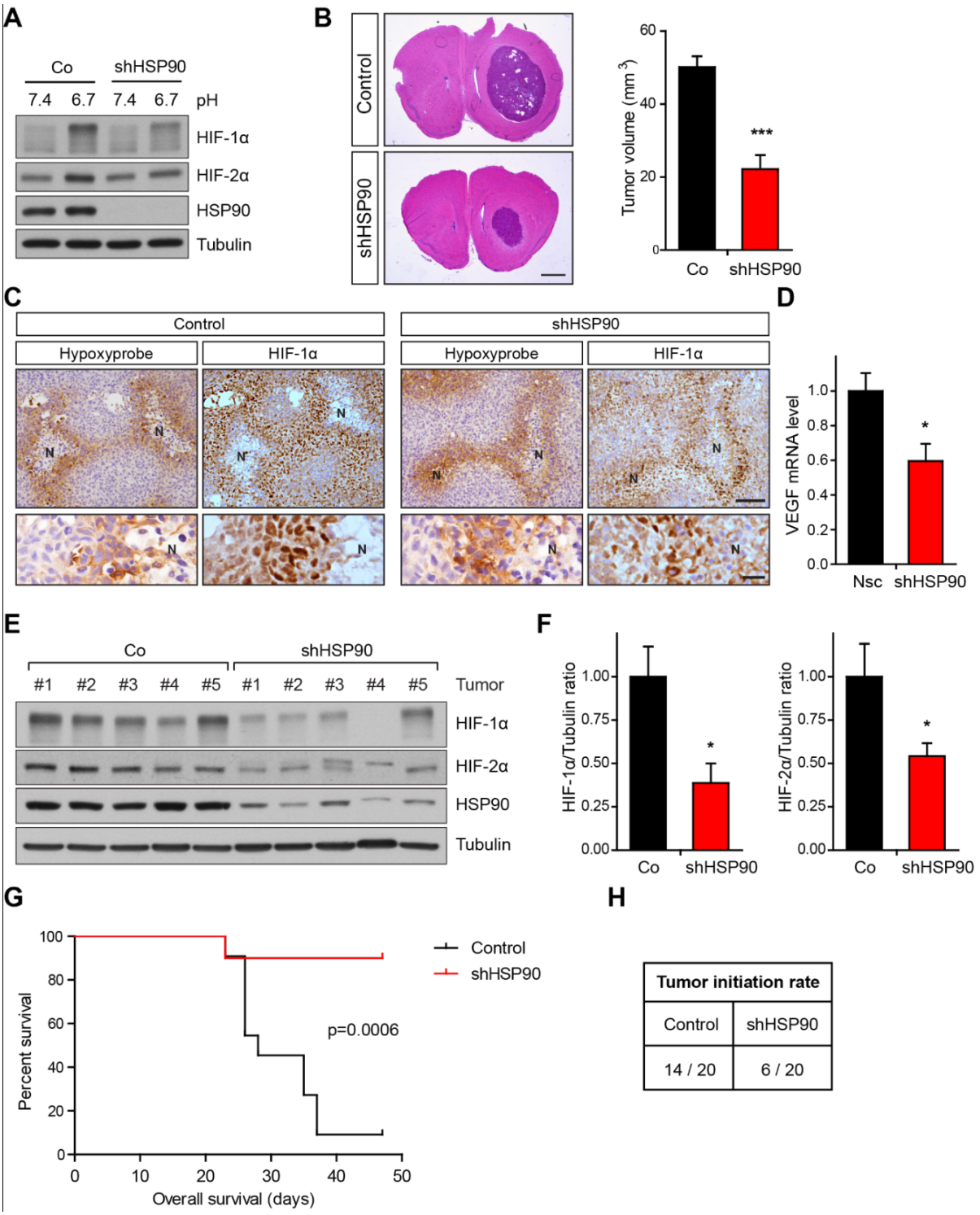

Figure 4.17. HSP90 inactivation suppresses the acidosis-induced HIF-α increase and tumor growth.

A, Silencing of HSP90α/β reduces HIF-α levels *in vitro*. Immunoblot of G55 cells stably transduced with non-silencing control (Co) or HSP90α/β shRNAs (shHSP90) and cultured at pH7.4 or 6.7 under hypoxia for 18 hours. **B-H,** Loss of HSP90 reduces tumor growth and intratumoral HIF-α levels and activity. Control and HSP90α/β shRNA G55 tumor cells were

orthotopically transplanted in immunocompromised mice. **B,** Tumor xenografts were HE-stained and the tumor volume was quantified (n=9). **C,** Immunohistochemical staining for Hypoxyprobe and HIF-1α in control and shHSP90 tumors. N, necrotic areas. **D,** The expression of the HIF target gene VEGFA was analyzed by qPCR in tumor samples (n=9) **E,** Immunoblot for HIF-1/2α and HSP90 in extracts from representative control and shHSP90 tumors. **F,** Quantification of HIF-1α and HIF-2α levels in control and shHSP90 tumors by immunoblot (n=9). **G, H,** HSP90 silencing promotes survival and reduces tumor initiating capacity. G55 cells stably transduced with non-silencing control or HSP90α/β shRNA were transplanted subcutaneously in immunocompromised mice. Loss of HSP90 increased morbidity-free survival of mice (n=10) (**G**) and reduced the tumor initiating capacity (**H**). Data are means ± SEM. **P*<0.05; ****P*<0.001. Scale bars, 1 mm (**B**), 100 µm (**C**), 20 µm (**C**, higher magnifications).

Similarly, inhibition of HSP90 by overexpressing the dominant negative form of HSP90 (Miao et al., 2008) also reduced the HIF-1α and HIF-2α levels (Fig. 4.18A). Importantly, HSP90 inhibition through the dominant negative form also resulted in reduced intracranial tumor growth (Fig. 4.18B) and in decreased HIF-1α and HIF-2α levels (Fig. 4.18C, D). Taken together, our findings show that acidosis increases HIF-α levels and CSC maintenance through HSP90 and inhibition of HSP90 abrogates tumorigenicity and intratumoral HIF-1/2α levels.

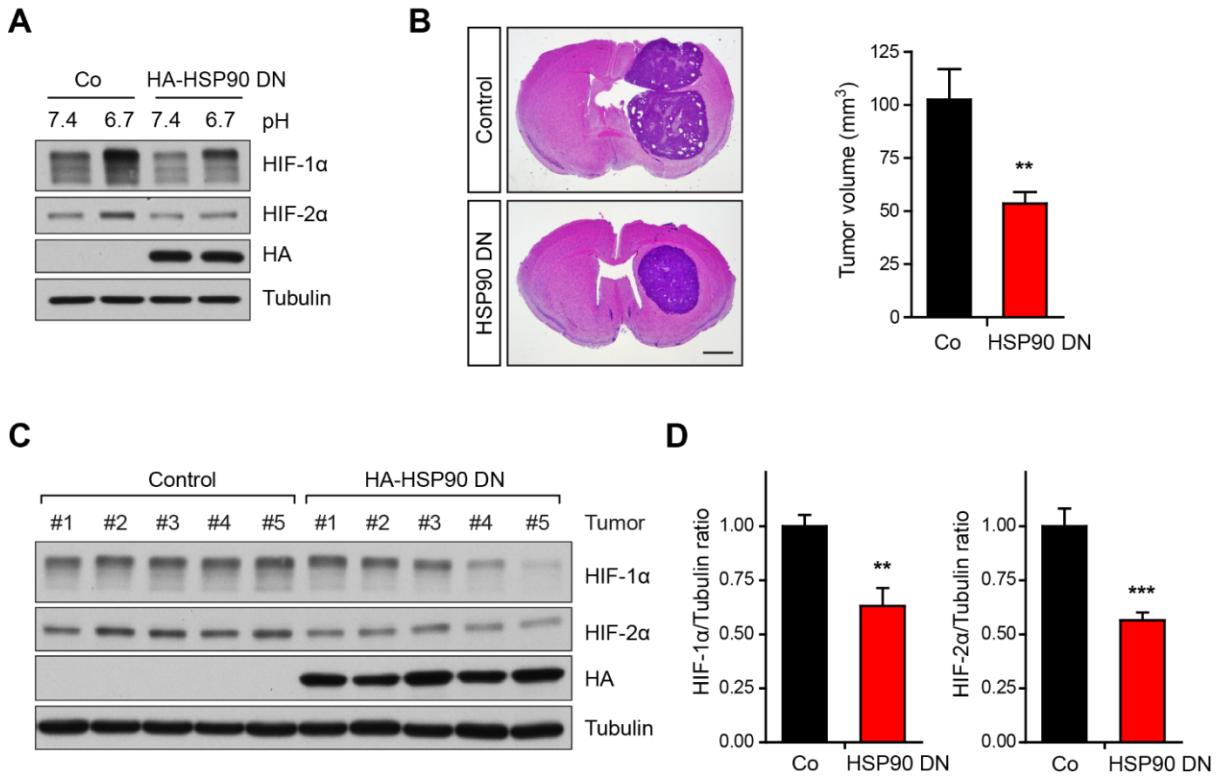

Figure 4.18. HSP90 inactivation by a dominant negative form of HSP90 reduces HIF-α levels and inhibits tumor growth.
A, Overexpression of dominant negative HSP90 (HSP90 DN) decreases HIF-α levels *in vitro*. Immunoblot of G55 control and HA-HSP90 DN expressing cells cultured at pH7.4 or 6.7 under hypoxia for 18 hours. **B-D,** Loss of HSP90 function reduces tumor growth and intratumoral HIF-α levels. G55 cells expressing GFP (control) or HA-tagged HSP90 DN, were orthotopically transplanted into immunocompromised mice. **B,** Tumor xenografts were HE-stained and the tumor volume was quantified (n=9-10). **C,** Immunoblot for HIF-1/2α and HA in extracts from representative control and HA-HSP90 DN tumors. **D,** Quantification of HIF-1α and HIF-2α levels in control and HA-HSP90 DN tumors (n=9-10). Data are means ± SEM. ***P*<0.01; ****P*<0.001. Scale bar, 1 mm (**B**).

4.2.2 High HSP90 expression in the hypoxic CSC niche

Next, analysis of human patient data from the TCGA glioblastoma cohort, demonstrated that high HSP90 expressing tumors also had higher expression levels of the HIF target gene VEGF and the cancer stem cell markers CD133 and Nestin (Fig. 4.19A). For further validation, 10 patient biopsies were stained for HIF-1α, HSP90 and CD133. Perinecrotic areas, which are characterized by severe hypoxia and presumed acidosis as a result of increased anaerobic glycolysis, displayed higher HIF-α levels. Notably, 10 out of 10 glioblastoma biopsies displayed increased HSP90

levels in the perinecrotic areas (Fig. 4.19B middle). In addition to coexpression of HIF-1α and HSP90, CSCs were also enriched in this area as shown by CD133 staining. Taken together, these findings demonstrate that microenvironmental factors such as hypoxia and acidosis in tumors synergistically regulate the hypoxic response and promote CSC maintenance in a HSP90 dependent manner.

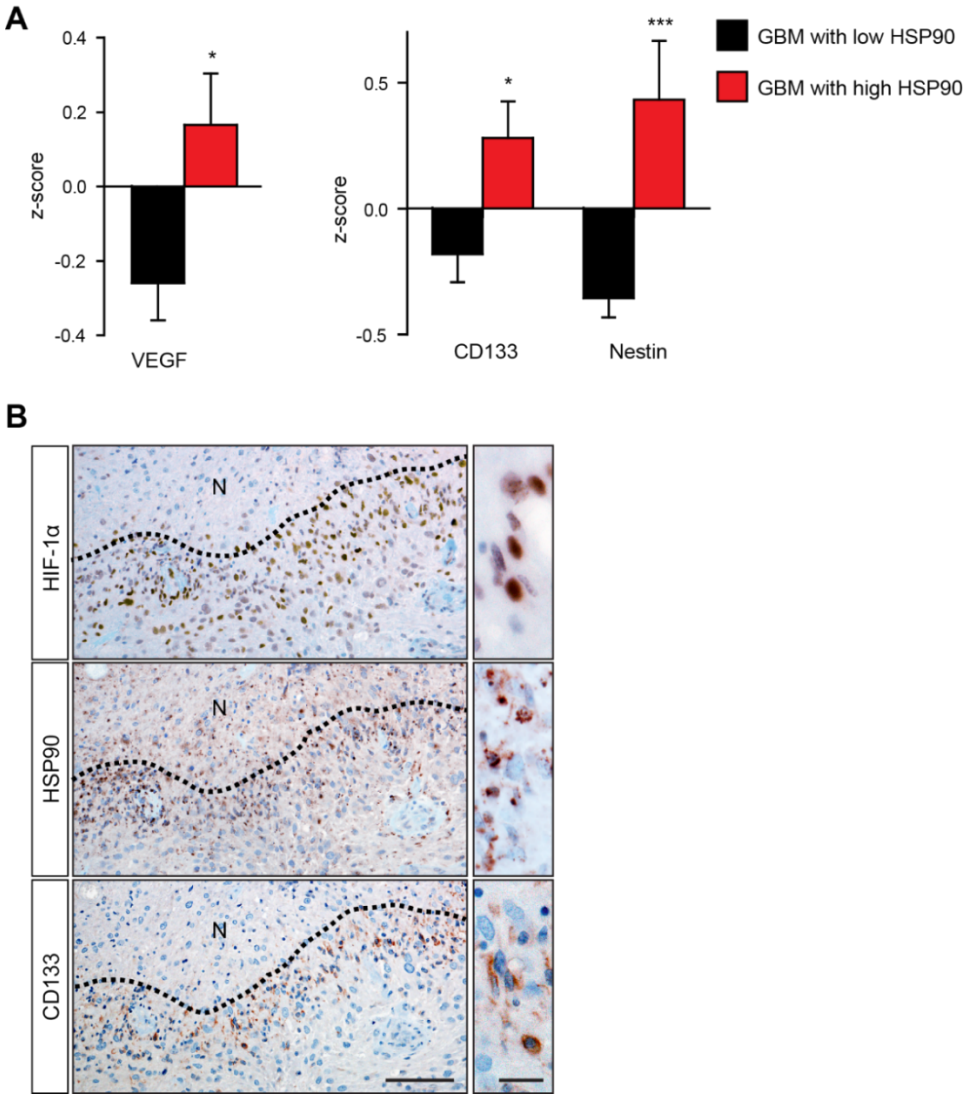

Figure 4.19. High HSP90 expression is observed in the hypoxic niche and correlates with hypoxic and stem cell markers in human glioblastomas.
A, Comparison of the HIF-target VEGFA and the glioma CSC markers CD133 and Nestin in glioblastomas with high and low HSP90 levels in the Cancer Genome Atlas (TCGA) cohort (n=154). **B,** Serial sections of human glioblastoma biopsies containing a perinecrotic (hypoxic) region were immunohistochemically stained for HIF-1α, HSP90 and CD133. The panels on the right show higher magnifications of the staining in the perinecrotic areas. N, necrosis. *P<0.05; ***P<0.001. Scale bars, 100 µm **(B)**, 20 µm **(B, inset)**.

4.3 The hypoxia regulated HIF-1α-ZEB2-ephrinB2 axis controls tumor invasion and anti-angiogenic resistance

The third part of the thesis focuses on the mechanisms of tumor invasion and anti-angiogenic resistance in glioblastoma. The project has been carried out in collaboration with the group of Prof. Amparo Acker-Palmer, Institute of Cell Biology and Neuroscience, Goethe University Frankfurt. Within the project, I focused on the impact of hypoxia and ephrinB2 in the regulation of *in vitro* and *in vivo* invasion, whereas Cornelia Depner and Helge zum Buttel focused on the regulation of ephrinB2 and the link to the anti-angiogenic resistance. The data presented in figure 20E and F was performed by Cornelia Depner. Intracranial transplantation of tumors presented in figure 21 was performed by Sascha Seidel and figure 21A was analyzed by Cornelia Depner.

4.3.1 Hypoxia increases invasion through downregulation of ephrinB2

Hypoxia regulated genes control the cellular responses to overcome stress conditions via modulating the cell metabolism, survival, motility and angiogenesis. Local invasiveness of glioblastomas is one of the reasons for tumor relapse and poor outcome (Huang et al., 2014, Span and Bussink, 2015). To examine the role and the mechanism of hypoxia on the invasive phenotype, we cultured the cells under hypoxia and analyzed the invasiveness of the glioblastoma cells. Small G55 spheres were seeded in a collagen gel allowing the cells to invade three-dimensionally, in a manner resembling the natural conditions of glioblastomas. Hypoxia treated G55 cells displayed increased invasiveness in the collagen matrix (Fig. 4.20A). In line with the collagen invasion assay, a modified Boyden chamber assay also showed that hypoxia treated cells invaded more through a membrane covered with matrigel (Fig. 4.20B, C).

EphrinBs are transmembrane proteins, which play a role in the regulation of a variety of cellular processes such as cell migration, axon guidance, cell adhesion, cell

proliferation and cell repulsion (Kania and Klein, 2016). Our results had demonstrated that ephrinB2 is frequently downregulated in glioblastomas compared to normal brain (Depner, et al., 2016). Therefore, to examine if ephrinB2 downregulation contributes to the invasive behavior of cells under hypoxia, we first analyzed ephrinB2 expression levels under hypoxia by qPCR. EphrinB2 levels were remarkably downregulated upon hypoxia. In addition, HIF-1α or HIF-2α silencing revealed that ephrinB2 downregulation is controlled by HIF-1α as evidenced by recovery of ephrinB2 levels in HIF-1α silenced cells under hypoxia (Fig. 4.20E). Since HIFs typically act as transcriptional activators, we sought to identify additional transcriptional regulators that could control ephrinB2 downstream of hypoxia and HIF-1α.

EMT regulators are known to be important for the mesenchymal phenotype in gliomas, which is associated with poor outcome and characterized by necrotic and hypoxic areas. EMT regulators function as transcriptional repressors and are elevated by hypoxia (Iser, et al., 2016). Therefore, we performed a siRNA screening against EMT regulators. Silencing of the transcriptional repressor ZEB2 led to highly upregulated ephrinB2 levels (Fig. 4.20F), indicating that ephrinB2 downregulation is mediated by ZEB2. Moreover, Cornelia Depner also showed that ZEB2 was highly upregulated upon hypoxia and HIF-1α silencing inhibited the ZEB2 upregulation (Depner, et al., 2016).

Of the two cell lines used in our experiments, LN229 cells formed highly invasive tumors, whereas G55 cells formed well-circumscribed tumors with smoother tumor rims (Depner, et al., 2016). Interestingly, analysis of ZEB2, ephrinB2 and EphB4 expression levels revealed that the highly invasive cell line LN229 expresses higher ZEB2 and lower ephrinB2 levels (Fig. 4.20D). Taken together, our data show that hypoxia promotes invasion through ZEB2 leading to ephrinB2 silencing.

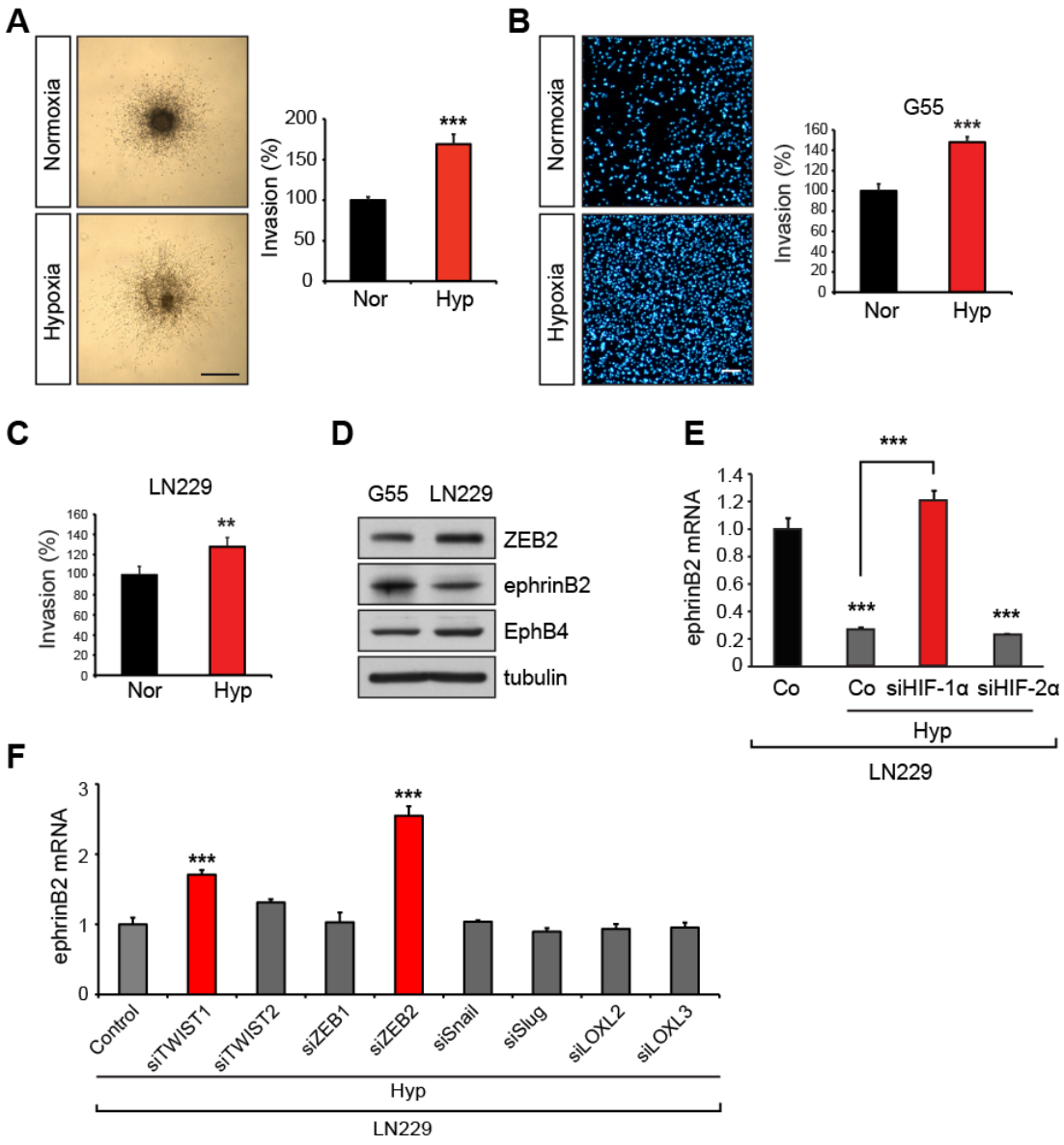

Figure 4.20. Hypoxia induces glioma cell invasion and downregulates ephrinB2 expression through HIF-1α.

A, Hypoxia induces glioblastoma invasion. Invasion of human G55 glioblastoma spheroids was quantified following incubation in a collagen gel at normoxia (21% O_2) or hypoxia (1% O_2) for 48 hours (n=7-11 spheroids). **B, C,** Invasion of G55 and LN229 glioblastoma cells cultured under normoxia (21% O_2) or hypoxia (1% O_2) for 24h was assessed using a modified Boyden chamber assay (n=6). **D,** Expression levels of ZEB2, ephrinB2 and the ephrinB2 receptor EphB4. Western blot for ZEB2, ephrinB2 and EphB4 in G55 and LN229 glioblastoma cells. **E,** Hypoxia downregulates ephrinB2 expression through HIF-1α. qPCR analysis of ephrinB2 mRNA levels in LN229 glioblastoma cells expressing control, HIF-1α or HIF-2α siRNA following exposure to 1% O_2 (Hyp) for 18 hours (n=3). **F,** ZEB2 mediates the HIF-1α-induced downregulation of ephrinB2. siRNA based screen of transcriptional EMT repressors in LN229 glioblastoma cells following exposure to 1% O_2 (Hyp) for 18 hours (n=3). Data are means ± SEM. ***P*<0.01; ****P*<0.001. Scale bar, 500 µm (**A**), 200µm (**B**).

4.3.2 Decreased ephrinB2 levels are associated with increased tumor invasiveness and resistance to antiangiogenic treatment

Since downregulation or loss of ephrinB2 occurs at high frequency in glioblastoma patients, we wanted to examine the consequence of ephrinB2 loss (Depner, et al., 2016). Therefore, an immortalized ephrinB2 knock-out astrocytoma model was used. Control and ephrinB2 knock-out cells were intracranially transplanted to investigate the effect of ephrinB2 loss on tumor growth and invasion. Notably, ephrinB2 deficient cells formed remarkably larger tumors with a highly invasive tumor front (Fig. 4.21A). To further confirm the role of ephrinB2 in the invasive phenotype, we restored ephrinB2 levels by reintroducing ephrinB2 in the ephrinB2 knock-out cells. EphrinB2 levels were analyzed by western blotting and exogenous ephrinB2 was detected with anti-ephrinB2 and anti-HA antibodies (Fig. 4.21B). Importantly, intracranial transplantation of the cells confirmed that the pro-invasive phenotype of ephrinB2 knock-out tumors was a direct result of ephrinB2 loss, as it was reverted by reintroduction of ephrinB2 (Fig. 4.21C).

Anti-angiogenic treatment has been reported to increase tumor invasion. Bevacizumab, an antiangiogenic anti-VEGF antibody, which decreases tumor vascularization and thereby creates a hypoxic tumor microenvironment, leads to increased tumor cell invasion/migration (Zhang, et al., 2015b, Tamura, et al., 2017). Our findings indicated that ZEB2-mediated ephrinB2 repression leads to enhanced tumor invasiveness under hypoxia, therefore we wanted to examine if ephrinB2 repression is also an important step in anti-angiogenic treatment-induced invasion. We showed that the HIF-1α-ZEB2-ephrinB2 pathway is activated following anti-angiogenic treatment (Depner, et al., 2016). To further verify that downregulation of ephrinB2 modulates the resistance to bevacizumab, we created ephrinB2 overexpressing G55 cells (Fig. 4.21D). Intriguingly, bevacizumab treated ephrinB2 overexpressing tumors exhibited reduced invasiveness compared to control tumors (Fig. 4.21E), as seen by a smoother tumor rim in ephrinB2 overexpressing tumors.

Together, these findings demonstrated that ephrinB2 downregulation functionally promotes tumor invasion and regulates the evasive resistance to anti-angiogenic treatment.

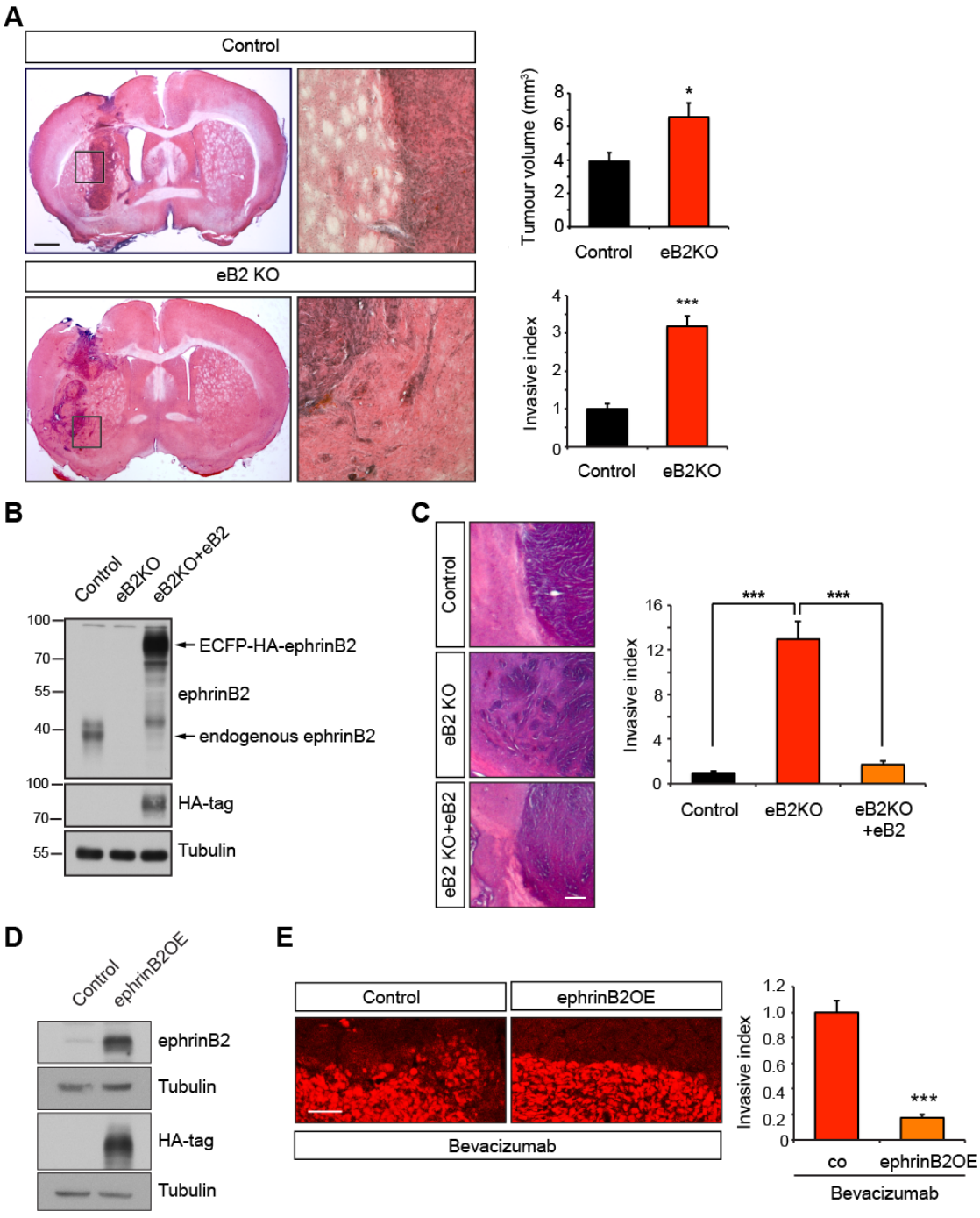

Figure 4.21. Loss of ephrinB2 increases tumor invasiveness.
A, Loss of ephrinB2 increases tumor invasion and growth. HE staining of intracranial control and ephrinB2 knock-out (KO) (eB2 KO) glioma xenografts (left) together with representative

pictures of tumor rims (right). Quantification of tumor volume in control and ephrinB2KO gliomas (n=10-11 tumors) (upper) and quantification of the invasive index of control and ephrinB2KO gliomas, assessed by measuring the area of tumor invading the brain parenchyma per tumor rim length (n=5 tumors). **B, C,** Reintroduction of ephrinB2 into ephrinB2 KO tumors reverts the pro-invasive phenotype. Levels of ephrinB2 assessed by immunoblot of control, ephrinB2KO (eB2KO) and ephrinB2KO glioma cells re-expressing exogenous ECFP-HA-ephrinB2 (eB2KO + eB2), probed with anti-ephrinB2 and HA antibodies (**B**). Quantification of the invasive index of control, ephrinB2KO and ephrinB2KO gliomas re-expressing ephrinB2 (**C;** n=7-9 tumors). **D,** Immunoblot for ephrinB2 in G55 cells expressing control vector or ephrinB2 (ephrinB2OE). **E,** EphrinB2 overexpression impairs the invasive phenotype elicited by bevacizumab. Invasive fronts of intracranial tumor xenografts of polyclonal G55 pools stably overexpressing control vector or ephrinB2 (ephrinB2OE) following bevacizumab treatment visualized using human nuclei staining (**E**, left). Quantification of invasion in the tumors (n=5-9 tumors) (**E**, right). Data are means + SEM. **P*< 0.05, ****P*<0.001; ANOVA *P*<0.0001 (**C**). Scale bar, 1 mm (**A**), 100µm (**C, E**).

5 Discussion

Hallmarks of cancer such as resistance to cell death, sustention of proliferative signals, evasion from growth suppressors, activation of invasion and metastasis, enabling of unlimited replication and induction of angiogenesis are capabilities of cancer cells that ensure tumor growth and are involved in the pathogenesis of cancer. Therefore, understanding the mechanisms involved in the control of cancer hallmarks remains one of the most important focuses in cancer research (Hanahan and Weinberg, 2011, Pavlova and Thompson, 2016). In this thesis study, we characterize different cancer hallmarks, such as metabolic reprograming, activation of invasion and induction of angiogenesis, all influenced by the contribution of the tumor microenvironment.

The first part of the study demonstrates the importance of metabolic reprogramming mediated by 2-OG levels. We show that reduced IDH1 levels increase HIF function by decreasing the level of 2-OG, a substrate used by PHDs, the master regulators of HIF-α. In parallel, we also characterized the function of IDH1 for an invasive and metastatic tumor phenotype. **In the second part**, we identified the acidic tumor microenvironment, acting through HSP90, as a stimulus of HIF function and CSC maintenance. Importantly, we revealed the function of HSP90 in tumor initiation and tumor hypoxia as a potential target to eliminate CSCs in the hypoxic/acidic niche. **In the third part** of the study, we elucidated the function of ephrinB2 reverse signaling for tumor invasion and anti-angiogenic treatment resistance. We show that repression of ephrinB2 is promoted by hypoxia and mediates an anti-angiogenic therapy-induced invasive tumor phenotype.

5.1 Impaired 2-OG levels controlled by IDH1 elevate the hypoxic response and the invasive/metastatic tumor phenotype

As a hallmark of cancer, reprogrammed cancer metabolism supports the acquisition and maintenance of malignant properties by providing energy and metabolites essential for sustaining tumor growth under fluctuating nutrient conditions (Hanahan and Weinberg, 2011, Pavlova and Thompson, 2016). To fulfill the metabolic demands, cancer cells rewire their metabolism, resulting in the Warburg effect - a metabolic shift from oxidative phosphorylation to glycolysis independent of oxygen availability (Warburg, 1956a). Studies during the last decade have demonstrated that metabolic reprogramming is not limited to the Warburg effect and can be driven by several factors. Among them are oncogene activation or loss of tumor suppressors, epigenetic changes, mitochondrial dysfunction and activation of HIF function. Importantly, these factors show complex interactions with each other (Scott, et al., 2011, Chen and Russo, 2012, Ward and Thompson, 2012, Phan, et al., 2014). Therefore, an improved understanding of metabolic reprogramming and the identification of metabolic dependencies that support accelerated proliferation, survival, invasion/migration and therapy resistance of cancer cells, is crucial for the development of effective therapeutic strategies.

Over the last decade, research on 2-OG and 2-OG regulated signaling pathways has been intensified and became highly attractive with the identification of single-mutation-driven accumulation of the 2-OG analogs succinate, fumarate and 2-HG, also described as oncometabolites, and their involvement in carcinogenesis (Sullivan et al., 2016). 2-OG is involved in a variety of metabolic and cellular pathways as a key intermediate of energy generation, a precursor of amino acid and lipid synthesis, and a signaling molecule involved in epigenetic and protein modifications (Zdzisinska, et al., 2017).

In this part of the study, we characterized the function of 2-OG homeostasis in tumor progression by targeting the 2-OG producing enzyme IDH1. We show that dysregulation of 2-OG levels mediated by IDH1 downregulation initiates adaptive responses such as HIF activation by altering the function of 2-OG dependent dioxygenases, in particular PHDs. In addition, we analyzed the effect of 2-OG dysregulation mediated by IDH1 silencing on cancer stem cell and an invasive/metastatic tumor phenotype and show that IDH1 silencing enhances CSC maintenance, as well as the invasive and metastatic capacity of cancer cells.

5.1.1 IDH1 silencing-mediated 2-OG decrease enhances the hypoxic response in a PHD dependent manner

Reduced oxygen supply is one of the characteristics of solid tumors and it is known that hypoxia can limit cell growth, but also promotes a more aggressive tumor phenotype by triggering survival signals, adaptive responses and immune evasion (Huang, et al., 2014, Muz, et al., 2015). Although the control of the hypoxic response by PHDs is well studied and both HIF-α isoforms are hydroxylated by all PHDs *in vitro* (Appelhoff, et al., 2004), the specific roles of each PHD in certain cellular contexts are still not completely understood. Several studies during the last few years focused on the tumor suppressive function of PHDs and the identification of new HIF independent binding and hydroxylation targets of PHDs (Nguyen and Duran, 2016, Zurlo, et al., 2016). Among the novel PHD binding partners identified in these studies are molecules involved in tumor growth and progression including FOXO3a, KIF1Bβ, ATF4, and EGFR suggesting a tumor suppressor function of PHDs (Koditz, et al., 2007, Schlisio et al., 2008, Garvalov, et al., 2014, Henze, et al., 2014, Zheng, et al., 2014). Interestingly, further evidence supporting a tumor suppressive function of PHDs has been recently reported, as genetic or functional inactivation of PHDs was observed in various tumor entities including glioblastoma (Chan et al., 2009, Hatzimichael et al., 2010, Henze, et al., 2014). Even if PHDs mainly function as oxygen sensors, PHD activity, in addition to oxygen, relies on the availability of Fe^{2+} as a co-factor and 2-OG as a co-substrate (McDonough, et al., 2010). Thus, PHDs

can potentially act as signaling hubs to sense and integrate various metabolic alterations in response to changes in cell physiology, exogenous signals and microenvironmental conditions. Indeed, it has been shown that succinate and fumarate can compete with 2-OG for binding to PHDs and, when bound to the enzyme, they inhibit its activity (Selak, et al., 2005, Koivunen, et al., 2007, MacKenzie, et al., 2007). To date, however, little is known about the role of 2-OG metabolizing enzymes in the regulation of prolyl hydroxylases and their downstream functions. A major 2-OG producing enzyme is isocitrate dehydrogenase (IDH), which converts isocitrate to 2-OG by oxidative decarboxylation (Dalziel, 1980, Xu, et al., 2004).

Given the fact that 2-OG is a key metabolite in the catalytic activation of 2-OG dependent enzymes, including PHDs, we hypothesized that the maintenance of cellular 2-OG levels by 2-OG metabolizing enzymes such as IDHs plays a pivotal role in the control of PHD activity. Therefore, we decided to examine the role of the 2-OG producing enzyme IDH in coordinating the cellular response to hypoxia. For defining the role of IDH1 and IDH2 in the regulation of the hypoxic response, which is tightly controlled by PHDs, we characterized IDH knock-down cells. In agreement with the above-mentioned hypothesis, our results show that IDH1 and/or IDH2 knock-down increased the HIF response under normoxia (Fig. 4.2, 4.3) and even further potentiated it under hypoxia (Fig. 4.1, 4.2, 4.3). Interestingly, the knock-down of IDH1 led to the strongest HIF-α stabilization compared to IDH2 loss of function alone, or in combination with IDH1 (Fig. 4.1C). Given the fact that IDH1 is localized in the cytoplasm, 2-OG produced by IDH1 is thought to be the primary source for cytoplasmic and nuclear 2-OG dependent dioxygenases (Losman and Kaelin, 2013), supporting our results that IDH1 is more influential on HIF-α stabilization. Moreover, comparison of expression levels of previously defined (Koivunen, et al., 2012) HIF-regulated genes in control and IDH1 knock-down cells revealed the activation of HIF mediated transcriptional programming in IDH1 silenced cells under both, normoxia and hypoxia (Fig. 4.2, 4.3A, 4.3B). These results are in line with a previous report, focusing on the characterization of IDH1 mutations, where it was shown that IDH1 knock-down elevates HIF-1α levels (Zhao, et al., 2009). Interestingly, Zhao *et al.* showed that IDH1 mutations influence IDH1 wildtype activity and mutant IDH1

mediated inhibition of wildtype IDH1 results in elevated HIF-1α levels, an effect which could be reversed by 2-OG treatment. However, subsequent studies revealed that IDH1 mutation associated effects are mostly mediated by D-2-HG, which is produced due to the neomorphic activity of mutant IDH1 and which competitively inhibits 2-OG dependent dioxygenases (Dang, et al., 2009, Ward, et al., 2010). Notably, the observed reduction of HIF-α levels upon overexpression of wildtype IDH1, but not of enzymatically inactive IDH1 (IDH1-3DN), underlines the importance of IDH1 levels as well as IDH1 enzymatic activity (Fig. 4.6A-D). In line with this, the inhibitory effect of IDH1 overexpression on downstream targets of HIFs was shown by reduced expression of CAIX, VEGFA and GLUT1 (Fig. 4.7A)

The aforementioned results lead to the assumption that impaired IDH levels abrogating the cellular 2-OG status are crucial for the catalytic activity of PHD. Notably, we show that IDH1 knock-down leads to the reduction of intracellular 2-OG levels (Fig. 4.4A), an observation also reported in recent studies (Zhao, et al., 2009, Calvert et al., 2017). Activation of HIF signaling is not only controlled by PHDs, but also by additional mechanisms (Keith, et al., 2011). Therefore, to determine whether the effect of IDH1 on HIF signaling is PHD/hydroxylation dependent, we analyzed the exogenous and endogenous HIF activity by using either wildtype HIF-α, or an undegradable mutant (HIF-1α mPPN), carrying point mutations at the PHD hydroxylation sites which therefore cannot be hydroxylated by PHDs. This method allowed us to detect the differentiation of hydroxylation dependent and independent regulation of HIF activity by assessing binding activity of HIF to HREs (Fig. 4.3A-C). Importantly, our results indicate that HIF-α activity upon IDH1 silencing is regulated in a PHD dependent manner, as wildtype HIF activity is increased upon IDH1 knock-down, whereas undegradable HIF-1α (mPPN) activity is unaffected (Fig. 4.3C). IDH1 silencing-mediated inhibition of PHD activity, triggering HIF signaling, was further confirmed by direct measurement of hydroxylated HIF-1α (Pro^{564}) under the presence of the proteasomal inhibitor MG132 (Fig. 4.3D). This method measures PHD activity by detecting the end product of the reaction performed by PHD (Tian et al., 2011). In line with our previous results pointing at a hydroxylation dependent HIF-α stabilization (Fig. 4.3C), we found that IDH1 silenced cells exhibit reduced HIF-α hydroxylation

leading to increased HIF-α levels. Interestingly, our results show that even if IDH2 is upregulated in IDH1 silenced cells (Fig. 4.1C), this is not sufficient to restore 2-OG levels (Fig.4. 4A), therefore evoking inhibition of PHD hydroxylase activity, HIF-α stabilization and subsequent HIF target gene activation.

Treatment concepts using 2-OG inhibitors for the activation of the HIF pathway by inhibiting PHDs have been proposed for diseases such as ischemic and inflammatory diseases, in which impaired HIF target gene expression are causative (Jaakkola et al., 2001, Cummins, et al., 2008, Eltzschig et al., 2014), based on the importance of 2-OG for PHD and HIF activity. The first evidence for a prominent role of 2-OG in cancer progression was found in paraganglioma and papillary renal cancers. As mentioned before, accumulation of succinate and fumarate leads to inhibition of 2-OG dependent dioxygenases by competitive inhibition, due to the binding activity of these metabolites to the 2-OG binding site, and subsequently results in carcinogenesis (Baysal, et al., 2000, Isaacs, et al., 2005, Selak, et al., 2005). Additional studies identified more TCA cycle intermediates, such as oxaloacetate, pyruvate, citrate and 2-HG as steric 2-OG analogues with an inhibiting function. However, succinate and fumarate remain the most potent inhibitors (Koivunen, et al., 2007, Dang, et al., 2009, Ward, et al., 2010, Xu, et al., 2011). By showing the antitumorigenic effects of 2-OG, further studies strengthened the notion that impaired 2-OG homeostasis is a key step in cancer progression (Matsumoto, et al., 2006, Matsumoto, et al., 2009, Tennant, et al., 2009, Rzeski, et al., 2012). Notably, our results show that reduced 2-OG levels activate the HIF pathway, known to be responsible for the activation of adaptive responses in the tumor microenvironment and associated with an aggressive tumor phenotype. Our results (Fig. 4.4C-F), as well as the aforementioned studies, show that administration of cell permeable 2-OG is able to restore the consequences of 2-OG dependent enzyme activity inhibition.

Interestingly, regional glutamine deficiency in the tumor core due to insufficient tumor vascularization, has been shown to elicit reduction in 2-OG levels, thereby inactivating 2-OG dependent enzymes, particularly JMJDs, leading to a promotion of cancer cell dedifferentiation (Hojfeldt and Helin, 2016, Pan, et al., 2016). In line with this study

and our own data, amino acid starvation has been shown to lead to 2-OG depletion and subsequent PHD inactivation (Duran, et al., 2013). In conclusion, our study, together with recent data from other groups, underlines the importance of 2-OG homeostasis in solid tumors and point to a central role of IDHs in the regulation of 2-OG, thereby altering PHD activity and the hypoxic response in glioblastoma.

5.1.2 Activation of PHD-controlled HIF-α-independent NF-κB signaling in IDH1 silenced cells

The function of PHDs are not limited to the activation of HIF signaling. An increasing number of studies identify new hydroxylation targets of PHDs and their functions. One of the first proposed PHD hydroxylase targets besides HIF-α is IKKβ, which participates in the control of NF-κB signaling. It has been suggested that, similarly to HIF-α, hydroxylated IKKβ is tagged for degradation; hence inactivation of PHDs results in active IKKβ and release of NF-κB for nuclear translocation to activate transcription of its target genes (Cummins, et al., 2006, Hamm, et al., 2013, Liu et al., 2017). Beside inflammation, oncogenic pathways, DNA damage and reduced PHD levels or hypoxia are known to induce NF-κB activity (Cummins, et al., 2006, Winning, et al., 2010, Xue, et al., 2010, Perkins, 2012). In line with these findings, we show that IDH1 silencing-mediated PHD inactivation also increased translocation of the NF-κB subunit p65 into the nucleus, thereby increasing NF-κB activity and the expression of known NF-κB target genes (Fig. 4.5A-E).

The discovery of the central role of NF-κB in inflammation, which initiates immunity and a chronic inflammatory microenvironment in tumors, led to detailed investigation of NF-κB signaling in cancer (Grivennikov et al., 2010, Ben-Neriah and Karin, 2011) and identified several NF-κB activating factors. Notably, these factors include the inflammatory tumor microenvironment, genetic alterations, oncogene activation (e.g. Ras), DNA damage and, as aforementioned, components of the tumor microenvironment such as hypoxia, which itself is known to regulate hallmarks of cancer (Hanahan and Weinberg, 2011, Perkins, 2012). Subsequently, aberrant NF-κB activation, which regulates important cellular processes such as proliferation,

angiogenesis, metastasis, invasion and tumor metabolism, was identified in a variety of cancers. On the other hand, depending on the cellular context and specific target gene expression, NF-κB can also promote apoptosis and genomic instability (Rayet and Gelinas, 1999, Perkins, 2012, Xia et al., 2014). Interestingly, a particular role of aberrant NF-κB activation altering CSC maintenance, EMT, therapy resistance, metabolism and angiogenesis, has been shown in glioblastoma (Cahill et al., 2016, Soubannier and Stifani, 2017). Importantly, our results indicated another cellular factor contributing to the control of NF-κB activation, as depletion of 2-OG resulted in NF-κB activation under basal conditions and was even further enhanced by combination with known NF-κB inducing signals (TNFα, hypoxia) (Fig. 4.5E). Notably, recovery of 2-OG levels reduced NF-κB target gene expression, further emphasizing the effect of 2-OG levels on NF-κB signaling (Fig. 4.5F). Recently, our findings were corroborated by another study on immune cell activation, showing that 2-OG acts as an anti-inflammatory metabolite by controlling NF-κB signaling through the modulation of IKKβ activity in a PHD-dependent mechanism (Liu, et al., 2017). Consistently, potential PHD activation by IDH1 overexpression lead to a lower NF-κB target gene expression (Fig. 4.7B). Taken together, our results identified a potential novel function of 2-OG in the regulation of NF-κB signaling, which is controlled by IDH1-maintained PHD activity. Additionally, our results underline the importance of 2-OG levels not only for PHD2 activity, which is widely recognized as the main oxygen sensor (PHD1 and PHD3 also regulate HIF-α, but under specific conditions; (Berra, et al., 2003, Schofield and Ratcliffe, 2004), but also for PHD1 and PHD3 activity, which are considered to be mediators of most HIF-α-independent effects (Nguyen and Duran, 2016, Zurlo, et al., 2016). An intimate crosstalk occurs between HIF and NF-κB, particularly in carcinogenesis, at and levels - from shared inducers to shared targets (D'Ignazio et al., 2016). Indeed, our results revealed that 2-OG is a key-shared regulatory metabolite controlling HIF and NF-κB signaling.

5.1.3 The potential role of 2-OG for the maintenance of the cancer stem cell phenotype

A large body of evidence indicates that solid tumors, including glioblastomas, are organized in a hierarchical manner with a distinct subset of tumor cells with self-renewal and differentiation capacity, the CSCs, at the top of the hierarchy (Reya, et al., 2001, Plaks, et al., 2015). As IDH1 silencing led to deregulated activation of HIF-α and NF-κB, two signaling pathways that are linked to CSC maintenance and therapy resistance (Heddleston et al., 2010, Sundar, et al., 2014, Cahill, et al., 2016, Soubannier and Stifani, 2017), we decided to examine the effect of IDH1-dependent regulation of 2-OG levels on the CSC phenotype. Importantly, expression levels of the well-established glioblastoma stem cell marker CD133, as well as the expression of previously identified glioblastoma stem cell signature genes were elevated in IDH1-silenced cells (Fig. 4.8A-D, 4.9A-D), whereas IDH1 overexpression resulted in decreased CD133 levels (Fig. 4.8E). Notably, along with the upregulation of CSC markers, we observed an increased self-renewal capacity upon IDH1 knock-down (Fig. 4.8G), emphasizing the key role of IDH1 for the CSC phenotype. Moreover, recovery of 2-OG levels in IDH1 knock-down cells reduced the percentage of the CD133 positive cell population and CD133 expression, underlining the role of 2-OG as an important regulator of CSC maintenance. In line with our observation of a 2-OG dependent regulation of the CSC phenotype, 2-OG has been shown to promote primed pluripotent stem cell (pPSC) differentiation (TeSlaa, et al., 2016). Intriguingly, in contrast to the effect of 2-OG in pPSCs, two recent studies observed that 2-OG supports embryonic stem cell (ESC) pluripotency, in which phosphoserine aminotransferase 1 (PSAT1) seems to be the metabolic enzyme regulating 2-OG levels (Carey, et al., 2015, Hwang, et al., 2016). Interestingly, in contrast to our results, a recent study observed that IDH1 knock-down in cells with low 2-OG levels, decreased cellular proliferation accompanied with increased expression of glial differentiation marker genes (Calvert, et al., 2017). In comparison to the aforementioned study, 2-OG levels are much higher in our cells (Fig. 4.4A), hinting at a crucial dependency of the outcome on 2-OG levels. This suggests that, given

different affinities of 2-OG dependent enzymes for 2-OG, the enzymes with lower affinity will be inhibited first. Therefore, the overall levels of 2-OG will define the enzymes and cellular processes influenced by it. Notably, a recent study demonstrated that the tumor core with hypoxic tumor areas also exhibits reduced 2-OG levels due to glutamine deficiency, leading to dedifferentiation of melanoma cells (Pan, et al., 2016). These results, which are in line with our observations showing regained stem cell characteristics when 2-OG levels are reduced, emphasize that intratumoral regional variations such as varying nutrient distributions within the tumor, not only impair the hypoxic response, but also 2-OG homeostasis and thereby tumor heterogeneity. Congruously with our findings that decreased 2-OG levels promote a CSC phenotype, expression of mutant IDH1/2, or absence of the 2-OG dependent enzyme TET2 resulted in impaired hematopoietic differentiation and increased the expression of stem cell marker genes (Figueroa, et al., 2010). Moreover, BCAT1 (branched-chain amino acids transaminase 1) has been shown to restrict 2-OG levels and inhibit TET2 in AML stem cells (Raffel et al., 2017).

Collectively, our data and recent publications strongly underscore the importance of 2-OG homeostasis for defining the CSC phenotype. Moreover, these observations suggest that the contribution of IDH1 for 2-OG maintenance and the effect of 2-OG on the stem cell state, possibly vary depending on cellular 2-OG levels and the cellular context, including 2-OG producing enzymes other than IDH1. Although, as we and other groups show, the individual roles for CSC maintenance of HIF-α and NF-κB signaling on the one hand and 2-OG on the other, have been investigated, it still remains unknown how pivotal HIF-α and NF-κB signaling are for 2-OG-mediated effects on the CSC phenotype.

5.1.4 Metabolic control of mesenchymal transition in glioblastoma

Accumulating evidence over the last decade demonstrates the existence of an EMT-like process, the so-called mesenchymal transition or alternatively glial-to-mesenchymal transition (GMT) in glioblastoma, and a link between CSC traits and this mesenchymal transition (Scheel and Weinberg, 2012, Iser, et al., 2016, Iwadate,

2016, Karsy, et al., 2016). Recent studies revealed that aggressive glioblastomas with highly invasive tumors, recurrent non-mesenchymal tumors and immortalized glioblastoma cells exhibit a mesenchymal phenotype (Phillips, et al., 2006, Verhaak, et al., 2010, Cheng, et al., 2012b, Louis, et al., 2016), suggesting that mesenchymal transition appears to be a mechanism to acquire a more aggressive tumor nature and therapy resistance.

EMT requires metabolic reprograming to support adaptation to harsh environmental changes during invasion and metastasis. However, to what extent EMT rewires the metabolism or how metabolic changes contribute to EMT is only partially understood. Importantly, although a recent study determined the differentially expressed metabolic genes in mesenchymal cells (Shaul et al., 2014), their roles in EMT still need to be elucidated. Interestingly, even if SDH, FH and IDH were not found to be expressed differentially in the aforementioned study, mutations of these genes have been shown to drive EMT and be associated with mesenchymal gene expression (Grassian et al., 2012, Loriot et al., 2012, Sciacovelli et al., 2016, Sciacovelli and Frezza, 2017). Accumulation of metabolites caused by these oncogenic mutations promote EMT and subsequent induction of invasion and metastasis (Grassian, et al., 2012, Loriot, et al., 2012, Aspuria et al., 2014, Colvin et al., 2016, Sciacovelli, et al., 2016), revealing the importance of metabolic homeostasis in the control of EMT. In agreement with these findings, our results show that deregulated 2-OG levels also promote EMT, as shown by elevated levels of EMT regulators, particularly Snail (Fig. 4.10). Although glioblastoma cells lack, or have only very low levels of epithelial genes such as E-cadherin (Lewis-Tuffin et al., 2010), known EMT regulators from epithelial cancers have been shown to be involved in mesenchymal transformation in glioblastoma (Iser, et al., 2016, Karsy, et al., 2016). Indeed, our findings also demonstrated that more invasive IDH1 knock-down cells (Fig. 4.11) also express significantly higher levels of these EMT regulators (Fig. 4.10G), indicating that cells with IDH1-mediated aberrant 2-OG levels acquire a shift towards mesenchymal phenotype.

The tumor microenvironment, including the hypoxic or inflammatory microenvironment, is known to induce EMT and invasion. A hypoxic or inflammatory

microenvironment results in recruitment of immune cells, which release signaling factors such as TGFβ, EGF, FGF and proteases, leading to initiation of EMT and invasion (Charles, et al., 2012, Hanahan and Coussens, 2012). Moreover, cells with a mesenchymal gene expression pattern are localized at the invasive tumor front (Spaderna et al., 2006, Depner, et al., 2016), supporting the hypothesis of a microenvironmental regulation of the mesenchymal phenotype. The well-established EMT-inducing cytokine TGFβ activates SMAD-dependent and SMAD-independent signaling. TGFβ-induced SMAD-dependent signaling activates the expression and activity of EMT regulators such as Snail, Slug, ZEB1, ZEB2 and Twist (Fuxe et al., 2010, Bellomo et al., 2016). Importantly, we also observed increased SMAD activity (Fig. 4.10A) accompanied by increased Snail transcription and protein levels in IDH1 and/or IDH2 knock-down cells, with IDH1 disruption showing a more robust effect (Fig. 4.10B, C). Moreover, IDH1 silencing resulted in a strong upregulation of Snail, whereas only mild changes were observed for ZEB2 and Slug (Fig. 4.10D). In addition to the EMT regulator Snail, the expression of the EMT marker gene CD44 was also significantly elevated (Fig. 4.10D). Importantly, restoring of 2-OG levels in IDH1 knock-down cells led to a reduction of Snail and CD44 expression (Fig. 4.10E, F), revealing a direct link between 2-OG levels and initiation of EMT. Of note, increased levels of CD44, an alternative CSC and EMT marker (Fig. 4.10E, F), provided additional evidence for our previous findings of increased CSC maintenance under reduced 2-OG levels (Fig. 4.8,4.9). Importantly, recent studies demonstrated the involvement of Snail and CD44 in mesenchymal transition, invasion and tumor progression in glioblastoma. Snail depletion has been shown to decrease the proliferative, invasive and migratory capacity of glioblastoma cells (Han, et al., 2011, Savary, et al., 2013, Dong et al., 2014, Myung, et al., 2014). Interestingly, another study reported elevated levels of Snail after irradiation in glioma cells and a Snail knock-down suppressed irradiation-mediated mesenchymal gene expression and invasion (Mahabir et al., 2014). CD44 itself is a modulator of EMT in breast cancer (Brown et al., 2011) and elevated levels of CD44 have been shown in the mesenchymal subtype of glioblastoma (Phillips, et al., 2006, Verhaak, et al., 2010). Interestingly, CD44 promotes tumor cell resistance via activation of the Hippo signaling pathway in

glioblastoma (Xu et al., 2010b). Moreover, CD44 has been shown to promote aggressive tumor growth and has been described as a CSC marker in glioblastoma (Anido, et al., 2010, Fu et al., 2013, Pietras et al., 2014).

HIF and NF-κB signaling are known activators of EMT and the CSC phenotype (Min et al., 2008, Karsy, et al., 2016, Yeo et al., 2017). As we found both of these signaling pathways activated upon IDH1 silencing, the observed increased mesenchymal gene expression, particularly Snail expression, can potentially be under the control of one, or both of these signaling pathways. Indeed, we confirmed an important role of HIF-α, but not NF-κB signaling in regulating Snail, as we observed reduced Snail expression levels upon HIF-α silencing in IDH1 knock-down cells (Fig. 4.12). Although we showed the involvement of HIF signaling, other pathways effected by IDH1 silencing seem to be also involved in the regulation of Snail levels, since HIF-1/2α knock-down only partially reverted the IDH1 mediated Snail upregulation.

In conclusion, our data underline the importance and functional contribution of 2-OG and IDH1, not only for the CSC phenotype, but also for mesenchymal transition in glioblastoma. Moreover, our findings demonstrate the simultaneous involvement of 2-OG in distinct key cellular processes implicated in tumor progression.

5.1.5 Microenvironmental regulation of IDH1

Since the identification of IDH mutations in various tumors, including glioma, AML and colon cancer during the last decade (Sjoblom, et al., 2006, Parsons, et al., 2008, Mardis, et al., 2009), isocitrate dehydrogenase enzymes (IDH1-3) have become a focus of intense research. While much recent research has focused on the role of mutant IDH in tumor development, much less is known about the role of wildtype IDH in varying tumor microenvironments.

IDH1 is known to contribute to lipid metabolism by regulating reductive carboxylation and to protection from oxidative stress by generating NADPH in developing astrocytes, adipocytes, hepatic cells and cancer cells (Jo, et al., 2002, Lee, et al., 2002, Koh et al., 2004, Lee, et al., 2004, Metallo, et al., 2011, Filipp, et al., 2012, Fendt

et al., 2013, Bogdanovic et al., 2014). Altered IDH1 levels have been reported in tumor cells, in which the expression levels were mostly compared to normal cells, suggesting a role of altered IDH1 levels during tumorigenesis (Robbins et al., 2012, Tan et al., 2012, Hu, et al., 2014, Calvert, et al., 2017, Wahl et al., 2017). However, it remains largely unclear at which stage in tumor development and by what molecular mechanisms IDHs are downregulated. Interestingly, IDH1 has been shown to be upregulated following intracerebral hemorrhage (a type of stroke) to regulate neuronal apoptosis (Chen et al., 2017), indicating microenvironmental based regulation of IDH1. In our work, we saw robust IDH1 downregulation upon FBS and TGFβ treatment (Fig. 4.13A-D), whereas only mild changes were observed for IDH2 and IDH3 levels (Fig. 4.13D). Moreover, recent studies showed that IDH1 expression is under the control of transcription factors or miRNAs. FOXO transcription factors, which are considered as tumor suppressors, have been shown to drive IDH1 wildtype and mutant transcriptional expression via binding to its promoter (Charitou et al., 2015). Interestingly, sterol regulatory element binding proteins (SREBPs), which are regulators of lipid metabolism, also directly regulate IDH1 transcription to support lipogenesis (Shechter, et al., 2003). In addition to SREBPs, miR-181a has also been reported to regulate lipid metabolism by targeting IDH1 (Chu, et al., 2015). A recent study identified IDH1, ACO2 (aconitase 2), IDH3A, and SUCLA2 (Succinyl-CoA synthetase Beta-A Chain) as NF-κB target genes, suggesting a NF-κB dependent molecular mechanism regulating the TCA cycle to support tumor metabolism (Zhou et al., 2017). Our results showed that IDH1 downregulation activates NF-κB in a 2-OG dependent manner (Fig. 4.5). Importantly, our findings and those of Zhou et al. conjointly propose a possible feedback loop for mutual regulation between IDH1 and NF-κB (Zhou, et al., 2017). Moreover, under endoplasmic reticulum (ER) stress, IDH1 has been shown to be upregulated by CHOP and C/EBPβ to induce hypoxia-regulated apoptosis. Consistent with our observations, IDH1 upregulation upon ER stress led to HIF-α degradation and inhibition of melanoma cell survival (Yang, et al., 2015). This supports the data by us and others that IDH1 is regulated in response to microenvironmental changes. Recently, HuR, a transcription factor activated upon stress conditions such as chemotherapy and nutrient withdrawal, has been also

shown to regulate IDH1 expression to promote survival of pancreatic cancer cells (Zarei et al., 2017). Taken together, our results demonstrate the importance of IDH1 levels and their microenvironmental regulation. However, the consequences of IDH1 regulation vary from promotion to inhibition of survival in different cell types, suggesting a cell context dependency.

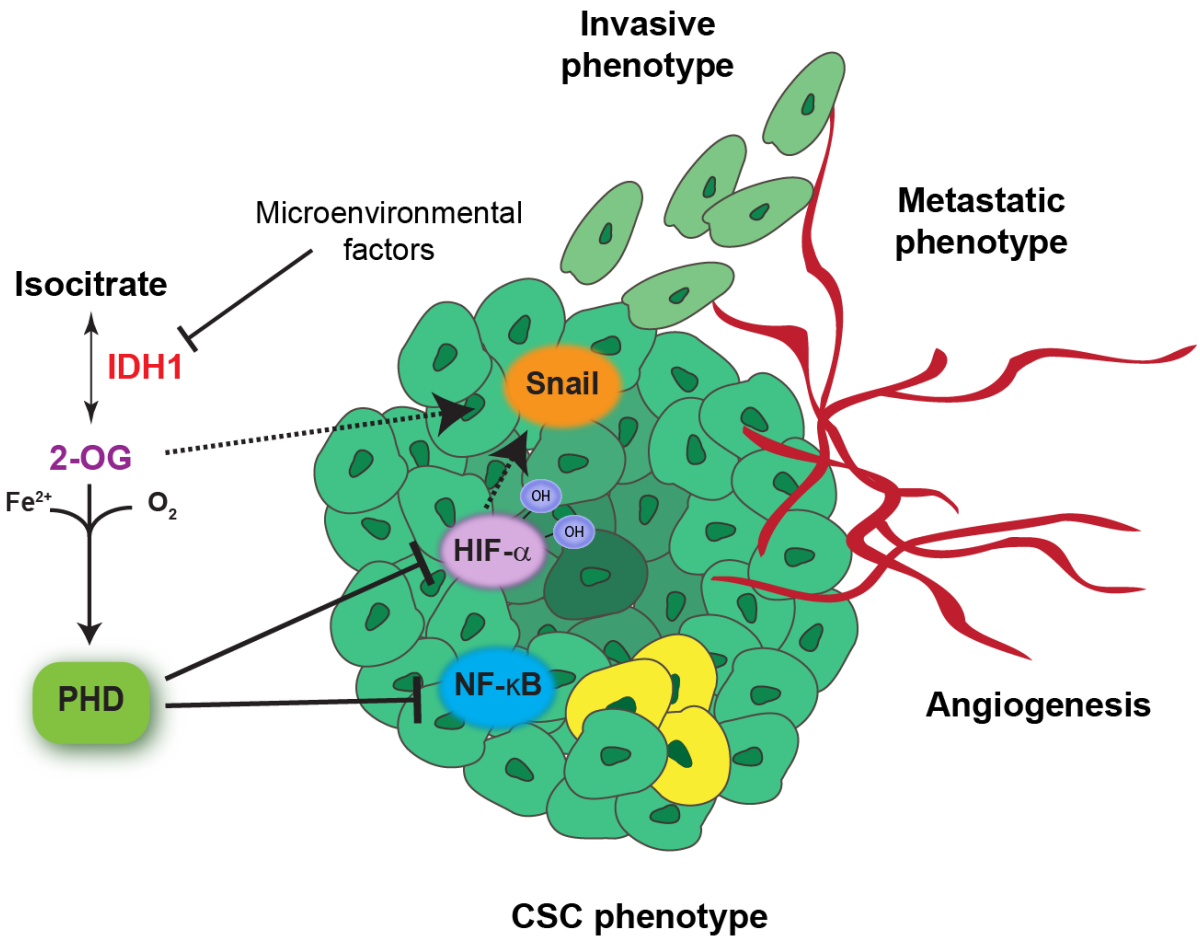

Figure 5.1. A model presenting the metabolic control of the tumor phenotype by IDH1 via regulation of 2-OG maintenance.
Altered IDH1 levels or activity regulate 2-OG levels, contributing to the control of the 2-OG-dependent PHD activity. Abrogated 2-OG levels and subsequent inhibition of PHD activity potentiate HIF-α and NF-κB-mediated signaling. Moreover, impaired 2-OG levels lead to a shift towards a mesenchymal phenotype and a strongly increased Snail expression, which is partially mediated by HIF signaling (dotted arrows).

5.1.6 The role of IDH1 and 2-OG in tumor growth and progression

Tumor hypoxia and activation of the HIF signaling pathway have been linked to many crucial aspects of tumor progression, including tumor angiogenesis, stem cell maintenance, metabolic reprogramming, EMT, metastasis/invasion and therapy resistance (Semenza, 2012). Considering the contribution of HIF-α to tumor progression, therapeutic targeting of the HIF pathway and development of inhibitors have been of great interest. There is a variety of promising HIF inhibitors that modulate the HIF pathway via different mechanisms, including the inhibition of mRNA or protein synthesis, HIF dimerization, DNA binding or transactivation (Semenza, 2012, Masoud and Li, 2015, Chen et al., 2016b, Cho et al., 2016). Our findings demonstrate that IDH1 levels, by regulating 2-OG homeostasis, control activation of the HIF-α and NF-κB pathways and the aforementioned biological processes associated with tumor progression *in vitro*. Our analysis of the TCGA glioblastoma cohort showed that low IDH1 levels correlated with shorter patient survival in glioblastoma (Fig. 4.14A). It is known that the IDH1 mutation status is associated with a better patient prognosis (Sanson et al., 2009). In addition, our findings imply that IDH1 expression levels might also contribute to patient outcome. This assumption was supported by increased tumor growth in IDH1 silenced cells (Fig. 4.14B). Consistently, 2-OG acts as an anti-tumorigenic metabolite (Matsumoto, et al., 2006, Matsumoto, et al., 2009, Tennant, et al., 2009, Rzeski, et al., 2012) and 2-OG starvation occurs due to the nutritional withdraw in tumors (Hojfeldt and Helin, 2016, Pan, et al., 2016). Our data, demonstrating the abrogated 2-OG homeostasis following IDH1 depletion, delineate an additional mechanism that impacts on tumor development and progression.

Importantly, our analysis revealed that IDH1-silenced tumors exhibit enhanced invasive characteristics (Fig. 4.14C-D), which is in line with our findings of an enhanced mesenchymal phenotype in IDH1-depleted cells. Moreover, IDH1 knock-down tumors showed increased tumor vascularization (Fig. 4.14E), supplying the essential nutrients for tumor growth and invasion. It is known that the tumor microenvironment, particularly hypoxia, controls the expression of genes like VEGFA, which mediates blood vessel growth, to promote tumor angiogenesis (Folkman, 2007).

Indeed, analysis of VEGFA expression in tumors revealed increased levels of VEGFA in IDH1 knock-down tumors. Moreover, congruously with our *in vitro* findings of increased CSC marker and NF-κB target gene expression in IDH1-silenced cells, IDH1 knock-down tumors also express higher levels of CD133 and CCL-2 (Fig. 4.14F). In agreement with our hypothesis, a recent study demonstrated that loss of 5-hydroxymethylcytosine (5-hmC), a prognostic marker for renal cell carcinoma (RCC), is mediated by IDH1 downregulation accompanied with lower levels of 2-OG. Notably, loss of 5-hmC or low levels of IDH1 correlate with shorter patient survival (Chen et al., 2016a). In contrast to our data, IDH1 knock-down has been shown to inhibit proliferation, as well as tumor formation through reduced lipid metabolism and increased ROS formation in glioblastoma (Calvert, et al., 2017). However, IDH1 silencing did not affect proliferation in our cells (data not shown) and resulted in moderate reduction of 2-OG levels. In the aforementioned study, IDH1 silencing led to severe 2-OG reduction or was performed in cells with extremely low basal 2-OG levels, which might provide an explanation for the divergent results. Given that IDH1 is needed for NADPH production and lipid metabolism, severe reduction of 2-OG is expected to influence these processes, and by that the proliferation and survival of the cells. Consistently, reductive carboxylation, a reaction performed by IDH isoforms to produce precursors of lipid metabolism from 2-OG and NADPH, has been already shown to support the tumor metabolism under hypoxia or in tumor cells with defective mitochondria (Metallo, et al., 2011, Mullen, et al., 2011, Filipp, et al., 2012, Fendt, et al., 2013, Mullen, et al., 2014) . Nevertheless, when absence of 2-OG is not as extreme as to alter these crucial metabolic processes, decreased 2-OG levels seem to activate the HIF pathway and the CSC phenotype as shown by us and others (Zhao, et al., 2009, Yang, et al., 2015, Pan, et al., 2016). Furthermore, some cells might rely more on IDH1 than other 2-OG metabolizing enzymes or other IDH isoforms to maintain the 2-OG levels. Critical contribution of other 2-OG metabolizing enzymes, such as IDH2, IDH3, BCAT1 and PSAT1, to 2-OG maintenance has recently been shown (Tanaka, et al., 2013, Zeng, et al., 2015, Zhang, et al., 2015a, Hwang, et al., 2016, Raffel, et al., 2017).

Breast and lung cancers are among the most common and lethal cancer types worldwide and in the vast majority of cases patient mortality from these cancers is due to distant metastasis. The strikingly increased invasiveness, mesenchymal phenotype and EMT marker expression upon IDH1 silencing in glioblastoma suggested a possible mechanism of tumor cell dissemination that may also be active in breast and lung cancer. Indeed, IDH1 absence resulted in increased HIF-α, as well as Snail levels in breast and lung cancer cells, similar to glioblastoma (Fig. 4.15A-E), indicating that EMT may be activated in carcinomas upon IDH1 depletion. In addition, IDH1-silenced cells exhibited increased colony formation capacity (Fig. 4.15F). Importantly, even if primary tumor size remained the same, IDH1 knock-down cells showed a significantly increased metastatic capacity *in vivo* (Fig. 4.15H), demonstrating the importance of IDH1 and 2-OG not only for invasion but also for metastasis. Interestingly, in line with our findings, IDH1 overexpression has been shown to be associated with decreased proliferation, invasion and metastasis in osteosarcoma (Hu, et al., 2014). Although IDH1 levels have been shown to be upregulated in lung adenocarcinoma compared to normal tissue (Tan, et al., 2012), analysis of lung adenocarcinoma patient data from TCGA revealed that lower IDH1 expression is associated with shorter patient survival (Fig. 4.15G). In conclusion, our results highlight the relevant and substantial role of IDH1 and 2-OG in the regulation of biological processes linked to tumor progression both in glioblastoma and in epithelial cancers (Fig. 5.1).

5.2 Acidosis promotes HIF function and cancer stem cell maintenance through HSP90

The rapid growth of tumors not only limits the nutrient/oxygen supply, but also removal of metabolic products, eventually causing an acidification of the tumor microenvironment (Chiche et al., 2009, Chiche, et al., 2010, Neri and Supuran, 2011). Accumulating evidence demonstrates that an acidic tumor microenvironment promotes the CSC phenotype (Hjelmeland, et al., 2011). However, it still remains unclear, through which mechanisms extracellular acidosis controls CSC maintenance within the hypoxic microenvironment.

In this part of the thesis, we demonstrated the synergistic effect of hypoxia and acidosis to enhance HIF function and potentiate CSC maintenance in glioblastoma controlled by HSP90. Importantly, our results show that the hypoxic response and the tumorigenic capacity of glioblastoma cells are suppressed following HSP90 inactivation. Furthermore, we found that glioblastoma patients expressing high levels of HSP90 also express higher levels of HIF target genes and CSC markers. These results highlight the potential relevance of HSP90 as a druggable target for designing new therapeutic strategies targeting CSCs (Fig. 5.2).

5.2.1 HIF dependent induction of the CSC phenotype under acidic stress

Many tumor types possess a hypoxic and acidic tumor microenvironment which controls several pathophysiological processes and responses involved in tumor progression. Glycolytic cancer cell metabolism, hypoxia and inefficient blood perfusion in tumors are the cause for the acidic tumor microenvironment. Importantly, acidosis regulates chemotherapy resistance, invasion, metastasis, angiogenesis and evasion from immune response. Interestingly, hypoxia also regulates these specific processes, implying that hypoxia and concomitant acidosis functionally contribute to a more aggressive tumor phenotype. (Honasoge and Sontheimer, 2013, Kato, et al., 2013, Kolosenko et al., 2017). So far, only few studies focused on the cellular responses activated by acidosis along with hypoxia, however, the molecular mechanisms underlying these responses still remain unclear.

To uncover the link between acidosis and hypoxia, we exposed glioblastoma cells to physiological (pH7.4) and acidic pH (pH6.7) under normoxia and hypoxia. Our results showed that an acidic pH upregulates HIF-1α and HIF-2α under normoxia (Fig. 4.16A). Similar to tumors in which decreased extracellular pH is accompanied by hypoxia, glioblastoma cells cultured under acidic pH and hypoxia showed even further increased HIF-α levels (Fig. 4.16A). Consistent with our observation, previous studies have also reported increased HIF-α levels under acidic conditions (Willam et al., 2006b, Hjelmeland, et al., 2011). Furthermore, our results, as well as those from other

groups, showed that low pH regulates VEGF expression, a HIF target gene and angiogenic factor (Fukumura, et al., 2001, Xu, et al., 2002, Filatova, et al., 2016). However, other studies reported a reduction of HIF-α levels under acidosis (Tang et al., 2012, Parks et al., 2013). To determine whether an acidic pH range is an important factor in the regulation of HIF-α, pH ranges of 7.2 to 6.1 were tested for the induction of HIF-α levels. Importantly, pH in the range of 6.7-6.9, values which have been measured in tumors (Gillies et al., 2004, Hjelmeland, et al., 2011), increased HIF-α levels, whereas lower pH ranges decreased the HIF-α expression (see (Filatova, et al., 2016)). Our data demonstrated that only a certain pH range, which is also detected in tumors, potentiates HIF function, suggesting a possible explanation for controversial results in previous reports. Of note, the specific pH range, which induces HIF function, might vary between different tumor entities and subtypes since the degree of hypoxia, blood perfusion to remove the acidic products and the expression of molecules involved in pH sensing differ.

One of the best-characterized niches where CSCs reside, is the hypoxic niche and hypoxia promotes the stem cell characteristics of cancer cells. (Heddleston, et al., 2009, Seidel, et al., 2010). Moreover, increased CSC marker gene expression and self-renewal capacity of glioblastoma cells have been shown under acidic conditions. Hjelmeland and co-workers reported increased expression of the CSC marker genes Olig2, Oct4 and Nanog, as well as enhanced sphere formation capacity, which was accompanied by increased HIF-α levels (Hjelmeland, et al., 2011). However, it is not clear whether an acidosis induced CSC phenotype is controlled directly by HIF-α, the major regulators of cellular response to hypoxia, or by other factors. In line with the enhanced CSC maker gene expression reported by the aforementioned study, we found that the expression of side population marker genes, which are associated with CSC maintenance in glioblastoma (Seidel, et al., 2010), was increased under acidic stress. Importantly, we demonstrated that acidosis enhances the CSC population and self-renewal capacity in a HIF-1/2α dependent manner, as the effects of acidosis on CSC features were abrogated in HIF-1/2α-silenced cells cultured under acidic conditions (Fig. 4.16).

5.2.2 HSP90 controlled HIF function under acidic conditions

Oxygen-dependent activation of HIF-α is predominantly mediated by a PHD/VHL dependent mechanism at the posttranslational level, especially under hypoxic conditions. However, besides a PHD/VHL dependent mechanism, additional mechanisms are involved in controlling HIF activity and levels. A previous study has shown that severe acidity under normoxic conditions leads to prolonged HIF-α stabilization and nucleolar sequestration of VHL, neutralizing its function (Mekhail et al., 2004). In contrast to these data, we determined that acidosis-induced HIF function is PHD/VHL independent, as HIF-α induction by acidosis was maintained in VHL deficient cells (Filatova, et al., 2016). Furthermore, acidosis-induced HIF-α levels were unaffected by the inhibition of PHD function (DMOG and DP treatment). In addition, low pH could also increase the levels of HIF-α proteins that carry a mutation at the PHD hydroxylation residues (HIF-1/2α mPPN), providing strong evidence for a PHD/VHL-independent HIF-α stabilization under acidosis (Filatova, et al., 2016). Another well-characterized mechanism for HIF-α stabilization is through their interaction with HSP90 (Katschinski, et al., 2004, Liu, et al., 2007). We could confirm that HSP90 controls HIF-α stabilization under acidosis, as acidosis-mediated HIF-α induction was abrogated following treatment with the HSP90 inhibitor geldanamycin. HSP90 expression was also induced under acidic conditions, allowing for increased interaction with, and thereby stabilization of HIF-α (Filatova, et al., 2016). Given the fact that acidosis promotes CSC characteristics through HSP90 mediated HIF activation, we wanted to corroborate the effect of acidosis and HSP90 on tumorigenicity, since CSCs show strong tumorigenic capacity. In agreement with this hypothesis, our results showed that HSP90 silencing reduced intracranial tumor growth indicating a reduction of tumor initiating capacity of the cells. Importantly, by assessing the HIF-α levels, we demonstrated that HSP90 silencing abrogates the synergistic increase of HIF function mediated by acidosis and hypoxia *in vivo* and *in vitro* (Fig. 4.17A-F). In line with these findings, we were able to show that HSP90 silencing decreased the tumor initiating capacity of cells and hence increased the survival of mice in a subcutaneous xenograft model (Fig. 4.17G, H). In addition to

these observations, inhibition of HSP90 function by overexpressing a dominant negative form of HSP90 led to a similar reduction of HIF function, tumor growth and intratumoral HIF-α levels, confirming our previous results (Fig. 4.18A-D). Taken together, our results underline the importance and functional contribution of acidosis for the maintenance of the CSC phenotype through HSP90, providing a novel mechanistic insight into this process. In agreement with our findings in glioblastoma, acidosis has also been shown to contribute to the CSC and invasive phenotype in prostate cancer as shown by increased CSC marker gene expression and MMP-9 secretion to promote invasion, although the molecular mechanism remained unclear (Huang et al., 2016).

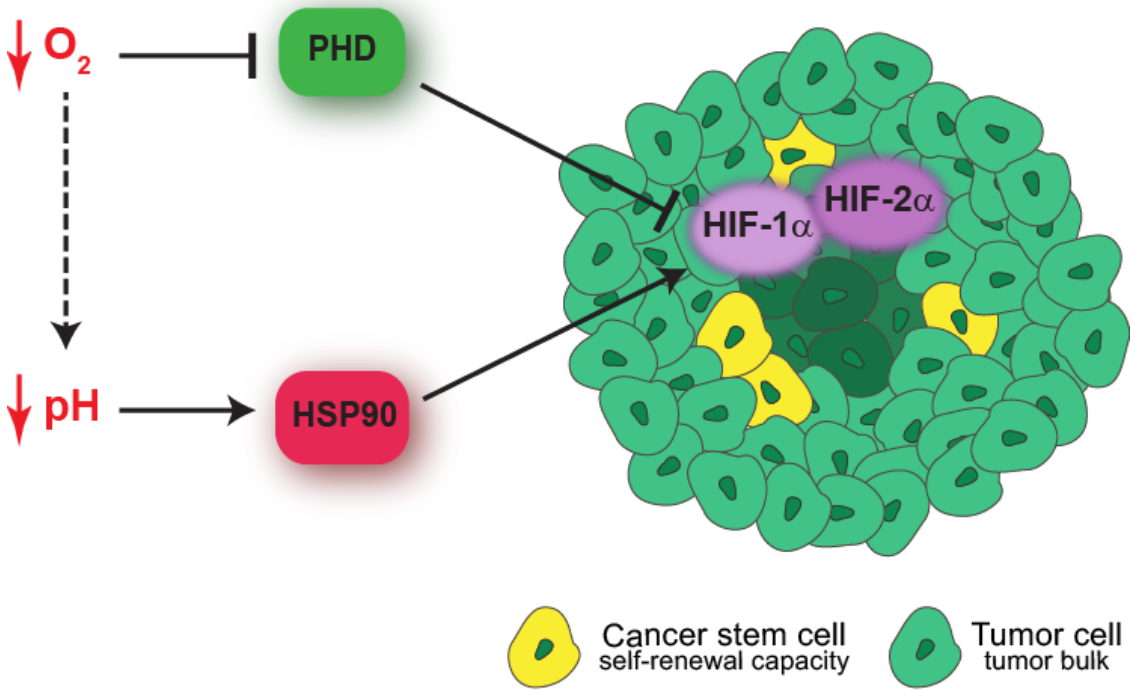

Figure 5.2. A model of the synergistic regulation of HIF function and self-renewal capacity of CSCs in the hypoxic/acidic niche.
Hypoxia and a hypoxia-induced acidic microenvironment concomitantly potentiate the hypoxic response and promote CSC maintenance. Hypoxia and acidosis act together through PHD and HSP90, respectively, to synergistically potentiate HIF-α mediated signaling and drive adaptive responses involved in tumor initiation and growth (redrawn and modified from (Filatova, et al., 2016)).

5.2.3 Targeting the hypoxic CSC niche through HSP90 inhbition

HSP90, a highly conserved chaperone protein, plays a pivotal role in stabilization and activation of more than 200 client proteins by assisting the folding, intracellular transport, maintenance, and degradation of these client proteins. Notably, HSP90 plays an even more critical role in cancer cells. HSP90-facilitated protection of mutated proteins and overexpressed oncoproteins from misfolding and degradation supports cancer cell survival (Whitesell and Lindquist, 2005, Trepel et al., 2010). HSP90 is frequently upregulated in several tumor types and is associated with poor patient prognosis and an aggressive tumor phenotype (Becker et al., 2004, Biaoxue et al., 2012, Cheng et al., 2012a, Wang et al., 2013b). Therefore, HSP90 has become an attractive molecular target and a variety of small molecular inhibitors, such as geldanamycin and its derivatives, which are currently under clinical evaluation, have been developed (Jhaveri et al., 2014, Garg et al., 2016). Our current data and recent publications by others strongly underscore the potential function of HSP90 as a CSC regulator. Inhibition of HSP90, alone or in combination with other therapeutics, has been shown to effectively eliminate CSCs, providing a potential approach to overcome CSC mediated chemotherapy resistance (Lee et al., 2012, Newman et al., 2012, Kim et al., 2015). Moreover, we demonstrated the key function of HSP90 in acidosis-dependent potentiation of HIF function and the resulting increase of CSC maintenance. The upregulation of HSP90 in the hypoxic niche and the correlation between HSP90 levels and HIF target gene and CSC marker genes expression levels (Fig. 4.19) demonstrated that targeting HSP90 might be clinically relevant, in particular to inhibit the synergistic effects of hypoxia and acidosis on HIF-α expression and a novel strategy to target CSC in the hypoxic niche. Reports from other groups have strengthened this assumption, as CSCs showed higher sensitivity to HSP90 inhibitors in glioblastoma (Sauvageot et al., 2009, Di et al., 2014).

5.3 Hypoxia mediates an invasive phenotype and anti-angiogenic therapy resistance through the activation of a HIF-1α-ZEB2-ephrinB2 axis

Low oxygenation resulting in enhanced tumor vascularization is one of the characteristics of malignant tumors like glioblastoma. Anti-angiogenic therapies targeting the tumor vasculature have been applied to deplete oxygen and nutrient supply in tumors. Even if anti-angiogenic therapy initially results in reduced tumor growth, tumor cells develop adaptive and evasive responses. Anti-angiogenic therapy-induced hypoxia plays an important role in these processes, in part through its ability to enhance tumor cell invasion. In this part of the thesis, we demonstrate that hypoxia is one of the key microenvironmental factors regulating the invasive phenotype. We show that hypoxia increases the invasion of glioblastoma cells by decreasing ephrinB2 levels and that ephrinB2 depletion itself increases tumor invasion and growth. Furthermore, re-expressing ephrinB2 in ephrinB2 depleted tumors or tumors subjected to anti-angiogenic treatment reverses the invasive capacity of tumor cells *in vivo*. These findings identify a common mechanism involved in tumor invasion, highlighting the importance of ZEB2/ephrinB2 as novel therapeutic targets to inhibit glioma invasion (Fig. 5.3).

5.3.1 Hypoxia induces invasion and downregulates ephrinB2

Tumor hypoxia is associated with an aggressive tumor phenotype, poor patient survival, treatment failure and increased metastasis/invasion. It is known that hypoxia has a dual function during cancer progression: tumor cells need oxygen and nutrient supply to support their metabolism and other cellular functions, therefore hypoxia inhibits tumor growth. On the other hand, hypoxia regulates metabolic adaptation to these stress conditions and selects for more aggressive tumor cells (Pennacchietti et al., 2003, Erler, et al., 2006, Keith, et al., 2011, Semenza, 2012). Indeed, we show that hypoxia treated cells exhibit increased invasive behavior *in vitro*, as demonstrated

in collagen invasion and Boyden chamber assays (Fig. 4.20A-C). Glioblastoma cells rarely metastasize to other organs. However, glioblastoma cells migrate, spread and disseminate into the surrounding brain tissue, which is the main factor limiting the success of the currently available therapies, leading to tumor recurrence (Rao, 2003). On that account, we wanted to identify the molecular mechanism underlying the hypoxia-induced invasive phenotype.

Eph/ephrin signaling is known to be involved in axon guidance and formation of stable tissue boundaries via mediating repulsive effects (Pasquale, 2008, Kania and Klein, 2016). Interestingly, Eph receptors and ephrins are also expressed in both tumor cells and stromal cells, mediating cell-cell communication by signal transduction. Dysregulated Eph and ephrin expression levels have been observed in various cancers leading to up or down regulation by different mechanisms. Chromosomal alterations, epigenetic regulation, changes in mRNA stability and transcriptional regulation are the mechanisms, which have been reported to lead to altered Eph or ephrin expression (Pasquale, 2010, Arvanitis and Davy, 2012). Importantly, ephrinB2 expression is frequently downregulated in gliomas compared to normal brain and the EFNB2 gene locus is also deleted with high frequency during glioma progression (Depner, et al., 2016). Moreover, we showed that hypoxia also downregulates ephrinB2. Downregulation of ephrinB2 is exclusively controlled by HIF-1α but not HIF-2α, as shown by recovered ephrinB2 levels in HIF-1α silenced cells (Fig. 4.20E). Since HIF-1α is a transcriptional activator, we performed an siRNA based screening against known EMT regulators, which function as transcriptional repressors and are upregulated upon hypoxia (Krishnamachary et al., 2006, Yang, et al., 2008, Joseph, et al., 2015, Kahlert, et al., 2015, Yeo, et al., 2017). We showed that ephrinB2 expression was increased by silencing of ZEB2 (Fig. 4.20F), which was upregulated upon hypoxia (Depner, et al., 2016), identifying ZEB2 as a putative repressor of ephrinB2. Furthermore, ephrinB2 promoter analysis and chromatin immunoprecipitation confirmed direct repression of ephrinB2 by HIF-1α-mediated upregulation of ZEB2 (Depner, et al., 2016). Interestingly, comparison of ephrinB2 and ZEB2 levels in the two cell lines LN229 and G55, which were used in this study, revealed that LN229 cells, which form highly invasive tumors when orthotopically

transplanted, expresses lower ephrinB2 and higher ZEB2 (Fig. 4.20D). These data demonstrate that hypoxic repression of ephrinB2 is mediated through the activation of the transcriptional repressor ZEB2.

5.3.2 Loss of ephrinB2 is associated with an invasive tumor phenotype

The dysregulation of Eph receptors and ephrins in cancers, particularly our findings of downregulation or loss of ephrinB2 in glioblastoma patients and hypoxic repression of ephrinB2 through ZEB2, a known EMT regulator, led us to further investigate the effect of ephrinB2 reverse signaling on tumor progression and invasion. In agreement with the repulsive effects of ephrinB2 reverse signaling in axon guidance, loss of ephrinB2 in gliomas markedly increased the invasive phenotype *in vivo*. Importantly, we showed that blockade or loss of ephrinB2 reverse signaling inhibits the repulsive signals promoting cell invasion into the surrounding brain parenchyma and enhancing tumor growth (Fig. 4.20A). To corroborate the role of ephrinB2 for the invasive phenotype, we performed a rescue experiment by overexpression of ephrinB2 in ephrinB2 deficient glioma cells. This reversed the pro-invasive phenotype, demonstrating the pivotal and direct role of ephrinB2 in the control of glioma cell invasion (Fig. 4.20B, C). A similar model has been reported for colorectal cancer, demonstrating that EphB signaling restricts the spreading of EphB expressing tumor cells into ephrinB1 expressing intestinal tissue. To overcome the repulsive EphB signal and invade into the surrounding intestinal tissue, tumor cells silence EphB expression (Batlle, et al., 2005, Cortina, et al., 2007).

Anti-angiogenic treatment has been shown to induce hypoxia and an invasive phenotype, associated with the development of therapy resistance (Zhang, et al., 2015b, Ronca, et al., 2017, Tamura, et al., 2017). However, little is known about the possible involvement of EMT regulators and ephrins in invasiveness and resistance following anti-angiogenic treatment. Notably, we show that ephrinB2 overexpression restricts tumor invasion evoked by bevacizumab treatment (Fig. 4.21D, E). Taken together, our data suggest a model in which hypoxic repression of ephrinB2 through

the hypoxic activation of ZEB2, increases the invasive capacity of tumor cells. Furthermore, tumor cells silence ephrinB2 expression by additional mechanisms, including genetic loss or epigenetic repression (Fig. 5.3).

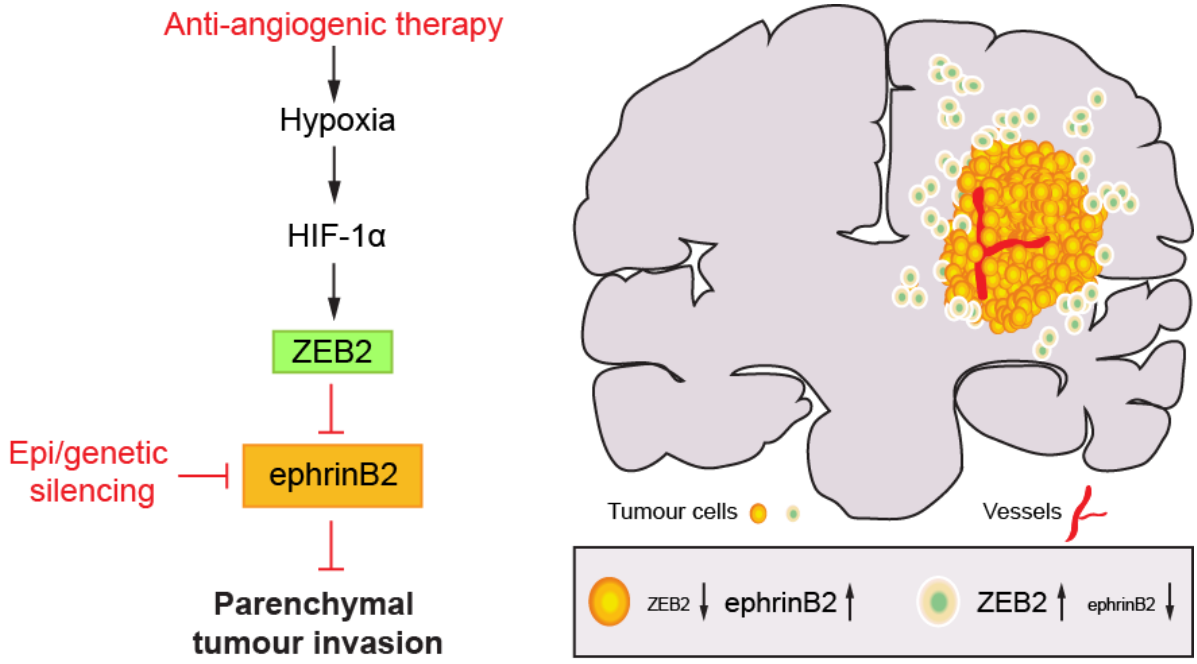

Figure 5.3. Model of the regulation of glioma invasion and evasive resistance by the HIF-1α-ZEB2-ephrinB2 axis.
The downregulation of ephrinB2 through genetic/epigenetic alterations and microenvironmental mechanisms, such as hypoxia, is a crucial step that promotes tumor invasion by abrogation of repulsive signals. The hypoxia and HIF-1α dependent control of ZEB2 and the ZEB2 mediated suppression of ephrinB2 is a central regulatory pathway that allows tumor cells to flexibly guide invasion in response to microenvironmental cues and promote evasive resistance to anti-angiogenic therapies in glioma. Our results identify the disruption of ZEB2 function as an attractive therapeutic strategy to inhibit tumor invasiveness and counteract anti-angiogenic resistance mechanisms (Depner, et al., 2016).

6 Bibliography

Akbay, E. A., Moslehi, J., Christensen, C. L., Saha, S., Tchaicha, J. H., Ramkissoon, S. H., Stewart, K. M., Carretero, J., Kikuchi, E., Zhang, H., Cohoon, T. J., Murray, S., Liu, W., Uno, K., Fisch, S., Jones, K., Gurumurthy, S., Gliser, C., Choe, S., Keenan, M., Son, J., Stanley, I., Losman, J. A., Padera, R., Bronson, R. T., Asara, J. M., Abdel-Wahab, O., Amrein, P. C., Fathi, A. T., Danial, N. N., Kimmelman, A. C., Kung, A. L., Ligon, K. L., Yen, K. E., Kaelin, W. G., Jr., Bardeesy, N. and Wong, K. K. (2014) D-2-hydroxyglutarate produced by mutant IDH2 causes cardiomyopathy and neurodegeneration in mice. Genes Dev. 28, 479-490

Al-Hajj, M., Wicha, M. S., Benito-Hernandez, A., Morrison, S. J. and Clarke, M. F. (2003) Prospective identification of tumorigenic breast cancer cells. Proc Natl Acad Sci U S A. 100, 3983-3988

Al Balushi, R. M., Cohen, J., Banks, M. and Paratz, J. D. (2013) The clinical role of glutamine supplementation in patients with multiple trauma: a narrative review. Anaesth Intensive Care. 41, 24-34

Ali, M. M., Roe, S. M., Vaughan, C. K., Meyer, P., Panaretou, B., Piper, P. W., Prodromou, C. and Pearl, L. H. (2006) Crystal structure of an Hsp90-nucleotide-p23/Sba1 closed chaperone complex. Nature. 440, 1013-1017

Amary, M. F., Bacsi, K., Maggiani, F., Damato, S., Halai, D., Berisha, F., Pollock, R., O'Donnell, P., Grigoriadis, A., Diss, T., Eskandarpour, M., Presneau, N., Hogendoorn, P. C., Futreal, A., Tirabosco, R. and Flanagan, A. M. (2011a) IDH1 and IDH2 mutations are frequent events in central chondrosarcoma and central and periosteal chondromas but not in other mesenchymal tumours. J Pathol. 224, 334-343

Amary, M. F., Damato, S., Halai, D., Eskandarpour, M., Berisha, F., Bonar, F., McCarthy, S., Fantin, V. R., Straley, K. S., Lobo, S., Aston, W., Green, C. L., Gale, R. E., Tirabosco, R., Futreal, A., Campbell, P., Presneau, N. and Flanagan, A. M. (2011b) Ollier disease and Maffucci syndrome are caused by somatic mosaic mutations of IDH1 and IDH2. Nat Genet. 43, 1262-1265

Anido, J., Saez-Borderias, A., Gonzalez-Junca, A., Rodon, L., Folch, G., Carmona, M. A., Prieto-Sanchez, R. M., Barba, I., Martinez-Saez, E., Prudkin, L., Cuartas, I., Raventos, C., Martinez-Ricarte, F., Poca, M. A., Garcia-Dorado, D., Lahn, M. M., Yingling, J. M., Rodon, J., Sahuquillo, J., Baselga, J. and Seoane, J. (2010) TGF-beta Receptor Inhibitors Target the CD44(high)/Id1(high) Glioma-Initiating Cell Population in Human Glioblastoma. Cancer Cell. 18, 655-668

Appelhoff, R. J., Tian, Y. M., Raval, R. R., Turley, H., Harris, A. L., Pugh, C. W., Ratcliffe, P. J. and Gleadle, J. M. (2004) Differential function of the prolyl hydroxylases PHD1, PHD2, and PHD3 in the regulation of hypoxia-inducible factor. J Biol Chem. 279, 38458-38465

Arvanitis, D. N. and Davy, A. (2012) Regulation and misregulation of Eph/ephrin expression. Cell Adh Migr. 6, 131-137

Aspuria, P. P., Lunt, S. Y., Varemo, L., Vergnes, L., Gozo, M., Beach, J. A., Salumbides, B., Reue, K., Wiedemeyer, W. R., Nielsen, J., Karlan, B. Y. and Orsulic, S. (2014) Succinate dehydrogenase inhibition leads to epithelial-mesenchymal transition and reprogrammed carbon metabolism. Cancer Metab. 2, 21

Bae, S. H., Jeong, J. W., Park, J. A., Kim, S. H., Bae, M. K., Choi, S. J. and Kim, K. W. (2004) Sumoylation increases HIF-1alpha stability and its transcriptional activity. Biochem Biophys Res Commun. 324, 394-400

Balkwill, F. R., Capasso, M. and Hagemann, T. (2012) The tumor microenvironment at a glance. J Cell Sci. 125, 5591-5596

Balss, J., Meyer, J., Mueller, W., Korshunov, A., Hartmann, C. and von Deimling, A. (2008) Analysis of the IDH1 codon 132 mutation in brain tumors. Acta Neuropathol. 116, 597-602

Bao, S., Wu, Q., McLendon, R. E., Hao, Y., Shi, Q., Hjelmeland, A. B., Dewhirst, M. W., Bigner, D. D. and Rich, J. N. (2006) Glioma stem cells promote radioresistance by preferential activation of the DNA damage response. Nature. 444, 756-760

Bardella, C., Al-Dalahmah, O., Krell, D., Brazauskas, P., Al-Qahtani, K., Tomkova, M., Adam, J., Serres, S., Lockstone, H., Freeman-Mills, L., Pfeffer, I., Sibson, N., Goldin, R., Schuster-Boeckler, B., Pollard, P. J., Soga, T., McCullagh, J. S., Schofield, C. J., Mulholland, P., Ansorge, O., Kriaucionis, S., Ratcliffe, P. J., Szele, F. G. and Tomlinson, I. (2016) Expression of Idh1R132H in the Murine Subventricular Zone Stem Cell Niche Recapitulates Features of Early Gliomagenesis. Cancer Cell. 30, 578-594

Batlle, E., Bacani, J., Begthel, H., Jonkheer, S., Gregorieff, A., van de Born, M., Malats, N., Sancho, E., Boon, E., Pawson, T., Gallinger, S., Pals, S. and Clevers, H. (2005) EphB receptor activity suppresses colorectal cancer progression. Nature. 435, 1126-1130

Baysal, B. E., Ferrell, R. E., Willett-Brozick, J. E., Lawrence, E. C., Myssiorek, D., Bosch, A., van der Mey, A., Taschner, P. E., Rubinstein, W. S., Myers, E. N., Richard, C. W., 3rd, Cornelisse, C. J., Devilee, P. and Devlin, B. (2000) Mutations in SDHD, a mitochondrial complex II gene, in hereditary paraganglioma. Science. 287, 848-851

Becker, B., Multhoff, G., Farkas, B., Wild, P. J., Landthaler, M., Stolz, W. and Vogt, T. (2004) Induction of Hsp90 protein expression in malignant melanomas and melanoma metastases. Exp Dermatol. 13, 27-32

Bell, E. L. and Chandel, N. S. (2007) Mitochondrial oxygen sensing: regulation of hypoxia-inducible factor by mitochondrial generated reactive oxygen species. Essays Biochem. 43, 17-27

Bellomo, C., Caja, L. and Moustakas, A. (2016) Transforming growth factor beta as regulator of cancer stemness and metastasis. Br J Cancer. 115, 761-769

Ben-Neriah, Y. and Karin, M. (2011) Inflammation meets cancer, with NF-kappaB as the matchmaker. Nat Immunol. 12, 715-723

Benita, Y., Kikuchi, H., Smith, A. D., Zhang, M. Q., Chung, D. C. and Xavier, R. J. (2009) An integrative genomics approach identifies Hypoxia Inducible Factor-1 (HIF-1)-target genes that form the core response to hypoxia. Nucleic Acids Res. 37, 4587-4602

Berchner-Pfannschmidt, U., Tug, S., Kirsch, M. and Fandrey, J. (2010) Oxygen-sensing under the influence of nitric oxide. Cell Signal. 22, 349-356

Berra, E., Benizri, E., Ginouves, A., Volmat, V., Roux, D. and Pouyssegur, J. (2003) HIF prolyl-hydroxylase 2 is the key oxygen sensor setting low steady-state levels of HIF-1alpha in normoxia. EMBO J. 22, 4082-4090

Berta, M. A., Mazure, N., Hattab, M., Pouyssegur, J. and Brahimi-Horn, M. C. (2007) SUMOylation of hypoxia-inducible factor-1alpha reduces its transcriptional activity. Biochem Biophys Res Commun. 360, 646-652

Biaoxue, R., Xiling, J., Shuanying, Y., Wei, Z., Xiguang, C., Jinsui, W. and Min, Z. (2012) Upregulation of Hsp90-beta and annexin A1 correlates with poor survival and lymphatic metastasis in lung cancer patients. J Exp Clin Cancer Res. 31, 70

Bilton, R., Mazure, N., Trottier, E., Hattab, M., Dery, M. A., Richard, D. E., Pouyssegur, J. and Brahimi-Horn, M. C. (2005) Arrest-defective-1 protein, an acetyltransferase, does not alter stability of hypoxia-inducible factor (HIF)-1alpha and is not induced by hypoxia or HIF. J Biol Chem. 280, 31132-31140

Binns, K. L., Taylor, P. P., Sicheri, F., Pawson, T. and Holland, S. J. (2000) Phosphorylation of tyrosine residues in the kinase domain and juxtamembrane region regulates the biological and catalytic activities of Eph receptors. Mol Cell Biol. 20, 4791-4805

Bleau, A. M., Hambardzumyan, D., Ozawa, T., Fomchenko, E. I., Huse, J. T., Brennan, C. W. and Holland, E. C. (2009) PTEN/PI3K/Akt pathway regulates the side population phenotype and ABCG2 activity in glioma tumor stem-like cells. Cell Stem Cell. 4, 226-235

Bogdanovic, E., Sadri, A. R., Catapano, M., Vance, J. E. and Jeschke, M. G. (2014) IDH1 regulates phospholipid metabolism in developing astrocytes. Neurosci Lett. 582, 87-92

Bogurcu, N., Seidel, S., Garvalov, B. K. and Acker, T. (2018) Analysis of Hypoxia and the Hypoxic Response in Tumor Xenografts. Methods Mol Biol. 1742, 283-300

Bohme, I. and Bosserhoff, A. K. (2016) Acidic tumor microenvironment in human melanoma. Pigment Cell Melanoma Res. 29, 508-523

Bonnet, D. and Dick, J. E. (1997) Human acute myeloid leukemia is organized as a hierarchy that originates from a primitive hematopoietic cell. Nat Med. 3, 730-737

Borger, D. R., Tanabe, K. K., Fan, K. C., Lopez, H. U., Fantin, V. R., Straley, K. S., Schenkein, D. P., Hezel, A. F., Ancukiewicz, M., Liebman, H. M., Kwak, E. L., Clark, J. W., Ryan, D. P., Deshpande, V., Dias-Santagata, D., Ellisen, L. W., Zhu, A. X. and Iafrate, A. J. (2012) Frequent mutation of isocitrate dehydrogenase (IDH)1 and IDH2 in cholangiocarcinoma identified through broad-based tumor genotyping. Oncologist. 17, 72-79

Borovski, T., De Sousa, E. M. F., Vermeulen, L. and Medema, J. P. (2011) Cancer stem cell niche: the place to be. Cancer Res. 71, 634-639

Bralten, L. B., Kloosterhof, N. K., Balvers, R., Sacchetti, A., Lapre, L., Lamfers, M., Leenstra, S., de Jonge, H., Kros, J. M., Jansen, E. E., Struys, E. A., Jakobs, C., Salomons, G. S., Diks, S. H., Peppelenbosch, M., Kremer, A., Hoogenraad, C. C., Smitt, P. A. and French, P. J. (2011) IDH1 R132H decreases proliferation of glioma cell lines in vitro and in vivo. Ann Neurol. 69, 455-463

Brennan, C. W., Verhaak, R. G., McKenna, A., Campos, B., Noushmehr, H., Salama, S. R., Zheng, S., Chakravarty, D., Sanborn, J. Z., Berman, S. H., Beroukhim, R., Bernard, B., Wu, C. J., Genovese, G., Shmulevich, I., Barnholtz-Sloan, J., Zou, L., Vegesna, R., Shukla, S. A., Ciriello, G., Yung, W. K., Zhang, W., Sougnez, C., Mikkelsen, T., Aldape, K., Bigner, D. D., Van Meir, E. G., Prados, M., Sloan, A., Black, K. L., Eschbacher, J., Finocchiaro, G., Friedman, W., Andrews, D. W., Guha, A., Iacocca, M., O'Neill, B. P., Foltz, G., Myers, J., Weisenberger, D. J., Penny, R., Kucherlapati, R., Perou, C. M., Hayes, D. N., Gibbs, R., Marra, M., Mills, G. B., Lander, E., Spellman, P., Wilson, R., Sander, C., Weinstein, J., Meyerson, M., Gabriel, S., Laird, P. W., Haussler, D., Getz, G., Chin, L. and Network, T. R. (2013) The somatic genomic landscape of glioblastoma. Cell. 155, 462-477

Briere, J. J., Favier, J., Benit, P., El Ghouzzi, V., Lorenzato, A., Rabier, D., Di Renzo, M. F., Gimenez-Roqueplo, A. P. and Rustin, P. (2005) Mitochondrial succinate is instrumental for HIF1alpha nuclear translocation in SDHA-mutant fibroblasts under normoxic conditions. Hum Mol Genet. 14, 3263-3269

Briggs, K. J., Koivunen, P., Cao, S., Backus, K. M., Olenchock, B. A., Patel, H., Zhang, Q., Signoretti, S., Gerfen, G. J., Richardson, A. L., Witkiewicz, A. K., Cravatt, B. F., Clardy, J. and Kaelin, W. G., Jr. (2016) Paracrine Induction of HIF by Glutamate in Breast Cancer: EglN1 Senses Cysteine. Cell. 166, 126-139

Brown, R. L., Reinke, L. M., Damerow, M. S., Perez, D., Chodosh, L. A., Yang, J. and Cheng, C. (2011) CD44 splice isoform switching in human and mouse epithelium is essential

for epithelial-mesenchymal transition and breast cancer progression. J Clin Invest. 121, 1064-1074

Bruick, R. K. and McKnight, S. L. (2001) A conserved family of prolyl-4-hydroxylases that modify HIF. Science. 294, 1337-1340

Bruna, A., Darken, R. S., Rojo, F., Ocana, A., Penuelas, S., Arias, A., Paris, R., Tortosa, A., Mora, J., Baselga, J. and Seoane, J. (2007) High TGFbeta-Smad activity confers poor prognosis in glioma patients and promotes cell proliferation depending on the methylation of the PDGF-B gene. Cancer Cell. 11, 147-160

Cahill, K. E., Morshed, R. A. and Yamini, B. (2016) Nuclear factor-kappaB in glioblastoma: insights into regulators and targeted therapy. Neuro Oncol. 18, 329-339

Cairns, R. A., Harris, I. S. and Mak, T. W. (2011) Regulation of cancer cell metabolism. Nat Rev Cancer. 11, 85-95

Calabrese, C., Poppleton, H., Kocak, M., Hogg, T. L., Fuller, C., Hamner, B., Oh, E. Y., Gaber, M. W., Finklestein, D., Allen, M., Frank, A., Bayazitov, I. T., Zakharenko, S. S., Gajjar, A., Davidoff, A. and Gilbertson, R. J. (2007) A perivascular niche for brain tumor stem cells. Cancer Cell. 11, 69-82

Calvert, A. E., Chalastanis, A., Wu, Y., Hurley, L. A., Kouri, F. M., Bi, Y., Kachman, M., May, J. L., Bartom, E., Hua, Y., Mishra, R. K., Schiltz, G. E., Dubrovskyi, O., Mazar, A. P., Peter, M. E., Zheng, H., James, C. D., Burant, C. F., Chandel, N. S., Davuluri, R. V., Horbinski, C. and Stegh, A. H. (2017) Cancer-Associated IDH1 Promotes Growth and Resistance to Targeted Therapies in the Absence of Mutation. Cell Rep. 19, 1858-1873

Cancer Genome Atlas Research, N. (2008) Comprehensive genomic characterization defines human glioblastoma genes and core pathways. Nature. 455, 1061-1068

Cancer Genome Atlas Research, N., Brat, D. J., Verhaak, R. G., Aldape, K. D., Yung, W. K., Salama, S. R., Cooper, L. A., Rheinbay, E., Miller, C. R., Vitucci, M., Morozova, O., Robertson, A. G., Noushmehr, H., Laird, P. W., Cherniack, A. D., Akbani, R., Huse, J. T., Ciriello, G., Poisson, L. M., Barnholtz-Sloan, J. S., Berger, M. S., Brennan, C., Colen, R. R., Colman, H., Flanders, A. E., Giannini, C., Grifford, M., Iavarone, A., Jain, R., Joseph, I., Kim, J., Kasaian, K., Mikkelsen, T., Murray, B. A., O'Neill, B. P., Pachter, L., Parsons, D. W., Sougnez, C., Sulman, E. P., Vandenberg, S. R., Van Meir, E. G., von Deimling, A., Zhang, H., Crain, D., Lau, K., Mallery, D., Morris, S., Paulauskis, J., Penny, R., Shelton, T., Sherman, M., Yena, P., Black, A., Bowen, J., Dicostanzo, K., Gastier-Foster, J., Leraas, K. M., Lichtenberg, T. M., Pierson, C. R., Ramirez, N. C., Taylor, C., Weaver, S., Wise, L., Zmuda, E., Davidsen, T., Demchok, J. A., Eley, G., Ferguson, M. L., Hutter, C. M., Mills Shaw, K. R., Ozenberger, B. A., Sheth, M., Sofia, H. J., Tarnuzzer, R., Wang, Z., Yang, L., Zenklusen, J. C., Ayala, B., Baboud, J., Chudamani, S., Jensen, M. A., Liu, J., Pihl, T., Raman, R., Wan, Y., Wu, Y., Ally, A., Auman, J. T., Balasundaram, M., Balu, S., Baylin, S. B., Beroukhim, R., Bootwalla, M. S., Bowlby, R., Bristow, C. A., Brooks, D., Butterfield, Y., Carlsen, R., Carter, S., Chin, L., Chu, A., Chuah, E., Cibulskis, K., Clarke, A., Coetzee, S. G., Dhalla, N., Fennell, T., Fisher, S., Gabriel, S., Getz, G., Gibbs, R., Guin, R., Hadjipanayis, A., Hayes, D. N., Hinoue, T., Hoadley, K., Holt, R. A., Hoyle, A. P., Jefferys, S. R., Jones, S., Jones, C. D., Kucherlapati, R., Lai, P. H., Lander, E., Lee, S., Lichtenstein, L., Ma, Y., Maglinte, D. T., Mahadeshwar, H. S., Marra, M. A., Mayo, M., Meng, S., Meyerson, M. L., Mieczkowski, P. A., Moore, R. A., Mose, L. E., Mungall, A. J., Pantazi, A., Parfenov, M., Park, P. J., Parker, J. S., Perou, C. M., Protopopov, A., Ren, X., Roach, J., Sabedot, T. S., Schein, J., Schumacher, S. E., Seidman, J. G., Seth, S., Shen, H., Simons, J. V., Sipahimalani, P., Soloway, M. G., Song, X., Sun, H., Tabak, B., Tam, A., Tan, D., Tang, J., Thiessen, N., Triche, T., Jr., Van Den Berg, D. J., Veluvolu, U., Waring, S., Weisenberger, D. J., Wilkerson, M. D., Wong, T., Wu, J., Xi, L., Xu, A. W.,

Yang, L., Zack, T. I., Zhang, J., Aksoy, B. A., Arachchi, H., Benz, C., Bernard, B., Carlin, D., Cho, J., DiCara, D., Frazer, S., Fuller, G. N., Gao, J., Gehlenborg, N., Haussler, D., Heiman, D. I., Iype, L., Jacobsen, A., Ju, Z., Katzman, S., Kim, H., Knijnenburg, T., Kreisberg, R. B., Lawrence, M. S., Lee, W., Leinonen, K., Lin, P., Ling, S., Liu, W., Liu, Y., Liu, Y., Lu, Y., Mills, G., Ng, S., Noble, M. S., Paull, E., Rao, A., Reynolds, S., Saksena, G., Sanborn, Z., Sander, C., Schultz, N., Senbabaoglu, Y., Shen, R., Shmulevich, I., Sinha, R., Stuart, J., Sumer, S. O., Sun, Y., Tasman, N., Taylor, B. S., Voet, D., Weinhold, N., Weinstein, J. N., Yang, D., Yoshihara, K., Zheng, S., Zhang, W., Zou, L., Abel, T., Sadeghi, S., Cohen, M. L., Eschbacher, J., Hattab, E. M., Raghunathan, A., Schniederjan, M. J., Aziz, D., Barnett, G., Barrett, W., Bigner, D. D., Boice, L., Brewer, C., Calatozzolo, C., Campos, B., Carlotti, C. G., Jr., Chan, T. A., Cuppini, L., Curley, E., Cuzzubbo, S., Devine, K., DiMeco, F., Duell, R., Elder, J. B., Fehrenbach, A., Finocchiaro, G., Friedman, W., Fulop, J., Gardner, J., Hermes, B., Herold-Mende, C., Jungk, C., Kendler, A., Lehman, N. L., Lipp, E., Liu, O., Mandt, R., McGraw, M., McLendon, R., McPherson, C., Neder, L., Nguyen, P., Noss, A., Nunziata, R., Ostrom, Q. T., Palmer, C., Perin, A., Pollo, B., Potapov, A., Potapova, O., Rathmell, W. K., Rotin, D., Scarpace, L., Schilero, C., Senecal, K., Shimmel, K., Shurkhay, V., Sifri, S., Singh, R., Sloan, A. E., Smolenski, K., Staugaitis, S. M., Steele, R., Thorne, L., Tirapelli, D. P., Unterberg, A., Vallurupalli, M., Wang, Y., Warnick, R., Williams, F., Wolinsky, Y., Bell, S., Rosenberg, M., Stewart, C., Huang, F., Grimsby, J. L., Radenbaugh, A. J. and Zhang, J. (2015) Comprehensive, Integrative Genomic Analysis of Diffuse Lower-Grade Gliomas. N Engl J Med. 372, 2481-2498

Carey, B. W., Finley, L. W., Cross, J. R., Allis, C. D. and Thompson, C. B. (2015) Intracellular alpha-ketoglutarate maintains the pluripotency of embryonic stem cells. Nature. 518, 413-416

Castro, B. A. and Aghi, M. K. (2014) Bevacizumab for glioblastoma: current indications, surgical implications, and future directions. Neurosurg Focus. 37, E9

Ceccarelli, C., Grodsky, N. B., Ariyaratne, N., Colman, R. F. and Bahnson, B. J. (2002) Crystal structure of porcine mitochondrial NADP+-dependent isocitrate dehydrogenase complexed with Mn2+ and isocitrate. Insights into the enzyme mechanism. J Biol Chem. 277, 43454-43462

Ceccarelli, M., Barthel, F. P., Malta, T. M., Sabedot, T. S., Salama, S. R., Murray, B. A., Morozova, O., Newton, Y., Radenbaugh, A., Pagnotta, S. M., Anjum, S., Wang, J., Manyam, G., Zoppoli, P., Ling, S., Rao, A. A., Grifford, M., Cherniack, A. D., Zhang, H., Poisson, L., Carlotti, C. G., Jr., Tirapelli, D. P., Rao, A., Mikkelsen, T., Lau, C. C., Yung, W. K., Rabadan, R., Huse, J., Brat, D. J., Lehman, N. L., Barnholtz-Sloan, J. S., Zheng, S., Hess, K., Rao, G., Meyerson, M., Beroukhim, R., Cooper, L., Akbani, R., Wrensch, M., Haussler, D., Aldape, K. D., Laird, P. W., Gutmann, D. H., Network, T. R., Noushmehr, H., Iavarone, A. and Verhaak, R. G. (2016) Molecular Profiling Reveals Biologically Discrete Subsets and Pathways of Progression in Diffuse Glioma. Cell. 164, 550-563

Cerami, E., Gao, J., Dogrusoz, U., Gross, B. E., Sumer, S. O., Aksoy, B. A., Jacobsen, A., Byrne, C. J., Heuer, M. L., Larsson, E., Antipin, Y., Reva, B., Goldberg, A. P., Sander, C. and Schultz, N. (2012) The cBio cancer genomics portal: an open platform for exploring multidimensional cancer genomics data. Cancer Discov. 2, 401-404

Cervera, A. M., Bayley, J. P., Devilee, P. and McCreath, K. J. (2009) Inhibition of succinate dehydrogenase dysregulates histone modification in mammalian cells. Mol Cancer. 8, 89

Chan, D. A., Kawahara, T. L., Sutphin, P. D., Chang, H. Y., Chi, J. T. and Giaccia, A. J. (2009) Tumor vasculature is regulated by PHD2-mediated angiogenesis and bone marrow-derived cell recruitment. Cancer Cell. 15, 527-538

Charitou, P., Rodriguez-Colman, M., Gerrits, J., van Triest, M., Groot Koerkamp, M., Hornsveld, M., Holstege, F., Verhoeven-Duif, N. M. and Burgering, B. M. (2015) FOXOs support the metabolic requirements of normal and tumor cells by promoting IDH1 expression. EMBO Rep. 16, 456-466

Charles, N., Ozawa, T., Squatrito, M., Bleau, A. M., Brennan, C. W., Hambardzumyan, D. and Holland, E. C. (2010) Perivascular nitric oxide activates notch signaling and promotes stem-like character in PDGF-induced glioma cells. Cell Stem Cell. 6, 141-152

Charles, N. A., Holland, E. C., Gilbertson, R., Glass, R. and Kettenmann, H. (2012) The brain tumor microenvironment. Glia. 60, 502-514

Chaudhry, I. H., O'Donovan, D. G., Brenchley, P. E., Reid, H. and Roberts, I. S. (2001) Vascular endothelial growth factor expression correlates with tumour grade and vascularity in gliomas. Histopathology. 39, 409-415

Chen, J. Q. and Russo, J. (2012) Dysregulation of glucose transport, glycolysis, TCA cycle and glutaminolysis by oncogenes and tumor suppressors in cancer cells. Biochim Biophys Acta. 1826, 370-384

Chen, K., Zhang, J., Guo, Z., Ma, Q., Xu, Z., Zhou, Y., Xu, Z., Li, Z., Liu, Y., Ye, X., Li, X., Yuan, B., Ke, Y., He, C., Zhou, L., Liu, J. and Ci, W. (2016a) Loss of 5-hydroxymethylcytosine is linked to gene body hypermethylation in kidney cancer. Cell Res. 26, 103-118

Chen, W., Hill, H., Christie, A., Kim, M. S., Holloman, E., Pavia-Jimenez, A., Homayoun, F., Ma, Y., Patel, N., Yell, P., Hao, G., Yousuf, Q., Joyce, A., Pedrosa, I., Geiger, H., Zhang, H., Chang, J., Gardner, K. H., Bruick, R. K., Reeves, C., Hwang, T. H., Courtney, K., Frenkel, E., Sun, X., Zojwalla, N., Wong, T., Rizzi, J. P., Wallace, E. M., Josey, J. A., Xie, Y., Xie, X. J., Kapur, P., McKay, R. M. and Brugarolas, J. (2016b) Targeting renal cell carcinoma with a HIF-2 antagonist. Nature. 539, 112-117

Chen, X., Wang, H., Yu, W., Chen, F., Wang, G., Shi, J. and Zhou, C. (2017) IDH1 Associated with Neuronal Apoptosis in Adult Rats Brain Following Intracerebral Hemorrhage. Cell Mol Neurobiol. 37, 831-841

Cheng, L., Huang, Z., Zhou, W., Wu, Q., Donnola, S., Liu, J. K., Fang, X., Sloan, A. E., Mao, Y., Lathia, J. D., Min, W., McLendon, R. E., Rich, J. N. and Bao, S. (2013) Glioblastoma stem cells generate vascular pericytes to support vessel function and tumor growth. Cell. 153, 139-152

Cheng, Q., Chang, J. T., Geradts, J., Neckers, L. M., Haystead, T., Spector, N. L. and Lyerly, H. K. (2012a) Amplification and high-level expression of heat shock protein 90 marks aggressive phenotypes of human epidermal growth factor receptor 2 negative breast cancer. Breast Cancer Res. 14, R62

Cheng, W. Y., Kandel, J. J., Yamashiro, D. J., Canoll, P. and Anastassiou, D. (2012b) A multi-cancer mesenchymal transition gene expression signature is associated with prolonged time to recurrence in glioblastoma. PLoS One. 7, e34705

Chesnelong, C., Chaumeil, M. M., Blough, M. D., Al-Najjar, M., Stechishin, O. D., Chan, J. A., Pieper, R. O., Ronen, S. M., Weiss, S., Luchman, H. A. and Cairncross, J. G. (2014) Lactate dehydrogenase A silencing in IDH mutant gliomas. Neuro Oncol. 16, 686-695

Chiche, J., Brahimi-Horn, M. C. and Pouyssegur, J. (2010) Tumour hypoxia induces a metabolic shift causing acidosis: a common feature in cancer. J Cell Mol Med. 14, 771-794

Chiche, J., Ilc, K., Laferriere, J., Trottier, E., Dayan, F., Mazure, N. M., Brahimi-Horn, M. C. and Pouyssegur, J. (2009) Hypoxia-inducible carbonic anhydrase IX and XII promote tumor cell growth by counteracting acidosis through the regulation of the intracellular pH. Cancer Res. 69, 358-368

Chin, R. M., Fu, X., Pai, M. Y., Vergnes, L., Hwang, H., Deng, G., Diep, S., Lomenick, B., Meli, V. S., Monsalve, G. C., Hu, E., Whelan, S. A., Wang, J. X., Jung, G., Solis, G. M.,

Fazlollahi, F., Kaweeteerawat, C., Quach, A., Nili, M., Krall, A. S., Godwin, H. A., Chang, H. R., Faull, K. F., Guo, F., Jiang, M., Trauger, S. A., Saghatelian, A., Braas, D., Christofk, H. R., Clarke, C. F., Teitell, M. A., Petrascheck, M., Reue, K., Jung, M. E., Frand, A. R. and Huang, J. (2014) The metabolite alpha-ketoglutarate extends lifespan by inhibiting ATP synthase and TOR. Nature. 510, 397-401

Cho, H., Du, X., Rizzi, J. P., Liberzon, E., Chakraborty, A. A., Gao, W., Carvo, I., Signoretti, S., Bruick, R. K., Josey, J. A., Wallace, E. M. and Kaelin, W. G. (2016) On-target efficacy of a HIF-2alpha antagonist in preclinical kidney cancer models. Nature. 539, 107-111

Chowdhury, R., Flashman, E., Mecinovic, J., Kramer, H. B., Kessler, B. M., Frapart, Y. M., Boucher, J. L., Clifton, I. J., McDonough, M. A. and Schofield, C. J. (2011a) Studies on the reaction of nitric oxide with the hypoxia-inducible factor prolyl hydroxylase domain 2 (EGLN1). J Mol Biol. 410, 268-279

Chowdhury, R., Yeoh, K. K., Tian, Y. M., Hillringhaus, L., Bagg, E. A., Rose, N. R., Leung, I. K., Li, X. S., Woon, E. C., Yang, M., McDonough, M. A., King, O. N., Clifton, I. J., Klose, R. J., Claridge, T. D., Ratcliffe, P. J., Schofield, C. J. and Kawamura, A. (2011b) The oncometabolite 2-hydroxyglutarate inhibits histone lysine demethylases. EMBO Rep. 12, 463-469

Chu, B., Wu, T., Miao, L., Mei, Y. and Wu, M. (2015) MiR-181a regulates lipid metabolism via IDH1. Sci Rep. 5, 8801

Cioffi, C. L., Liu, X. Q., Kosinski, P. A., Garay, M. and Bowen, B. R. (2003) Differential regulation of HIF-1 alpha prolyl-4-hydroxylase genes by hypoxia in human cardiovascular cells. Biochem Biophys Res Commun. 303, 947-953

Cohen, M. H., Shen, Y. L., Keegan, P. and Pazdur, R. (2009) FDA drug approval summary: bevacizumab (Avastin) as treatment of recurrent glioblastoma multiforme. Oncologist. 14, 1131-1138

Collins, A. T., Berry, P. A., Hyde, C., Stower, M. J. and Maitland, N. J. (2005) Prospective identification of tumorigenic prostate cancer stem cells. Cancer Res. 65, 10946-10951

Colvin, H., Nishida, N., Konno, M., Haraguchi, N., Takahashi, H., Nishimura, J., Hata, T., Kawamoto, K., Asai, A., Tsunekuni, K., Koseki, J., Mizushima, T., Satoh, T., Doki, Y., Mori, M. and Ishii, H. (2016) Oncometabolite D-2-Hydroxyglurate Directly Induces Epithelial-Mesenchymal Transition and is Associated with Distant Metastasis in Colorectal Cancer. Sci Rep. 6, 36289

Cortina, C., Palomo-Ponce, S., Iglesias, M., Fernandez-Masip, J. L., Vivancos, A., Whissell, G., Huma, M., Peiro, N., Gallego, L., Jonkheer, S., Davy, A., Lloreta, J., Sancho, E. and Batlle, E. (2007) EphB-ephrin-B interactions suppress colorectal cancer progression by compartmentalizing tumor cells. Nat Genet. 39, 1376-1383

Covello, K. L., Kehler, J., Yu, H., Gordan, J. D., Arsham, A. M., Hu, C. J., Labosky, P. A., Simon, M. C. and Keith, B. (2006) HIF-2alpha regulates Oct-4: effects of hypoxia on stem cell function, embryonic development, and tumor growth. Genes Dev. 20, 557-570

Crespo, I., Vital, A. L., Gonzalez-Tablas, M., Patino Mdel, C., Otero, A., Lopes, M. C., de Oliveira, C., Domingues, P., Orfao, A. and Tabernero, M. D. (2015) Molecular and Genomic Alterations in Glioblastoma Multiforme. Am J Pathol. 185, 1820-1833

Csermely, P., Schnaider, T., Soti, C., Prohaszka, Z. and Nardai, G. (1998) The 90-kDa molecular chaperone family: structure, function, and clinical applications. A comprehensive review. Pharmacol Ther. 79, 129-168

Cummins, E. P., Berra, E., Comerford, K. M., Ginouves, A., Fitzgerald, K. T., Seeballuck, F., Godson, C., Nielsen, J. E., Moynagh, P., Pouyssegur, J. and Taylor, C. T. (2006) Prolyl hydroxylase-1 negatively regulates IkappaB kinase-beta, giving insight into hypoxia-induced NFkappaB activity. Proc Natl Acad Sci U S A. 103, 18154-18159

Cummins, E. P., Seeballuck, F., Keely, S. J., Mangan, N. E., Callanan, J. J., Fallon, P. G. and Taylor, C. T. (2008) The hydroxylase inhibitor dimethyloxalylglycine is protective in a murine model of colitis. Gastroenterology. 134, 156-165

D'Ignazio, L., Bandarra, D. and Rocha, S. (2016) NF-kappaB and HIF crosstalk in immune responses. FEBS J. 283, 413-424

Dalerba, P., Cho, R. W. and Clarke, M. F. (2007) Cancer stem cells: models and concepts. Annu Rev Med. 58, 267-284

Dalziel, K. (1980) Isocitrate dehydrogenase and related oxidative decarboxylases. FEBS Lett. 117 Suppl, K45-55

Dang, L. and Su, S. M. (2017) Isocitrate Dehydrogenase Mutation and (R)-2-Hydroxyglutarate: From Basic Discovery to Therapeutics Development. Annu Rev Biochem. 86, 305-331

Dang, L., White, D. W., Gross, S., Bennett, B. D., Bittinger, M. A., Driggers, E. M., Fantin, V. R., Jang, H. G., Jin, S., Keenan, M. C., Marks, K. M., Prins, R. M., Ward, P. S., Yen, K. E., Liau, L. M., Rabinowitz, J. D., Cantley, L. C., Thompson, C. B., Vander Heiden, M. G. and Su, S. M. (2009) Cancer-associated IDH1 mutations produce 2-hydroxyglutarate. Nature. 462, 739-744

Davidson, T., Chen, H., Garrick, M. D., D'Angelo, G. and Costa, M. (2005) Soluble nickel interferes with cellular iron homeostasis. Mol Cell Biochem. 279, 157-162

DeBerardinis, R. J., Lum, J. J., Hatzivassiliou, G. and Thompson, C. B. (2008) The biology of cancer: metabolic reprogramming fuels cell growth and proliferation. Cell Metab. 7, 11-20

DeBerardinis, R. J., Mancuso, A., Daikhin, E., Nissim, I., Yudkoff, M., Wehrli, S. and Thompson, C. B. (2007) Beyond aerobic glycolysis: transformed cells can engage in glutamine metabolism that exceeds the requirement for protein and nucleotide synthesis. Proc Natl Acad Sci U S A. 104, 19345-19350

Dengler, V. L., Galbraith, M. D. and Espinosa, J. M. (2014) Transcriptional regulation by hypoxia inducible factors. Crit Rev Biochem Mol Biol. 49, 1-15

Denko, N. C. (2008) Hypoxia, HIF1 and glucose metabolism in the solid tumour. Nat Rev Cancer. 8, 705-713

Depner, C., Zum Buttel, H., Bogurcu, N., Cuesta, A. M., Aburto, M. R., Seidel, S., Finkelmeier, F., Foss, F., Hofmann, J., Kaulich, K., Barbus, S., Segarra, M., Reifenberger, G., Garvalov, B. K., Acker, T. and Acker-Palmer, A. (2016) EphrinB2 repression through ZEB2 mediates tumour invasion and anti-angiogenic resistance. Nat Commun. 7, 12329

Di, K., Keir, S. T., Alexandru-Abrams, D., Gong, X., Nguyen, H., Friedman, H. S. and Bota, D. A. (2014) Profiling Hsp90 differential expression and the molecular effects of the Hsp90 inhibitor IPI-504 in high-grade glioma models. J Neurooncol. 120, 473-481

Dimova, I., Popivanov, G. and Djonov, V. (2014) Angiogenesis in cancer - general pathways and their therapeutic implications. J BUON. 19, 15-21

Dioum, E. M., Chen, R., Alexander, M. S., Zhang, Q., Hogg, R. T., Gerard, R. D. and Garcia, J. A. (2009) Regulation of hypoxia-inducible factor 2alpha signaling by the stress-responsive deacetylase sirtuin 1. Science. 324, 1289-1293

Dong, Q., Cai, N., Tao, T., Zhang, R., Yan, W., Li, R., Zhang, J., Luo, H., Shi, Y., Luan, W., Zhang, Y., You, Y., Wang, Y. and Liu, N. (2014) An axis involving SNAI1, microRNA-128 and SP1 modulates glioma progression. PLoS One. 9, e98651

Donnarumma, F., Wintersteiger, R., Schober, M., Greilberger, J., Matzi, V., Maier, A., Schwarz, M. and Ortner, A. (2013) Simultaneous quantitation of alpha-ketoglutaric acid and 5-hydroxymethylfurfural in plasma by HPLC with UV and fluorescence detection. Anal Sci. 29, 1177-1182

Donnem, T., Hu, J., Ferguson, M., Adighibe, O., Snell, C., Harris, A. L., Gatter, K. C. and Pezzella, F. (2013) Vessel co-option in primary human tumors and metastases: an obstacle to effective anti-angiogenic treatment? Cancer Med. 2, 427-436

Duncan, C. G., Barwick, B. G., Jin, G., Rago, C., Kapoor-Vazirani, P., Powell, D. R., Chi, J. T., Bigner, D. D., Vertino, P. M. and Yan, H. (2012) A heterozygous IDH1R132H/WT mutation induces genome-wide alterations in DNA methylation. Genome Res. 22, 2339-2355

Duran, R. V., MacKenzie, E. D., Boulahbel, H., Frezza, C., Heiserich, L., Tardito, S., Bussolati, O., Rocha, S., Hall, M. N. and Gottlieb, E. (2013) HIF-independent role of prolyl hydroxylases in the cellular response to amino acids. Oncogene. 32, 4549-4556

Elias, M. C., Tozer, K. R., Silber, J. R., Mikheeva, S., Deng, M., Morrison, R. S., Manning, T. C., Silbergeld, D. L., Glackin, C. A., Reh, T. A. and Rostomily, R. C. (2005) TWIST is expressed in human gliomas and promotes invasion. Neoplasia. 7, 824-837

Eltzschig, H. K., Bratton, D. L. and Colgan, S. P. (2014) Targeting hypoxia signalling for the treatment of ischaemic and inflammatory diseases. Nat Rev Drug Discov. 13, 852-869

Emily G. Armitage, Helen L. Kotze and William, K. J. (2014) Correlation-based network analysis of cancer metabolism. Springer New York

Engqvist, M., Drincovich, M. F., Flugge, U. I. and Maurino, V. G. (2009) Two D-2-hydroxy-acid dehydrogenases in Arabidopsis thaliana with catalytic capacities to participate in the last reactions of the methylglyoxal and beta-oxidation pathways. J Biol Chem. 284, 25026-25037

Eph Nomenclature, C. Unified Nomenclature for Eph Family Receptors and Their Ligands, the Ephrins. In Cell ed.)^eds.). pp. 403-404, Elsevier

Epstein, A. C., Gleadle, J. M., McNeill, L. A., Hewitson, K. S., O'Rourke, J., Mole, D. R., Mukherji, M., Metzen, E., Wilson, M. I., Dhanda, A., Tian, Y. M., Masson, N., Hamilton, D. L., Jaakkola, P., Barstead, R., Hodgkin, J., Maxwell, P. H., Pugh, C. W., Schofield, C. J. and Ratcliffe, P. J. (2001) C. elegans EGL-9 and mammalian homologs define a family of dioxygenases that regulate HIF by prolyl hydroxylation. Cell. 107, 43-54

Erler, J. T., Bennewith, K. L., Nicolau, M., Dornhofer, N., Kong, C., Le, Q. T., Chi, J. T., Jeffrey, S. S. and Giaccia, A. J. (2006) Lysyl oxidase is essential for hypoxia-induced metastasis. Nature. 440, 1222-1226

Essmann, C. L., Martinez, E., Geiger, J. C., Zimmer, M., Traut, M. H., Stein, V., Klein, R. and Acker-Palmer, A. (2008) Serine phosphorylation of ephrinB2 regulates trafficking of synaptic AMPA receptors. Nat Neurosci. 11, 1035-1043

Fan, J., Kamphorst, J. J., Mathew, R., Chung, M. K., White, E., Shlomi, T. and Rabinowitz, J. D. (2013) Glutamine-driven oxidative phosphorylation is a major ATP source in transformed mammalian cells in both normoxia and hypoxia. Mol Syst Biol. 9, 712

Fendt, S. M., Bell, E. L., Keibler, M. A., Olenchock, B. A., Mayers, J. R., Wasylenko, T. M., Vokes, N. I., Guarente, L., Vander Heiden, M. G. and Stephanopoulos, G. (2013) Reductive glutamine metabolism is a function of the alpha-ketoglutarate to citrate ratio in cells. Nat Commun. 4, 2236

Ferlay, J., Steliarova-Foucher, E., Lortet-Tieulent, J., Rosso, S., Coebergh, J. W., Comber, H., Forman, D. and Bray, F. (2013) Cancer incidence and mortality patterns in Europe: estimates for 40 countries in 2012. Eur J Cancer. 49, 1374-1403

Ferluga, S., Hantgan, R., Goldgur, Y., Himanen, J. P., Nikolov, D. B. and Debinski, W. (2013) Biological and structural characterization of glycosylation on ephrin-A1, a preferred ligand for EphA2 receptor tyrosine kinase. J Biol Chem. 288, 18448-18457

Figueroa, M. E., Abdel-Wahab, O., Lu, C., Ward, P. S., Patel, J., Shih, A., Li, Y., Bhagwat, N., Vasanthakumar, A., Fernandez, H. F., Tallman, M. S., Sun, Z., Wolniak, K., Peeters, J. K., Liu, W., Choe, S. E., Fantin, V. R., Paietta, E., Lowenberg, B., Licht, J. D., Godley, L. A., Delwel, R., Valk, P. J., Thompson, C. B., Levine, R. L. and Melnick, A.

(2010) Leukemic IDH1 and IDH2 mutations result in a hypermethylation phenotype, disrupt TET2 function, and impair hematopoietic differentiation. Cancer Cell. 18, 553-567

Filatova, A., Seidel, S., Bogurcu, N., Graf, S., Garvalov, B. K. and Acker, T. (2016) Acidosis Acts through HSP90 in a PHD/VHL-Independent Manner to Promote HIF Function and Stem Cell Maintenance in Glioma. Cancer Res. 76, 5845-5856

Filipp, F. V., Scott, D. A., Ronai, Z. A., Osterman, A. L. and Smith, J. W. (2012) Reverse TCA cycle flux through isocitrate dehydrogenases 1 and 2 is required for lipogenesis in hypoxic melanoma cells. Pigment Cell Melanoma Res. 25, 375-383

Folkins, C., Man, S., Xu, P., Shaked, Y., Hicklin, D. J. and Kerbel, R. S. (2007) Anticancer therapies combining antiangiogenic and tumor cell cytotoxic effects reduce the tumor stem-like cell fraction in glioma xenograft tumors. Cancer Res. 67, 3560-3564

Folkman, J. (2007) Angiogenesis: an organizing principle for drug discovery? Nat Rev Drug Discov. 6, 273-286

Frattini, V., Trifonov, V., Chan, J. M., Castano, A., Lia, M., Abate, F., Keir, S. T., Ji, A. X., Zoppoli, P., Niola, F., Danussi, C., Dolgalev, I., Porrati, P., Pellegatta, S., Heguy, A., Gupta, G., Pisapia, D. J., Canoll, P., Bruce, J. N., McLendon, R. E., Yan, H., Aldape, K., Finocchiaro, G., Mikkelsen, T., Prive, G. G., Bigner, D. D., Lasorella, A., Rabadan, R. and Iavarone, A. (2013) The integrated landscape of driver genomic alterations in glioblastoma. Nat Genet. 45, 1141-1149

Fu, J. and Taubman, M. B. (2010) Prolyl hydroxylase EGLN3 regulates skeletal myoblast differentiation through an NF-kappaB-dependent pathway. J Biol Chem. 285, 8927-8935

Fu, J., Yang, Q. Y., Sai, K., Chen, F. R., Pang, J. C., Ng, H. K., Kwan, A. L. and Chen, Z. P. (2013) TGM2 inhibition attenuates ID1 expression in CD44-high glioma-initiating cells. Neuro Oncol. 15, 1353-1365

Fukumura, D., Xu, L., Chen, Y., Gohongi, T., Seed, B. and Jain, R. K. (2001) Hypoxia and acidosis independently up-regulate vascular endothelial growth factor transcription in brain tumors in vivo. Cancer Res. 61, 6020-6024

Fuxe, J., Vincent, T. and Garcia de Herreros, A. (2010) Transcriptional crosstalk between TGF-beta and stem cell pathways in tumor cell invasion: role of EMT promoting Smad complexes. Cell Cycle. 9, 2363-2374

Gale, N. W., Holland, S. J., Valenzuela, D. M., Flenniken, A., Pan, L., Ryan, T. E., Henkemeyer, M., Strebhardt, K., Hirai, H., Wilkinson, D. G., Pawson, T., Davis, S. and Yancopoulos, G. D. (1996) Eph receptors and ligands comprise two major specificity subclasses and are reciprocally compartmentalized during embryogenesis. Neuron. 17, 9-19

Gallego, O. (2015) Nonsurgical treatment of recurrent glioblastoma. Curr Oncol. 22, e273-281

Gao, J., Aksoy, B. A., Dogrusoz, U., Dresdner, G., Gross, B., Sumer, S. O., Sun, Y., Jacobsen, A., Sinha, R., Larsson, E., Cerami, E., Sander, C. and Schultz, N. (2013) Integrative analysis of complex cancer genomics and clinical profiles using the cBioPortal. Sci Signal. 6, pl1

Garg, G., Khandelwal, A. and Blagg, B. S. (2016) Anticancer Inhibitors of Hsp90 Function: Beyond the Usual Suspects. Adv Cancer Res. 129, 51-88

Garvalov, B. K. and Acker, T. (2011) Cancer stem cells: a new framework for the design of tumor therapies. J Mol Med (Berl). 89, 95-107

Garvalov, B. K., Foss, F., Henze, A. T., Bethani, I., Graf-Hochst, S., Singh, D., Filatova, A., Dopeso, H., Seidel, S., Damm, M., Acker-Palmer, A. and Acker, T. (2014) PHD3 regulates EGFR internalization and signalling in tumours. Nat Commun. 5, 5577

Gatenby, R. A. and Gillies, R. J. (2004) Why do cancers have high aerobic glycolysis? Nat Rev Cancer. 4, 891-899

Geng, H., Harvey, C. T., Pittsenbarger, J., Liu, Q., Beer, T. M., Xue, C. and Qian, D. Z. (2011) HDAC4 protein regulates HIF1alpha protein lysine acetylation and cancer cell response to hypoxia. J Biol Chem. 286, 38095-38102

Gentleman, R. C., Carey, V. J., Bates, D. M., Bolstad, B., Dettling, M., Dudoit, S., Ellis, B., Gautier, L., Ge, Y., Gentry, J., Hornik, K., Hothorn, T., Huber, W., Iacus, S., Irizarry, R., Leisch, F., Li, C., Maechler, M., Rossini, A. J., Sawitzki, G., Smith, C., Smyth, G., Tierney, L., Yang, J. Y. and Zhang, J. (2004) Bioconductor: open software development for computational biology and bioinformatics. Genome Biol. 5, R80

Gilbert, M. R., Dignam, J. J., Armstrong, T. S., Wefel, J. S., Blumenthal, D. T., Vogelbaum, M. A., Colman, H., Chakravarti, A., Pugh, S., Won, M., Jeraj, R., Brown, P. D., Jaeckle, K. A., Schiff, D., Stieber, V. W., Brachman, D. G., Werner-Wasik, M., Tremont-Lukats, I. W., Sulman, E. P., Aldape, K. D., Curran, W. J., Jr. and Mehta, M. P. (2014) A randomized trial of bevacizumab for newly diagnosed glioblastoma. N Engl J Med. 370, 699-708

Gillies, R. J., Raghunand, N., Garcia-Martin, M. L. and Gatenby, R. A. (2004) pH imaging. A review of pH measurement methods and applications in cancers. IEEE Eng Med Biol Mag. 23, 57-64

Global Burden of Disease Cancer, C. (2015) The global burden of cancer 2013

Gorlach, A., Camenisch, G., Kvietikova, I., Vogt, L., Wenger, R. H. and Gassmann, M. (2000) Efficient translation of mouse hypoxia-inducible factor-1alpha under normoxic and hypoxic conditions. Biochim Biophys Acta. 1493, 125-134

Gradin, K., McGuire, J., Wenger, R. H., Kvietikova, I., fhitelaw, M. L., Toftgard, R., Tora, L., Gassmann, M. and Poellinger, L. (1996) Functional interference between hypoxia and dioxin signal transduction pathways: competition for recruitment of the Arnt transcription factor. Mol Cell Biol. 16, 5221-5231

Gradin, K., Takasaki, C., Fujii-Kuriyama, Y. and Sogawa, K. (2002) The transcriptional activation function of the HIF-like factor requires phosphorylation at a conserved threonine. J Biol Chem. 277, 23508-23514

Grassian, A. R., Lin, F., Barrett, R., Liu, Y., Jiang, W., Korpal, M., Astley, H., Gitterman, D., Henley, T., Howes, R., Levell, J., Korn, J. M. and Pagliarini, R. (2012) Isocitrate dehydrogenase (IDH) mutations promote a reversible ZEB1/microRNA (miR)-200-dependent epithelial-mesenchymal transition (EMT). J Biol Chem. 287, 42180-42194

Grauer, O. M., Nierkens, S., Bennink, E., Toonen, L. W., Boon, L., Wesseling, P., Sutmuller, R. P. and Adema, G. J. (2007) CD4+FoxP3+ regulatory T cells gradually accumulate in gliomas during tumor growth and efficiently suppress antiglioma immune responses in vivo. Int J Cancer. 121, 95-105

Grivennikov, S. I., Greten, F. R. and Karin, M. (2010) Immunity, inflammation, and cancer. Cell. 140, 883-899

Gucciardo, E., Sugiyama, N. and Lehti, K. (2014) Eph- and ephrin-dependent mechanisms in tumor and stem cell dynamics. Cell Mol Life Sci. 71, 3685-3710

Hamerlik, P., Lathia, J. D., Rasmussen, R., Wu, Q., Bartkova, J., Lee, M., Moudry, P., Bartek, J., Jr., Fischer, W., Lukas, J., Rich, J. N. and Bartek, J. (2012) Autocrine VEGF-VEGFR2-Neuropilin-1 signaling promotes glioma stem-like cell viability and tumor growth. J Exp Med. 209, 507-520

Hamm, A., Veschini, L., Takeda, Y., Costa, S., Delamarre, E., Squadrito, M. L., Henze, A. T., Wenes, M., Serneels, J., Pucci, F., Roncal, C., Anisimov, A., Alitalo, K., De Palma, M. and Mazzone, M. (2013) PHD2 regulates arteriogenic macrophages through TIE2 signalling. EMBO Mol Med. 5, 843-857

Han, S. P., Kim, J. H., Han, M. E., Sim, H. E., Kim, K. S., Yoon, S., Baek, S. Y., Kim, B. S. and Oh, S. O. (2011) SNAI1 is involved in the proliferation and migration of glioblastoma cells. Cell Mol Neurobiol. 31, 489-496

Hanahan, D. and Coussens, L. M. (2012) Accessories to the crime: functions of cells recruited to the tumor microenvironment. Cancer Cell. 21, 309-322

Hanahan, D. and Weinberg, R. A. (2011) Hallmarks of cancer: the next generation. Cell. 144, 646-674

Hatzimichael, E., Dasoula, A., Shah, R., Syed, N., Papoudou-Bai, A., Coley, H. M., Dranitsaris, G., Bourantas, K. L., Stebbing, J. and Crook, T. (2010) The prolyl-hydroxylase EGLN3 and not EGLN1 is inactivated by methylation in plasma cell neoplasia. Eur J Haematol. 84, 47-51

Heddleston, J. M., Hitomi, M., Venere, M., Flavahan, W. A., Yang, K., Kim, Y., Minhas, S., Rich, J. N. and Hjelmeland, A. B. (2011) Glioma stem cell maintenance: the role of the microenvironment. Curr Pharm Des. 17, 2386-2401

Heddleston, J. M., Li, Z., Lathia, J. D., Bao, S., Hjelmeland, A. B. and Rich, J. N. (2010) Hypoxia inducible factors in cancer stem cells. Br J Cancer. 102, 789-795

Heddleston, J. M., Li, Z., McLendon, R. E., Hjelmeland, A. B. and Rich, J. N. (2009) The hypoxic microenvironment maintains glioblastoma stem cells and promotes reprogramming towards a cancer stem cell phenotype. Cell Cycle. 8, 3274-3284

Henze, A. T. and Acker, T. (2010) Feedback regulators of hypoxia-inducible factors and their role in cancer biology. Cell Cycle. 9, 2749-2763

Henze, A. T., Garvalov, B. K., Seidel, S., Cuesta, A. M., Ritter, M., Filatova, A., Foss, F., Dopeso, H., Essmann, C. L., Maxwell, P. H., Reifenberger, G., Carmeliet, P., Acker-Palmer, A. and Acker, T. (2014) Loss of PHD3 allows tumours to overcome hypoxic growth inhibition and sustain proliferation through EGFR. Nat Commun. 5, 5582

Henze, A. T., Riedel, J., Diem, T., Wenner, J., Flamme, I., Pouyseggur, J., Plate, K. H. and Acker, T. (2010) Prolyl hydroxylases 2 and 3 act in gliomas as protective negative feedback regulators of hypoxia-inducible factors. Cancer Res. 70, 357-366

Hermanussen, M. and Tresguerres, J. A. (2005) How much glutamate is toxic in paediatric parenteral nutrition? Acta Paediatr. 94, 16-19

Himanen, J. P. and Nikolov, D. B. (2003) Eph signaling: a structural view. Trends Neurosci. 26, 46-51

Himanen, J. P., Rajashankar, K. R., Lackmann, M., Cowan, C. A., Henkemeyer, M. and Nikolov, D. B. (2001) Crystal structure of an Eph receptor-ephrin complex. Nature. 414, 933-938

Himanen, J. P., Yermekbayeva, L., Janes, P. W., Walker, J. R., Xu, K., Atapattu, L., Rajashankar, K. R., Mensinga, A., Lackmann, M., Nikolov, D. B. and Dhe-Paganon, S. (2010) Architecture of Eph receptor clusters. Proc Natl Acad Sci U S A. 107, 10860-10865

Hirai, H., Maru, Y., Hagiwara, K., Nishida, J. and Takaku, F. (1987) A novel putative tyrosine kinase receptor encoded by the eph gene. Science. 238, 1717-1720

Hirsila, M., Koivunen, P., Gunzler, V., Kivirikko, K. I. and Myllyharju, J. (2003) Characterization of the human prolyl 4-hydroxylases that modify the hypoxia-inducible factor. J Biol Chem. 278, 30772-30780

Hiwatashi, Y., Kanno, K., Takasaki, C., Goryo, K., Sato, T., Torii, S., Sogawa, K. and Yasumoto, K. (2011) PHD1 interacts with ATF4 and negatively regulates its transcriptional activity without prolyl hydroxylation. Exp Cell Res. 317, 2789-2799

Hjelmeland, A. B., Wu, Q., Heddleston, J. M., Choudhary, G. S., MacSwords, J., Lathia, J. D., McLendon, R., Lindner, D., Sloan, A. and Rich, J. N. (2011) Acidic stress promotes a glioma stem cell phenotype. Cell Death Differ. 18, 829-840

Hoelzinger, D. B., Demuth, T. and Berens, M. E. (2007) Autocrine factors that sustain glioma invasion and paracrine biology in the brain microenvironment. J Natl Cancer Inst. 99, 1583-1593

Hojfeldt, J. W. and Helin, K. (2016) Regional tumour glutamine supply affects chromatin and cell identity. Nat Cell Biol. 18, 1027-1029

Holmquist-Mengelbier, L., Fredlund, E., Lofstedt, T., Noguera, R., Navarro, S., Nilsson, H., Pietras, A., Vallon-Christersson, J., Borg, A., Gradin, K., Poellinger, L. and Pahlman, S. (2006) Recruitment of HIF-1alpha and HIF-2alpha to common target genes is differentially regulated in neuroblastoma: HIF-2alpha promotes an aggressive phenotype. Cancer Cell. 10, 413-423

Honasoge, A. and Sontheimer, H. (2013) Involvement of tumor acidification in brain cancer pathophysiology. Front Physiol. 4, 316

Hu, C. J., Sataur, A., Wang, L., Chen, H. and Simon, M. C. (2007) The N-terminal transactivation domain confers target gene specificity of hypoxia-inducible factors HIF-1alpha and HIF-2alpha. Mol Biol Cell. 18, 4528-4542

Hu, X., Liu, Y., Qin, C., Pan, Z., Luo, J., Yu, A. and Cheng, Z. (2014) Up-regulated isocitrate dehydrogenase 1 suppresses proliferation, migration and invasion in osteosarcoma: in vitro and in vivo. Cancer Lett. 346, 114-121

Huang, D., Li, C. and Zhang, H. (2014) Hypoxia and cancer cell metabolism. Acta Biochim Biophys Sin (Shanghai). 46, 214-219

Huang, J., Zhao, Q., Mooney, S. M. and Lee, F. S. (2002) Sequence determinants in hypoxia-inducible factor-1alpha for hydroxylation by the prolyl hydroxylases PHD1, PHD2, and PHD3. J Biol Chem. 277, 39792-39800

Huang, S., Tang, Y., Peng, X., Cai, X., Wa, Q., Ren, D., Li, Q., Luo, J., Li, L., Zou, X. and Huang, S. (2016) Acidic extracellular pH promotes prostate cancer bone metastasis by enhancing PC-3 stem cell characteristics, cell invasiveness and VEGF-induced vasculogenesis of BM-EPCs. Oncol Rep. 36, 2025-2032

Huang, Y. and Rao, A. (2014) Connections between TET proteins and aberrant DNA modification in cancer. Trends Genet. 30, 464-474

Huse, J. T. and Aldape, K. D. (2014) The evolving role of molecular markers in the diagnosis and management of diffuse glioma. Clin Cancer Res. 20, 5601-5611

Huusko, P., Ponciano-Jackson, D., Wolf, M., Kiefer, J. A., Azorsa, D. O., Tuzmen, S., Weaver, D., Robbins, C., Moses, T., Allinen, M., Hautaniemi, S., Chen, Y., Elkahloun, A., Basik, M., Bova, G. S., Bubendorf, L., Lugli, A., Sauter, G., Schleutker, J., Ozcelik, H., Elowe, S., Pawson, T., Trent, J. M., Carpten, J. D., Kallioniemi, O. P. and Mousses, S. (2004) Nonsense-mediated decay microarray analysis identifies mutations of EPHB2 in human prostate cancer. Nat Genet. 36, 979-983

Hwang, I. Y., Kwak, S., Lee, S., Kim, H., Lee, S. E., Kim, J. H., Kim, Y. A., Jeon, Y. K., Chung, D. H., Jin, X., Park, S., Jang, H., Cho, E. J. and Youn, H. D. (2016) Psat1-Dependent Fluctuations in alpha-Ketoglutarate Affect the Timing of ESC Differentiation. Cell Metab. 24, 494-501

Isaacs, J. S., Jung, Y. J., Mimnaugh, E. G., Martinez, A., Cuttitta, F. and Neckers, L. M. (2002) Hsp90 regulates a von Hippel Lindau-independent hypoxia-inducible factor-1 alpha-degradative pathway. J Biol Chem. 277, 29936-29944

Isaacs, J. S., Jung, Y. J., Mole, D. R., Lee, S., Torres-Cabala, C., Chung, Y. L., Merino, M., Trepel, J., Zbar, B., Toro, J., Ratcliffe, P. J., Linehan, W. M. and Neckers, L. (2005) HIF overexpression correlates with biallelic loss of fumarate hydratase in renal cancer: novel role of fumarate in regulation of HIF stability. Cancer Cell. 8, 143-153

Iser, I. C., Pereira, M. B., Lenz, G. and Wink, M. R. (2016) The Epithelial-to-Mesenchymal Transition-Like Process in Glioblastoma: An Updated Systematic Review and In Silico Investigation. Med Res Rev

Itsumi, M., Inoue, S., Elia, A. J., Murakami, K., Sasaki, M., Lind, E. F., Brenner, D., Harris, I. S., Chio, II, Afzal, S., Cairns, R. A., Cescon, D. W., Elford, A. R., Ye, J., Lang, P. A., Li, W. Y., Wakeham, A., Duncan, G. S., Haight, J., You-Ten, A., Snow, B., Yamamoto,

K., Ohashi, P. S. and Mak, T. W. (2015) Idh1 protects murine hepatocytes from endotoxin-induced oxidative stress by regulating the intracellular NADP(+)/NADPH ratio. Cell Death Differ. 22, 1837-1845

Iwadate, Y. (2016) Epithelial-mesenchymal transition in glioblastoma progression. Oncol Lett. 11, 1615-1620

Iwadate, Y., Matsutani, T., Hirono, S., Shinozaki, N. and Saeki, N. (2016) Transforming growth factor-beta and stem cell markers are highly expressed around necrotic areas in glioblastoma. J Neurooncol. 129, 101-107

Iwai, K., Yamanaka, K., Kamura, T., Minato, N., Conaway, R. C., Conaway, J. W., Klausner, R. D. and Pause, A. (1999) Identification of the von Hippel-lindau tumor-suppressor protein as part of an active E3 ubiquitin ligase complex. Proc Natl Acad Sci U S A. 96, 12436-12441

Iyer, N. V., Kotch, L. E., Agani, F., Leung, S. W., Laughner, E., Wenger, R. H., Gassmann, M., Gearhart, J. D., Lawler, A. M., Yu, A. Y. and Semenza, G. L. (1998) Cellular and developmental control of O2 homeostasis by hypoxia-inducible factor 1 alpha. Genes Dev. 12, 149-162

Izquierdo-Garcia, J. L., Viswanath, P., Eriksson, P., Cai, L., Radoul, M., Chaumeil, M. M., Blough, M., Luchman, H. A., Weiss, S., Cairncross, J. G., Phillips, J. J., Pieper, R. O. and Ronen, S. M. (2015) IDH1 Mutation Induces Reprogramming of Pyruvate Metabolism. Cancer Res. 75, 2999-3009

Jaakkola, P., Mole, D. R., Tian, Y. M., Wilson, M. I., Gielbert, J., Gaskell, S. J., von Kriegsheim, A., Hebestreit, H. F., Mukherji, M., Schofield, C. J., Maxwell, P. H., Pugh, C. W. and Ratcliffe, P. J. (2001) Targeting of HIF-alpha to the von Hippel-Lindau ubiquitylation complex by O2-regulated prolyl hydroxylation. Science. 292, 468-472

Jackson, E. L. and Alvarez-Buylla, A. (2008) Characterization of adult neural stem cells and their relation to brain tumors. Cells Tissues Organs. 188, 212-224

Janes, P. W., Nievergall, E. and Lackmann, M. (2012) Concepts and consequences of Eph receptor clustering. Semin Cell Dev Biol. 23, 43-50

Jeong, J. W., Bae, M. K., Ahn, M. Y., Kim, S. H., Sohn, T. K., Bae, M. H., Yoo, M. A., Song, E. J., Lee, K. J. and Kim, K. W. (2002) Regulation and destabilization of HIF-1alpha by ARD1-mediated acetylation. Cell. 111, 709-720

Jhaveri, K., Ochiana, S. O., Dunphy, M. P., Gerecitano, J. F., Corben, A. D., Peter, R. I., Janjigian, Y. Y., Gomes-DaGama, E. M., Koren, J., 3rd, Modi, S. and Chiosis, G. (2014) Heat shock protein 90 inhibitors in the treatment of cancer: current status and future directions. Expert Opin Investig Drugs. 23, 611-628

Jiang, B. H., Rue, E., Wang, G. L., Roe, R. and Semenza, G. L. (1996) Dimerization, DNA binding, and transactivation properties of hypoxia-inducible factor 1. J Biol Chem. 271, 17771-17778

Jiang, B. H., Zheng, J. Z., Leung, S. W., Roe, R. and Semenza, G. L. (1997) Transactivation and inhibitory domains of hypoxia-inducible factor 1alpha. Modulation of transcriptional activity by oxygen tension. J Biol Chem. 272, 19253-19260

Jimenez-Valerio, G. and Casanovas, O. (2017) Angiogenesis and Metabolism: Entwined for Therapy Resistance. Trends Cancer. 3, 10-18

Jo, S. H., Lee, S. H., Chun, H. S., Lee, S. M., Koh, H. J., Lee, S. E., Chun, J. S., Park, J. W. and Huh, T. L. (2002) Cellular defense against UVB-induced phototoxicity by cytosolic NADP(+)-dependent isocitrate dehydrogenase. Biochem Biophys Res Commun. 292, 542-549

Jokilehto, T. and Jaakkola, P. M. (2010) The role of HIF prolyl hydroxylases in tumour growth. J Cell Mol Med. 14, 758-770

Joseph, J. V., Conroy, S., Pavlov, K., Sontakke, P., Tomar, T., Eggens-Meijer, E., Balasubramaniyan, V., Wagemakers, M., den Dunnen, W. F. and Kruyt, F. A. (2015)

Hypoxia enhances migration and invasion in glioblastoma by promoting a mesenchymal shift mediated by the HIF1alpha-ZEB1 axis. Cancer Lett. 359, 107-116

Joseph, J. V., Conroy, S., Tomar, T., Eggens-Meijer, E., Bhat, K., Copray, S., Walenkamp, A. M., Boddeke, E., Balasubramanyian, V., Wagemakers, M., den Dunnen, W. F. and Kruyt, F. A. (2014) TGF-beta is an inducer of ZEB1-dependent mesenchymal transdifferentiation in glioblastoma that is associated with tumor invasion. Cell Death Dis. 5, e1443

Junghans, P., Derno, M., Pierzynowski, S., Hennig, U., Eberhard Rudolph, P. and Souffrant, W. B. (2006) Intraduodenal infusion of alpha-ketoglutarate decreases whole body energy expenditure in growing pigs. Clin Nutr. 25, 489-496

Kaelin, W. G., Jr. and Ratcliffe, P. J. (2008) Oxygen sensing by metazoans: the central role of the HIF hydroxylase pathway. Mol Cell. 30, 393-402

Kahlert, U. D., Maciaczyk, D., Doostkam, S., Orr, B. A., Simons, B., Bogiel, T., Reithmeier, T., Prinz, M., Schubert, J., Niedermann, G., Brabletz, T., Eberhart, C. G., Nikkhah, G. and Maciaczyk, J. (2012) Activation of canonical WNT/beta-catenin signaling enhances in vitro motility of glioblastoma cells by activation of ZEB1 and other activators of epithelial-to-mesenchymal transition. Cancer Lett. 325, 42-53

Kahlert, U. D., Nikkhah, G. and Maciaczyk, J. (2013) Epithelial-to-mesenchymal(-like) transition as a relevant molecular event in malignant gliomas. Cancer Lett. 331, 131-138

Kahlert, U. D., Suwala, A. K., Raabe, E. H., Siebzehnrubl, F. A., Suarez, M. J., Orr, B. A., Bar, E. E., Maciaczyk, J. and Eberhart, C. G. (2015) ZEB1 Promotes Invasion in Human Fetal Neural Stem Cells and Hypoxic Glioma Neurospheres. Brain Pathol. 25, 724-732

Kallio, P. J., Pongratz, I., Gradin, K., McGuire, J. and Poellinger, L. (1997) Activation of hypoxia-inducible factor 1alpha: posttranscriptional regulation and conformational change by recruitment of the Arnt transcription factor. Proc Natl Acad Sci U S A. 94, 5667-5672

Kalluri, R. and Weinberg, R. A. (2009) The basics of epithelial-mesenchymal transition. J Clin Invest. 119, 1420-1428

Kalousi, A., Mylonis, I., Politou, A. S., Chachami, G., Paraskeva, E. and Simos, G. (2010) Casein kinase 1 regulates human hypoxia-inducible factor HIF-1. J Cell Sci. 123, 2976-2986

Kania, A. and Klein, R. (2016) Mechanisms of ephrin-Eph signalling in development, physiology and disease. Nat Rev Mol Cell Biol. 17, 240-256

Karcher, S., Steiner, H. H., Ahmadi, R., Zoubaa, S., Vasvari, G., Bauer, H., Unterberg, A. and Herold-Mende, C. (2006) Different angiogenic phenotypes in primary and secondary glioblastomas. Int J Cancer. 118, 2182-2189

Karsy, M., Guan, J., Jensen, R., Huang, L. E. and Colman, H. (2016) The Impact of Hypoxia and Mesenchymal Transition on Glioblastoma Pathogenesis and Cancer Stem Cells Regulation. World Neurosurg. 88, 222-236

Kato, Y., Lambert, C. A., Colige, A. C., Mineur, P., Noel, A., Frankenne, F., Foidart, J. M., Baba, M., Hata, R., Miyazaki, K. and Tsukuda, M. (2005) Acidic extracellular pH induces matrix metalloproteinase-9 expression in mouse metastatic melanoma cells through the phospholipase D-mitogen-activated protein kinase signaling. J Biol Chem. 280, 10938-10944

Kato, Y., Ozawa, S., Miyamoto, C., Maehata, Y., Suzuki, A., Maeda, T. and Baba, Y. (2013) Acidic extracellular microenvironment and cancer. Cancer Cell Int. 13, 89

Katschinski, D. M., Le, L., Schindler, S. G., Thomas, T., Voss, A. K. and Wenger, R. H. (2004) Interaction of the PAS B domain with HSP90 accelerates hypoxia-inducible factor-1alpha stabilization. Cell Physiol Biochem. 14, 351-360

Kaufhold, S. and Bonavida, B. (2014) Central role of Snail1 in the regulation of EMT and resistance in cancer: a target for therapeutic intervention. J Exp Clin Cancer Res. 33, 62

Keating, G. M. (2014) Bevacizumab: a review of its use in advanced cancer. Drugs. 74, 1891-1925

Keith, B., Johnson, R. S. and Simon, M. C. (2011) HIF1alpha and HIF2alpha: sibling rivalry in hypoxic tumour growth and progression. Nat Rev Cancer. 12, 9-22

Kickingereder, P., Sahm, F., Radbruch, A., Wick, W., Heiland, S., Deimling, A., Bendszus, M. and Wiestler, B. (2015) IDH mutation status is associated with a distinct hypoxia/angiogenesis transcriptome signature which is non-invasively predictable with rCBV imaging in human glioma. Sci Rep. 5, 16238

Kim, C. F., Jackson, E. L., Woolfenden, A. E., Lawrence, S., Babar, I., Vogel, S., Crowley, D., Bronson, R. T. and Jacks, T. (2005) Identification of bronchioalveolar stem cells in normal lung and lung cancer. Cell. 121, 823-835

Kim, H. B., Lee, S. H., Um, J. H., Kim, M. J., Hyun, S. K., Gong, E. J., Oh, W. K., Kang, C. D. and Kim, S. H. (2015) Sensitization of chemo-resistant human chronic myeloid leukemia stem-like cells to Hsp90 inhibitor by SIRT1 inhibition. Int J Biol Sci. 11, 923-934

Kim, J. W., Tchernyshyov, I., Semenza, G. L. and Dang, C. V. (2006) HIF-1-mediated expression of pyruvate dehydrogenase kinase: a metabolic switch required for cellular adaptation to hypoxia. Cell Metab. 3, 177-185

Kim, S., Kim, S. Y., Ku, H. J., Jeon, Y. H., Lee, H. W., Lee, J., Kwon, T. K., Park, K. M. and Park, J. W. (2014) Suppression of tumorigenesis in mitochondrial NADP(+)-dependent isocitrate dehydrogenase knock-out mice. Biochim Biophys Acta. 1842, 135-143

Kim, Y. W., Koul, D., Kim, S. H., Lucio-Eterovic, A. K., Freire, P. R., Yao, J., Wang, J., Almeida, J. S., Aldape, K. and Yung, W. K. (2013) Identification of prognostic gene signatures of glioblastoma: a study based on TCGA data analysis. Neuro Oncol. 15, 829-839

Knizetova, P., Ehrmann, J., Hlobilkova, A., Vancova, I., Kalita, O., Kolar, Z. and Bartek, J. (2008) Autocrine regulation of glioblastoma cell cycle progression, viability and radioresistance through the VEGF-VEGFR2 (KDR) interplay. Cell Cycle. 7, 2553-2561

Koditz, J., Nesper, J., Wottawa, M., Stiehl, D. P., Camenisch, G., Franke, C., Myllyharju, J., Wenger, R. H. and Katschinski, D. M. (2007) Oxygen-dependent ATF-4 stability is mediated by the PHD3 oxygen sensor. Blood. 110, 3610-3617

Koh, H. J., Lee, S. M., Son, B. G., Lee, S. H., Ryoo, Z. Y., Chang, K. T., Park, J. W., Park, D. C., Song, B. J., Veech, R. L., Song, H. and Huh, T. L. (2004) Cytosolic NADP+-dependent isocitrate dehydrogenase plays a key role in lipid metabolism. J Biol Chem. 279, 39968-39974

Koh, M. Y., Lemos, R., Jr., Liu, X. and Powis, G. (2011) The hypoxia-associated factor switches cells from HIF-1alpha- to HIF-2alpha-dependent signaling promoting stem cell characteristics, aggressive tumor growth and invasion. Cancer Res. 71, 4015-4027

Koivunen, P., Hirsila, M., Remes, A. M., Hassinen, I. E., Kivirikko, K. I. and Myllyharju, J. (2007) Inhibition of hypoxia-inducible factor (HIF) hydroxylases by citric acid cycle intermediates: possible links between cell metabolism and stabilization of HIF. J Biol Chem. 282, 4524-4532

Koivunen, P., Lee, S., Duncan, C. G., Lopez, G., Lu, G., Ramkissoon, S., Losman, J. A., Joensuu, P., Bergmann, U., Gross, S., Travins, J., Weiss, S., Looper, R., Ligon, K. L., Verhaak, R. G., Yan, H. and Kaelin, W. G., Jr. (2012) Transformation by the (R)-enantiomer of 2-hydroxyglutarate linked to EGLN activation. Nature. 483, 484-488

Kolosenko, I., Avnet, S., Baldini, N., Viklund, J. and De Milito, A. (2017) Therapeutic implications of tumor interstitial acidification. Semin Cancer Biol. 43, 119-133

Kranendijk, M., Struys, E. A., Gibson, K. M., Wickenhagen, W. V., Abdenur, J. E., Buechner, J., Christensen, E., de Kremer, R. D., Errami, A., Gissen, P., Gradowska, W., Hobson, E., Islam, L., Korman, S. H., Kurczynski, T., Maranda, B., Meli, C., Rizzo, C., Sansaricq, C., Trefz, F. K., Webster, R., Jakobs, C. and Salomons, G. S. (2010a) Evidence for genetic heterogeneity in D-2-hydroxyglutaric aciduria. Hum Mutat. 31, 279-283

Kranendijk, M., Struys, E. A., Salomons, G. S., Van der Knaap, M. S. and Jakobs, C. (2012) Progress in understanding 2-hydroxyglutaric acidurias. J Inherit Metab Dis. 35, 571-587

Kranendijk, M., Struys, E. A., van Schaftingen, E., Gibson, K. M., Kanhai, W. A., van der Knaap, M. S., Amiel, J., Buist, N. R., Das, A. M., de Klerk, J. B., Feigenbaum, A. S., Grange, D. K., Hofstede, F. C., Holme, E., Kirk, E. P., Korman, S. H., Morava, E., Morris, A., Smeitink, J., Sukhai, R. N., Vallance, H., Jakobs, C. and Salomons, G. S. (2010b) IDH2 mutations in patients with D-2-hydroxyglutaric aciduria. Science. 330, 336

Krebs, H. A. and Johnson, W. A. (1980) The role of citric acid in intermediate metabolism in animal tissues. FEBS Lett. 117 Suppl, K1-10

Krishnamachary, B., Zagzag, D., Nagasawa, H., Rainey, K., Okuyama, H., Baek, J. H. and Semenza, G. L. (2006) Hypoxia-inducible factor-1-dependent repression of E-cadherin in von Hippel-Lindau tumor suppressor-null renal cell carcinoma mediated by TCF3, ZFHX1A, and ZFHX1B. Cancer Res. 66, 2725-2731

Kroeze, L. I., van der Reijden, B. A. and Jansen, J. H. (2015) 5-Hydroxymethylcytosine: An epigenetic mark frequently deregulated in cancer. Biochim Biophys Acta. 1855, 144-154

Krone, P. H. and Sass, J. B. (1994) HSP 90 alpha and HSP 90 beta genes are present in the zebrafish and are differentially regulated in developing embryos. Biochem Biophys Res Commun. 204, 746-752

Kucharzewska, P. and Belting, M. (2013) Emerging roles of extracellular vesicles in the adaptive response of tumour cells to microenvironmental stress. J Extracell Vesicles. 2,

Kuiper, C. and Vissers, M. C. (2014) Ascorbate as a co-factor for fe- and 2-oxoglutarate dependent dioxygenases: physiological activity in tumor growth and progression. Front Oncol. 4, 359

Lamouille, S., Xu, J. and Derynck, R. (2014) Molecular mechanisms of epithelial-mesenchymal transition. Nat Rev Mol Cell Biol. 15, 178-196

Lando, D., Peet, D. J., Gorman, J. J., Whelan, D. A., Whitelaw, M. L. and Bruick, R. K. (2002) FIH-1 is an asparaginyl hydroxylase enzyme that regulates the transcriptional activity of hypoxia-inducible factor. Genes Dev. 16, 1466-1471

Lathia, J. D., Gallagher, J., Heddleston, J. M., Wang, J., Eyler, C. E., Macswords, J., Wu, Q., Vasanji, A., McLendon, R. E., Hjelmeland, A. B. and Rich, J. N. (2010) Integrin alpha 6 regulates glioblastoma stem cells. Cell Stem Cell. 6, 421-432

Lau, K. W., Tian, Y. M., Raval, R. R., Ratcliffe, P. J. and Pugh, C. W. (2007) Target gene selectivity of hypoxia-inducible factor-alpha in renal cancer cells is conveyed by post-DNA-binding mechanisms. Br J Cancer. 96, 1284-1292

Le, A., Lane, A. N., Hamaker, M., Bose, S., Gouw, A., Barbi, J., Tsukamoto, T., Rojas, C. J., Slusher, B. S., Zhang, H., Zimmerman, L. J., Liebler, D. C., Slebos, R. J., Lorkiewicz, P. K., Higashi, R. M., Fan, T. W. and Dang, C. V. (2012) Glucose-independent glutamine metabolism via TCA cycling for proliferation and survival in B cells. Cell Metab. 15, 110-121

Lee, C. H., Hong, H. M., Chang, Y. Y. and Chang, W. W. (2012) Inhibition of heat shock protein (Hsp) 27 potentiates the suppressive effect of Hsp90 inhibitors in targeting breast cancer stem-like cells. Biochimie. 94, 1382-1389

Lee, J. M., Dedhar, S., Kalluri, R. and Thompson, E. W. (2006) The epithelial-mesenchymal transition: new insights in signaling, development, and disease. J Cell Biol. 172, 973-981

Lee, S. H., Jo, S. H., Lee, S. M., Koh, H. J., Song, H., Park, J. W., Lee, W. H. and Huh, T. L. (2004) Role of NADP+-dependent isocitrate dehydrogenase (NADP+-ICDH) on cellular defence against oxidative injury by gamma-rays. Int J Radiat Biol. 80, 635-642

Lee, S. M., Koh, H. J., Park, D. C., Song, B. J., Huh, T. L. and Park, J. W. (2002) Cytosolic NADP(+)-dependent isocitrate dehydrogenase status modulates oxidative damage to cells. Free Radic Biol Med. 32, 1185-1196

Leenders, W. P., Kusters, B. and de Waal, R. M. (2002) Vessel co-option: how tumors obtain blood supply in the absence of sprouting angiogenesis. Endothelium. 9, 83-87

Lewis-Tuffin, L. J., Rodriguez, F., Giannini, C., Scheithauer, B., Necela, B. M., Sarkaria, J. N. and Anastasiadis, P. Z. (2010) Misregulated E-cadherin expression associated with an aggressive brain tumor phenotype. PLoS One. 5, e13665

Li, H., Ko, H. P. and Whitlock, J. P. (1996) Induction of phosphoglycerate kinase 1 gene expression by hypoxia. Roles of Arnt and HIF1alpha. J Biol Chem. 271, 21262-21267

Li, Z., Bao, S., Wu, Q., Wang, H., Eyler, C., Sathornsumetee, S., Shi, Q., Cao, Y., Lathia, J., McLendon, R. E., Hjelmeland, A. B. and Rich, J. N. (2009) Hypoxia-inducible factors regulate tumorigenic capacity of glioma stem cells. Cancer Cell. 15, 501-513

Liao, Y., Lu, W., Che, Q., Yang, T., Qiu, H., Zhang, H., He, X., Wang, J., Qiu, M., Zou, Y., Gu, W. and Wan, X. (2014) SHARP1 suppresses angiogenesis of endometrial cancer by decreasing hypoxia-inducible factor-1alpha level. PLoS One. 9, e99907

Lieb, M. E., Menzies, K., Moschella, M. C., Ni, R. and Taubman, M. B. (2002) Mammalian EGLN genes have distinct patterns of mRNA expression and regulation. Biochem Cell Biol. 80, 421-426

Lin, A. P., Abbas, S., Kim, S. W., Ortega, M., Bouamar, H., Escobedo, Y., Varadarajan, P., Qin, Y., Sudderth, J., Schulz, E., Deutsch, A., Mohan, S., Ulz, P., Neumeister, P., Rakheja, D., Gao, X., Hinck, A., Weintraub, S. T., DeBerardinis, R. J., Sill, H., Dahia, P. L. and Aguiar, R. C. (2015) D2HGDH regulates alpha-ketoglutarate levels and dioxygenase function by modulating IDH2. Nat Commun. 6, 7768

Liu, C., Tu, Y., Sun, X., Jiang, J., Jin, X., Bo, X., Li, Z., Bian, A., Wang, X., Liu, D., Wang, Z. and Ding, L. (2011) Wnt/beta-Catenin pathway in human glioma: expression pattern and clinical/prognostic correlations. Clin Exp Med. 11, 105-112

Liu, G., Yuan, X., Zeng, Z., Tunici, P., Ng, H., Abdulkadir, I. R., Lu, L., Irvin, D., Black, K. L. and Yu, J. S. (2006) Analysis of gene expression and chemoresistance of CD133+ cancer stem cells in glioblastoma. Mol Cancer. 5, 67

Liu, P. S., Wang, H., Li, X., Chao, T., Teav, T., Christen, S., Di Conza, G., Cheng, W. C., Chou, C. H., Vavakova, M., Muret, C., Debackere, K., Mazzone, M., Huang, H. D., Fendt, S. M., Ivanisevic, J. and Ho, P. C. (2017) alpha-ketoglutarate orchestrates macrophage activation through metabolic and epigenetic reprogramming. Nat Immunol. 18, 985-994

Liu, Y. V., Baek, J. H., Zhang, H., Diez, R., Cole, R. N. and Semenza, G. L. (2007) RACK1 competes with HSP90 for binding to HIF-1alpha and is required for O(2)-independent and HSP90 inhibitor-induced degradation of HIF-1alpha. Mol Cell. 25, 207-217

Lodola, A., Giorgio, C., Incerti, M., Zanotti, I. and Tognolini, M. (2017) Targeting Eph/ephrin system in cancer therapy. Eur J Med Chem

Loenarz, C. and Schofield, C. J. (2011) Physiological and biochemical aspects of hydroxylations and demethylations catalyzed by human 2-oxoglutarate oxygenases. Trends Biochem Sci. 36, 7-18

Lofstedt, T., Fredlund, E., Holmquist-Mengelbier, L., Pietras, A., Ovenberger, M., Poellinger, L. and Pahlman, S. (2007) Hypoxia inducible factor-2alpha in cancer. Cell Cycle. 6, 919-926

Lorger, M. (2012) Tumor microenvironment in the brain. Cancers (Basel). 4, 218-243

Loriot, C., Burnichon, N., Gadessaud, N., Vescovo, L., Amar, L., Libe, R., Bertherat, J., Plouin, P. F., Jeunemaitre, X., Gimenez-Roqueplo, A. P. and Favier, J. (2012) Epithelial to mesenchymal transition is activated in metastatic pheochromocytomas and paragangliomas caused by SDHB gene mutations. J Clin Endocrinol Metab. 97, E954-962

Losman, J. A. and Kaelin, W. G., Jr. (2013) What a difference a hydroxyl makes: mutant IDH, (R)-2-hydroxyglutarate, and cancer. Genes Dev. 27, 836-852

Losman, J. A., Looper, R. E., Koivunen, P., Lee, S., Schneider, R. K., McMahon, C., Cowley, G. S., Root, D. E., Ebert, B. L. and Kaelin, W. G., Jr. (2013) (R)-2-hydroxyglutarate is sufficient to promote leukemogenesis and its effects are reversible. Science. 339, 1621-1625

Louis, D. N., Ohgaki, H., Wiestler, O. D., Cavenee, W. K., Burger, P. C., Jouvet, A., Scheithauer, B. W. and Kleihues, P. (2007) The 2007 WHO classification of tumours of the central nervous system. Acta Neuropathol. 114, 97-109

Louis, D. N., Perry, A., Reifenberger, G., von Deimling, A., Figarella-Branger, D., Cavenee, W. K., Ohgaki, H., Wiestler, O. D., Kleihues, P. and Ellison, D. W. (2016) The 2016 World Health Organization Classification of Tumors of the Central Nervous System: a summary. Acta Neuropathol. 131, 803-820

Lowry, O. H., Rosebrough, N. J., Farr, A. L. and Randall, R. J. (1951) Protein measurement with the Folin phenol reagent. J Biol Chem. 193, 265-275

Lu, C., Ward, P. S., Kapoor, G. S., Rohle, D., Turcan, S., Abdel-Wahab, O., Edwards, C. R., Khanin, R., Figueroa, M. E., Melnick, A., Wellen, K. E., O'Rourke, D. M., Berger, S. L., Chan, T. A., Levine, R. L., Mellinghoff, I. K. and Thompson, C. B. (2012) IDH mutation impairs histone demethylation and results in a block to cell differentiation. Nature. 483, 474-478

Mabjeesh, N. J., Post, D. E., Willard, M. T., Kaur, B., Van Meir, E. G., Simons, J. W. and Zhong, H. (2002) Geldanamycin induces degradation of hypoxia-inducible factor 1alpha protein via the proteosome pathway in prostate cancer cells. Cancer Res. 62, 2478-2482

MacKenzie, E. D., Selak, M. A., Tennant, D. A., Payne, L. J., Crosby, S., Frederiksen, C. M., Watson, D. G. and Gottlieb, E. (2007) Cell-permeating alpha-ketoglutarate derivatives alleviate pseudohypoxia in succinate dehydrogenase-deficient cells. Mol Cell Biol. 27, 3282-3289

Mahabir, R., Tanino, M., Elmansuri, A., Wang, L., Kimura, T., Itoh, T., Ohba, Y., Nishihara, H., Shirato, H., Tsuda, M. and Tanaka, S. (2014) Sustained elevation of Snail promotes glial-mesenchymal transition after irradiation in malignant glioma. Neuro Oncol. 16, 671-685

Mahase, S., Rattenni, R. N., Wesseling, P., Leenders, W., Baldotto, C., Jain, R. and Zagzag, D. (2017) Hypoxia-Mediated Mechanisms Associated with Antiangiogenic Treatment Resistance in Glioblastomas. Am J Pathol. 187, 940-953

Mani, S. A., Guo, W., Liao, M. J., Eaton, E. N., Ayyanan, A., Zhou, A. Y., Brooks, M., Reinhard, F., Zhang, C. C., Shipitsin, M., Campbell, L. L., Polyak, K., Brisken, C., Yang, J. and Weinberg, R. A. (2008) The epithelial-mesenchymal transition generates cells with properties of stem cells. Cell. 133, 704-715

Mardis, E. R., Ding, L., Dooling, D. J., Larson, D. E., McLellan, M. D., Chen, K., Koboldt, D. C., Fulton, R. S., Delehaunty, K. D., McGrath, S. D., Fulton, L. A., Locke, D. P., Magrini, V. J., Abbott, R. M., Vickery, T. L., Reed, J. S., Robinson, J. S., Wylie, T., Smith, S. M., Carmichael, L., Eldred, J. M., Harris, C. C., Walker, J., Peck, J. B., Du, F., Dukes, A. F., Sanderson, G. E., Brummett, A. M., Clark, E., McMichael, J. F., Meyer, R. J., Schindler, J. K., Pohl, C. S., Wallis, J. W., Shi, X., Lin, L., Schmidt, H., Tang, Y., Haipek, C., Wiechert, M. E., Ivy, J. V., Kalicki, J., Elliott, G., Ries, R. E., Payton, J. E., Westervelt, P., Tomasson, M. H., Watson, M. A., Baty, J., Heath, S., Shannon, W. D., Nagarajan, R., Link, D. C., Walter, M. J., Graubert, T. A., DiPersio, J. F., Wilson, R. K. and Ley, T. J. (2009) Recurring mutations found by sequencing an acute myeloid leukemia genome. N Engl J Med. 361, 1058-1066

Markolovic, S., Wilkins, S. E. and Schofield, C. J. (2015) Protein Hydroxylation Catalyzed by 2-Oxoglutarate-dependent Oxygenases. J Biol Chem. 290, 20712-20722

Masoud, G. N. and Li, W. (2015) HIF-1alpha pathway: role, regulation and intervention for cancer therapy. Acta Pharm Sin B. 5, 378-389

Matsumoto, K., Imagawa, S., Obara, N., Suzuki, N., Takahashi, S., Nagasawa, T. and Yamamoto, M. (2006) 2-Oxoglutarate downregulates expression of vascular endothelial growth factor and erythropoietin through decreasing hypoxia-inducible factor-1alpha and inhibits angiogenesis. J Cell Physiol. 209, 333-340

Matsumoto, K., Obara, N., Ema, M., Horie, M., Naka, A., Takahashi, S. and Imagawa, S. (2009) Antitumor effects of 2-oxoglutarate through inhibition of angiogenesis in a murine tumor model. Cancer Sci. 100, 1639-1647

Maxwell, P. H., Wiesener, M. S., Chang, G. W., Clifford, S. C., Vaux, E. C., Cockman, M. E., Wykoff, C. C., Pugh, C. W., Maher, E. R. and Ratcliffe, P. J. (1999) The tumour suppressor protein VHL targets hypoxia-inducible factors for oxygen-dependent proteolysis. Nature. 399, 271-275

McDonough, M. A., Loenarz, C., Chowdhury, R., Clifton, I. J. and Schofield, C. J. (2010) Structural studies on human 2-oxoglutarate dependent oxygenases. Curr Opin Struct Biol. 20, 659-672

McMahon, S., Charbonneau, M., Grandmont, S., Richard, D. E. and Dubois, C. M. (2006) Transforming growth factor beta1 induces hypoxia-inducible factor-1 stabilization through selective inhibition of PHD2 expression. J Biol Chem. 281, 24171-24181

McNeill, L. A., Hewitson, K. S., Claridge, T. D., Seibel, J. F., Horsfall, L. E. and Schofield, C. J. (2002) Hypoxia-inducible factor asparaginyl hydroxylase (FIH-1) catalyses hydroxylation at the beta-carbon of asparagine-803. Biochem J. 367, 571-575

Mekhail, K., Gunaratnam, L., Bonicalzi, M. E. and Lee, S. (2004) HIF activation by pH-dependent nucleolar sequestration of VHL. Nat Cell Biol. 6, 642-647

Mellai, M., Caldera, V., Annovazzi, L. and Schiffer, D. (2013) The Distribution and Significance of IDH Mutations in Gliomas. In Evolution of the Molecular Biology of Brain Tumors and the Therapeutic Implications (Lichtor, T., ed.). p. Ch. 10, InTech, Rijeka

Metallo, C. M., Gameiro, P. A., Bell, E. L., Mattaini, K. R., Yang, J., Hiller, K., Jewell, C. M., Johnson, Z. R., Irvine, D. J., Guarente, L., Kelleher, J. K., Vander Heiden, M. G., Iliopoulos, O. and Stephanopoulos, G. (2011) Reductive glutamine metabolism by IDH1 mediates lipogenesis under hypoxia. Nature. 481, 380-384

Metellus, P., Colin, C., Taieb, D., Guedj, E., Nanni-Metellus, I., de Paula, A. M., Colavolpe, C., Fuentes, S., Dufour, H., Barrie, M., Chinot, O., Ouafik, L. and Figarella-Branger, D. (2011) IDH mutation status impact on in vivo hypoxia biomarkers expression: new insights from a clinical, nuclear imaging and immunohistochemical study in 33 glioma patients. J Neurooncol. 105, 591-600

Metzen, E., Berchner-Pfannschmidt, U., Stengel, P., Marxsen, J. H., Stolze, I., Klinger, M., Huang, W. Q., Wotzlaw, C., Hellwig-Burgel, T., Jelkmann, W., Acker, H. and Fandrey,

J. (2003) Intracellular localisation of human HIF-1 alpha hydroxylases: implications for oxygen sensing. J Cell Sci. 116, 1319-1326

Miao, R. Q., Fontana, J., Fulton, D., Lin, M. I., Harrison, K. D. and Sessa, W. C. (2008) Dominant-negative Hsp90 reduces VEGF-stimulated nitric oxide release and migration in endothelial cells. Arterioscler Thromb Vasc Biol. 28, 105-111

Mikhaylova, O., Ignacak, M. L., Barankiewicz, T. J., Harbaugh, S. V., Yi, Y., Maxwell, P. H., Schneider, M., Van Geyte, K., Carmeliet, P., Revelo, M. P., Wyder, M., Greis, K. D., Meller, J. and Czyzyk-Krzeska, M. F. (2008) The von Hippel-Lindau tumor suppressor protein and Egl-9-Type proline hydroxylases regulate the large subunit of RNA polymerase II in response to oxidative stress. Mol Cell Biol. 28, 2701-2717

Mikheeva, S. A., Mikheev, A. M., Petit, A., Beyer, R., Oxford, R. G., Khorasani, L., Maxwell, J. P., Glackin, C. A., Wakimoto, H., Gonzalez-Herrero, I., Sanchez-Garcia, I., Silber, J. R., Horner, P. J. and Rostomily, R. C. (2010) TWIST1 promotes invasion through mesenchymal change in human glioblastoma. Mol Cancer. 9, 194

Min, C., Eddy, S. F., Sherr, D. H. and Sonenshein, G. E. (2008) NF-kappaB and epithelial to mesenchymal transition of cancer. J Cell Biochem. 104, 733-744

Minet, E., Arnould, T., Michel, G., Roland, I., Mottet, D., Raes, M., Remacle, J. and Michiels, C. (2000) ERK activation upon hypoxia: involvement in HIF-1 activation. FEBS Lett. 468, 53-58

Miroshnikova, Y. A., Mouw, J. K., Barnes, J. M., Pickup, M. W., Lakins, J. N., Kim, Y., Lobo, K., Persson, A. I., Reis, G. F., McKnight, T. R., Holland, E. C., Phillips, J. J. and Weaver, V. M. (2016) Tissue mechanics promote IDH1-dependent HIF1alpha-tenascin C feedback to regulate glioblastoma aggression. Nat Cell Biol. 18, 1336-1345

Modrek, A. S., Bayin, N. S. and Placantonakis, D. G. (2014) Brain stem cells as the cell of origin in glioma. World J Stem Cells. 6, 43-52

Monne, M., Miniero, D. V., Iacobazzi, V., Bisaccia, F. and Fiermonte, G. (2013) The mitochondrial oxoglutarate carrier: from identification to mechanism. J Bioenerg Biomembr. 45, 1-13

Montagner, M., Enzo, E., Forcato, M., Zanconato, F., Parenti, A., Rampazzo, E., Basso, G., Leo, G., Rosato, A., Bicciato, S., Cordenonsi, M. and Piccolo, S. (2012) SHARP1 suppresses breast cancer metastasis by promoting degradation of hypoxia-inducible factors. Nature. 487, 380-384

Moore, C. E., Mikolajek, H., Regufe da Mota, S., Wang, X., Kenney, J. W., Werner, J. M. and Proud, C. G. (2015) Elongation Factor 2 Kinase Is Regulated by Proline Hydroxylation and Protects Cells during Hypoxia. Mol Cell Biol. 35, 1788-1804

Moschetta, M., Mishima, Y., Sahin, I., Manier, S., Glavey, S., Vacca, A., Roccaro, A. M. and Ghobrial, I. M. (2014) Role of endothelial progenitor cells in cancer progression. Biochim Biophys Acta. 1846, 26-39

Mottet, D., Dumont, V., Deccache, Y., Demazy, C., Ninane, N., Raes, M. and Michiels, C. (2003) Regulation of hypoxia-inducible factor-1alpha protein level during hypoxic conditions by the phosphatidylinositol 3-kinase/Akt/glycogen synthase kinase 3beta pathway in HepG2 cells. J Biol Chem. 278, 31277-31285

Moustakas, A. and Heldin, C. H. (2016) Mechanisms of TGFbeta-Induced Epithelial-Mesenchymal Transition. J Clin Med. 5,

Mullen, A. R., Hu, Z., Shi, X., Jiang, L., Boroughs, L. K., Kovacs, Z., Boriack, R., Rakheja, D., Sullivan, L. B., Linehan, W. M., Chandel, N. S. and DeBerardinis, R. J. (2014) Oxidation of alpha-ketoglutarate is required for reductive carboxylation in cancer cells with mitochondrial defects. Cell Rep. 7, 1679-1690

Mullen, A. R., Wheaton, W. W., Jin, E. S., Chen, P. H., Sullivan, L. B., Cheng, T., Yang, Y., Linehan, W. M., Chandel, N. S. and DeBerardinis, R. J. (2011) Reductive carboxylation supports growth in tumour cells with defective mitochondria. Nature. 481, 385-388

Murray-Rust, T. A., Oldham, N. J., Hewitson, K. S. and Schofield, C. J. (2006) Purified recombinant hARD1 does not catalyse acetylation of Lys532 of HIF-1alpha fragments in vitro. FEBS Lett. 580, 1911-1918

Muz, B., de la Puente, P., Azab, F. and Azab, A. K. (2015) The role of hypoxia in cancer progression, angiogenesis, metastasis, and resistance to therapy. Hypoxia (Auckl). 3, 83-92

Myers, A. L., Williams, R. F., Ng, C. Y., Hartwich, J. E. and Davidoff, A. M. (2010) Bevacizumab-induced tumor vessel remodeling in rhabdomyosarcoma xenografts increases the effectiveness of adjuvant ionizing radiation. J Pediatr Surg. 45, 1080-1085

Myllyla, R., Majamaa, K., Gunzler, V., Hanauske-Abel, H. M. and Kivirikko, K. I. (1984) Ascorbate is consumed stoichiometrically in the uncoupled reactions catalyzed by prolyl 4-hydroxylase and lysyl hydroxylase. J Biol Chem. 259, 5403-5405

Myung, J. K., Choi, S. A., Kim, S. K., Wang, K. C. and Park, S. H. (2014) Snail plays an oncogenic role in glioblastoma by promoting epithelial mesenchymal transition. Int J Clin Exp Pathol. 7, 1977-1987

Nagaishi, M., Paulus, W., Brokinkel, B., Vital, A., Tanaka, Y., Nakazato, Y., Giangaspero, F. and Ohgaki, H. (2012) Transcriptional factors for epithelial-mesenchymal transition are associated with mesenchymal differentiation in gliosarcoma. Brain Pathol. 22, 670-676

Nakada, M., Niska, J. A., Miyamori, H., McDonough, W. S., Wu, J., Sato, H. and Berens, M. E. (2004) The phosphorylation of EphB2 receptor regulates migration and invasion of human glioma cells. Cancer Res. 64, 3179-3185

Neri, D. and Supuran, C. T. (2011) Interfering with pH regulation in tumours as a therapeutic strategy. Nat Rev Drug Discov. 10, 767-777

Newman, B., Liu, Y., Lee, H. F., Sun, D. and Wang, Y. (2012) HSP90 inhibitor 17-AAG selectively eradicates lymphoma stem cells. Cancer Res. 72, 4551-4561

Nguyen, T. L. and Duran, R. V. (2016) Prolyl hydroxylase domain enzymes and their role in cell signaling and cancer metabolism. Int J Biochem Cell Biol. 80, 71-80

Nicolaidis, S. (2015) Biomarkers of glioblastoma multiforme. Metabolism. 64, S22-27

Noren, N. K., Foos, G., Hauser, C. A. and Pasquale, E. B. (2006) The EphB4 receptor suppresses breast cancer cell tumorigenicity through an Abl-Crk pathway. Nat Cell Biol. 8, 815-825

Noren, N. K., Lu, M., Freeman, A. L., Koolpe, M. and Pasquale, E. B. (2004) Interplay between EphB4 on tumor cells and vascular ephrin-B2 regulates tumor growth. Proc Natl Acad Sci U S A. 101, 5583-5588

Noushmehr, H., Weisenberger, D. J., Diefes, K., Phillips, H. S., Pujara, K., Berman, B. P., Pan, F., Pelloski, C. E., Sulman, E. P., Bhat, K. P., Verhaak, R. G., Hoadley, K. A., Hayes, D. N., Perou, C. M., Schmidt, H. K., Ding, L., Wilson, R. K., Van Den Berg, D., Shen, H., Bengtsson, H., Neuvial, P., Cope, L. M., Buckley, J., Herman, J. G., Baylin, S. B., Laird, P. W., Aldape, K. and Cancer Genome Atlas Research, N. (2010) Identification of a CpG island methylator phenotype that defines a distinct subgroup of glioma. Cancer Cell. 17, 510-522

Nowell, P. C. (1976) The clonal evolution of tumor cell populations. Science. 194, 23-28

Ogden, A. T., Waziri, A. E., Lochhead, R. A., Fusco, D., Lopez, K., Ellis, J. A., Kang, J., Assanah, M., McKhann, G. M., Sisti, M. B., McCormick, P. C., Canoll, P. and Bruce, J. N. (2008) Identification of A2B5+CD133- tumor-initiating cells in adult human gliomas. Neurosurgery. 62, 505-514; discussion 514-505

Ohgaki, H. and Kleihues, P. (2013) The definition of primary and secondary glioblastoma. Clin Cancer Res. 19, 764-772

Oliver, K. M., Taylor, C. T. and Cummins, E. P. (2009) Hypoxia. Regulation of NFkappaB signalling during inflammation: the role of hydroxylases. Arthritis Res Ther. 11, 215

Ostrom, Q. T., Gittleman, H., Fulop, J., Liu, M., Blanda, R., Kromer, C., Wolinsky, Y., Kruchko, C. and Barnholtz-Sloan, J. S. (2015) CBTRUS Statistical Report: Primary Brain and Central Nervous System Tumors Diagnosed in the United States in 2008-2012. Neuro Oncol. 17 Suppl 4, iv1-iv62

Owen, O. E., Kalhan, S. C. and Hanson, R. W. (2002) The key role of anaplerosis and cataplerosis for citric acid cycle function. J Biol Chem. 277, 30409-30412

Palmer, A., Zimmer, M., Erdmann, K. S., Eulenburg, V., Porthin, A., Heumann, R., Deutsch, U. and Klein, R. (2002) EphrinB phosphorylation and reverse signaling: regulation by Src kinases and PTP-BL phosphatase. Mol Cell. 9, 725-737

Pan, M., Reid, M. A., Lowman, X. H., Kulkarni, R. P., Tran, T. Q., Liu, X., Yang, Y., Hernandez-Davies, J. E., Rosales, K. K., Li, H., Hugo, W., Song, C., Xu, X., Schones, D. E., Ann, D. K., Gradinaru, V., Lo, R. S., Locasale, J. W. and Kong, M. (2016) Regional glutamine deficiency in tumours promotes dedifferentiation through inhibition of histone demethylation. Nat Cell Biol. 18, 1090-1101

Pansuriya, T. C., van Eijk, R., d'Adamo, P., van Ruler, M. A., Kuijjer, M. L., Oosting, J., Cleton-Jansen, A. M., van Oosterwijk, J. G., Verbeke, S. L., Meijer, D., van Wezel, T., Nord, K. H., Sangiorgi, L., Toker, B., Liegl-Atzwanger, B., San-Julian, M., Sciot, R., Limaye, N., Kindblom, L. G., Daugaard, S., Godfraind, C., Boon, L. M., Vikkula, M., Kurek, K. C., Szuhai, K., French, P. J. and Bovee, J. V. (2011) Somatic mosaic IDH1 and IDH2 mutations are associated with enchondroma and spindle cell hemangioma in Ollier disease and Maffucci syndrome. Nat Genet. 43, 1256-1261

Parks, S. K., Mazure, N. M., Counillon, L. and Pouyssegur, J. (2013) Hypoxia promotes tumor cell survival in acidic conditions by preserving ATP levels. J Cell Physiol. 228, 1854-1862

Parsons, D. W., Jones, S., Zhang, X., Lin, J. C., Leary, R. J., Angenendt, P., Mankoo, P., Carter, H., Siu, I. M., Gallia, G. L., Olivi, A., McLendon, R., Rasheed, B. A., Keir, S., Nikolskaya, T., Nikolsky, Y., Busam, D. A., Tekleab, H., Diaz, L. A., Jr., Hartigan, J., Smith, D. R., Strausberg, R. L., Marie, S. K., Shinjo, S. M., Yan, H., Riggins, G. J., Bigner, D. D., Karchin, R., Papadopoulos, N., Parmigiani, G., Vogelstein, B., Velculescu, V. E. and Kinzler, K. W. (2008) An integrated genomic analysis of human glioblastoma multiforme. Science. 321, 1807-1812

Pasquale, E. B. (2008) Eph-ephrin bidirectional signaling in physiology and disease. Cell. 133, 38-52

Pasquale, E. B. (2010) Eph receptors and ephrins in cancer: bidirectional signalling and beyond. Nat Rev Cancer. 10, 165-180

Patel, A. and Sant, S. (2016) Hypoxic tumor microenvironment: Opportunities to develop targeted therapies. Biotechnol Adv. 34, 803-812

Paul, I., Bhattacharya, S., Chatterjee, A. and Ghosh, M. K. (2013) Current Understanding on EGFR and Wnt/beta-Catenin Signaling in Glioma and Their Possible Crosstalk. Genes Cancer. 4, 427-446

Pavlova, N. N. and Thompson, C. B. (2016) The Emerging Hallmarks of Cancer Metabolism. Cell Metab. 23, 27-47

Pennacchietti, S., Michieli, P., Galluzzo, M., Mazzone, M., Giordano, S. and Comoglio, P. M. (2003) Hypoxia promotes invasive growth by transcriptional activation of the met protooncogene. Cancer Cell. 3, 347-361

Perkins, N. D. (2012) The diverse and complex roles of NF-kappaB subunits in cancer. Nat Rev Cancer. 12, 121-132

Petrella, B. L., Lohi, J. and Brinckerhoff, C. E. (2005) Identification of membrane type-1 matrix metalloproteinase as a target of hypoxia-inducible factor-2 alpha in von Hippel-Lindau renal cell carcinoma. Oncogene. 24, 1043-1052

Phan, L. M., Yeung, S. C. and Lee, M. H. (2014) Cancer metabolic reprogramming: importance, main features, and potentials for precise targeted anti-cancer therapies. Cancer Biol Med. 11, 1-19

Phillips, H. S., Kharbanda, S., Chen, R., Forrest, W. F., Soriano, R. H., Wu, T. D., Misra, A., Nigro, J. M., Colman, H., Soroceanu, L., Williams, P. M., Modrusan, Z., Feuerstein, B. G. and Aldape, K. (2006) Molecular subclasses of high-grade glioma predict prognosis, delineate a pattern of disease progression, and resemble stages in neurogenesis. Cancer Cell. 9, 157-173

Piccolo, S., Enzo, E. and Montagner, M. (2013) p63, Sharp1, and HIFs: master regulators of metastasis in triple-negative breast cancer. Cancer Res. 73, 4978-4981

Pietras, A., Katz, A. M., Ekstrom, E. J., Wee, B., Halliday, J. J., Pitter, K. L., Werbeck, J. L., Amankulor, N. M., Huse, J. T. and Holland, E. C. (2014) Osteopontin-CD44 signaling in the glioma perivascular niche enhances cancer stem cell phenotypes and promotes aggressive tumor growth. Cell Stem Cell. 14, 357-369

Pitulescu, M. E. and Adams, R. H. (2010) Eph/ephrin molecules--a hub for signaling and endocytosis. Genes Dev. 24, 2480-2492

Plaks, V., Kong, N. and Werb, Z. (2015) The cancer stem cell niche: how essential is the niche in regulating stemness of tumor cells? Cell Stem Cell. 16, 225-238

Plaut, G. W., Cook, M. and Aogaichi, T. (1983) The subcellular location of isozymes of NADP-isocitrate dehydrogenase in tissues from pig, ox and rat. Biochim Biophys Acta. 760, 300-308

Postigo, A. A., Depp, J. L., Taylor, J. J. and Kroll, K. L. (2003) Regulation of Smad signaling through a differential recruitment of coactivators and corepressors by ZEB proteins. EMBO J. 22, 2453-2462

Pugh, C. W. and Ratcliffe, P. J. (2003) Regulation of angiogenesis by hypoxia: role of the HIF system. Nat Med. 9, 677-684

Qi, S., Song, Y., Peng, Y., Wang, H., Long, H., Yu, X., Li, Z., Fang, L., Wu, A., Luo, W., Zhen, Y., Zhou, Y., Chen, Y., Mai, C., Liu, Z. and Fang, W. (2012) ZEB2 mediates multiple pathways regulating cell proliferation, migration, invasion, and apoptosis in glioma. PLoS One. 7, e38842

Raffel, S., Falcone, M., Kneisel, N., Hansson, J., Wang, W., Lutz, C., Bullinger, L., Poschet, G., Nonnenmacher, Y., Barnert, A., Bahr, C., Zeisberger, P., Przybylla, A., Sohn, M., Tonjes, M., Erez, A., Adler, L., Jensen, P., Scholl, C., Frohling, S., Cocciardi, S., Wuchter, P., Thiede, C., Florcken, A., Westermann, J., Ehninger, G., Lichter, P., Hiller, K., Hell, R., Herrmann, C., Ho, A. D., Krijgsveld, J., Radlwimmer, B. and Trumpp, A. (2017) BCAT1 restricts alphaKG levels in AML stem cells leading to IDHmut-like DNA hypermethylation. Nature. 551, 384-388

Rahman, R., Catalano, P. J., Reardon, D. A., Norden, A. D., Wen, P. Y., Lee, E. Q., Nayak, L., Beroukhim, R., Dunn, I. F., Golby, A. J., Johnson, M. D., Chiocca, E. A., Claus, E. B., Alexander, B. M. and Arvold, N. D. (2015) Incidence, risk factors, and reasons for hospitalization among glioblastoma patients receiving chemoradiation. J Neurooncol. 124, 137-146

Ran, F. A., Hsu, P. D., Wright, J., Agarwala, V., Scott, D. A. and Zhang, F. (2013) Genome engineering using the CRISPR-Cas9 system. Nat Protoc. 8, 2281-2308

Rao, J. S. (2003) Molecular mechanisms of glioma invasiveness: the role of proteases. Nat Rev Cancer. 3, 489-501

Ravi, R., Mookerjee, B., Bhujwalla, Z. M., Sutter, C. H., Artemov, D., Zeng, Q., Dillehay, L. E., Madan, A., Semenza, G. L. and Bedi, A. (2000) Regulation of tumor angiogenesis by p53-induced degradation of hypoxia-inducible factor 1alpha. Genes Dev. 14, 34-44

Rayet, B. and Gelinas, C. (1999) Aberrant rel/nfkb genes and activity in human cancer. Oncogene. 18, 6938-6947

Reya, T., Morrison, S. J., Clarke, M. F. and Weissman, I. L. (2001) Stem cells, cancer, and cancer stem cells. Nature. 414, 105-111

Ribatti, D. and Djonov, V. (2012) Intussusceptive microvascular growth in tumors. Cancer Lett. 316, 126-131

Ricci-Vitiani, L., Lombardi, D. G., Pilozzi, E., Biffoni, M., Todaro, M., Peschle, C. and De Maria, R. (2007) Identification and expansion of human colon-cancer-initiating cells. Nature. 445, 111-115

Ricci-Vitiani, L., Pallini, R., Biffoni, M., Todaro, M., Invernici, G., Cenci, T., Maira, G., Parati, E. A., Stassi, G., Larocca, L. M. and De Maria, R. (2010) Tumour vascularization via endothelial differentiation of glioblastoma stem-like cells. Nature. 468, 824-828

Richard, D. E., Berra, E., Gothie, E., Roux, D. and Pouyssegur, J. (1999) p42/p44 mitogen-activated protein kinases phosphorylate hypoxia-inducible factor 1alpha (HIF-1alpha) and enhance the transcriptional activity of HIF-1. J Biol Chem. 274, 32631-32637

Ritchie, M. E., Phipson, B., Wu, D., Hu, Y., Law, C. W., Shi, W. and Smyth, G. K. (2015) limma powers differential expression analyses for RNA-sequencing and microarray studies. Nucleic Acids Res. 43, e47

Robbins, D., Wittwer, J. A., Codarin, S., Circu, M. L., Aw, T. Y., Huang, T. T., Van Remmen, H., Richardson, A., Wang, D. B., Witt, S. N., Klein, R. L. and Zhao, Y. (2012) Isocitrate dehydrogenase 1 is downregulated during early skin tumorigenesis which can be inhibited by overexpression of manganese superoxide dismutase. Cancer Sci. 103, 1429-1433

Roe, J. S. and Youn, H. D. (2006) The positive regulation of p53 by the tumor suppressor VHL. Cell Cycle. 5, 2054-2056

Rohle, D., Popovici-Muller, J., Palaskas, N., Turcan, S., Grommes, C., Campos, C., Tsoi, J., Clark, O., Oldrini, B., Komisopoulou, E., Kunii, K., Pedraza, A., Schalm, S., Silverman, L., Miller, A., Wang, F., Yang, H., Chen, Y., Kernytsky, A., Rosenblum, M. K., Liu, W., Biller, S. A., Su, S. M., Brennan, C. W., Chan, T. A., Graeber, T. G., Yen, K. E. and Mellinghoff, I. K. (2013) An inhibitor of mutant IDH1 delays growth and promotes differentiation of glioma cells. Science. 340, 626-630

Ronca, R., Benkheil, M., Mitola, S., Struyf, S. and Liekens, S. (2017) Tumor angiogenesis revisited: Regulators and clinical implications. Med Res Rev

Rose, N. R., McDonough, M. A., King, O. N., Kawamura, A. and Schofield, C. J. (2011) Inhibition of 2-oxoglutarate dependent oxygenases. Chem Soc Rev. 40, 4364-4397

Rzeski, W., Walczak, K., Juszczak, M., Langner, E., Pozarowski, P., Kandefer-Szerszen, M. and Pierzynowski, S. G. (2012) Alpha-ketoglutarate (AKG) inhibits proliferation of colon adenocarcinoma cells in normoxic conditions. Scand J Gastroenterol. 47, 565-571

Salminen, A., Kaarniranta, K., Hiltunen, M. and Kauppinen, A. (2014) Krebs cycle dysfunction shapes epigenetic landscape of chromatin: novel insights into mitochondrial regulation of aging process. Cell Signal. 26, 1598-1603

Sanchez-Tillo, E., Siles, L., de Barrios, O., Cuatrecasas, M., Vaquero, E. C., Castells, A. and Postigo, A. (2011) Expanding roles of ZEB factors in tumorigenesis and tumor progression. Am J Cancer Res. 1, 897-912

Sanson, M., Marie, Y., Paris, S., Idbaih, A., Laffaire, J., Ducray, F., El Hallani, S., Boisselier, B., Mokhtari, K., Hoang-Xuan, K. and Delattre, J. Y. (2009) Isocitrate dehydrogenase 1 codon 132 mutation is an important prognostic biomarker in gliomas. J Clin Oncol. 27, 4150-4154

Sasaki, M., Knobbe, C. B., Itsumi, M., Elia, A. J., Harris, I. S., Chio, II, Cairns, R. A., McCracken, S., Wakeham, A., Haight, J., Ten, A. Y., Snow, B., Ueda, T., Inoue, S., Yamamoto, K., Ko, M., Rao, A., Yen, K. E., Su, S. M. and Mak, T. W. (2012a) D-2-

hydroxyglutarate produced by mutant IDH1 perturbs collagen maturation and basement membrane function. Genes Dev. 26, 2038-2049

Sasaki, M., Knobbe, C. B., Munger, J. C., Lind, E. F., Brenner, D., Brustle, A., Harris, I. S., Holmes, R., Wakeham, A., Haight, J., You-Ten, A., Li, W. Y., Schalm, S., Su, S. M., Virtanen, C., Reifenberger, G., Ohashi, P. S., Barber, D. L., Figueroa, M. E., Melnick, A., Zuniga-Pflucker, J. C. and Mak, T. W. (2012b) IDH1(R132H) mutation increases murine haematopoietic progenitors and alters epigenetics. Nature. 488, 656-659

Sauvageot, C. M., Weatherbee, J. L., Kesari, S., Winters, S. E., Barnes, J., Dellagatta, J., Ramakrishna, N. R., Stiles, C. D., Kung, A. L., Kieran, M. W. and Wen, P. Y. (2009) Efficacy of the HSP90 inhibitor 17-AAG in human glioma cell lines and tumorigenic glioma stem cells. Neuro Oncol. 11, 109-121

Savary, K., Caglayan, D., Caja, L., Tzavlaki, K., Bin Nayeem, S., Bergstrom, T., Jiang, Y., Uhrbom, L., Forsberg-Nilsson, K., Westermark, B., Heldin, C. H., Ferletta, M. and Moustakas, A. (2013) Snail depletes the tumorigenic potential of glioblastoma. Oncogene. 32, 5409-5420

Sawamiphak, S., Seidel, S., Essmann, C. L., Wilkinson, G. A., Pitulescu, M. E., Acker, T. and Acker-Palmer, A. (2010) Ephrin-B2 regulates VEGFR2 function in developmental and tumour angiogenesis. Nature. 465, 487-491

Scheel, C. and Weinberg, R. A. (2012) Cancer stem cells and epithelial-mesenchymal transition: concepts and molecular links. Semin Cancer Biol. 22, 396-403

Schlisio, S., Kenchappa, R. S., Vredeveld, L. C., George, R. E., Stewart, R., Greulich, H., Shahriari, K., Nguyen, N. V., Pigny, P., Dahia, P. L., Pomeroy, S. L., Maris, J. M., Look, A. T., Meyerson, M., Peeper, D. S., Carter, B. D. and Kaelin, W. G., Jr. (2008) The kinesin KIF1Bbeta acts downstream from EglN3 to induce apoptosis and is a potential 1p36 tumor suppressor. Genes Dev. 22, 884-893

Schmidt, N. O., Westphal, M., Hagel, C., Ergun, S., Stavrou, D., Rosen, E. M. and Lamszus, K. (1999) Levels of vascular endothelial growth factor, hepatocyte growth factor/scatter factor and basic fibroblast growth factor in human gliomas and their relation to angiogenesis. Int J Cancer. 84, 10-18

Schneider, C. A., Rasband, W. S. and Eliceiri, K. W. (2012) NIH Image to ImageJ: 25 years of image analysis. Nat Methods. 9, 671-675

Schofield, C. J. and Ratcliffe, P. J. (2004) Oxygen sensing by HIF hydroxylases. Nat Rev Mol Cell Biol. 5, 343-354

Schofield, C. J. and Zhang, Z. (1999) Structural and mechanistic studies on 2-oxoglutarate-dependent oxygenases and related enzymes. Curr Opin Struct Biol. 9, 722-731

Sciacovelli, M. and Frezza, C. (2017) Metabolic reprogramming and epithelial-to-mesenchymal transition in cancer. FEBS J. 284, 3132-3144

Sciacovelli, M., Goncalves, E., Johnson, T. I., Zecchini, V. R., da Costa, A. S., Gaude, E., Drubbel, A. V., Theobald, S. J., Abbo, S. R., Tran, M. G., Rajeeve, V., Cardaci, S., Foster, S., Yun, H., Cutillas, P., Warren, A., Gnanapragasam, V., Gottlieb, E., Franze, K., Huntly, B., Maher, E. R., Maxwell, P. H., Saez-Rodriguez, J. and Frezza, C. (2016) Fumarate is an epigenetic modifier that elicits epithelial-to-mesenchymal transition. Nature. 537, 544-547

Scott, D. A., Richardson, A. D., Filipp, F. V., Knutzen, C. A., Chiang, G. G., Ronai, Z. A., Osterman, A. L. and Smith, J. W. (2011) Comparative metabolic flux profiling of melanoma cell lines: beyond the Warburg effect. J Biol Chem. 286, 42626-42634

Seftor, R. E., Hess, A. R., Seftor, E. A., Kirschmann, D. A., Hardy, K. M., Margaryan, N. V. and Hendrix, M. J. (2012) Tumor cell vasculogenic mimicry: from controversy to therapeutic promise. Am J Pathol. 181, 1115-1125

Seidel, S., Garvalov, B. K. and Acker, T. (2015) Isolation and culture of primary glioblastoma cells from human tumor specimens. Methods Mol Biol. 1235, 263-275

Seidel, S., Garvalov, B. K., Wirta, V., von Stechow, L., Schanzer, A., Meletis, K., Wolter, M., Sommerlad, D., Henze, A. T., Nister, M., Reifenberger, G., Lundeberg, J., Frisen, J. and Acker, T. (2010) A hypoxic niche regulates glioblastoma stem cells through hypoxia inducible factor 2 alpha. Brain. 133, 983-995

Selak, M. A., Armour, S. M., MacKenzie, E. D., Boulahbel, H., Watson, D. G., Mansfield, K. D., Pan, Y., Simon, M. C., Thompson, C. B. and Gottlieb, E. (2005) Succinate links TCA cycle dysfunction to oncogenesis by inhibiting HIF-alpha prolyl hydroxylase. Cancer Cell. 7, 77-85

Semenza, G. L. (2001) HIF-1 and mechanisms of hypoxia sensing. Curr Opin Cell Biol. 13, 167-171

Semenza, G. L. (2012) Hypoxia-inducible factors: mediators of cancer progression and targets for cancer therapy. Trends Pharmacol Sci. 33, 207-214

Semenza, G. L., Nejfelt, M. K., Chi, S. M. and Antonarakis, S. E. (1991) Hypoxia-inducible nuclear factors bind to an enhancer element located 3' to the human erythropoietin gene. Proc Natl Acad Sci U S A. 88, 5680-5684

Seoane, J. (2006) Escaping from the TGFbeta anti-proliferative control. Carcinogenesis. 27, 2148-2156

Seoane, J., Le, H. V., Shen, L., Anderson, S. A. and Massague, J. (2004) Integration of Smad and forkhead pathways in the control of neuroepithelial and glioblastoma cell proliferation. Cell. 117, 211-223

Sequist, L. V., Heist, R. S., Shaw, A. T., Fidias, P., Rosovsky, R., Temel, J. S., Lennes, I. T., Digumarthy, S., Waltman, B. A., Bast, E., Tammireddy, S., Morrissey, L., Muzikansky, A., Goldberg, S. B., Gainor, J., Channick, C. L., Wain, J. C., Gaissert, H., Donahue, D. M., Muniappan, A., Wright, C., Willers, H., Mathisen, D. J., Choi, N. C., Baselga, J., Lynch, T. J., Ellisen, L. W., Mino-Kenudson, M., Lanuti, M., Borger, D. R., Iafrate, A. J., Engelman, J. A. and Dias-Santagata, D. (2011) Implementing multiplexed genotyping of non-small-cell lung cancers into routine clinical practice. Ann Oncol. 22, 2616-2624

Shaul, Y. D., Freinkman, E., Comb, W. C., Cantor, J. R., Tam, W. L., Thiru, P., Kim, D., Kanarek, N., Pacold, M. E., Chen, W. W., Bierie, B., Possemato, R., Reinhardt, F., Weinberg, R. A., Yaffe, M. B. and Sabatini, D. M. (2014) Dihydropyrimidine accumulation is required for the epithelial-mesenchymal transition. Cell. 158, 1094-1109

Shechter, I., Dai, P., Huo, L. and Guan, G. (2003) IDH1 gene transcription is sterol regulated and activated by SREBP-1a and SREBP-2 in human hepatoma HepG2 cells: evidence that IDH1 may regulate lipogenesis in hepatic cells. J Lipid Res. 44, 2169-2180

Shen, Q., Wang, Y., Kokovay, E., Lin, G., Chuang, S. M., Goderie, S. K., Roysam, B. and Temple, S. (2008) Adult SVZ stem cells lie in a vascular niche: a quantitative analysis of niche cell-cell interactions. Cell Stem Cell. 3, 289-300

Siebzehnrubl, F. A., Silver, D. J., Tugertimur, B., Deleyrolle, L. P., Siebzehnrubl, D., Sarkisian, M. R., Devers, K. G., Yachnis, A. T., Kupper, M. D., Neal, D., Nabilsi, N. H., Kladde, M. P., Suslov, O., Brabletz, S., Brabletz, T., Reynolds, B. A. and Steindler, D. A. (2013) The ZEB1 pathway links glioblastoma initiation, invasion and chemoresistance. EMBO Mol Med. 5, 1196-1212

Silver, J. D., Ritchie, M. E. and Smyth, G. K. (2009) Microarray background correction: maximum likelihood estimation for the normal-exponential convolution. Biostatistics. 10, 352-363

Singh, S. K., Clarke, I. D., Terasaki, M., Bonn, V. E., Hawkins, C., Squire, J. and Dirks, P. B. (2003) Identification of a cancer stem cell in human brain tumors. Cancer Res. 63, 5821-5828

Singh, S. K., Hawkins, C., Clarke, I. D., Squire, J. A., Bayani, J., Hide, T., Henkelman, R. M., Cusimano, M. D. and Dirks, P. B. (2004) Identification of human brain tumour initiating cells. Nature. 432, 396-401

Sjoblom, T., Jones, S., Wood, L. D., Parsons, D. W., Lin, J., Barber, T. D., Mandelker, D., Leary, R. J., Ptak, J., Silliman, N., Szabo, S., Buckhaults, P., Farrell, C., Meeh, P., Markowitz, S. D., Willis, J., Dawson, D., Willson, J. K., Gazdar, A. F., Hartigan, J., Wu, L., Liu, C., Parmigiani, G., Park, B. H., Bachman, K. E., Papadopoulos, N., Vogelstein, B., Kinzler, K. W. and Velculescu, V. E. (2006) The consensus coding sequences of human breast and colorectal cancers. Science. 314, 268-274

Smirnova, N. A., Hushpulian, D. M., Speer, R. E., Gaisina, I. N., Ratan, R. R. and Gazaryan, I. G. (2012) Catalytic mechanism and substrate specificity of HIF prolyl hydroxylases. Biochemistry (Mosc). 77, 1108-1119

Son, M. J., Woolard, K., Nam, D. H., Lee, J. and Fine, H. A. (2009) SSEA-1 is an enrichment marker for tumor-initiating cells in human glioblastoma. Cell Stem Cell. 4, 440-452

Soubannier, V. and Stifani, S. (2017) NF-kappaB Signalling in Glioblastoma. Biomedicines. 5,

Spaderna, S., Schmalhofer, O., Hlubek, F., Berx, G., Eger, A., Merkel, S., Jung, A., Kirchner, T. and Brabletz, T. (2006) A transient, EMT-linked loss of basement membranes indicates metastasis and poor survival in colorectal cancer. Gastroenterology. 131, 830-840

Span, P. N. and Bussink, J. (2015) Biology of hypoxia. Semin Nucl Med. 45, 101-109

Steenweg, M. E., Jakobs, C., Errami, A., van Dooren, S. J., Adeva Bartolome, M. T., Aerssens, P., Augoustides-Savvapoulou, P., Baric, I., Baumann, M., Bonafe, L., Chabrol, B., Clarke, J. T., Clayton, P., Coker, M., Cooper, S., Falik-Zaccai, T., Gorman, M., Hahn, A., Hasanoglu, A., King, M. D., de Klerk, H. B., Korman, S. H., Lee, C., Meldgaard Lund, A., Mejaski-Bosnjak, V., Pascual-Castroviejo, I., Raadhyaksha, A., Rootwelt, T., Roubertie, A., Ruiz-Falco, M. L., Scalais, E., Schimmel, U., Seijo-Martinez, M., Suri, M., Sykut-Cegielska, J., Trefz, F. K., Uziel, G., Valayannopoulos, V., Vianey-Saban, C., Vlaho, S., Vodopiutz, J., Wajner, M., Walter, J., Walter-Derbort, C., Yapici, Z., Zafeiriou, D. I., Spreeuwenberg, M. D., Celli, J., den Dunnen, J. T., van der Knaap, M. S. and Salomons, G. S. (2010) An overview of L-2-hydroxyglutarate dehydrogenase gene (L2HGDH) variants: a genotype-phenotype study. Hum Mutat. 31, 380-390

Stehle, P., Zander, J., Mertes, N., Albers, S., Puchstein, C., Lawin, P. and Furst, P. (1989) Effect of parenteral glutamine peptide supplements on muscle glutamine loss and nitrogen balance after major surgery. Lancet. 1, 231-233

Stein, J., Boehles, H. J., Blumenstein, I., Goeters, C., Schulz, R. and Working group for developing the guidelines for parenteral nutrition of The German Association for Nutritional, M. (2009) Amino acids - Guidelines on Parenteral Nutrition, Chapter 4. Ger Med Sci. 7, Doc24

Struys, E. A. (2013) 2-Hydroxyglutarate is not a metabolite; D-2-hydroxyglutarate and L-2-hydroxyglutarate are! Proc Natl Acad Sci U S A. 110, E4939

Stupp, R., Mason, W. P., van den Bent, M. J., Weller, M., Fisher, B., Taphoorn, M. J., Belanger, K., Brandes, A. A., Marosi, C., Bogdahn, U., Curschmann, J., Janzer, R. C., Ludwin, S. K., Gorlia, T., Allgeier, A., Lacombe, D., Cairncross, J. G., Eisenhauer, E., Mirimanoff, R. O., European Organisation for, R., Treatment of Cancer Brain, T., Radiotherapy, G. and National Cancer Institute of Canada Clinical Trials, G. (2005) Radiotherapy plus concomitant and adjuvant temozolomide for glioblastoma. N Engl J Med. 352, 987-996

Sturm, D., Witt, H., Hovestadt, V., Khuong-Quang, D. A., Jones, D. T., Konermann, C., Pfaff, E., Tonjes, M., Sill, M., Bender, S., Kool, M., Zapatka, M., Becker, N., Zucknick, M., Hielscher, T., Liu, X. Y., Fontebasso, A. M., Ryzhova, M., Albrecht, S., Jacob, K., Wolter, M., Ebinger, M., Schuhmann, M. U., van Meter, T., Fruhwald, M. C., Hauch,

H., Pekrun, A., Radlwimmer, B., Niehues, T., von Komorowski, G., Durken, M., Kulozik, A. E., Madden, J., Donson, A., Foreman, N. K., Drissi, R., Fouladi, M., Scheurlen, W., von Deimling, A., Monoranu, C., Roggendorf, W., Herold-Mende, C., Unterberg, A., Kramm, C. M., Felsberg, J., Hartmann, C., Wiestler, B., Wick, W., Milde, T., Witt, O., Lindroth, A. M., Schwartzentruber, J., Faury, D., Fleming, A., Zakrzewska, M., Liberski, P. P., Zakrzewski, K., Hauser, P., Garami, M., Klekner, A., Bognar, L., Morrissy, S., Cavalli, F., Taylor, M. D., van Sluis, P., Koster, J., Versteeg, R., Volckmann, R., Mikkelsen, T., Aldape, K., Reifenberger, G., Collins, V. P., Majewski, J., Korshunov, A., Lichter, P., Plass, C., Jabado, N. and Pfister, S. M. (2012) Hotspot mutations in H3F3A and IDH1 define distinct epigenetic and biological subgroups of glioblastoma. Cancer Cell. 22, 425-437

Sullivan, L. B., Gui, D. Y. and Heiden, M. G. V. (2016) Altered metabolite levels in cancer: implications for tumour biology and cancer therapy. Nat Rev Cancer. 16, 680-693

Sundar, S. J., Hsieh, J. K., Manjila, S., Lathia, J. D. and Sloan, A. (2014) The role of cancer stem cells in glioblastoma. Neurosurg Focus. 37, E6

Swietach, P., Vaughan-Jones, R. D. and Harris, A. L. (2007) Regulation of tumor pH and the role of carbonic anhydrase 9. Cancer Metastasis Rev. 26, 299-310

Taal, W., Oosterkamp, H. M., Walenkamp, A. M., Dubbink, H. J., Beerepoot, L. V., Hanse, M. C., Buter, J., Honkoop, A. H., Boerman, D., de Vos, F. Y., Dinjens, W. N., Enting, R. H., Taphoorn, M. J., van den Berkmortel, F. W., Jansen, R. L., Brandsma, D., Bromberg, J. E., van Heuvel, I., Vernhout, R. M., van der Holt, B. and van den Bent, M. J. (2014) Single-agent bevacizumab or lomustine versus a combination of bevacizumab plus lomustine in patients with recurrent glioblastoma (BELOB trial): a randomised controlled phase 2 trial. Lancet Oncol. 15, 943-953

Takeda, K., Cowan, A. and Fong, G. H. (2007) Essential role for prolyl hydroxylase domain protein 2 in oxygen homeostasis of the adult vascular system. Circulation. 116, 774-781

Takeda, K., Ho, V. C., Takeda, H., Duan, L. J., Nagy, A. and Fong, G. H. (2006) Placental but not heart defects are associated with elevated hypoxia-inducible factor alpha levels in mice lacking prolyl hydroxylase domain protein 2. Mol Cell Biol. 26, 8336-8346

Takeda, N., Maemura, K., Imai, Y., Harada, T., Kawanami, D., Nojiri, T., Manabe, I. and Nagai, R. (2004) Endothelial PAS domain protein 1 gene promotes angiogenesis through the transactivation of both vascular endothelial growth factor and its receptor, Flt-1. Circ Res. 95, 146-153

Tamura, R., Tanaka, T., Miyake, K., Tabei, Y., Ohara, K., Sampetrean, O., Kono, M., Mizutani, K., Yamamoto, Y., Murayama, Y., Tamiya, T., Yoshida, K. and Sasaki, H. (2016) Histopathological investigation of glioblastomas resected under bevacizumab treatment. Oncotarget. 7, 52423-52435

Tamura, R., Tanaka, T., Miyake, K., Yoshida, K. and Sasaki, H. (2017) Bevacizumab for malignant gliomas: current indications, mechanisms of action and resistance, and markers of response. Brain Tumor Pathol. 34, 62-77

Tan, F., Jiang, Y., Sun, N., Chen, Z., Lv, Y., Shao, K., Li, N., Qiu, B., Gao, Y., Li, B., Tan, X., Zhou, F., Wang, Z., Ding, D., Wang, J., Sun, J., Hang, J., Shi, S., Feng, X., He, F. and He, J. (2012) Identification of isocitrate dehydrogenase 1 as a potential diagnostic and prognostic biomarker for non-small cell lung cancer by proteomic analysis. Mol Cell Proteomics. 11, M111 008821

Tanaka, H., Sasayama, T., Tanaka, K., Nakamizo, S., Nishihara, M., Mizukawa, K., Kohta, M., Koyama, J., Miyake, S., Taniguchi, M., Hosoda, K. and Kohmura, E. (2013) MicroRNA-183 upregulates HIF-1alpha by targeting isocitrate dehydrogenase 2 (IDH2) in glioma cells. J Neurooncol. 111, 273-283

Tang, X., Lucas, J. E., Chen, J. L., LaMonte, G., Wu, J., Wang, M. C., Koumenis, C. and Chi, J. T. (2012) Functional interaction between responses to lactic acidosis and hypoxia regulates genomic transcriptional outputs. Cancer Res. 72, 491-502

Tarhonskaya, H., Rydzik, A. M., Leung, I. K., Loik, N. D., Chan, M. C., Kawamura, A., McCullagh, J. S., Claridge, T. D., Flashman, E. and Schofield, C. J. (2014) Non-enzymatic chemistry enables 2-hydroxyglutarate-mediated activation of 2-oxoglutarate oxygenases. Nat Commun. 5, 3423

Tavazoie, M., Van der Veken, L., Silva-Vargas, V., Louissaint, M., Colonna, L., Zaidi, B., Garcia-Verdugo, J. M. and Doetsch, F. (2008) A specialized vascular niche for adult neural stem cells. Cell Stem Cell. 3, 279-288

Team, R. C. (2007) R: A Language and Environment for Statistical Computing. ed.)^eds.), R Foundation for Statistical Computing

Tefferi, A., Jimma, T., Sulai, N. H., Lasho, T. L., Finke, C. M., Knudson, R. A., McClure, R. F. and Pardanani, A. (2012) IDH mutations in primary myelofibrosis predict leukemic transformation and shortened survival: clinical evidence for leukemogenic collaboration with JAK2V617F. Leukemia. 26, 475-480

Teng, L., Nakada, M., Furuyama, N., Sabit, H., Furuta, T., Hayashi, Y., Takino, T., Dong, Y., Sato, H., Sai, Y., Miyamoto, K., Berens, M. E., Zhao, S. G. and Hamada, J. (2013) Ligand-dependent EphB1 signaling suppresses glioma invasion and correlates with patient survival. Neuro Oncol. 15, 1710-1720

Tennant, D. A., Frezza, C., MacKenzie, E. D., Nguyen, Q. D., Zheng, L., Selak, M. A., Roberts, D. L., Dive, C., Watson, D. G., Aboagye, E. O. and Gottlieb, E. (2009) Reactivating HIF prolyl hydroxylases under hypoxia results in metabolic catastrophe and cell death. Oncogene. 28, 4009-4021

Terunuma, A., Putluri, N., Mishra, P., Mathe, E. A., Dorsey, T. H., Yi, M., Wallace, T. A., Issaq, H. J., Zhou, M., Killian, J. K., Stevenson, H. S., Karoly, E. D., Chan, K., Samanta, S., Prieto, D., Hsu, T. Y., Kurley, S. J., Putluri, V., Sonavane, R., Edelman, D. C., Wulff, J., Starks, A. M., Yang, Y., Kittles, R. A., Yfantis, H. G., Lee, D. H., Ioffe, O. B., Schiff, R., Stephens, R. M., Meltzer, P. S., Veenstra, T. D., Westbrook, T. F., Sreekumar, A. and Ambs, S. (2014) MYC-driven accumulation of 2-hydroxyglutarate is associated with breast cancer prognosis. J Clin Invest. 124, 398-412

TeSlaa, T., Chaikovsky, A. C., Lipchina, I., Escobar, S. L., Hochedlinger, K., Huang, J., Graeber, T. G., Braas, D. and Teitell, M. A. (2016) alpha-Ketoglutarate Accelerates the Initial Differentiation of Primed Human Pluripotent Stem Cells. Cell Metab. 24, 485-493

Thol, F., Weissinger, E. M., Krauter, J., Wagner, K., Damm, F., Wichmann, M., Gohring, G., Schumann, C., Bug, G., Ottmann, O., Hofmann, W. K., Schlegelberger, B., Ganser, A. and Heuser, M. (2010) IDH1 mutations in patients with myelodysplastic syndromes are associated with an unfavorable prognosis. Haematologica. 95, 1668-1674

Tian, Y. M., Yeoh, K. K., Lee, M. K., Eriksson, T., Kessler, B. M., Kramer, H. B., Edelmann, M. J., Willam, C., Pugh, C. W., Schofield, C. J. and Ratcliffe, P. J. (2011) Differential sensitivity of hypoxia inducible factor hydroxylation sites to hypoxia and hydroxylase inhibitors. J Biol Chem. 286, 13041-13051

Tomlinson, I. P., Alam, N. A., Rowan, A. J., Barclay, E., Jaeger, E. E., Kelsell, D., Leigh, I., Gorman, P., Lamlum, H., Rahman, S., Roylance, R. R., Olpin, S., Bevan, S., Barker, K., Hearle, N., Houlston, R. S., Kiuru, M., Lehtonen, R., Karhu, A., Vilkki, S., Laiho, P., Eklund, C., Vierimaa, O., Aittomaki, K., Hietala, M., Sistonen, P., Paetau, A., Salovaara, R., Herva, R., Launonen, V., Aaltonen, L. A. and Multiple Leiomyoma, C. (2002) Germline mutations in FH predispose to dominantly inherited uterine fibroids, skin leiomyomata and papillary renal cell cancer. Nat Genet. 30, 406-410

Toth, J., Cutforth, T., Gelinas, A. D., Bethoney, K. A., Bard, J. and Harrison, C. J. (2001) Crystal structure of an ephrin ectodomain. Dev Cell. 1, 83-92

Trepel, J., Mollapour, M., Giaccone, G. and Neckers, L. (2010) Targeting the dynamic HSP90 complex in cancer. Nat Rev Cancer. 10, 537-549

Tso, C. L., Freije, W. A., Day, A., Chen, Z., Merriman, B., Perlina, A., Lee, Y., Dia, E. Q., Yoshimoto, K., Mischel, P. S., Liau, L. M., Cloughesy, T. F. and Nelson, S. F. (2006a) Distinct transcription profiles of primary and secondary glioblastoma subgroups. Cancer Res. 66, 159-167

Tso, C. L., Shintaku, P., Chen, J., Liu, Q., Liu, J., Chen, Z., Yoshimoto, K., Mischel, P. S., Cloughesy, T. F., Liau, L. M. and Nelson, S. F. (2006b) Primary glioblastomas express mesenchymal stem-like properties. Mol Cancer Res. 4, 607-619

Tsukada, Y., Fang, J., Erdjument-Bromage, H., Warren, M. E., Borchers, C. H., Tempst, P. and Zhang, Y. (2006) Histone demethylation by a family of JmjC domain-containing proteins. Nature. 439, 811-816

Turcan, S., Rohle, D., Goenka, A., Walsh, L. A., Fang, F., Yilmaz, E., Campos, C., Fabius, A. W., Lu, C., Ward, P. S., Thompson, C. B., Kaufman, A., Guryanova, O., Levine, R., Heguy, A., Viale, A., Morris, L. G., Huse, J. T., Mellinghoff, I. K. and Chan, T. A. (2012) IDH1 mutation is sufficient to establish the glioma hypermethylator phenotype. Nature. 483, 479-483

Vaupel, P., Kallinowski, F. and Okunieff, P. (1989) Blood flow, oxygen and nutrient supply, and metabolic microenvironment of human tumors: a review. Cancer Res. 49, 6449-6465

Velpula, K. K., Dasari, V. R., Tsung, A. J., Dinh, D. H. and Rao, J. S. (2011) Cord blood stem cells revert glioma stem cell EMT by down regulating transcriptional activation of Sox2 and Twist1. Oncotarget. 2, 1028-1042

Venneti, S., Felicella, M. M., Coyne, T., Phillips, J. J., Gorovets, D., Huse, J. T., Kofler, J., Lu, C., Tihan, T., Sullivan, L. M., Santi, M., Judkins, A. R., Perry, A. and Thompson, C. B. (2013) Histone 3 lysine 9 trimethylation is differentially associated with isocitrate dehydrogenase mutations in oligodendrogliomas and high-grade astrocytomas. J Neuropathol Exp Neurol. 72, 298-306

Verhaak, R. G., Hoadley, K. A., Purdom, E., Wang, V., Qi, Y., Wilkerson, M. D., Miller, C. R., Ding, L., Golub, T., Mesirov, J. P., Alexe, G., Lawrence, M., O'Kelly, M., Tamayo, P., Weir, B. A., Gabriel, S., Winckler, W., Gupta, S., Jakkula, L., Feiler, H. S., Hodgson, J. G., James, C. D., Sarkaria, J. N., Brennan, C., Kahn, A., Spellman, P. T., Wilson, R. K., Speed, T. P., Gray, J. W., Meyerson, M., Getz, G., Perou, C. M., Hayes, D. N. and Cancer Genome Atlas Research, N. (2010) Integrated genomic analysis identifies clinically relevant subtypes of glioblastoma characterized by abnormalities in PDGFRA, IDH1, EGFR, and NF1. Cancer Cell. 17, 98-110

Vital, A. L., Tabernero, M. D., Castrillo, A., Rebelo, O., Tao, H., Gomes, F., Nieto, A. B., Resende Oliveira, C., Lopes, M. C. and Orfao, A. (2010) Gene expression profiles of human glioblastomas are associated with both tumor cytogenetics and histopathology. Neuro Oncol. 12, 991-1003

Voron, T., Colussi, O., Marcheteau, E., Pernot, S., Nizard, M., Pointet, A. L., Latreche, S., Bergaya, S., Benhamouda, N., Tanchot, C., Stockmann, C., Combe, P., Berger, A., Zinzindohoue, F., Yagita, H., Tartour, E., Taieb, J. and Terme, M. (2015) VEGF-A modulates expression of inhibitory checkpoints on CD8+ T cells in tumors. J Exp Med. 212, 139-148

Wahl, D. R., Dresser, J., Wilder-Romans, K., Parsels, J. D., Zhao, S. G., Davis, M., Zhao, L., Kachman, M., Wernisch, S., Burant, C. F., Morgan, M. A., Feng, F. Y., Speers, C., Lyssiotis, C. A. and Lawrence, T. S. (2017) Glioblastoma Therapy Can Be Augmented by Targeting IDH1-Mediated NADPH Biosynthesis. Cancer Res. 77, 960-970

Wahl, D. R. and Venneti, S. (2015) 2-Hydoxyglutarate: D/Riving Pathology in gLiomaS. Brain Pathol. 25, 760-768

Wallin, J. J., Bendell, J. C., Funke, R., Sznol, M., Korski, K., Jones, S., Hernandez, G., Mier, J., He, X., Hodi, F. S., Denker, M., Leveque, V., Canamero, M., Babitski, G., Koeppen, H., Ziai, J., Sharma, N., Gaire, F., Chen, D. S., Waterkamp, D., Hegde, P. S. and McDermott, D. F. (2016) Atezolizumab in combination with bevacizumab enhances antigen-specific T-cell migration in metastatic renal cell carcinoma. Nat Commun. 7, 12624

Wang, F., Travins, J., DeLaBarre, B., Penard-Lacronique, V., Schalm, S., Hansen, E., Straley, K., Kernytsky, A., Liu, W., Gliser, C., Yang, H., Gross, S., Artin, E., Saada, V., Mylonas, E., Quivoron, C., Popovici-Muller, J., Saunders, J. O., Salituro, F. G., Yan, S., Murray, S., Wei, W., Gao, Y., Dang, L., Dorsch, M., Agresta, S., Schenkein, D. P., Biller, S. A., Su, S. M., de Botton, S. and Yen, K. E. (2013a) Targeted inhibition of mutant IDH2 in leukemia cells induces cellular differentiation. Science. 340, 622-626

Wang, G. L. and Semenza, G. L. (1995) Purification and characterization of hypoxia-inducible factor 1. J Biol Chem. 270, 1230-1237

Wang, J., Cui, S., Zhang, X., Wu, Y. and Tang, H. (2013b) High expression of heat shock protein 90 is associated with tumor aggressiveness and poor prognosis in patients with advanced gastric cancer. PLoS One. 8, e62876

Wang, R., Chadalavada, K., Wilshire, J., Kowalik, U., Hovinga, K. E., Geber, A., Fligelman, B., Leversha, M., Brennan, C. and Tabar, V. (2010a) Glioblastoma stem-like cells give rise to tumour endothelium. Nature. 468, 829-833

Wang, S. D., Rath, P., Lal, B., Richard, J. P., Li, Y., Goodwin, C. R., Laterra, J. and Xia, S. (2012) EphB2 receptor controls proliferation/migration dichotomy of glioblastoma by interacting with focal adhesion kinase. Oncogene. 31, 5132-5143

Wang, Y., Nakayama, M., Pitulescu, M. E., Schmidt, T. S., Bochenek, M. L., Sakakibara, A., Adams, S., Davy, A., Deutsch, U., Luthi, U., Barberis, A., Benjamin, L. E., Makinen, T., Nobes, C. D. and Adams, R. H. (2010b) Ephrin-B2 controls VEGF-induced angiogenesis and lymphangiogenesis. Nature. 465, 483-486

Warburg, O. (1956a) On respiratory impairment in cancer cells. Science. 124, 269-270

Warburg, O. (1956b) On the origin of cancer cells. Science. 123, 309-314

Ward, P. S., Patel, J., Wise, D. R., Abdel-Wahab, O., Bennett, B. D., Coller, H. A., Cross, J. R., Fantin, V. R., Hedvat, C. V., Perl, A. E., Rabinowitz, J. D., Carroll, M., Su, S. M., Sharp, K. A., Levine, R. L. and Thompson, C. B. (2010) The common feature of leukemia-associated IDH1 and IDH2 mutations is a neomorphic enzyme activity converting alpha-ketoglutarate to 2-hydroxyglutarate. Cancer Cell. 17, 225-234

Ward, P. S. and Thompson, C. B. (2012) Metabolic reprogramming: a cancer hallmark even warburg did not anticipate. Cancer Cell. 21, 297-308

Welti, J., Loges, S., Dimmeler, S. and Carmeliet, P. (2013) Recent molecular discoveries in angiogenesis and antiangiogenic therapies in cancer. J Clin Invest. 123, 3190-3200

Westphal, M., Hansel, M., Hamel, W., Kunzmann, R. and Holzel, F. (1994) Karyotype analyses of 20 human glioma cell lines. Acta Neurochir (Wien). 126, 17-26

Whitesell, L. and Lindquist, S. L. (2005) HSP90 and the chaperoning of cancer. Nat Rev Cancer. 5, 761-772

Willam, C., Maxwell, P. H., Nichols, L., Lygate, C., Tian, Y. M., Bernhardt, W., Wiesener, M., Ratcliffe, P. J., Eckardt, K. U. and Pugh, C. W. (2006a) HIF prolyl hydroxylases in the rat; organ distribution and changes in expression following hypoxia and coronary artery ligation. J Mol Cell Cardiol. 41, 68-77

Willam, C., Warnecke, C., Schefold, J. C., Kugler, J., Koehne, P., Frei, U., Wiesener, M. and Eckardt, K. U. (2006b) Inconsistent effects of acidosis on HIF-alpha protein and its target genes. Pflugers Arch. 451, 534-543

Wilson, T. A., Karajannis, M. A. and Harter, D. H. (2014) Glioblastoma multiforme: State of the art and future therapeutics. Surg Neurol Int. 5, 64

Winkler, F., Kozin, S. V., Tong, R. T., Chae, S. S., Booth, M. F., Garkavtsev, I., Xu, L., Hicklin, D. J., Fukumura, D., di Tomaso, E., Munn, L. L. and Jain, R. K. (2004) Kinetics of vascular normalization by VEGFR2 blockade governs brain tumor response to radiation: role of oxygenation, angiopoietin-1, and matrix metalloproteinases. Cancer Cell. 6, 553-563

Winning, S., Splettstoesser, F., Fandrey, J. and Frede, S. (2010) Acute hypoxia induces HIF-independent monocyte adhesion to endothelial cells through increased intercellular adhesion molecule-1 expression: the role of hypoxic inhibition of prolyl hydroxylase activity for the induction of NF-kappa B. J Immunol. 185, 1786-1793

Wise, D. R., Ward, P. S., Shay, J. E., Cross, J. R., Gruber, J. J., Sachdeva, U. M., Platt, J. M., DeMatteo, R. G., Simon, M. C. and Thompson, C. B. (2011) Hypoxia promotes isocitrate dehydrogenase-dependent carboxylation of alpha-ketoglutarate to citrate to support cell growth and viability. Proc Natl Acad Sci U S A. 108, 19611-19616

Wong, B. W., Kuchnio, A., Bruning, U. and Carmeliet, P. (2013) Emerging novel functions of the oxygen-sensing prolyl hydroxylase domain enzymes. Trends Biochem Sci. 38, 3-11

Wu, N., Yang, M., Gaur, U., Xu, H., Yao, Y. and Li, D. (2016) Alpha-Ketoglutarate: Physiological Functions and Applications. Biomol Ther (Seoul). 24, 1-8

Wykosky, J. and Debinski, W. (2008) The EphA2 receptor and ephrinA1 ligand in solid tumors: function and therapeutic targeting. Mol Cancer Res. 6, 1795-1806

Xia, Y., Shen, S. and Verma, I. M. (2014) NF-kappaB, an active player in human cancers. Cancer Immunol Res. 2, 823-830

Xiao, D., Zeng, L., Yao, K., Kong, X., Wu, G. and Yin, Y. (2016) The glutamine-alpha-ketoglutarate (AKG) metabolism and its nutritional implications. Amino Acids. 48, 2067-2080

Xiao, M., Yang, H., Xu, W., Ma, S., Lin, H., Zhu, H., Liu, L., Liu, Y., Yang, C., Xu, Y., Zhao, S., Ye, D., Xiong, Y. and Guan, K. L. (2012) Inhibition of alpha-KG-dependent histone and DNA demethylases by fumarate and succinate that are accumulated in mutations of FH and SDH tumor suppressors. Genes Dev. 26, 1326-1338

Xu, D., Yao, Y., Lu, L., Costa, M. and Dai, W. (2010a) Plk3 functions as an essential component of the hypoxia regulatory pathway by direct phosphorylation of HIF-1alpha. J Biol Chem. 285, 38944-38950

Xu, H., Rahimpour, S., Nesvick, C. L., Zhang, X., Ma, J., Zhang, M., Zhang, G., Wang, L., Yang, C., Hong, C. S., Germanwala, A. V., Elder, J. B., Ray-Chaudhury, A., Yao, Y., Gilbert, M. R., Lonser, R. R., Heiss, J. D., Brady, R. O., Mao, Y., Qin, J. and Zhuang, Z. (2015) Activation of hypoxia signaling induces phenotypic transformation of glioma cells: implications for bevacizumab antiangiogenic therapy. Oncotarget. 6, 11882-11893

Xu, L., Fukumura, D. and Jain, R. K. (2002) Acidic extracellular pH induces vascular endothelial growth factor (VEGF) in human glioblastoma cells via ERK1/2 MAPK signaling pathway: mechanism of low pH-induced VEGF. J Biol Chem. 277, 11368-11374

Xu, W., Yang, H., Liu, Y., Yang, Y., Wang, P., Kim, S. H., Ito, S., Yang, C., Wang, P., Xiao, M. T., Liu, L. X., Jiang, W. Q., Liu, J., Zhang, J. Y., Wang, B., Frye, S., Zhang, Y., Xu, Y. H., Lei, Q. Y., Guan, K. L., Zhao, S. M. and Xiong, Y. (2011) Oncometabolite 2-hydroxyglutarate is a competitive inhibitor of alpha-ketoglutarate-dependent dioxygenases. Cancer Cell. 19, 17-30

Xu, X., Zhao, J., Xu, Z., Peng, B., Huang, Q., Arnold, E. and Ding, J. (2004) Structures of human cytosolic NADP-dependent isocitrate dehydrogenase reveal a novel self-regulatory mechanism of activity. J Biol Chem. 279, 33946-33957

Xu, Y., Stamenkovic, I. and Yu, Q. (2010b) CD44 attenuates activation of the hippo signaling pathway and is a prime therapeutic target for glioblastoma. Cancer Res. 70, 2455-2464

Xue, J., Li, X., Jiao, S., Wei, Y., Wu, G. and Fang, J. (2010) Prolyl hydroxylase-3 is down-regulated in colorectal cancer cells and inhibits IKKbeta independent of hydroxylase activity. Gastroenterology. 138, 606-615

Yan, B., Jiao, S., Zhang, H. S., Lv, D. D., Xue, J., Fan, L., Wu, G. H. and Fang, J. (2011) Prolyl hydroxylase domain protein 3 targets Pax2 for destruction. Biochem Biophys Res Commun. 409, 315-320

Yan, H., Parsons, D. W., Jin, G., McLendon, R., Rasheed, B. A., Yuan, W., Kos, I., Batinic-Haberle, I., Jones, S., Riggins, G. J., Friedman, H., Friedman, A., Reardon, D., Herndon, J., Kinzler, K. W., Velculescu, V. E., Vogelstein, B. and Bigner, D. D. (2009) IDH1 and IDH2 mutations in gliomas. N Engl J Med. 360, 765-773

Yang, H. W., Menon, L. G., Black, P. M., Carroll, R. S. and Johnson, M. D. (2010) SNAI2/Slug promotes growth and invasion in human gliomas. BMC Cancer. 10, 301

Yang, J., Staples, O., Thomas, L. W., Briston, T., Robson, M., Poon, E., Simoes, M. L., El-Emir, E., Buffa, F. M., Ahmed, A., Annear, N. P., Shukla, D., Pedley, B. R., Maxwell, P. H., Harris, A. L. and Ashcroft, M. (2012) Human CHCHD4 mitochondrial proteins regulate cellular oxygen consumption rate and metabolism and provide a critical role in hypoxia signaling and tumor progression. J Clin Invest. 122, 600-611

Yang, M., Su, H., Soga, T., Kranc, K. R. and Pollard, P. J. (2014) Prolyl hydroxylase domain enzymes: important regulators of cancer metabolism. Hypoxia (Auckl). 2, 127-142

Yang, M. H., Wu, M. Z., Chiou, S. H., Chen, P. M., Chang, S. Y., Liu, C. J., Teng, S. C. and Wu, K. J. (2008) Direct regulation of TWIST by HIF-1alpha promotes metastasis. Nat Cell Biol. 10, 295-305

Yang, X., Du, T., Wang, X., Zhang, Y., Hu, W., Du, X., Miao, L. and Han, C. (2015) IDH1, a CHOP and C/EBPbeta-responsive gene under ER stress, sensitizes human melanoma cells to hypoxia-induced apoptosis. Cancer Lett. 365, 201-210

Yao, X. H., Ping, Y. F., Chen, J. H., Xu, C. P., Chen, D. L., Zhang, R., Wang, J. M. and Bian, X. W. (2008) Glioblastoma stem cells produce vascular endothelial growth factor by activation of a G-protein coupled formylpeptide receptor FPR. J Pathol. 215, 369-376

Yasumoto, K., Kowata, Y., Yoshida, A., Torii, S. and Sogawa, K. (2009) Role of the intracellular localization of HIF-prolyl hydroxylases. Biochim Biophys Acta. 1793, 792-797

Ye, J., Gu, Y., Zhang, F., Zhao, Y., Yuan, Y., Hao, Z., Sheng, Y., Li, W. Y., Wakeham, A., Cairns, R. A. and Mak, T. W. (2017) IDH1 deficiency attenuates gluconeogenesis in mouse liver by impairing amino acid utilization. Proc Natl Acad Sci U S A. 114, 292-297

Yeo, C. D., Kang, N., Choi, S. Y., Kim, B. N., Park, C. K., Kim, J. W., Kim, Y. K. and Kim, S. J. (2017) The role of hypoxia on the acquisition of epithelial-mesenchymal transition and cancer stemness: a possible link to epigenetic regulation. Korean J Intern Med. 32, 589-599

Yeung, S. J., Pan, J. and Lee, M. H. (2008) Roles of p53, MYC and HIF-1 in regulating glycolysis - the seventh hallmark of cancer. Cell Mol Life Sci. 65, 3981-3999

Young, R. M., Jamshidi, A., Davis, G. and Sherman, J. H. (2015) Current trends in the surgical management and treatment of adult glioblastoma. Ann Transl Med. 3, 121

Yuan, Y., Hilliard, G., Ferguson, T. and Millhorn, D. E. (2003) Cobalt inhibits the interaction between hypoxia-inducible factor-alpha and von Hippel-Lindau protein by direct binding to hypoxia-inducible factor-alpha. J Biol Chem. 278, 15911-15916

Yun, Z. and Lin, Q. (2014) Hypoxia and regulation of cancer cell stemness. Adv Exp Med Biol. 772, 41-53

Zagzag, D., Nomura, M., Friedlander, D. R., Blanco, C. Y., Gagner, J. P., Nomura, N. and Newcomb, E. W. (2003) Geldanamycin inhibits migration of glioma cells in vitro: a potential role for hypoxia-inducible factor (HIF-1alpha) in glioma cell invasion. J Cell Physiol. 196, 394-402

Zarei, M., Lal, S., Parker, S. J., Nevler, A., Vaziri-Gohar, A., Dukleska, K., Mambelli-Lisboa, N. C., Moffat, C., Blanco, F. F., Chand, S. N., Jimbo, M., Cozzitorto, J. A., Jiang, W., Yeo, C. J., Londin, E. R., Seifert, E. L., Metallo, C. M., Brody, J. R. and Winter, J. M. (2017) Posttranscriptional Upregulation of IDH1 by HuR Establishes a Powerful Survival Phenotype in Pancreatic Cancer Cells. Cancer Res. 77, 4460-4471

Zarkoob, H., Taube, J. H., Singh, S. K., Mani, S. A. and Kohandel, M. (2013) Investigating the link between molecular subtypes of glioblastoma, epithelial-mesenchymal transition, and CD133 cell surface protein. PLoS One. 8, e64169

Zdzisinska, B., Zurek, A. and Kandefer-Szerszen, M. (2017) Alpha-Ketoglutarate as a Molecule with Pleiotropic Activity: Well-Known and Novel Possibilities of Therapeutic Use. Arch Immunol Ther Exp (Warsz). 65, 21-36

Zeng, L., Morinibu, A., Kobayashi, M., Zhu, Y., Wang, X., Goto, Y., Yeom, C. J., Zhao, T., Hirota, K., Shinomiya, K., Itasaka, S., Yoshimura, M., Guo, G., Hammond, E. M., Hiraoka, M. and Harada, H. (2015) Aberrant IDH3alpha expression promotes malignant tumor growth by inducing HIF-1-mediated metabolic reprogramming and angiogenesis. Oncogene. 34, 4758-4766

Zhang, D., Wang, Y., Shi, Z., Liu, J., Sun, P., Hou, X., Zhang, J., Zhao, S., Zhou, B. P. and Mi, J. (2015a) Metabolic reprogramming of cancer-associated fibroblasts by IDH3alpha downregulation. Cell Rep. 10, 1335-1348

Zhang, J., Tian, X. J. and Xing, J. (2016) Signal Transduction Pathways of EMT Induced by TGF-beta, SHH, and WNT and Their Crosstalks. J Clin Med. 5,

Zhang, M., Ye, G., Li, J. and Wang, Y. (2015b) Recent advance in molecular angiogenesis in glioblastoma: the challenge and hope for anti-angiogenic therapy. Brain Tumor Pathol. 32, 229-236

Zhao, C., Wang, A., Lu, F., Chen, H., Fu, P., Zhao, X. and Chen, H. (2017) Overexpression of junctional adhesion molecule-A and EphB2 predicts poor survival in lung adenocarcinoma patients. Tumour Biol. 39, 1010428317691000

Zhao, S., Lin, Y., Xu, W., Jiang, W., Zha, Z., Wang, P., Yu, W., Li, Z., Gong, L., Peng, Y., Ding, J., Lei, Q., Guan, K. L. and Xiong, Y. (2009) Glioma-derived mutations in IDH1 dominantly inhibit IDH1 catalytic activity and induce HIF-1alpha. Science. 324, 261-265

Zheng, X., Zhai, B., Koivunen, P., Shin, S. J., Lu, G., Liu, J., Geisen, C., Chakraborty, A. A., Moslehi, J. J., Smalley, D. M., Wei, X., Chen, X., Chen, Z., Beres, J. M., Zhang, J., Tsao, J. L., Brenner, M. C., Zhang, Y., Fan, C., DePinho, R. A., Paik, J., Gygi, S. P., Kaelin, W. G., Jr. and Zhang, Q. (2014) Prolyl hydroxylation by EglN2 destabilizes FOXO3a by blocking its interaction with the USP9x deubiquitinase. Genes Dev. 28, 1429-1444

Zhong, L., D'Urso, A., Toiber, D., Sebastian, C., Henry, R. E., Vadysirisack, D. D., Guimaraes, A., Marinelli, B., Wikstrom, J. D., Nir, T., Clish, C. B., Vaitheesvaran, B., Iliopoulos, O., Kurland, I., Dor, Y., Weissleder, R., Shirihai, O. S., Ellisen, L. W., Espinosa, J. M. and Mostoslavsky, R. (2010) The histone deacetylase Sirt6 regulates glucose homeostasis via Hif1alpha. Cell. 140, 280-293

Zhou, F., Xu, X., Wu, J., Wang, D. and Wang, J. (2017) NF-kappaB controls four genes encoding core enzymes of tricarboxylic acid cycle. Gene. 621, 12-20

Zurlo, G., Guo, J., Takada, M., Wei, W. and Zhang, Q. (2016) New Insights into Protein Hydroxylation and Its Important Role in Human Diseases. Biochim Biophys Acta. 1866, 208-220

7 List of figures and tables

7.1 List of figures

Figure 1.1. Summary of most frequent molecular abnormalities found in primary and secondary glioblastomas.....11

Figure 1.2. The tumor microenvironment in the brain. 15

Figure 1.3. The regulation of HIF-α levels and transactivity.....18

Figure 1.4. The biological pathways activated by HIF-1α and HIF-2α.....22

Figure 1.5. Regulation of PHD activity.....25

Figure 1.6. Cancer stem cell model.....29

Figure 1.7. The metabolic processes producing 2-OG. 35

Figure 1.8. Structure of IDH1 homodimer and IDH1 conformational changes. 39

Figure 1.9. The reactions catalyzed by IDH wild-type (IDH^{wt}) and IDH mutant (IDH^{mut}) enyzmes. 44

Figure 1.10. The acidic tumor microenvironment. 47

Figure 1.11. Structure of Eph receptors and ephrin ligands.....53

Figure 4.1. IDH1 knock-down increases HIF-α levels and HIF target genes expression.... 105

Figure 4.2. Increased expression levels of HIF-regulated genes. 106

Figure 4.3. PHD dependent reduction of HIF-α hydroxylation leads to increased HIF activity and delayed reoxygenation in IDH1 silenced cells. 108

Figure 4.4. IDH1 knock-down results in reduced 2-OG levels and addition of Dm-2-OG reverts the IDH1 knock-down effects. 110

Figure 4.5. Regulation of the NF-κB pathway by IDH1 silencing. 112

Figure 4.6. IDH1 overexpression reduces the hypoxic response.....114

Figure 4.7. IDH1 overexpression reduces expression of HIF-α and NF-κB target genes... 115

Figure 4.8. Enrichment of cancer stem cells by IDH1 silencing. 117

Figure 4.9. Addition of Dm-2-OG abrogates the increased self-renewal capacity upon knock-down of IDH1. 119

Figure 4.10. IDH1 silencing enhances TGFβ signaling and increases Snail expression levels. 121

Figure 4.11. IDH1 silencing enhances the invasion capacity of tumor cells. 123

Figure 4.12. HIF-1/2α silencing but not RelA silencing reduces Snail expression levels upon IDH1 silencing.....124

Figure 4.13. Regulation of IDH1 by microenvironmental stimuli. 126

Figure 4.14. Reduced IDH1 levels correlate with poor GBM patient prognosis, increased tumor growth and invasion. 128

Figure 4.15. IDH1 silencing in breast and lung cancer cell lines 130

Figure 4.16. Acidosis induces HIF-α function and CSC self-renewal. 133

Figure 4.17. HSP90 inactivation suppresses the acidosis-induced HIF-α increase and tumor growth. 135

Figure 4.18. HSP90 inactivation by a dominant negative form of HSP90 reduces HIF-α levels and inhibits tumor growth. 137

Figure 4.19. High HSP90 expression is observed in the hypoxic niche and correlates with hypoxic and stem cell markers in human glioblastomas. 138

Figure 4.20. Hypoxia induces glioma cell invasion and downregulates ephrinB2 expression through HIF-1α. 141

Figure 4.21. Loss of ephrinB2 increases tumor invasiveness. 143

Figure 5.1. A model presenting the metabolic control of the tumor phenotype by IDH1 via regulation of 2-OG maintenance. 159

Figure 5.2. A model of the synergistic regulation of HIF function and self-renewal capacity of CSCs in the hypoxic/acidic niche. 166

Figure 5.3. Model of the regulation of glioma invasion and evasive resistance by the HIF-1α-ZEB2-ephrinB2 axis. 171

7.2 List of tables

Table 1.1. Examples of gliomas according to the 2016 WHO classification of central nervous system tumors (Louis, et al., 2016)....10

Table 3.1. Antibiotics for selection of bacterial cells....62

Table 3.2. Antibiotics for selection of mammalian cells....62

Table 3.3. Primary antibodies. WB; western blotting, IHC; Immunohistochemistry, IF; Immunofluorescence 63

Table 3.4. Secondary antibodies. WB; western blotting, IHC; Immunohistochemistry, IF; Immunofluorescence 64

Table 3.5. Cell pools generated in this work 66

Table 3.6. Primers for quantitative real time PCR....70

Table 3.7. qPCR program used for SYBR green method 83

8 Abbreviations

°C	degree Celsius
2-HG	2-hydroxglutarate
2-OG	2-oxoglutarate
5-hmC	5-hydroxy-methylcytosine
5-mC	5-methylcytosine
ALKBH	alkylated DNA repair protein alkB
AML	acute myeloid leukemia
ANG2	angiopoietin 2
APS	Ammonium persulfate
ARD1	acetyl-transferase arrest defective 1
ASPHD2	aspartate beta–hydroxylase domain-containing protein 2
ATF4	Activating transcription factor 4
ATP	adenosine tri-phosphate
ATRX	Alpha Thalassemia Retardation Syndrome X-Linked
bFGF	basic fibroblast growth factor
bHLH	basic Helix-Loop-Helix
BME	Basal Medium Eagle
Bmi1	B-cell specific Moloney murine leukemia virus integration site 1
BNIP3	BCL2/adenovirus E1B 19 kDa protein-interacting protein 3
bp	base pair
BSA	bovine serum albumin
C-P4H	collagen prolyl 4-hydroxlase
C/EBPβ	CCAAT-enhancer-binding protein
CAF	cancer-associated fibroblasts
CAIX	carbonic anhydrase IX
CBP	CREB binding protein
CD	cluster of differentiation
CHOP	CCAAT-enhancer-binding protein homologous protein
CKII	casein kinase II
CMV	cytomegalovirus
Co	control
CPS	cryoprotection solution
CSC	cancer stem cell
CXCR4	C-X-C chemokine receptor type 4
D-2-HGA	D-2-hydroxyglutaric acid
D-2-HGDH	D-2-hydroxyglutarate dehydrogenase
DAB	3,3'-diaminobenzidine
DAPI	4',6-diamidino-2-phenylindole
DEPC	Diethylpyrocarbonate
DMEM	Dulbeccos's modified eagle medium
DMOG	Dimethyloxaloyl glycine
DMSO	dimethyl sulfoxide
DNA	deoxyribonucleic acid
dNTP	deoxy-trinucleotide-phosphate
E. coli	Escherichia coli
ECFP	Enhanced cyan fluorescent protein

ECL	enhanced chemiluminescence
EDTA	ethylenediaminetetraacetic acid
EGF	epidermal growth factor
EGFR	epidermal growth factor receptor
EGLN	egg laying nine
Egr-1	Early growth response protein 1)
EMT	epithelial to mesenchymal transition
Eph	Erythropoietin-producing human hepatocellular
EPO	erythropoietin
EPOR	erythropoietin receptor
ER	endoplasmic reticulum
ERK	extracellular signal–regulated kinase
ESC	embryonic stem cell
FACS	fluorescence activated cell sorting
FAP	Fibroblast activation protein alpha
FBS	fetal bovine serum
FCS	fetal calf serum
FGF	fibroblast growth factor
FH	fumarate hydratase
FIH	factor inhibiting HIF
FITC	Fluorescein isothiocyanate
FOXO3a	Forkhead box O3
fw	forward
GABRA1	gamma-aminobutyric acid type A receptor alpha1
GFP	Green fluorescent protein
GFPT	glutamine--fructose-6-phosphate transaminase
GLS	Glutaminase
GLUD	glutamate dehydrogenase
GLUT1	Glucose transporter 1
GLUT3	Glucose transporter 3
GOT	Aspartate transaminase
GPI	glycosylphosphatidylinositol
GSC	glioblastoma stem cells
GSK3β	glycogen synthase kinase 3β
h	hour
HA	Human influenza hemagglutinin
HBS	HEPES buffered saline
HDAC	histone deacetylases
HE	hematoxylin/eosin
HEPES	4-(2-hydroxyethyl)-1-piperazineethanesulfonic acid
HGF	Hepatocyte growth factor
HIF	hypoxia inducible factor
HK	hexokinase
HMGA2	High-mobility group AT-hook 2
HPLC-MS	High-performance liquid chromatography-mass spectrometry
HPRT	hypoxanthine phosphoribosyltransferase
HRE	hypoxic response element
HRPO	Horseradish Peroxidase
HSP90	heat shock protein 90
Hyp	Hypoxia
ID2	DNA-binding protein inhibitor

IDH1	isocitrate dehydrogenase 1
IF	immunofluorescence
IHC	immunohistochemistry
IL-8	Interleukin-8
IκBα	IκB kinase
JMJD	Jumonji-domain-containing demethylase
kb	kilo base pair
KO	knock-out
L1CAM	L1 cell adhesion molecule
LB	Luria-Bertani
LDHA	lactate dehydrogenase A
LOH	loss of heterozygosity
LOX	lysyl oxidase
luc	luciferase
M-MuLV	Moloney Murine Leukemia Virus
MAML3	Mastermind Like Transcriptional Coactivator 3
MCT4	monocarboxylate transporter 4
MDM2	Mouse double minute 2 homolog
MDS	myelodysplastic syndrome
MEM	Minimum essential medium
MERTK	Proto-oncogene tyrosine-protein kinase MER
MFI	mean fluorescence intensity
mg	milligram
MGMT	O^6- methylguanine-DNA-methyltransferase
miRNA	micro RNA
ml	milliliter
MMP	matrix metalloproteinase-
MOI	multiplicity of infection
mRNA	messenger RNA
MTA3	Metastasis-associated protein 3
mTOR	mammalian target of rapamycin
NAD	Nicotinamide adenine dinucleotide
NADP	Nicotinamide adenine dinucleotide phosphate
NEFL	Neurofilament Light
NF-κB	nuclear factor kappa-light-chain-enhancer of activated B cells
NF1	neurofibromin 1
NFATc2	nuclear factor of activated T cells 2
NFE2L2	nuclear factor (erythroid-derived 2)-like 2
ng	nanogram
nM	nanomolar
NO	nitric oxide
Nor	Normoxia
Oct4	octamer-binding transcription factor 4
ODD	oxygen dependent degradation domain
OS	overall survival
P4H	Prolyl 4-hydroxylase
P4HA1	Prolyl 4-hydroxylase subunit alpha-1
PAGE	Poly Acrylamide Gel Electrophoresis
PARP-1	Poly [ADP-ribose] polymerase 1
PAS	PER, ARNT, SIM
Pax2	paired box gene 2

PB	phosphate buffer
PBS	phosphate buffered saline
PCR	polymerase chain reaction
PDGF	platelet-derived growth factor
PDGF-B	platelet-derived growth factor subunit B
PDGFR	platelet-derived growth factor receptor
PDGFRA	platelet-derived growth factor receptor alpha
PDK1	pyruvate dehydrogenase kinase 1
PDZ	postsynaptic density-95/disc large/zonula occludens-1
PE	Phycoerythrin
PFA	paraformaldehyde
PFS	progression-free survival
pH	potentia Hydrogenii
PHD	prolyl hydroxylase domain
pHEMA	Poly (2-hydroxyethyl) methacrylate
PKA	protein kinase A
PKM	pyruvate kinase
PLK3	polo-like kinase
PLOD	procollagen lysyl hydroxylase
pPSC	primed pluripotent stem cell
PSAT	Phosphoserine aminotransferase
PTEN	phosphatase and tensin homolog
PTP	phosphotyrosine binding domain-containing proteins
PVDF	polyvinylidenfluorid
pVHL	von Hippel-Lindau tumor-suppressor protein
qPCR	quantitative real time polymerase chain reaction
RACK1	Receptor of activated protein C kinase 1
RB	retinoblastoma protein
rev	reverse
RLU	Relative luminometer units/Relative light units
RNA	ribonucleic acid
ROS	reactive oxygen species
rpm	rounds per minute
RT	room temperature
RTK	receptor tyrosine kinase
SAM	sterile α motif
SBE	SMAD binding element
SDH	succinate dehydrogenase
SDS	sodium dodecyl sulfate
SEM	standard error of mean
SFU	sphere forming units
SHARP1	Basic helix-loop-helix family, member e41 (BHLHE41)
SLC12A5	Potassium-chloride transporter member 5
Sox2	SRY (sex determining region Y)-box 2
SREBP	sterol regulatory element-binding proteins
STAT3	Signal transducer and activator of transcription 3
SYT1	Synaptotagmin-1
TAD	transactivation domain
TAM	tumor-associated macrophage
TBE	tris-borate-EDTA
TBS	tris buffered saline

TCA cycle	tricarboxylic acid cycle
TCGA	The Cancer Genome Atlas
TEMED	N,N,N',N' Tetramethylethylenediamine
TET	Ten-eleven translocation methylcytosine dioxygenase
TGFβ	transforming growth factor β
TNF-α	tumor necrosis factor alpha
TP53	tumor protein 53
TSM	Tumor sphere medium
TU	transducing units
UPLC-MS	Ultra-performance liquid chromatography-mass spectrometry
UPR	unfolded protein response
V	voltage
VEGF	vascular endothelial growth factor
VEGFR	vascular endothelial growth factor receptor
WB	western blot
WHO	World Health Organization
Wnt	Wingless-type MMTV integration site family
YKL40	Chitinase-3-like protein 1 (CHI3L1)
Zeb	Zinc finger E-box-binding homeobox
α-KG	α-ketoglutarate
µg	microgram
µl	microliter

9 Publications based on the work presented in this dissertation

Böğürcü N, Zukunft S, Fleming I, Wilhelm J, Garvalov BK, Acker T

Metabolic control of PHD function and the hypoxic response by isocitrate dehydrogenase 1 (IDH1)

Manuscript under preparation.

Böğürcü N*, Seidel S*, Garvalov BK, Acker T (2018)

Analysis of hypoxia and the hypoxic response in tumor xenografts.

Methods Mol Biol. 2018;1742:283-300. doi: 10.1007/978-1-4939-7665-2_25.

*Equally contributing authors

Filatova A*, Seidel S*, **Böğürcü N***, Gräf S, Garvalov BK, Acker T (2016)

Acidosis acts through HSP90 in a PHD/VHL-independent manner to promote HIF function and stem cell maintenance in glioma.

Cancer Research 2016 Oct 1, 76(19):5845-5856. DOI: 10.1158/0008-5472.CAN-15-2630

*Equally contributing authors

Depner CA*, zum Buttel H*, **Böğürcü N***, Cuesta AM, Aburto MR, Seidel S, Finkelmeier F, Foss F, Hofmann J, Kaulich K, Barbus S, Segarra M, Reifenberger G, Garvalov BK, Acker T, Acker-Palmer A (2016).

EphrinB2 repression through ZEB2 mediates tumour invasion and anti-angiogenic resistance.

NATURE COMMUNICATIONS | 7:12329 | DOI: 10.1038/ncomms12329 |, 29 Jul 2016

*Equally contributing authors

10 Acknowledgments

My deepest appreciations go to the people who constantly supported me on a professional and personal level. Without you, I would have never achieved my goals!

First of all, I would like to express my gratitude to my supervisor Prof. Till Acker for giving me the opportunity to work in his institute, and for his support and guidance. I am grateful to our research laboratory head Dr. Boyan Garvalov for his excellent guidance, patience, motivation, immense knowledge and for the fruitful discussions. Thank you Boyan, your guidance helped me in all the time of research and writing of this thesis. I learned a lot from you!

I would like to thank Prof. Stefanie Dimmeler for her interest in my studies and for accepting the supervision of this work. Furthermore, I would like to thank Prof. Amparo Acker-Palmer for giving me the opportunity to work together and for allowing me access to her animal facility.

Moreover, many thanks to the GGL (Giessen Graduate School for the Life Sciences) and the Ph.D. program of the veterinary medical and human medical faculty for the courses, trainings and support during my PhD, which helped me to improve myself.

I would also like to thank to all the current and former members of the Institute of Neuropathology in Giessen for their cooperation, feedback, and of course friendship. Thank you Sabine, Sarah, Annette, Manuela, Jose, Omelyan, Conny, Anne-Therese, Attila, Miao, Huike, Nadja, Carmen, Marion, Sandra, Rebecca, Phuong, Hildegard, Anne, Gudrun, Kerstin and Alina for all the fun, happiness, success and desperation we have and had together.

My deepest and greatest thanks go to my love and colleague Sascha Seidel. Without you, I would have never achieved my goals! It is a great experience to share happy and desperate feelings as well as success with you.

Son olarak beni sürekli destekleyen, benimle sevinip, benimle üzülen aileme cok tesekkür ederim